Sultam Synthesis Via Intramolecular C-H Amination of Hydroxylamines

Jasper Adam May Quartus

Thesis submitted to the University of Ottawa
in partial Fulfillment of the requirements for the
M. Sc. Degree in Chemistry and Biomolecular Sciences

Department of Chemistry and Biomolecular Sciences
Faculty of Science
University of Ottawa

Abstract

Nitrogen is a vital element for the existence of life, as shown by its frequent presence in essential biomolecules, and inclusion into valuable drugs. Sulfonamides and their heterocycle counterpart, sultams, are *N*-containing functional groups and metabolically stable amide isosteres. Sulfa drugs, which contain these moieties, have a broad spectrum of medical applications. The industrial value of sultams has prompted the development of novel methods for their synthesis, and metal-catalyzed C-H amination reactions with nitrene precursors have recently shown promise.

The current thesis presents a survey of conditions for benzo[*d*]sultam synthesis via intramolecular C-H amination of *N*-acyloxysulfonamides. Initially, using $Ru(Bpy)_3(PF_6)_2$ as a photocatalyst and Et_3N as a base enabled benzo[*d*]sultam formation by tertiary C-H amidation. The photoredox conditions were optimized to accommodate other 2,6-disubstituted-*N*-acyloxysulfonamides upon omission of the base, which consistently gave sulfonamide byproducts. Control reactions indicated that a thermal base-induced reaction was simultaneously occurring, both enabling productive C-H amidation and byproduct formation. Systematic optimization of base-induced conditions enabled sultam synthesis from 2,6-dialkyl- and tertiary *ortho*-monoalkyl-precursors in moderate yield, but sulfonamide formation still impeded the reaction.

I. Graphical Abstract: Intramolecular C-H amidation of N-acyloxysulfonamides.

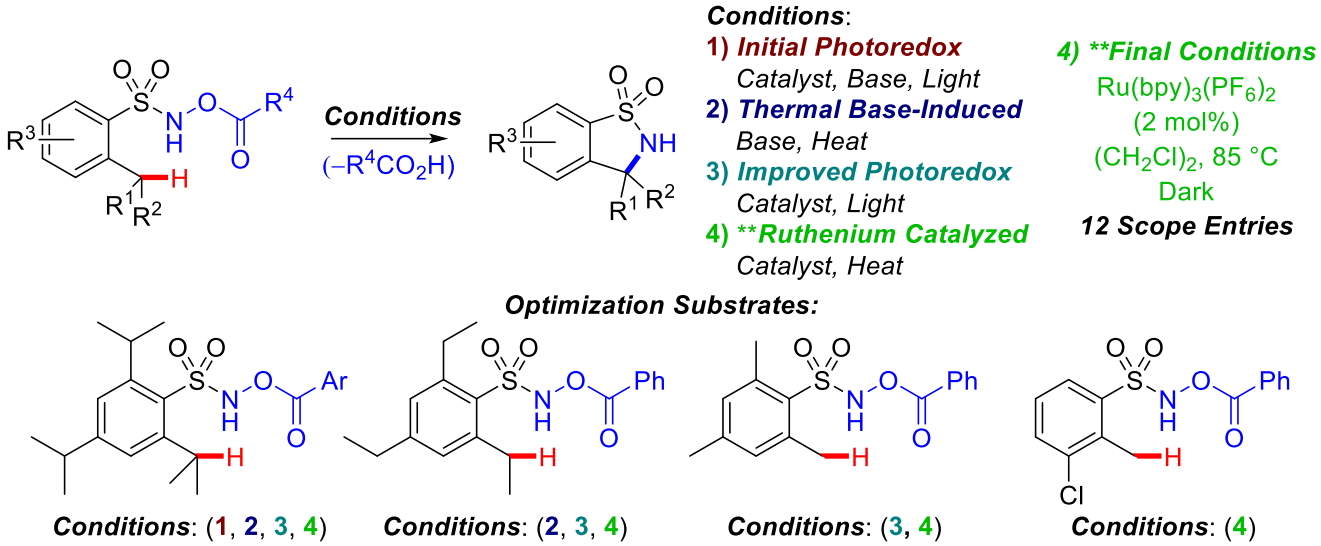

An additional control reaction indicated that a thermal Ruthenium-catalyzed C-H amidation reaction was possible. Indeed, heating *N*-acyloxysulfonamides in the presence of $Ru(Bpy)_3(PF_6)_2$ and in the absence of light and base enabled efficient C-H amidation, particularly with DCE as a solvent. A representative scope of 12 benzo[*d*]sultams was then synthesized including entries derived from *ortho*-monoalkyl-*N*-acyloxyarylsulfonamides.

Aside from optimizing an efficient reaction for the synthesis of benzo[*d*]sultams through the cyclization of *N*-acyloxyarylsulfonamides, including the challenging primary C-H amidation of *ortho*monomethyl-substrates, the unique reaction conditions developed in this thesis set precedent for future investigation of hydroxylamine derived nitrene precursors. The optimization and design of superior ruthenium catalysts could allow for more challenging C-H amination reactions with hydroxysulfonamide derivatives and similar *N*-oxy nitrene precursors.

Aknowledgements

First and foremost, I would like to thank André for allowing me to join his group; it has been an amazing opportunity to not only build my skills in the lab, but to also solidify my understanding of chemistry. André has always been very helpful and supportive in guiding me with my research and has been extremely understanding throughout the struggles that were posed by writing my thesis during a pandemic. André is also great to talk to about any topic in chemistry; whether it is related to my own research or not, it is always an interesting discussion. Additionally, our group meetings are a great way to improve the speed at which one can solve chemistry problems and would be a benefit to any aspiring chemist.

But it is not only the group meetings themselves that benefit a chemist in training; we are all lucky to be part of a group composed of brilliant scientists. Overall, the most interesting and engaging chemistry conversations occurred within our office. In fact, throughout my entire education I may have learned the most by simply sitting with Ryan, Meredith, Dilan and William during my Honours. The interesting chemistry conversations continued further when I moved to my new seat during my Master's, and for this I must thank Binjie, David, Josh, Alshimaa and once again William. Perhaps the best part of working in the office was that many of the conversations were hilarious, and we all had a lot of fun. But we always had a lot of fun, whether it was at 3 brewers getting drinks and food, partying at conferences, going skating, bowling and mountain climbing, or doing Karaoke. These activities are only a few of the many things I would to thank you all for, and I wish that I made time to do even more. It is also worth mentioning that ever since I can remember, my main interests have been science and music, so it was pretty awesome to have three additional full-fledged metalheads in the group—Ryan, Dilan and William—and that everyone else also had great music tastes.

I would really like to thank the co-author of my first paper and the current paper being prepared with the results in this thesis. Without Ryan, I would be completely lost with my research, and would not have been able to successfully navigate the optimization process. He also gave me a great deal of help editing my thesis, even after graduating with his Ph.D., and for this I will be forever grateful. Ryan was not the only expert on nitrene chemistry in our lab, however. Dilan was very helpful, particularly toward the initial stages of optimization, and while helping me to catch up on and solidify my understanding of previous research and prepare for conferences. She was also always good to talk to about future careers in industry and about her own experience in graduate school. Meredith is the current certified nitrene expert in our lab, and I need to thank her as well for a variety of insights throughout my optimization studies, for helping me to prepare for conferences, and always thinking of helpful ideas to improve my chemistry in sub-group meetings.

I would like to thank William and David for the times we could bounce ideas of each other at the most difficult parts of our projects; you have both helped me through many obstacles in my research. It was interesting to see our projects evolve together. You were also both great to study with for the classes we took, it was a lot more enjoyable to work through the material together. We also had some great times away from campus, even just to go for a nice Costco trip, but we should definitely hit up a comedy show again and actually try to go skiing together someday!

I would also like to thank the newer members of the group—Frédéric, Sherif, Myroslava, Huy, and Geneviève—it was always great to talk to aspiring students about chemistry, and their cool new projects after being away from the lab during the pandemic. I wish you all a great future in the group and beyond.

Some of the people I need to thank the most, however, are my family— my Mom, my Dad, and my brother Emmitt. With their tremendous support, I was able to achieve my goals. Additionally,

it was always nice to come home and spend time with you all; the nostalgia of returning home for a break has always been one of my best memories throughout my education. I would also like to thank my amazing partner Kirsten for always being there for me when I needed it, even in my most difficult situations. Spend time with you was always one of the things I looked most forward to throughout my studies. I would also like to thank Kirsten's family has also always been very supportive, including when they allowed Kirsten and I live at their home at the height of the pandemic. It is also important to thank the rest of my family, which I could not name here as I have twenty first-cousins and twenty aunts and uncles. I could never thank any of you enough for all you have done to help me reach success.

I would also like to thank a couple of my close friends: Derick, Calum and Emma. In some ways the fun times we had together were the most important for getting me through school. I am excited for many great times together in the future, and hopefully things can return to normal soon so we can get together.

I would also like to thank my amazing dog Benji, the best boy who I've been lucky to have throughout the pandemic.

Thank you to anyone else who I was unable to name that has had a positive impact on my graduate degree, my studies as a whole, or my life in general.

Table of Contents

List of Figures

List of Schemes

List of Tables

List of Abbreviations

[M] – generic metal

[O] – generic oxidant

Å – angstrom

°C – degrees Celsius

*α*KG – *α*-ketoglutarate

A – alanine

Ac – acetyl

Acac – acetylacetonate ligand

Ar – generic aryl

B3LYP – Becke-3-Lee-Yang-Parr

BDE – bond dissociation energy

BDFE – bond dissociation free energy

Bn – benzyl

Boc – *tert*-butyloxycarbonyl

BOX – bis(oxazoline) ligands

Bpy – 2,2′-bypyridine

BTMG – 2-tert-butyl-1,1,3,3-tetramethylguanidine

Bz – benzoyl

C – carbon, cysteine

calcd - calculated

cm – centimeter

CMD – concerted metalation deprotonation

Cy – cyclohexyl

CYP450 – Cytochrome P450 enzyme

$CYP450_{LM3,4}$ – rabbit liver microsomal cytochrome P450

$CYP450_{BM3}$ – cytochrome P450 from Bacillus megaterium

D – dextrorotatory

DBU – 1,8-diazabicyclo[5.4.0]undec-7-ene

DCE – 1,2-dichloroethane

DFT – density functional theory

DIPEA – *N*,*N*-diisopropylethylamine

DIPT – diisopropyl tartrate

DMAP – 4-dimethylaminopyridine

DME – dimethoxy Ethane

DMF – N,N-dimethylformamide

DMG – directed metalation group

DMSO – dimethyl sulfoxide

DNA – deoxyribonucleic acid

DOM – directed ortho metalation

dr – diastereomeric ratio

dtbbpy – 4,4′-di-tert-butyl-2,2′-dipyridyl

E – generic electrophile

E – Ger., entgegen

$E_{1/2}$ - Half Wave Potential

EDG – electron-donating group

ee – enantiomeric excess

EI – electron impact

EIF_4E – eukaryotic translation initiation factor 4E

EnT – energy transfer

equiv – stoichiometric equivalent

er – enantiomeric ratio

Et – ethyl

ET – triplet energy

EWG – electron-withdrawing group

F – phenylalanine

FTIR – Fourier transform infrared

g – gram

h – hour

H – histidine

HAT – hydrogen atom transfer

H-L-F – Hofmann–Löffler–Freytag

HIV – human immunodeficiency virus

HRMS – high-resolution mass spectroscopy

Hz – Hertz

hυ – light; electromagnetic radiation

I – isoleucine

i-Pr – isopropyl

IR – infrared

ISC – intersystem crossing

J – coupling constant

k – rate constant

K – Kelvin

kcal – kilocalorie

KIE – kinetic isotope effect

L – generic ligand

L – liter, levorotatory

LED – light-emitting diodes

LG – generic leaving group

m – meta

M – molar, methionine

ML_n – generic metal with *n* ligands

Me – methyl

MeCN – acetonitrile

mins – minutes

ml – millilitre

mmol – millimole

mol – mole

MOPS – (3-(N-morpholino)propanesulfonic acid)

My – myoglobin

n-Bu – *n*-butyl

NHC – *N*-heterocyclic carbene

NMR – nuclear magnetic resonance

NOE – nuclear Overhauser effect

NSAID – nonsteroidal anti-inflammatory drug

Nuc – generic nucleophile

o – ortho

p – para

PCET – proton coupled electron transfer

PG – protecting group

Ph – phenyl

Phebox – phenyl-bisoxazoline

Piv – pivalyl / pivaloyl group

PIX – mesoporphyrin IX:

ppm – parts per million

Ppy – 2-Phenylpyridine

*Ps*EFE – *Pseudomonas savastanoi* ethylene forming enzyme

PTAB – trimethylphenylammonium tribromide

pyr – pyridine

Py_5Me_2 – 2,6-bis(1,1-bis(2-pyridyl)ethyl)pyridine

Quinox P – 2,3-bis(*tert*-butylmethylphosphino)quinoxaline

R – generic group, arginine

R – Latin, rectus

R_F – retention factor

RNA – ribonucleic acid

rt – room temperature

S – serine

S – Latin, sinister

SCE – saturated calomel electrode

SET – singlet electron transfer

S_NAr – nucleophilic aromatic substitution

syn – together, same side

T – tyrosine

t-Bu – *tert*-butyl

*t*Bu-Nicox – (S)-methyl 6-(4-(tert-butyl)-4,5-dihydrooxazol-2-yl)nicotinate

^{t}Butpy – 4,4',4''-tri-tert-butyl-2,2':6',2''-terpyridine

temp. – temperature

Tf – trifluoromethanesulfonyl

THF – tetrahydrofuran

TLC – thin-layer chromatography

TMG - 1,1,3,3-Tetramethylguanidine

TMSCl – trimethylsilyl chloride

TON – turnover number

TPP – tetraphenylporphyrin

TTN – total turnover number

Ts – *para*-toluenesulfonyl

TS – transition state

UV – ultraviolet

V – valine, volts

VNS – vicarious nucleophilic substitution

W – watts

WHO – World Health Organization

X – generic halide, generic leaving group

Z – Ger., zusammen

Δ – thermolysis

δ – chemical shift in parts per million

μm – micrometer

μW – microwave

Chapter 1: Introduction

1.1 Nitrogen Containing Molecules

The value of nitrogen atoms in organic molecules cannot be overstated. All the proteins present in biological organisms, from enzymes to receptors, consist of amino acid chains connected by amide bonds (**Figure 1, A**). The purine and pyrimidine nucleobases present in DNA contain 2-5 necessary nitrogen atoms each (**Figure 1, B**) to participate in the hydrogen bonding interactions that maintain the double helix of DNA. The ferrous iron atom located at the core of hemoglobin oxygen transport enzymes is stabilized by coordination of Heme B, a pyrrole-based porphyrin ligand (**Figure 1, C**). The eight most common neurotransmitters all contain at least one nitrogen atom (**Figure 1, D**). With its importance for bond forming reactions and intermolecular interactions, the nitrogen atom is comparable to carbon and oxygen for its importance into biological systems.

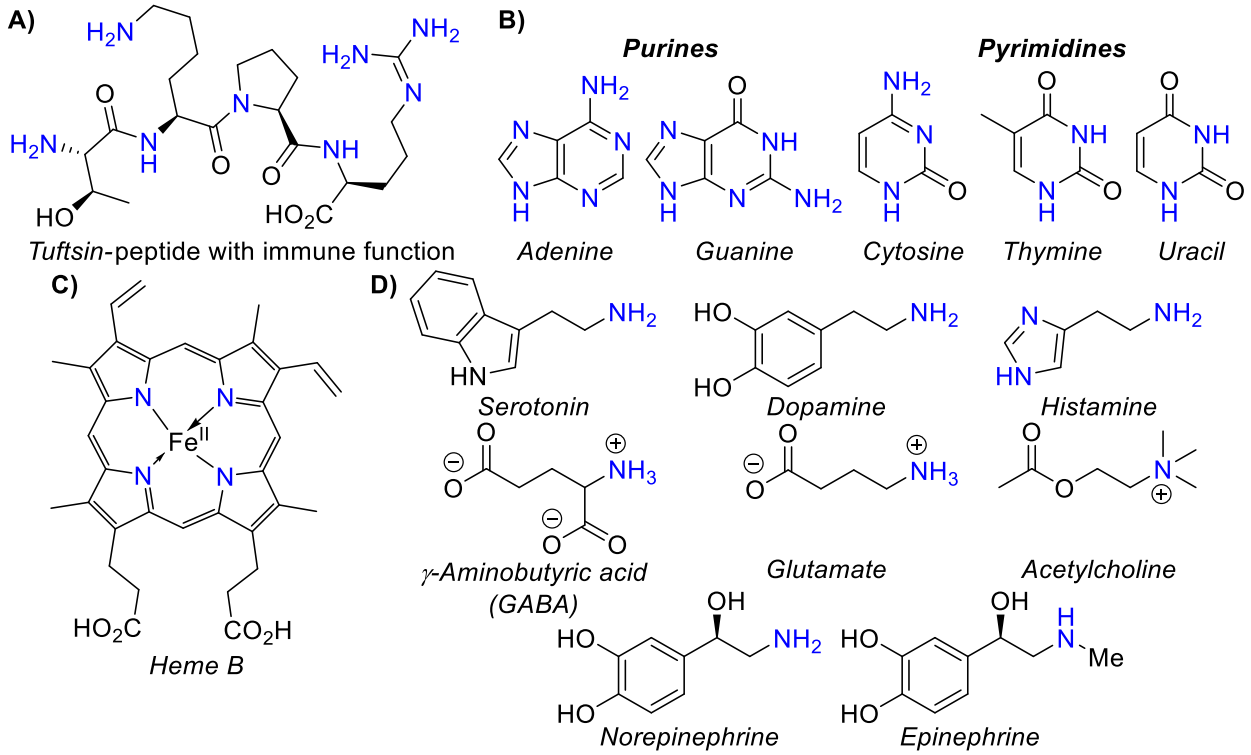

Figure 1. Nitrogen atom presence in important biomolecules.

With the vital bioactivities induced by nitrogen function groups, it is not surprising that 84% of small-molecule drugs contain at least one nitrogen atom, and over 15% of industrial reactions in the pharmaceutical sector involve the formation of a nitrogen-carbon bond.[1–3] On top of this, 59% of small molecule drugs contain at least one nitrogen-heterocycle.[3] From a historical perspective, some of the most ground-breaking discoveries in medicine involved drugs containing a nitrogen heterocycle. The 1928 discovery of Penicillin derivatives, which contain distinctive β-lactam heterocycles (**Figure 2, A**), lead to the treatment of many serious bacterial infections.[4,5] The pteridine containing folic acid derivatives, aminopterin and amethopterin (**Figure 2, B**), were the first compounds used for chemotherapy in 1947.[6–8] The approval of the first benzodiazepine anxiolytics, chlordiazepoxide in 1960 and diazepam (**Figure 2, C**) in 1963, revolutionized the management of mental disorders.[9] The piperidine / quinoline containing antiretroviral medication saquinavir was the first HIV protease inhibitor approved in 1988 (**Figure 2, D**).[10] Even the best-selling drug of all time, atorvastatin, has a pyrrole ring embedded in its core (**Figure 2, E**).[11,12] Overall, it is safe to say that nitrogen heterocycles play an essential role in the field of medicine.

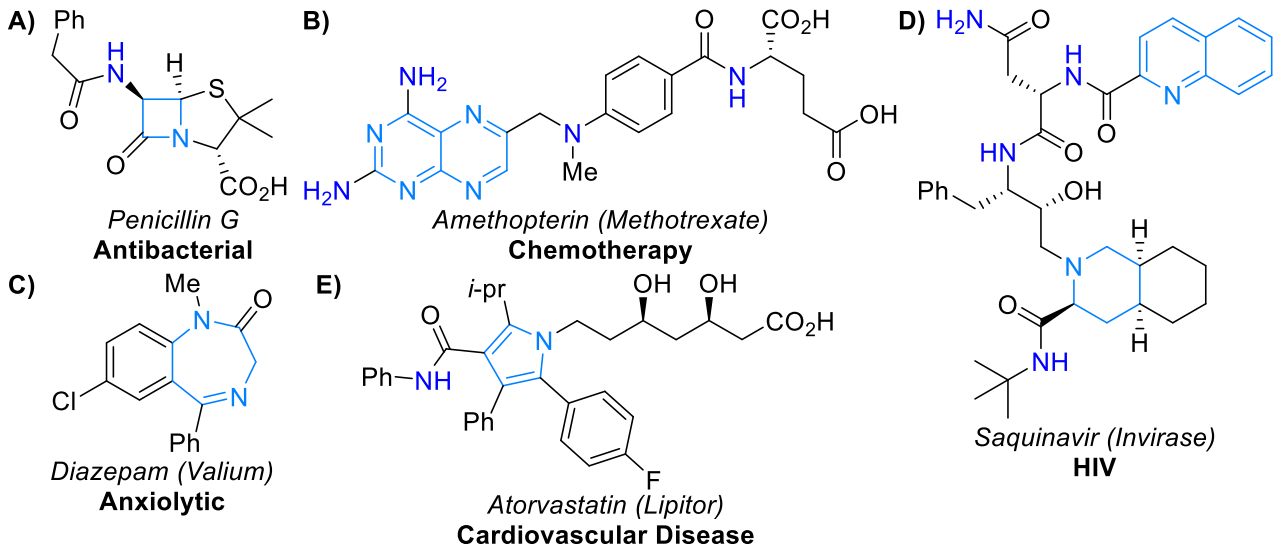

Figure 2. Historically ground-breaking drugs with Nitrogen heterocycles.

1.2 Sulfonamides

Sulfonamides are a relatively inert class of functional group represented by the general formula $R^1S(=O)_2NR^2R^3$ which act as an isostere of the amide functionality.[13] In 1932 Gerhard Domagk discovered that Protosil, an azo dye bearing a sulfonamide group, showed potent antibacterial effects.[14] The antimicrobial action was induced by a bioactive metabolite also containing a sulfonamide group, sulfanilamide, indicating that Protosil was in fact a prodrug (**Scheme 1**).[15,16]

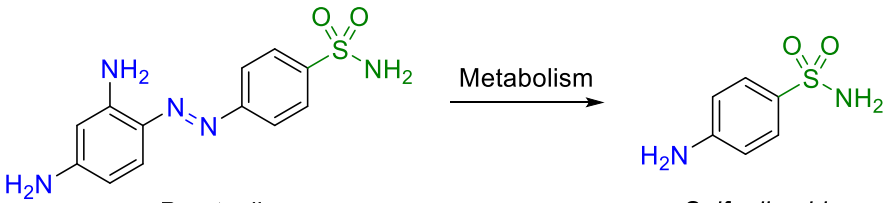

Prontosil
Prodrug

Sulfanilamide
Anitbacterial

Scheme 1. Azo dye Protosil represents a prodrug for sulfanilamide, an early antibiotic.

Since this discovery, several valuable sulfonamide-based (sulfa) drugs have been developed to elicit a variety of biological activities, several of which are included in the "WHO Model List of Essential Medicines".[17–19] Early research led to additional antibacterial sulfa drugs such as the dihydropteroate synthase inhibitor sulfamethoxazole in 1961 (**Figure 3, A**).[20] In 1952, the carbonic anhydrase inhibitor acetazolamide was introduced to treat glaucoma, epilepsy and edema (**Figure 3, B**).[21,22] The diuretic furosemide was then brought into the market in the following decade (**Figure 3, C**).[23,24] Several other sulfa drugs have been successfully marketed including the NSAID celecoxib (Celebrex),[25,26] the well-known erectile dysfunction medication Sildenafil (Viagra),[27,28] the HIV protease inhibitor amprenavir,[29,30] and sumatriptan, a serotonin receptor agonist used to treat migraines and cluster headaches (**Figure 3, D-G**).[31,32] An analysis of common drugs showed the sulfonamide group is the 22nd most common side chain in known drugs.[33–35]

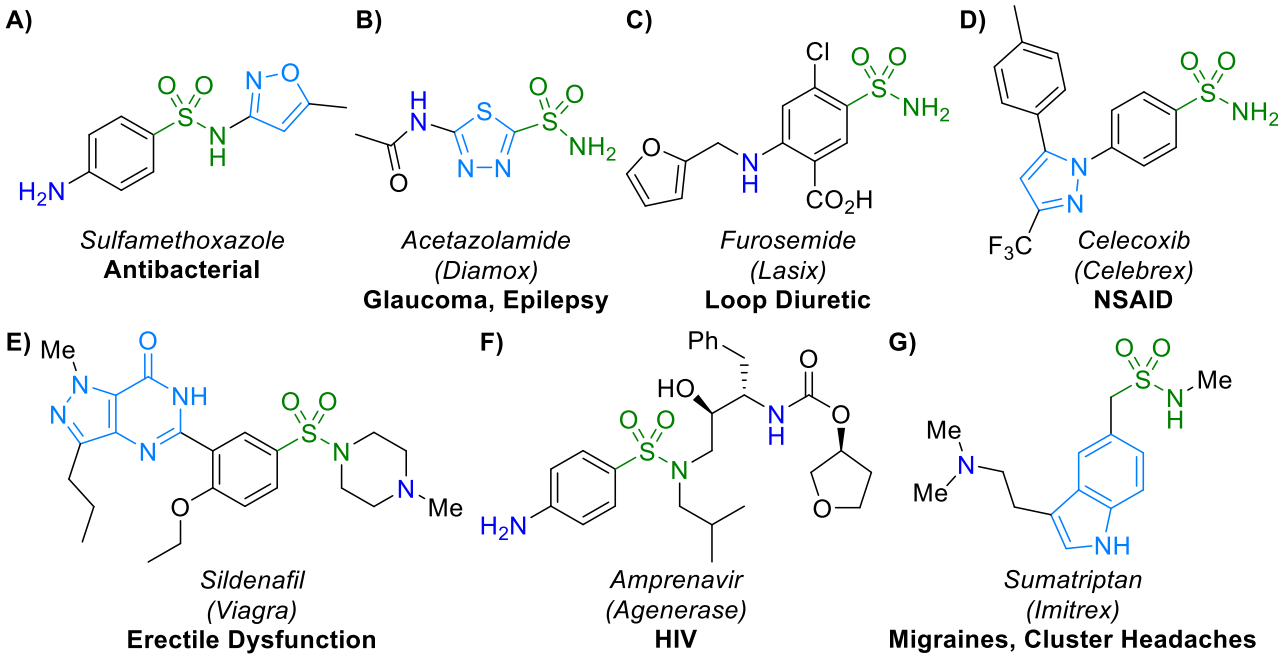

Figure 3. Valuable drugs containing sulfonamide functional groups.

The bioactivity of sulfonamides relates to their bioisosterism with other functional groups, namely amides, but also other carbonyl, sulfonyl and phosphonyl-based groups.[36] Unlike amides, sulfonamides have tetrahedral sulfur atoms, and the nitrogen atom is more pyramidal. This geometry makes the sulfonamide bond dihedral angle below 90° rather than 180°.[35] Importantly, the increased N-H acidity (sulfonamide pK_a = 17.5[37], amide pK_a = 25.5[38]) renders them far better hydrogen bond donors, and the N-H acidity can be selectively tuned for divergent drug design.[35] The sulfonamide motif is also more resistant to metabolism than amide functionalities.[39] Research assessing sulfonamide bioactivity has led to several patents disclosing drug candidates for a variety of diseases including: Alzheimer's, anxiety, cancer, diabetes, insomnia, osteoporosis and epilepsy.[35,36,40–45] Others compounds have antibacterial, antiviral, antifungal, antitubulin, antipsychotic, antidandruff and diuretic action.[35,36,40–45] The bioactivity of sulfonamide compounds allows for agricultural applications.[35,42] In terms of synthetic applications, proline sulfonamides are used as organocatalysts[46] and *N*-alkylsulfonamides (tosylamides) act as carbon electrophiles.[47]

1.3 Sultams

Sultams are heterocyclic sulfonamides, and like the relationship between sulfonamides and amides, sultams are isosteres of lactams. This isosterism extends to related cyclic sulfamate and sulfamide heterocycles, which represent the sulfonyl counterparts for cyclic carbamates and ureas, respectively (**Figure 4, A**). Sultams are conventionally classified by the same system applied to lactams, using Greek prefixes (α = 3, β = 4, γ = 5, δ = 6, ε = 7) to denote the ring size (**Figure 4, B**). Sultams derivatives that are annulated with an aromatic ring are referred to as benzosultams.

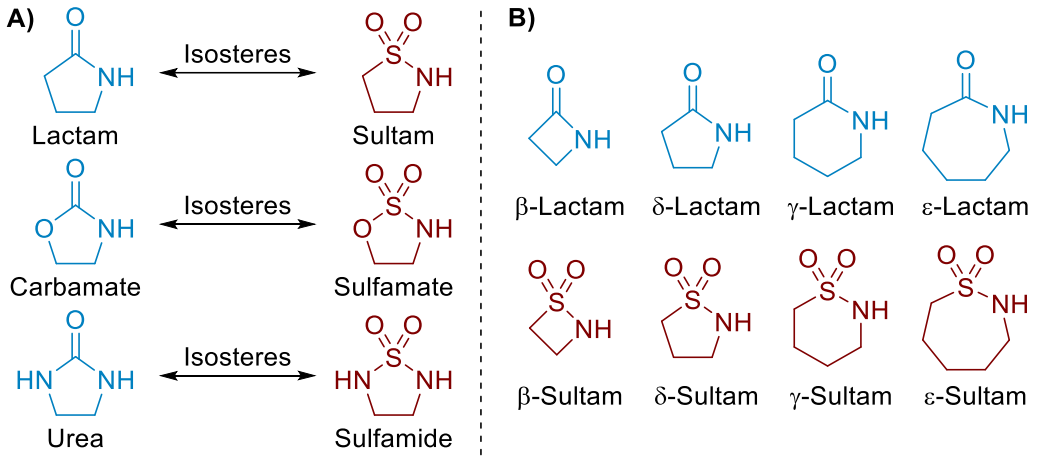

Figure 4. Structural and isosteric relationships of carbonyl and sulfonyl heterocycles.

1.3.1 Usage of Sultams

Sultams have several synthetic and medical applications, but they have the longest history as chiral auxiliaries, with Oppolzer's sultam as the most well-known example (**Figure 5, A**).[39,48–50] Chiral benzosultams have also been used.[39,48–50] Sultams also have application as directed metalation groups (DMGs), protecting groups and electrophilic fluorinating agents (*N*-fluorosultams).[48,49,51] Sultams also exhibit valuable biological activities, and the moiety has appeared in several drugs.[49] Piroxicam and meloxicam are NSAID drugs that treat rheumatic diseases (**Figure 5, B**).[52–54] Sultiame[55–57] and brinzolamide[58,59] are carbonic anhydrase inhibitors (**Figure 5, C-D**) that are

prescribed for distinct ailments, epilepsy[55–57] and glaucoma,[58,59] respectively. Hydrochlorothiazide is a diuretic used to treat high blood pressure, swelling and diabetes insipidus (**Figure 5, E**).[60,61] Interestingly, sultiame, brinzolamide and hydrochlorothiazide also contain free sulfonamide moieties (**Figure 5, C-E**). A range of other bioactivities have been found including antibacterial, antiviral, antifungal, antimalarial, anticancer, antidiabetic, antipsychotic and hypoglycemic action, serotonin receptor agonism and inhibitory action towards a range of enzymes such as calpain I, serine proteases, cyclooxygenase-2, HIV integrase, lipoxygenase, and matrix metallopeptidase-2.[35,36,40–45,49] In 2020, a patent disclosed nicotinamide-based benzosultams as $Na_V1.8$ voltage-gated sodium ion channel inhibitors, with implications for the treatment of epilepsy, migraine, and pain management (**Figure 5, F**).[62] Another patent in 2021 described a tricyclic sultam that inhibits EIF_4E, and could lead to the development of new cancer drugs (**Figure 5, F**).[63] Like sulfonamides, sultams have also been researched for use in agricultural fields as pesticides[50] and herbicides.[64] Sultam compounds clearly show potential for the future use in synthesis, medicine and agriculture.

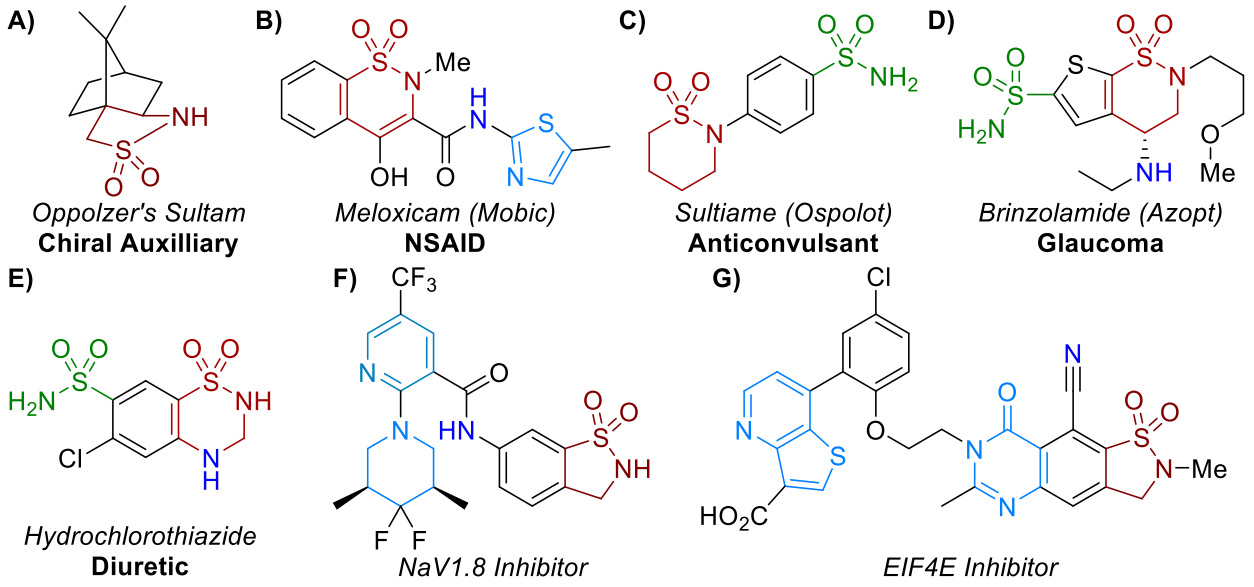

Figure 5. Important molecules containing sultam heterocycles.

1.3.2 Synthesis of γ-Sultams

A range of methods have been developed for sultam synthesis and several review articles survey this literature.[39,48–50,64–66] The formation of monocyclic and polycyclic sultams, including both aliphatic and benzo-annulated variants, with a range of ring sizes and fused ring numbers has been achieved. The results presented in this thesis focus on the development of methods for synthesis of five membered benzosultams through C-H amination reactions. Due to the array of published methods and the specific results obtained here, this review will focus on γ-benzosultams. Some sultam synthesis routes have taken advantage of C-H amination methodology and will be summarized with thorough introduction in **Chapter 1.4**, where C-H amination is the focus.

Benzosultams

A summary of synthetic routes toward the two major classes of γ-benzosultams, benzo[*d*]sultams (1,2-benzisothiazoline 1,1-dioxides) and the isomeric benzo[*c*]sultams (2,1-benzisothiazoline 2,2-dioxides) is covered here. The former class possess a benzenesulfonamide group and a nitrogen atom at the benzylic position. In the latter class this arrangement is reversed; the nitrogen atom is bound to the aromatic ring, and the sulfonyl group is benzylic (**Figure 6**).

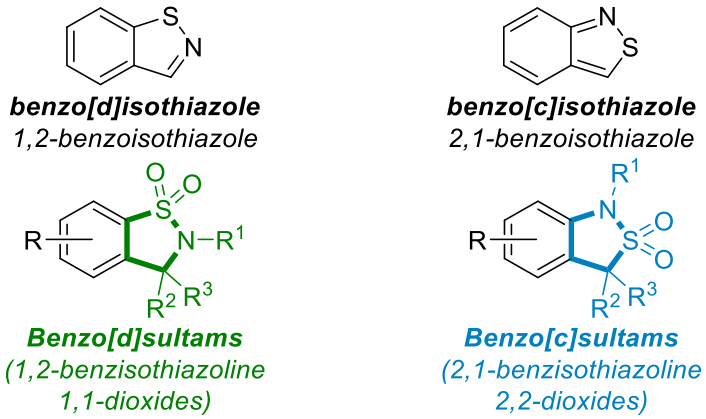

Figure 6. Connectivity of benzisothiazoles and the two major classes of benzosultams.

Substitution Reactions in the Synthesis of Benzosultams

Conceptually, one of the simplest ways to form sultams is through intramolecular nucleophilic substitution reactions. Indeed, one of the first successful benzo[*d*]sultam synthesis was achieved by reacting triphenylcarbinol-o-sulfonic methylamide with fuming HCl at 150 °C (**Scheme 2**).[65,67]

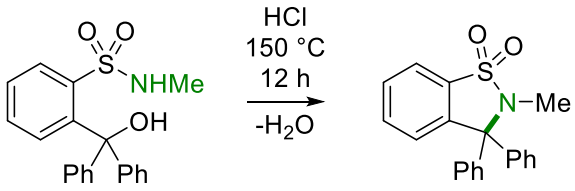

Scheme 2. Early example of sultam formation through a substitution reaction.

This nucleophilic cyclization method was later expanded to other 3,3-disubstituted benzosultams; directed *ortho* metalation (DOM) with *N*-methyl- and *N*-phenyl-benzenesulfonamides, followed by ketone addition gave the desired benzylic alcohols and excess heating or treatment with acid allowed the cyclodehydration reactions to ensue.[68] Alas, *N*-deprotection of the sultams was difficult. Liu's group further improved this DOM-substitution sequence.[69,70] Carbinol sulfonamides derived from the lithiation-ketone addition procedure with *N*-*tert*-butyl benzene sulfonamides were treated with NaI (2 equiv.) and TMSCl under reflux, thus enabling sequential *N*-deprotection and cyclization for high yields of free N-H benzo[*d*]sultams and the first examples of spirocyclic sultam synthesis (**Scheme 3**).

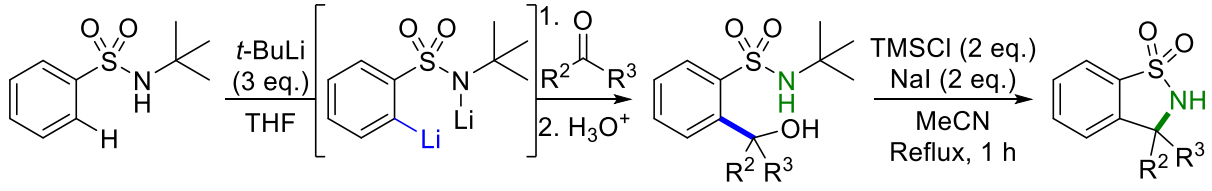

Scheme 3. TMSCl-NaI-MeCN reagent-mediated deprotection/cyclization.

Liu then extended these reaction conditions to include catalytic iodine, enabling the reaction of carbinol sulfonamides derived from aromatic aldehydes to synthesize 3-aryl benzo[*d*]sultams.[71]

Mechanistic evidence suggested these reactions proceed through sequential formation of an iodosilane, a silyl ether, and a benzyl-iodide. After a century of intermittent research, the mild conditions developed allow for a simple sultam synthesis through nucleophilic substitution.

Sultams can also form by intramolecular epoxide opening, reactivity exploited for the asymmetric synthesis of β-hydroxybenzo[*d*]sultams.[72] Sharpless epoxidation[73] of an allylic alcohol-containing sulfonamide furnished an epoxy-alcohol (99% ee) and regioselective cyclization was achieved using Ti(O*i*Pr)$_4$ as a Lewis acid. Finally, diol cleavage and reduction give the product (**Scheme 4**).

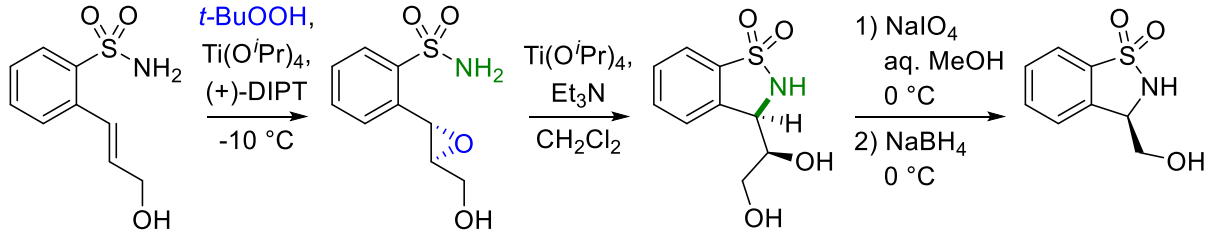

Scheme 4. Asymmetric synthesis of a β-hydroxysultam through epoxide ring opening.

Benzo[*c*]sultams have also been synthesized through substitution reactions. Refluxing sodium 2-aminobenzylsulfonate in phosphorus oxychloride enables the intermediate formation of a sulfonyl chloride, which undergoes intramolecular substitution by the *ortho*-aniline group (**Scheme 5**).[74]

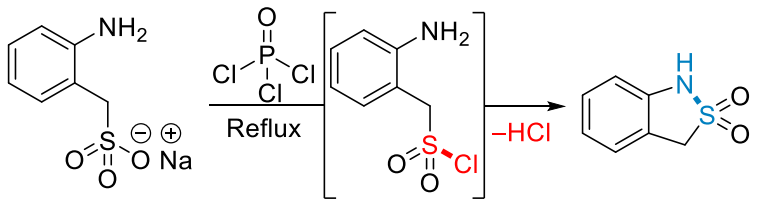

Scheme 5. Benzo[*c*]sultam synthesis by chlorodehydration of a sodium sulfonate.

Synthesis of Sultams from N-Sulfonylimines

A variety of methods for the synthesis of benzo[*d*]sultams rely on their unsaturated counterparts, *N*-sulfonylimines, as precursors. These transformations are often achieved with advanced variants of traditional π-bond manipulation reactions (**Figure 7**).[75–82] Examples that enable stereoselective

sultam synthesis include: hydrogenation[75] (**A**), metal catalyzed 1,2-insertion with alkyl[76] (**B**) aryl[77] (**C**) and alkynyl[78] (**D**) nucleophiles, cross-dehydrogenative coupling[79] (**E**), cycloadditions[80] (**F**), aza-Darzens reactions[81] (**G**), and NHC-catalyzed homoenolate additions (**H**).[82]

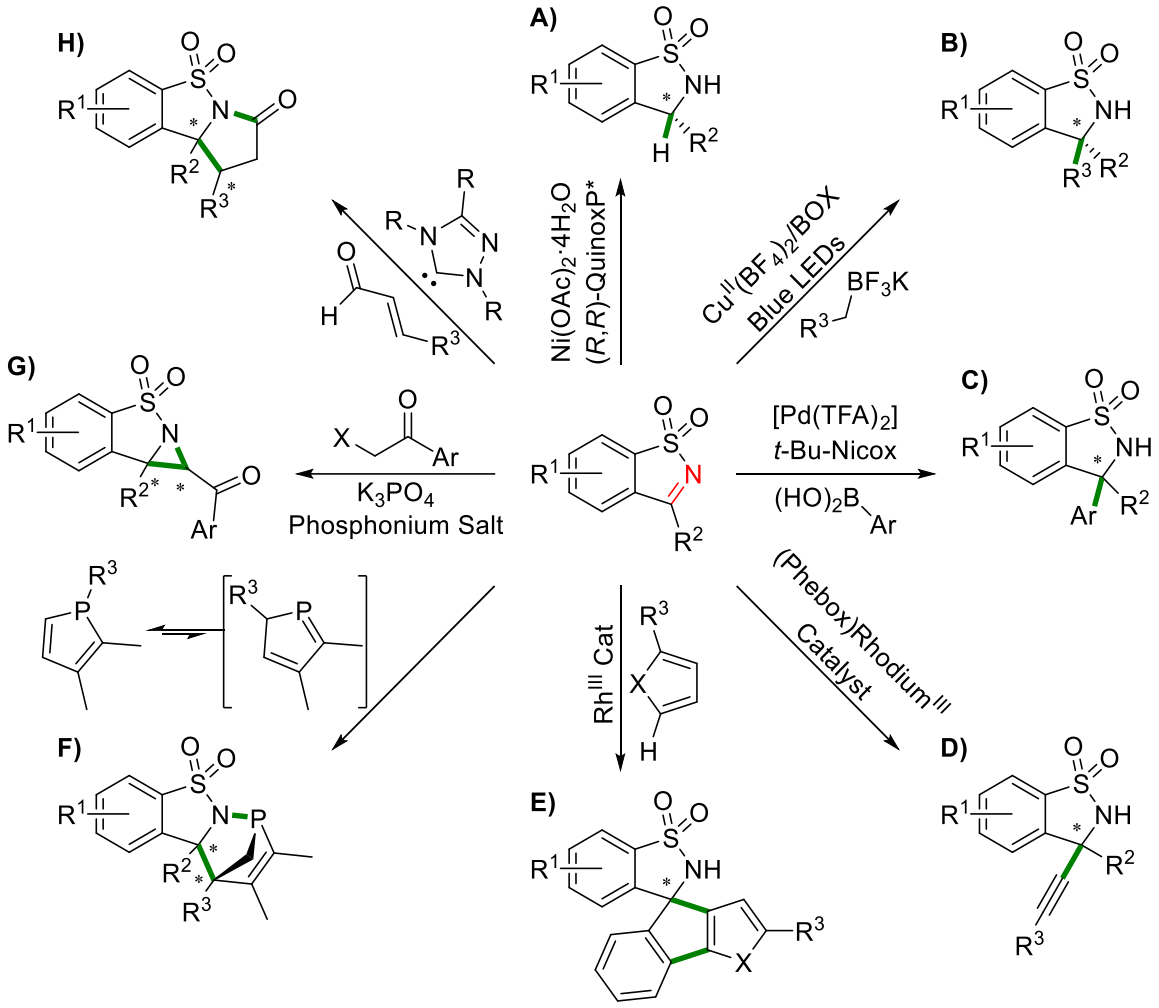

Figure 7. Various reactions to synthesize benzo[*d*]sultams from *N*-sulfonylimines.

Sultam Synthesis via Nucleophilic Aromatic Substitution

Synthetic routes toward benzo[*c*]sultams often make use of S_NAr reactions.[66] The simplest example employing an S_NAr reaction to close a sultam ring involves the displacement of a fluoride atom in an *N*-alkyl-*N*-methanesulfonyl-2-fluoro-5-nitroaniline under basic conditions (**Figure 8, A**).[66,83] An alternative S_NAr mechanism can also be used to form nitro-substituted

benzo[*c*]sultams; vicarious nucleophilic substitution (VNS) of a chlorine atom is possible when using *N*-chloromethane-sulfonyl-3-nitroanilines (**Figure 8, B**).[66,84,85] The generation of a benzyne intermediate is another mechanistic regime that enables benzo[*c*]sultam synthesis.[86–88] Nitrogen and carbon nucleophiles can both attack the benzyne in an intramolecular fashion (**Figure 8, C**).

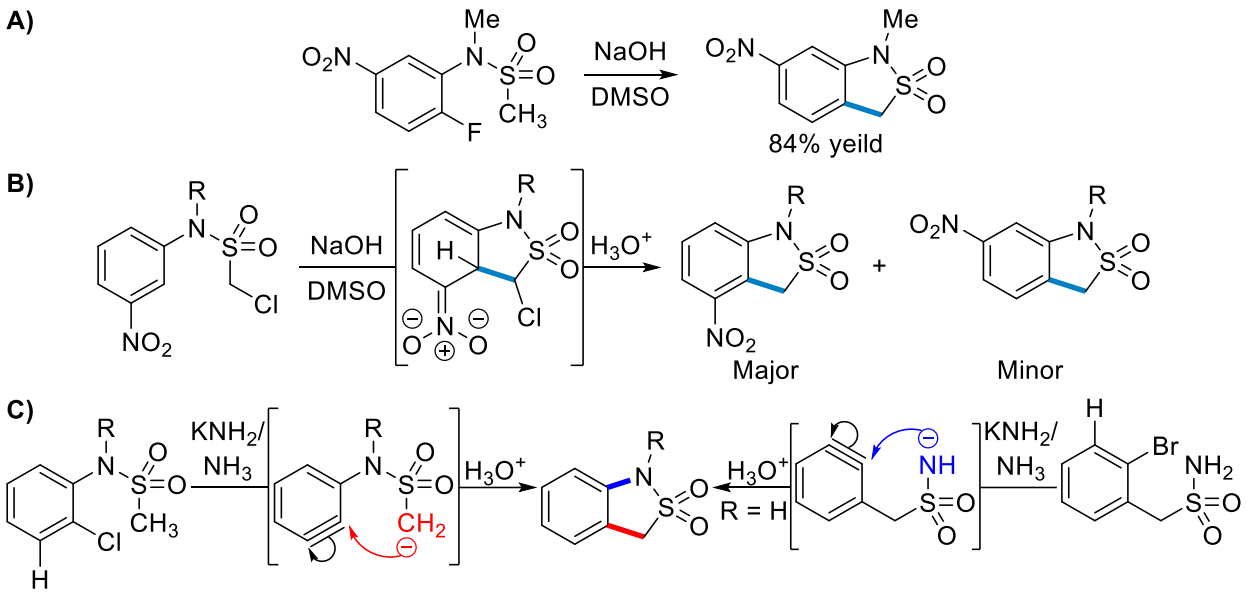

Figure 8. Synthesis of benzo[*c*]sultams through nucleophilic aromatic substitution reactions.

Benzo[*d*]sultams can also be synthesized via S_NAr; Penso reported the synthesis of 3-carboxy substituted tetrafluoro benzo[*d*]sultams by enolization of carboxy sulfonamides.[89] An improved enantiodivergent variant enabled access to both monofluoro-3-carboxy-benzosultam enantiomers starting from enantiopure sulfonamides by altering the base ratio of BTMG:DBU (**Scheme 6**).[90]

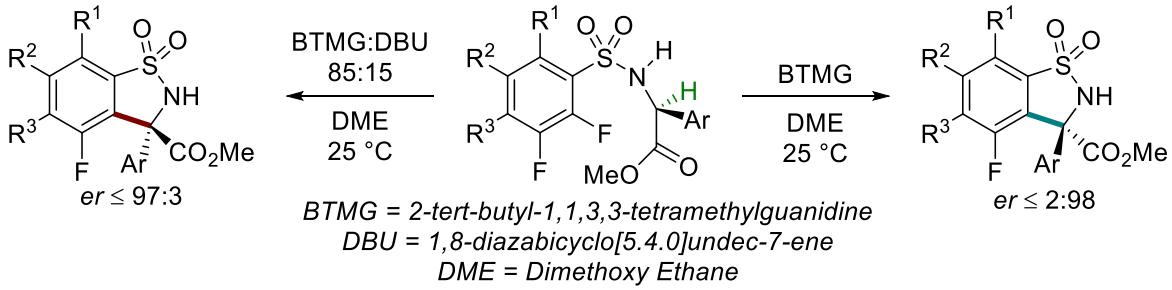

Scheme 6. Enantiodivergent synthesis of chiral benzo[*d*]sultams by S_NAr.

Benzosultam Synthesis Through Addition to π-Bonds

The intramolecular hydroamination of π-bonds by aryl sulfonamides represents yet another unique sultam synthesis method. Tao and Gilbertson showed that intramolecular hydrosulfonamidation of *ortho*-alkynes occurs in under ten minutes at room temperature using trifluoromethanesulfonimide as an acid catalyst and triethylsilane as a hydride source, affording *N*-substituted benzo[*d*]sultams. Using *ortho*-alkynyl-*N*-benzylsulfonamides with electron rich *N*-benzyl aromatic groups at 50° C instead allows direct formation of the free N-H sultams (**Scheme 7**). Unfortunately, the reaction only works with terminal *ortho*-alkynes, thus only 3-methyl-substituted sultams can be formed.[91]

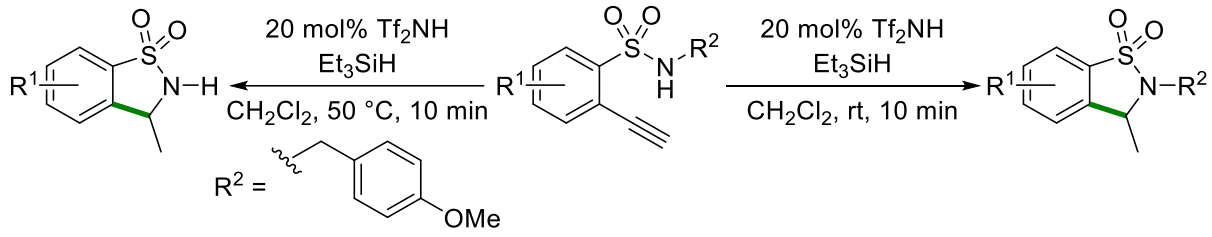

Scheme 7. Sultams from acid catalyzed hydroamination of *ortho*-alkynyl-arylsulfonamides.

Transition Metal Catalyzed Benzosultam Synthesis

Several literature examples exist for the synthesis of both benzo[*d*]sultams and benzo[*c*]sultams using transition metal catalysis techniques.[3,5–7] Dating back to 1986, a benzo[*c*]sultam was synthesized from 2-chlorophenylmethanesulfonamide through a high temperature intramolecular Ullmann-type amination with copper bronze in the presence of a base (**Scheme 8**).[74]

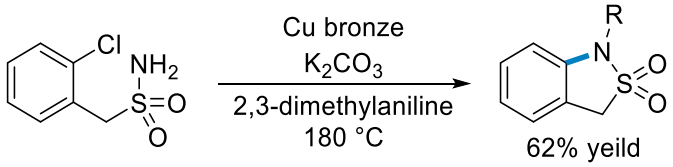

Scheme 8. Early catalytic example: Ullmann-type sultam synthesis using copper bronze.

The most common approach to generate benzo[*d*]sultams by transition metal catalysis is through Heck-type olefination reactions. For example, Reau's group applied a 5-*exo* Heck cyclization to generate tricyclic benzo[*d*]sultams from brominated *N*-benzenesulfonyl enamines (**Scheme 9**).[92]

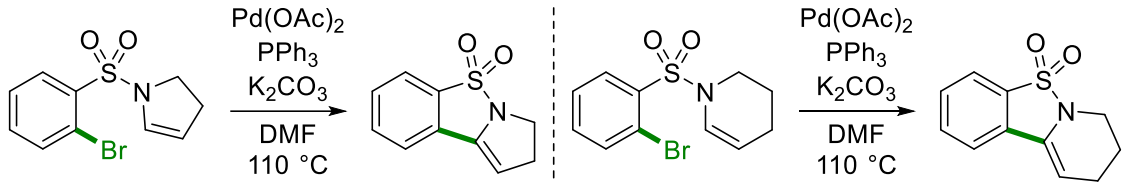

Scheme 9. Tricyclic benzo[*d*]sultams through 5-*exo* Heck cyclization of sulfonyl enamines.

In most other cases the Heck reaction generates a C-C bond between a benzenesulfonamide and an alkene, and the resulting olefin undergoes intramolecular amination. Hanson and colleagues published an early example of this by developing a one-pot three component protocol for the synthesis of benzo[*d*]sultams through a domino Heck-aza-Michael pathway (**Scheme 10**).[93]

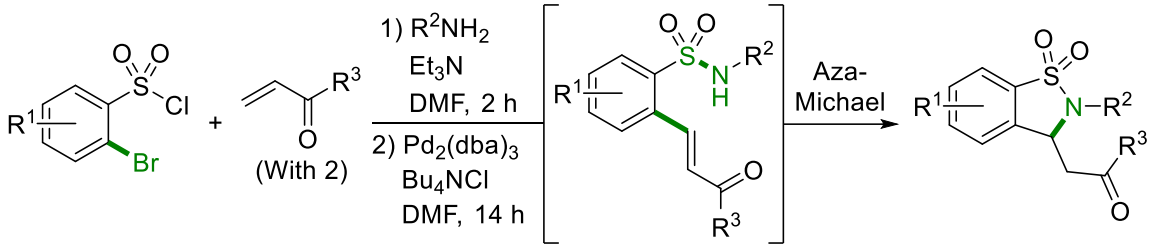

Scheme 10. One-pot three component domino Heck-aza-Michael pathway to benzo[*d*]sultams.

Several later publications disclosed *N*-acylsulfonamide directed tandem C-H olefination-Michael cyclization reactions catalyzed by $[RhCp^*Cl_2]_2$ (**Scheme 9, A**).[94–96] Unfortunately, double olefination occurred for the majority of substrates without *ortho*-substituents in the C-H olefination processes and a stoichiometric oxidant was required. In 2020, Liu's group developed a more efficient ruthenium (II) catalyzed tandem C-H olefination-cyclization process with *N*-acylsulfonamides for selective mono-alkenylation with O_2 as the oxidant (**Scheme 9**, **B**).[97]

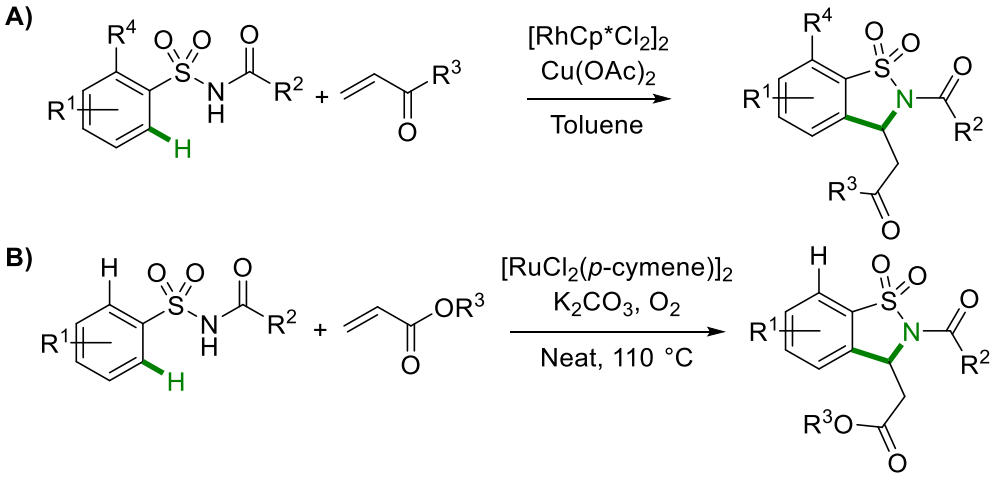

Figure 9. Catalytic tandem *ortho*-C-H olefination-cyclization reactions forming benzosultams.

Douglas et al. disclosed another sultam synthesis featuring an olefin insertion step in 2018.[98] A palladium catalyzed intramolecular aminocyanation reaction of *N*-sulfonylcyanamides allowed for the formation of 3,3-disubtituted benzo[*d*]sultams. The mechanism featured Lewis-acid promoted oxidative addition of an N-CN bond and C-CN bond forming reductive elimination (**Scheme 11**).

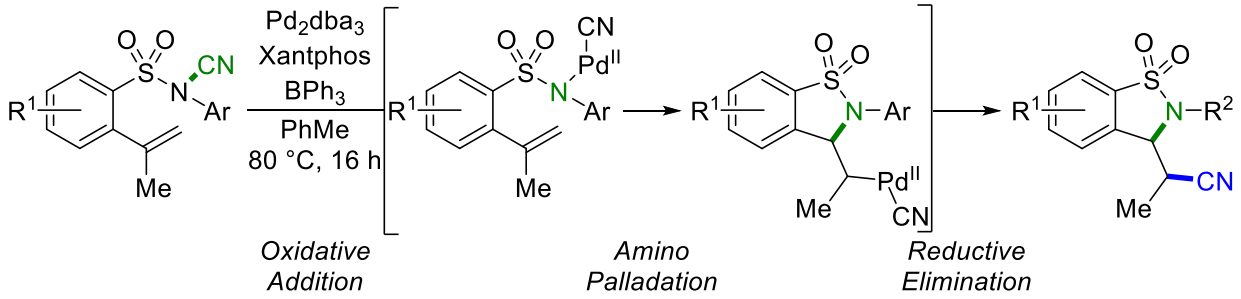

Scheme 11. Benzo[*d*]sultam synthesis through intramolecular aminocyanation of alkenes.

Aside from C-H olefination, other transition metal catalyzed C-H activation processes can be used to synthesize benzosultams. Fagnou's group published a synthetic route toward benzo[*d*]sultams using palladium catalyzed C(sp^3)-H bond activation α- to the nitrogen atoms in 2-bromo-*N*-methylbenzenesulfonamides, thus allowing for intramolecular alkane arylation (**Scheme 12**).[99]

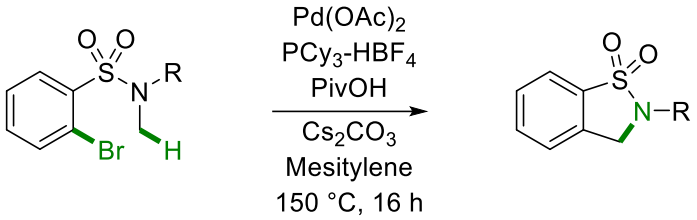

Scheme 12. Intramolecular alkane arylation via activation of α-sulfonamido C(sp^3)-H bonds.

Laha's group described a synthesis of heterobiarylsultams through palladium-catalyzed oxidative C-C coupling of *N*-arylsulfonyl indoles and *N*-arylsulfonyl pyrroles (**Scheme 13**).[100] Cesium pivalate and pivalic acid likely enabled CMD-based C-H activation, and silver acetate acted as a mild oxidant. This represented the first biaryl coupling involving a sulfonamide moiety.

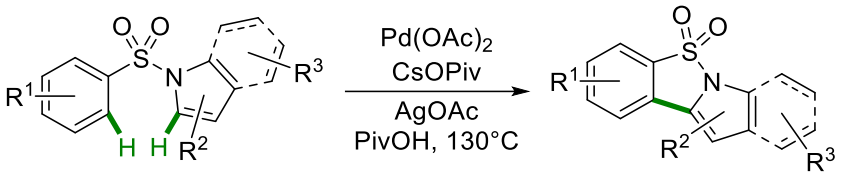

Scheme 13. Biarylsultam synthesis through palladium-catalyzed oxidative C-C coupling.

Yang and Xu published a method for *N*-arylbenzo[*c*]sultam synthesis via intramolecular aromatic C-H insertion with a rhodium carbenoid, the first record of diazosulfonamides as synthetic precursors.[101] Symmetrical *N*,*N*-diaryl diazosulfonamides reacted efficiently but unsymmetrical precursors gave only slight selectivity for the electron rich aromatic ring (**Figure 10, A**). Alas, conditions for the intramolecular aliphatic C-H insertion of *N*,*N*-dialkyl diazosulfonamides could not be developed.[102] Changing the catalyst to $Cu(acac)_2$ and altering the diazo transfer reagents to contain ketone diazo-adjacent groups rather than carboxylates, however, allowed for the aromatic C-H insertion of *N*-alkyl-*N*-aryl diazosulfonamides, albeit in low yield (**Figure 10, B**).[102]

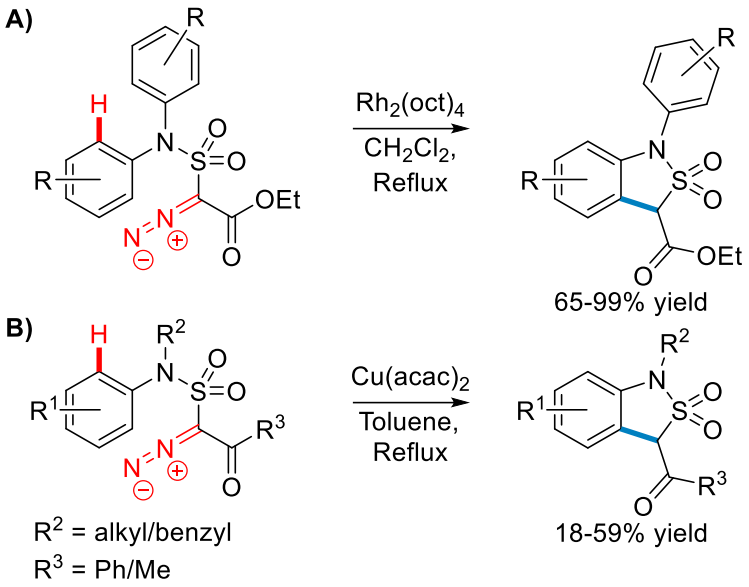

Figure 10. Benzo[*c*]sultam synthesis by C-H insertion with a rhodium carbenoid.

1.4 C-H Amination

The construction of nitrogen-carbon bonds has traditionally relied on classical reactions such as nucleophilic substitution, reductive amination, and rearrangement of carboxylic acid derivatives.[103] The modern application of transition metal catalysis has evolved robust amination methods including cross coupling, allylic amination and hydroamination (**Figure 11.**).[103] While these methods are reliable, they generally require starting materials that are pre-functionalized at the desired position to allow nitrogen incorporation. This generates stoichiometric waste and adds steps to synthetic processes, increasing environmental impact and operating costs.[104–106]

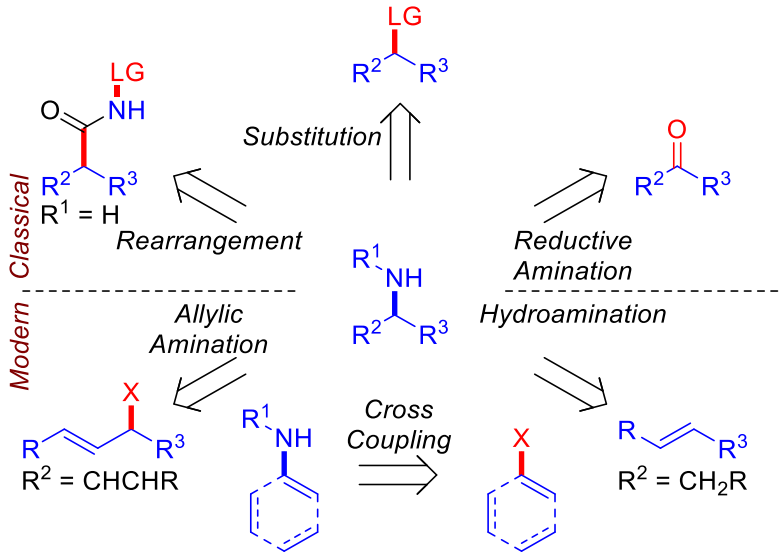

Figure 11. Classical and modern methods toward the formation of amines.

The direct amination of C-H bonds avoids manipulation of existing functional groups and can circumvent disadvantages of common amination reactions.[104–106] Alas, C-H functionalization is a difficult objective; C-H bonds are relatively strong (C{sp^3}-H ≈ 100 kcal/mol),[107] and are ubiquitous in organic molecules, raising regioselectivity and chemoselectivity issues.[108] Despite the obstacles, C-H amination methodology has seen significant progress and continues to develop.

Three main strategies have been adopted to enable C-H amination (**Figure 12**).[103,106] The most common amination method is "C-H activation", where C-H bond cleavage leads to the formation of an organometallic intermediate through an inner sphere mechanism.[103,106] This method will not be described in detail here as it likely does not directly relate to the research undertaken. The other common C-H amination manifold employs nitrenes / nitrenoids as reactive intermediates to enable "C-H insertion", which proceeds through an outer sphere mechanism without organometallic intermediacy.[103,106] C-H amination is also possible with *N*-centered radical intermediates generated from appropriate precursors using radical initiator systems or by photoredox catalysis.[103,106,109–111] This method is less common but has been applied more frequently in recent years.

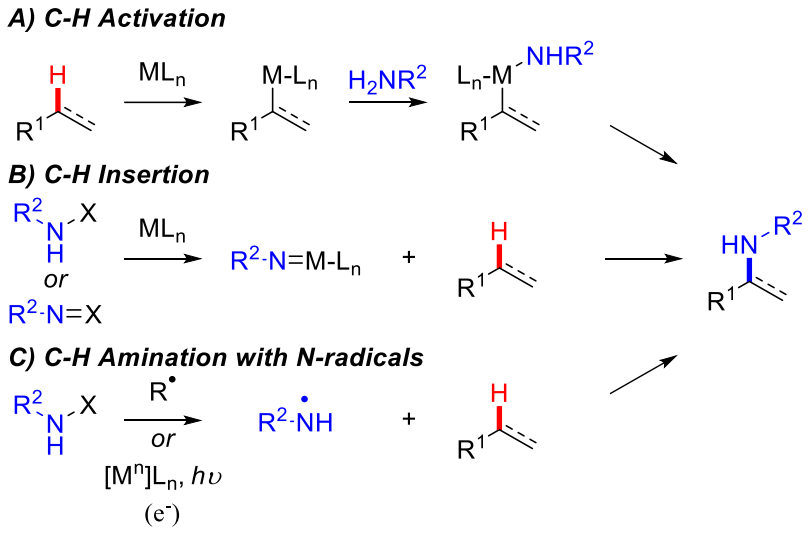

Figure 12. Three primary methods that enable C-H bond amination.

1.4.1 Nitrenes

Nitrenes are a highly reactive, short lived organic species that consist of an uncharged monovalent nitrogen atom with a sextet of electrons.[104,106,112–115] Nitrenes are the nitrogen analogues of carbenes; these species both have six valence electrons and thus exhibit reactivity consistent with their electron deficiency (**Figure 13**).[112–116]

Figure 13. Comparative structures of sub-valent species: carbenes, nitrenes and oxenes.

Free nitrenes can exist in either the singlet (S_0) or triplet (T_1) spin state.[106,112,114–116] Singlet nitrenes have an empty *p* orbital and a $\sigma(sp^2)$ orbital containing an electron pair, giving them ambiphilic character.[114–116] The reactivity of singlet nitrenes is dominated by electrophilicity as a result of their electron deficiency.[112,116–118] In contrast, triplet nitrenes have two unpaired electrons with the same spin, one located in each the *p* and $\sigma(sp^2)$ orbitals, and thus behave as electrophilic diradical species.[112,114,115] Since triplet nitrenes obey Hund's Rule and have no empty orbitals they are more stable and generally represent the nitrene ground state.[112,114,115,119] Free nitrenes are often generated in the singlet state, after which they undergo intersystem crossing to the triplet state (**Figure 14**).[112,114,115,120,121]

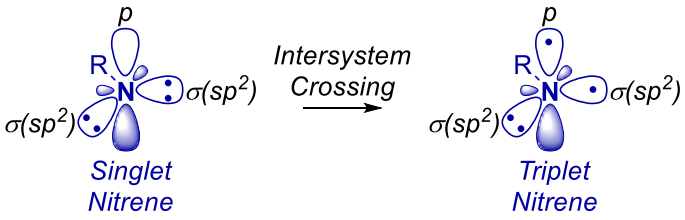

Figure 14. Singlet and triplet spin states for nitrenes.

Reactivity of Nitrenes

The ambiphilic nature of nitrenes leads to distinct reactivity. Singlet nitrenes tend to undergo concerted reactions and are particularly reactive toward insertion into C(sp^3)-H bonds and alkene aziridination (**Figure 15, A**).[112,114] They also undergo sp^2 aromatic C-H insertion, which proceeds by sequential aziridination-rearomatization. Azepines can be produced as side products through electrocyclic aziridine ring opening. (**Figure 15, B**).[112,122–124]

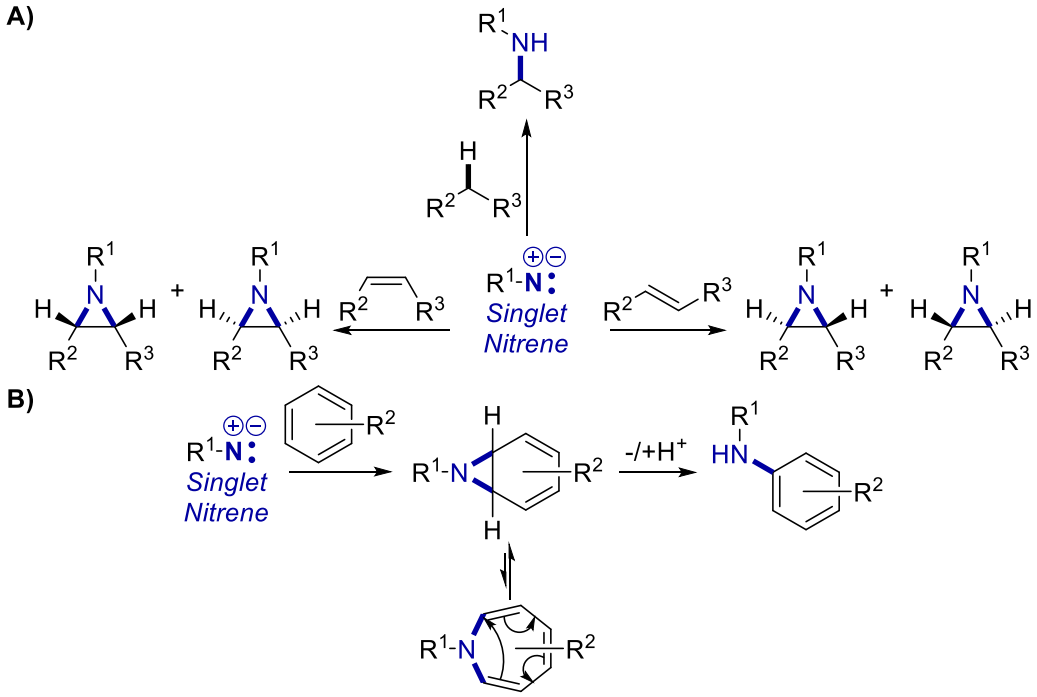

Figure 15. C-H insertion and aziridination reactivity of singlet nitrenes.

Singlet nitrenes also undergo rearrangement reactions; the most well-known example is the photoinduced Curtius Rearrangement of acyl nitrenes generated from azides (**Figure 16, A**).[112,114,125,126] This reaction enables the formation of an isocyanate through the [1,2] migration of a carbon atom to the empty orbital of the nitrene. Some trisubstituted aliphatic nitrenes can undergo rearrangement to form imines, particularly those substituted with triarylmethanes, as shown in the 1,2-aryl rearrangement of a triarylmethyl azide (**Figure 16, B**).[112,114,115] Nitrene intermediates may

also be present in the related Stieglitz Rearrangement of triarylmethyl- *O*-acyl-hydroxylamines (**Figure 16, C**).[114–116] In contrast, arylnitrenes often rearrange to azirines, followed by a second rearrangement to the corresponding azacycloheptatetraenes. (**Figure 16, D**).[120,127,128]

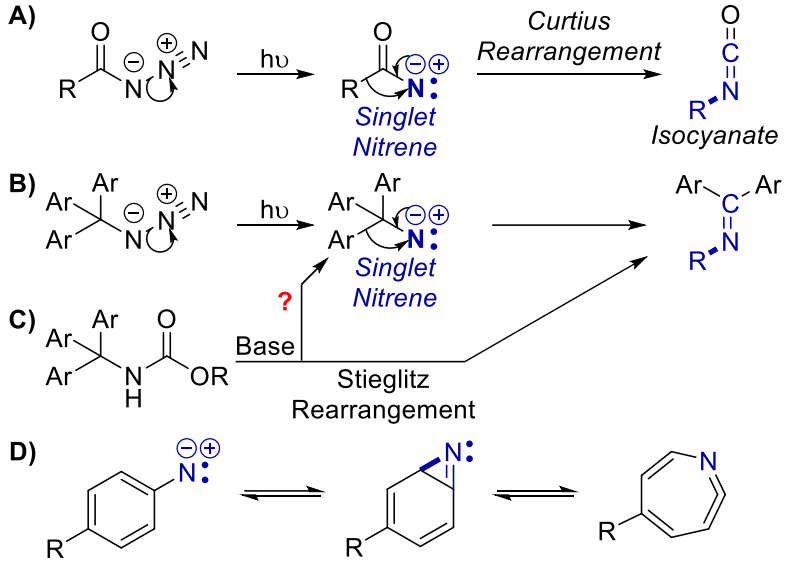

Figure 16. Rearrangement reactivity of singlet nitrenes.

The X-H insertion reactivity of singlet nitrenes is not limited to the reaction of C-H bonds, they can also undergo insertion with X-H bonds of various heteroatoms. Additionally, the nucleophilic attack of singlet nitrenes with Lewis bases forms ylides (**Figure 17**).[112,114,116]

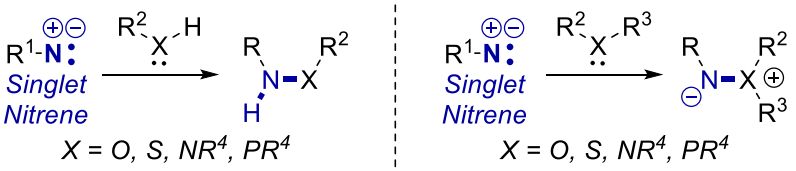

Figure 17. X-H insertion reactivity of singlet nitrenes and ylide formation from Lewis bases.

Nitrenes in the triplet state undergo alternate reactions. Triplet nitrenes undergo aziridination, but the mechanism is stepwise and lacks stereospecificity.[112,114–116] Addition of the alkene to the nitrene forms a carbon-centered radical that can rotate freely before rebound (**Figure 18, A**).[112,114,115] Triplet nitrenes tend to abstract hydrogen from solvent molecules (**Figure 18, B**), but

non-stereospecific C-H insertion is also possible. [123,124,129–132] They can also dimerize to form azo compounds (**Figure 18, C**).[114–116,120,131–133] Singlet nitrene reactions often compete with intersystem crossing to the triplet state, thus small quantities of triplet products are formed.[114,115,120,123,131,132,134]

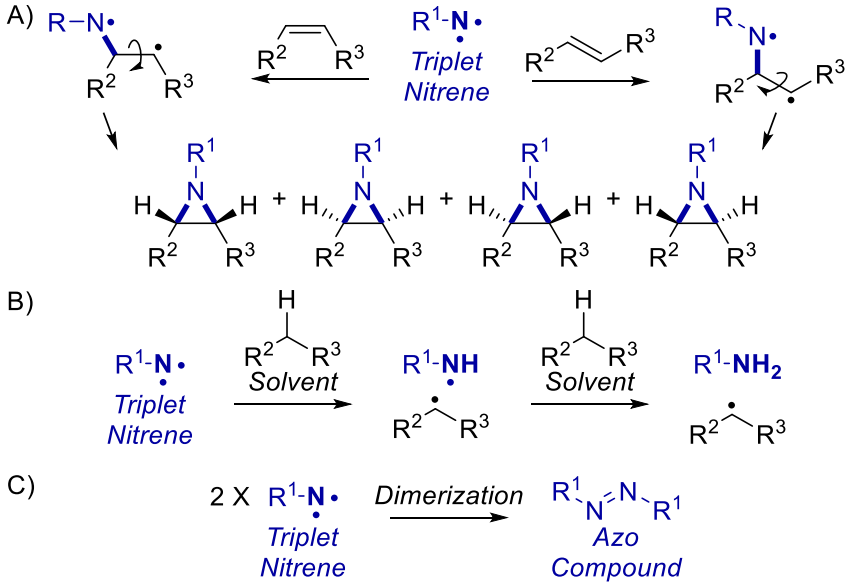

Figure 18. Typical reactivity of triplet nitrenes.

Due to the electrophilic nature of nitrenes, electron rich C-H bonds at activated positions tend to be more reactive toward insertion, and the reactivity generally correlates with the C-H bond strength.[108,117] The general reactivity trend for C-H bond insertion is as follows: allylic > α-ethereal > tertiary > benzylic > secondary > primary (**Figure 19**). If alkenes are present in the molecule, aziridination tends to compete with C-H insertion. Intramolecular C-H insertion leading to appropriate ring sizes is favoured over the formation of a strained bicycle through aziridination.[117]

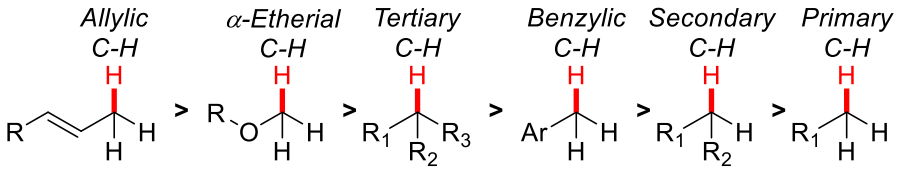

Figure 19. Typical selectivity trend for C-H insertion reactivity of free nitrenes.

Nitrenoids and Metal Nitrenes

The high reactivity, poor selectivity, and instability of free nitrenes limits their applicability, therefore most advances in synthetic chemistry involve reagents that enable controlled nitrene reactivity.[106,117] In general, the term "nitrenoid" is used to describe reagents with a trivalent nitrogen atom that exhibit properties of nitrenes and are capable of nitrogen atom transfer (**Figure 20, A**).[114] Specifically, nitrenoids are the nitrogen analogue of carbenoids (e.g. Simmons-Smith reagent, $IZnCH_2I$) where the reactive atom is bound to both a leaving group and a metal (**Figure 20, B**), and thus possesses both electrophilic and nucleophilic character.[116,135–137] Chloramine T is an example of a commercially available nitrenoid reagent (**Figure 20, C**).[116]

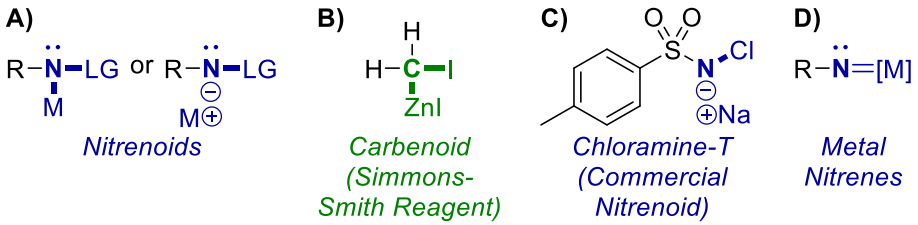

Figure 20. Reagents possessing the atom transfer capacity of free sub-valent species.

Transition metal stabilized nitrenes are commonly referred to as metal nitrenoids, but they do not possess a leaving group and instead contain a sub-valent nitrogen atom stabilized by a metal atom via π-backbonding (**Figure 20, D**).[138] Overall, metal nitrene species enable much more controlled reactivity than free nitrenes, and catalysts can be tuned to allow for regioselective and chemoselective C-H insertion and aziridination reactions.[106,117,139]

Reactivity of Nitrenoids and Metal-Nitrenes

Due to their ambiphilic character, nitrenoids react in a similar manner to singlet nitrenes.[116] They undergo electrophilic amination reactions through direct nucleophilic attack, similar to S_N2 substitution (**Figure 21, A**). The Hoffman and Lossen rearrangements occur through a concerted

mechanism from the corresponding nitrenoids generated by deprotonation of the parent *N*-bromoamides and hydroxamic acid derivatives, respectively (**Figure 21, B**).[116] Nitrenoids can react through "eliminative dimerization reactions" to form azobenzenes (**Figure 21, C**), but unlike free triplet nitrenes, these products are not accompanied by azepine or hydrogen abstraction products.[116]

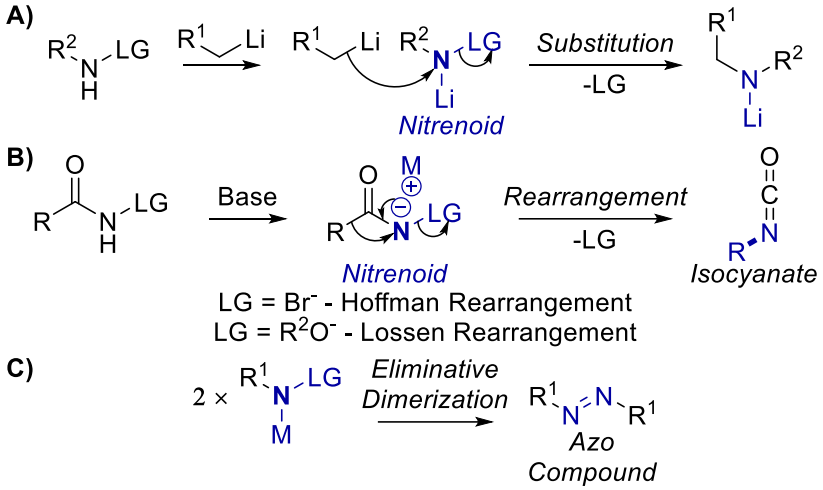

Figure 21. Typical reactivity observed with nitrenoids.

Metal stabilized nitrenes, like their free counterparts, undergo C-H insertion and aziridination reactions, but with more control and selectivity.[106,117,140] Thus, the majority of synthetic advances in nitrene chemistry have been achieved with metal-nitrenes. The nature of metal catalysts can be tuned to defy typical reactivity trends, enabling chemoselective insertion into strong C-H bonds in the presence of weaker bonds (secondary over tertiary), or to enable allylic C-H amination over aziridination.[117,138,141,142] Metal-nitrenes react in concerted or stepwise pathways depending on the properties of the metal catalyst.[106,117] Sometimes the selectivity trends for different C-H bonds are reversed with metal-nitrenes, particularly for intermolecular reactions; there is some evidence that the intermolecular C-H aminations involve triplet metal-nitrenes.[143]

Nitrene/Nitrenoid Precursors

Most nitrene and nitrenoid precursors have one thing in common: the presence of an electron withdrawing group bound to the nitrogen atom, which weakens the N-X bond (**Figure 22**). For nitrenoids, the other atom bound to nitrogen is most often another nitrogen atom, an oxygen atom, or a halogen.[106,116,117,141]

Free nitrenes can be generated upon thermolysis or photolysis of azides (**Figure 22, A, Column 1**)[112,114,115] and through heating of isocyanates (**Figure 22, A, Column 5**)[144–148], triggering the loss of nitrogen or carbon monoxide gas, respectively. Certain hydroxylamine derivatives generate free nitrenes under basic conditions, but the oxygen atom must have a very stable leaving group such as a sulfonate (**Figure 22, A, Column 2**).[106,114–116,149,150] Free nitrenes can also be generated to some degree from iminoiodinanes (**Figure 22, A, Column 4**)[114,134,140,151] and other haloamines (**Figure 22, A, Column 3**).[103,105,106,116,134,149]

Precursors for nitrenoids and free nitrenes are similar, but nitrenoids tend to have less stable leaving groups, or an additional electron withdrawing group at the nitrogen atom (**Figure 22, B**). Nitrenoids form by lithiation of hydroxylamines (**Figure 22, B, Column 2, Row I**), aside from *O*-sulfonyl derivatives, which often give free nitrenes (**Figure 22, A, Column 2**). In contrast, the lithiation of electron poor *N*-tosyloxycarbamates can form nitrenoids (**Figure 22, B, Column 2, Row II**).[116] *N*-chloroalkylamines and Chloramine T act as nitrenoids (**Figure 22, B, Column 3, Rows I-II**), yet some *N*-chloroanilines give free nitrene products (**Figure 22, A, Column 3**).[116]

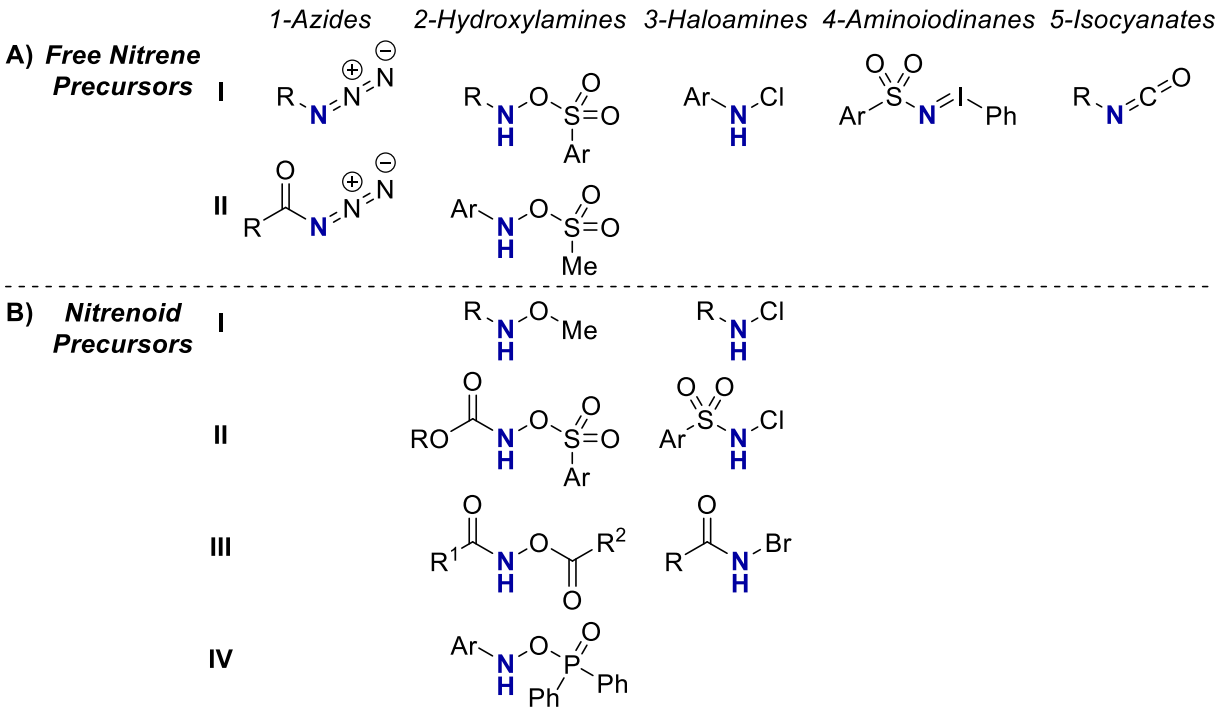

Figure 22. Precursors for free nitrenes, nitrenoids and metal-nitrenes.

Useful and robust nitrene transfer reactions are generally achieved using transition metal-nitrene complexes.[106,117,140] Precursors for metal-nitrenes are similar to those used to generate free nitrenes or are nitrenoids themselves; they possess weak, polarizable N-X bonds that are oxidative cleaved with a transition metal catalyst. The most common metal-nitrene precursors are azides, iminoiodinanes, hydroxylamines and chloroamines.[106,108,117,139] Iminoiodinanes can often be generated in situ with an amine and a hypervalent iodine (III) oxidant, such as iodobenzene diacetate or iodosobenzene, but the drawback is formation of stoichiometric iodobenzene byproducts.[152–154] Azides and chloroamines avoid this issue, as nitrogen gas and chloride salts are the only byproducts. With sulfonyloxy carbamates, the sulfonate byproduct is easily removed by acidic workup or filtration.[155–157]

Hydroxylamine Derivates – Nitrenes via Cleavage of N-O Bonds

Minimal progress has been made toward the development of controlled reactions featuring free nitrene intermediates with hydroxylamine-based precursors. Lwowski showed that salts of *N*-*p*-nitrobenzene-sulfonoxybenzenesulfonamide (Nitrenoid **I**) react at room temperature in alcohols to produce sulfamates **III**, and form *N*,*N*′-diphenylsulfamide **VI** by reaction in aniline (**Figure 23**).[158] As the authors described, *N*-sulfonyloxysulfonamides are likely susceptible to a Lossen-type rearrangement, allowing the transient formation of a reactive *N*-sulfonylimine intermediate (**II**) that is attacked by a nucleophile. Low yields of benzenesulfonamide (**IV**) from nitrene reduction and *N*-methoxybenzenesulfonamide (**V**) from nitrene O-H insertion show that free nitrene formation is minimal and that rearrangement may occur directly from the nitrenoid salt.

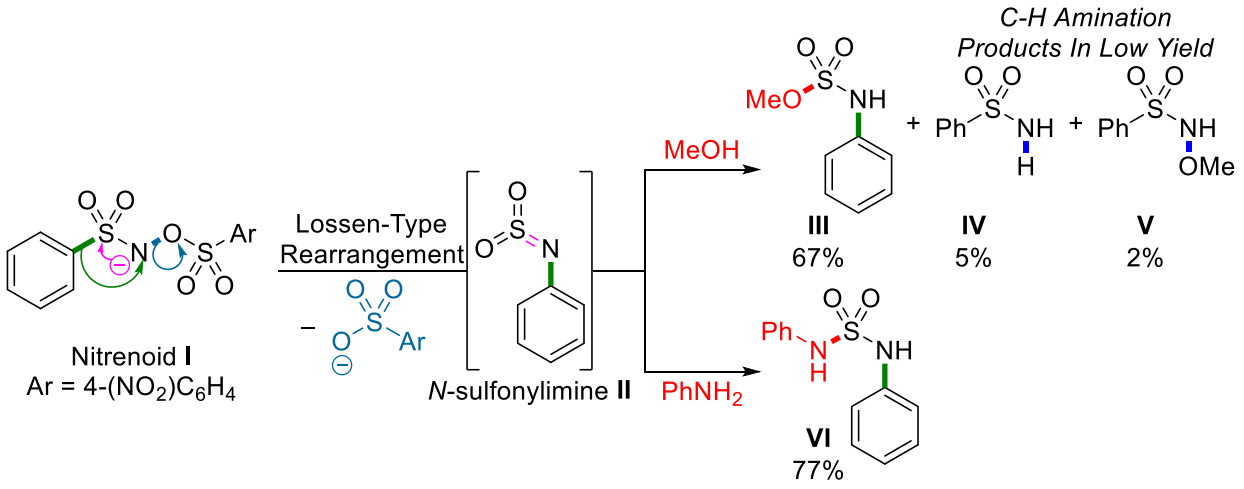

Figure 23. Lwowski's decomposition of *N*-*p*-nitrobenzenesulfonoxybenzenesulfonamide salts.

Pantaine's group capitalized on this side reactivity and disclosed methods for the synthesis of unsymmetrical sulfamides via base-induced Lossen-type rearrangement of *N*-arylsulfonyloxy benzenesulfonamides, followed by nucleophilic attack of the intermediate *N*-sulfonylimine by an amine (**Scheme 14**).[159,160] Interestingly, the conditions were similar to those used for thermal base-induced C-H amination reactivity in this research (**Chapter 2.3**); triethylamine was used as a base

to induce the rearrangement, and the reactions was conducted in CH_2Cl_2 at room temperature. Their conditions are differentiated by the ejection of a more stabilized sulfonate leaving group as opposed to a carboxylate. Indeed, their investigation of an acetate leaving group did not produce sulfamate product, and no information was given about the products obtained in this reaction.

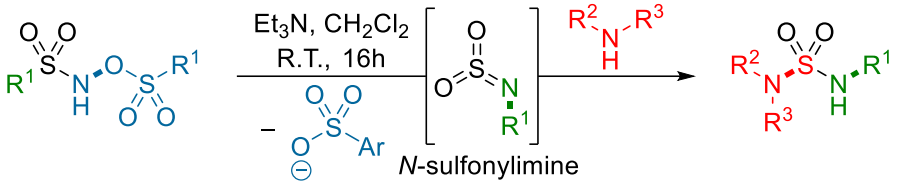

Scheme 14. Unsymmetrical sulfamides synthesis: Lossen-type rearrangement and reaction with amines.

It is worth noting that our group attempted to optimize a base-induced thermal reaction for the C-H amidation of *N*-acyloxyureas. Unfortunately, several substrates gave hydrazide derivatives derived from an Aza-Lossen rearrangement; a later paper exploited this side reactivity.[161]

Like the related reactions of azides and iminoiodinanes, chemoselective nitrogen atom transfer reactions with hydroxylamine-based nitrene precursors tend to rely on transition metal catalysis for stability and controlled reactivity. Hélène Lebel developed the first metal catalyzed nitrene-transfer reactions of *N*-oxycarbamates under rhodium[155–157,162–166] and copper[167–169] catalysis. Key players such as Glorius,[170,171] Chang,[172–175] Y. Li,[176,177] X. Li,[178,179] Jiao,[180–182] Falck,[183–186] Morandi,[187,188] Ueda,[189–191] Zhao,[192,193] and Meggers,[194–197] have further evolved this research. While a range hydroxylamine derived reagents are applied as metal-nitrene precursors (**Figure 24**), substrates with benzoate leaving groups have been used in palladium,[198] rhodium[199–203] and iron[204] catalyzed C-H amination reactions. Our group developed the C-H amidation of *N*-acyloxyureas via photoredox catalysis using $Ru(Bpy)_3$, and mechanistic studies suggested a triplet nitrene intermediate.[205–207] Meggers' lab[194–197] simultaneously developed ruthenium-catalyzed C-

H amination reactions with *N*-aroyloxy precursors using pyridyl-substituted NHC ligands. Dioxazolones[208–210] and anthranils[178,211] have also been adopted as *N*-oxy nitrene precursors.

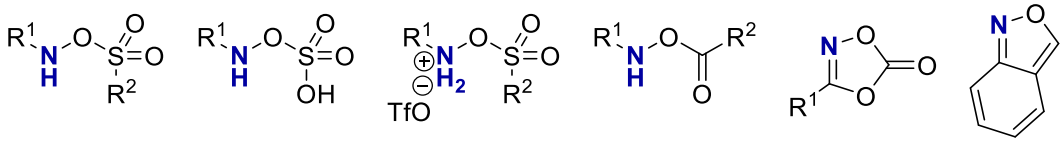

Figure 24. Common hydroxylamine derived metal-nitrene precursors.

Common Mechanisms for C-H Insertion Reactions of Metal-Nitrenes

Metal-nitrenes undergo two distinct mechanistic pathways for C-H amination reactions: either a concerted or stepwise C-H insertion is possible.[106,117,140] In either mechanism, the reaction initiates with nitrene formation though oxidative N-X bond cleavage by the catalyst. In the concerted mechanism, the new C-N and N-H bonds form simultaneously with the cleavage of the C-H bond, which is usually enabled through the alignment of a three-membered transition state. The aminated product is produced simultaneously with regeneration of the reduced catalyst (**Figure 25**).

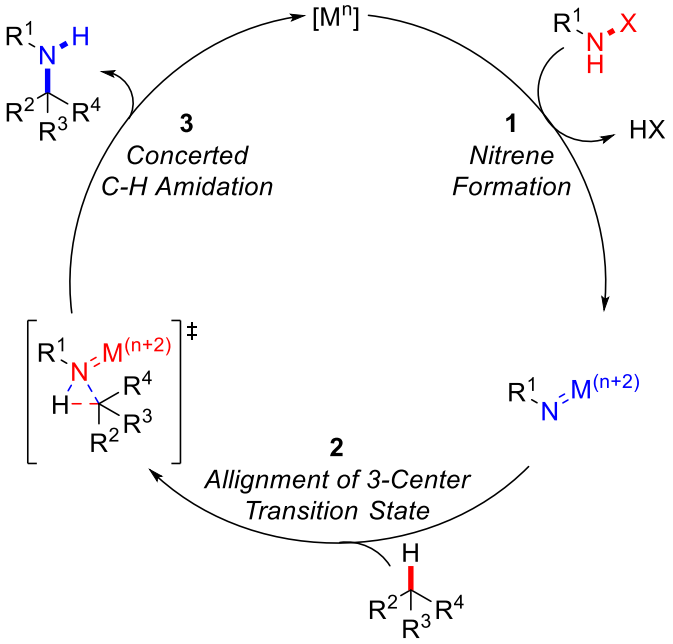

Figure 25. General mechanism for concerted C-H amination with metal-nitrenes.

Following the initial nitrene formation, the stepwise pathway instead proceeds through a preliminary hydrogen atom abstraction to form an N-H bond and a carbon centered radical. Subsequent radical rebound forms the C-N bond and regenerates the reduced catalyst (**Figure 26**).

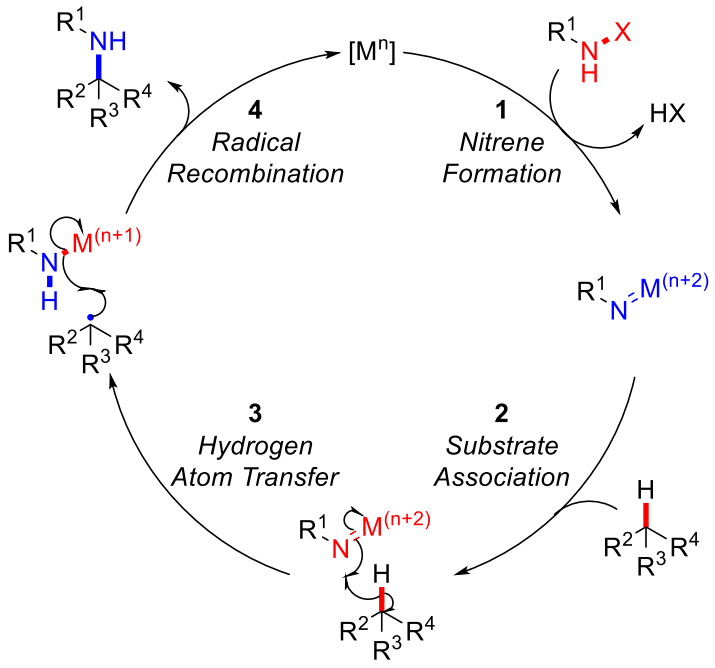

Figure 26. General mechanism for stepwise C-H amination with metal-nitrenes.

It is common for first row transition metals (copper, iron, cobalt, manganese) to follow the stepwise C-H amination pathway while evidence for both pathways has been found for heavier transition metals (rhodium, ruthenium, iridium).[105,106,117] Researchers use a combination of experiments to determine the likely pathway for catalyst systems including kinetic isotope effect studies, radical clock probes, computational studies, and the investigation of product stereochemistry.[106,108,117,140]

1.4.2 Nitrogen-Centered Radicals in C-H Amination

Formation of Nitrogen-Centered Radicals

Nitrogen-centered radicals represent another highly reactive class of nitrogen species used in C-H amination reactions. Like nitrenes, the generation of *N*-centered radicals commonly involves the cleavage of a weak N-X bond, necessitating the presence of a leaving group bound to the nitrogen atom.[106,109–111,212,213] In contrast to nitrene generation, *N*-radicals are formed by N-X bond homolytic cleavage rather than heterolytic cleavage (**Figure 27**). Several common aminating reagents are employed for the homolytic generation of *N*-radicals (**Figure 28**).[106,109,212]

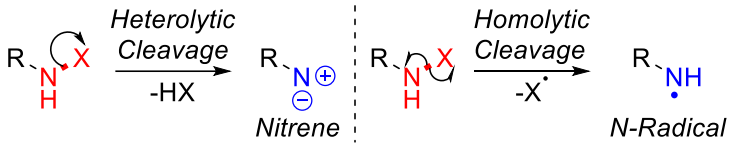

Figure 27. Heterolytic vs homolytic cleavage of N-X bonds.

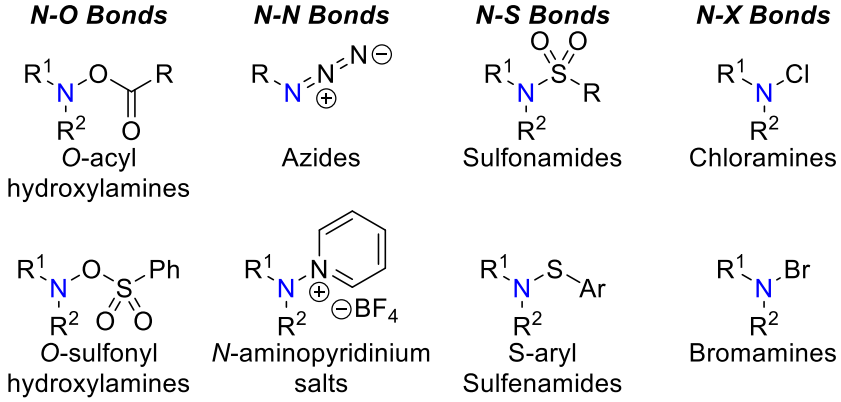

Figure 28. Common reagents for C-H amination reactions of Nitrogen-centered radicals.

Three methods are traditionally used for the generation of *N*-centered radicals from N-X precursors.[110,212] Similar to C-X bonds, N-X bonds can be reduced by a metal to generate *N*-radicals, either through an oxidative addition-type manifold, or through direct single electron transfer (**Figure 29, A**). The use of radical initiators coupled with hydrides from group 14,

particularly stannanes, is also common (**Figure 29, B**). Overall, the homolytic cleavage of N-X precursors by UV-irradiation is the simplest method for *N*-radical generation (**Figure 29, C**), but this method lacks selectivity and introduces decomposition reactions.[109]

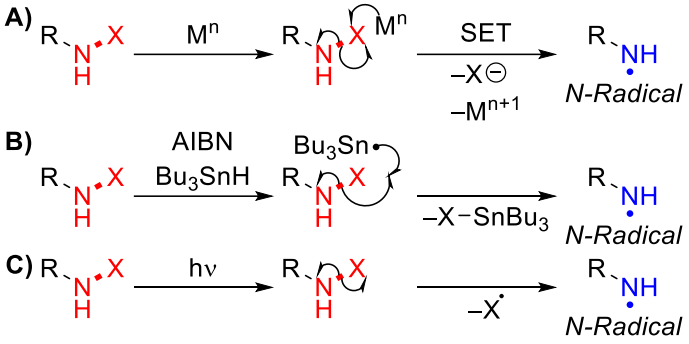

Figure 29. Traditional methods for *N*-radical generation.

More recently, photoredox catalysis has had a significant impact in the field of *N*-radical chemistry.[106,109–111,214] Starting from N-X precursors, the oxidative quench of an excited state photocatalyst enables single electron transfer and subsequent homolytic cleavage of the N-X bond (**Figure 30, A**). Photoredox catalysis has also enabled the development of novel methods for *N*-radical generation that bypass the need for N-X precursors. The presence of base in certain photoredox processes can allow for nitrogen atom deprotonation and subsequent anion oxidation by the excited state photocatalyst through a reductive quench (**Figure 30, B**).[109,110,215] Using a base, a reductive quench may be possible even if the N-H bond present in the amination substrate is weakly acidic. The base can associate with the substrate N-H via hydrogen bonding, allowing the excited state photocatalyst to oxidize the hydrogen-bond complex at the N-H σ-bond via proton-coupled electron transfer (PCET), to afford the reduced catalyst, a protonated base, and an *N*-radical (**Figure 30, C**).[106,109–111] With oxidizing catalysts, a final method for *N*-radical generation through a reductive quench involves the direct oxidation of amines to the corresponding aminium radical cation (**Figure 30, D**).[109,214]

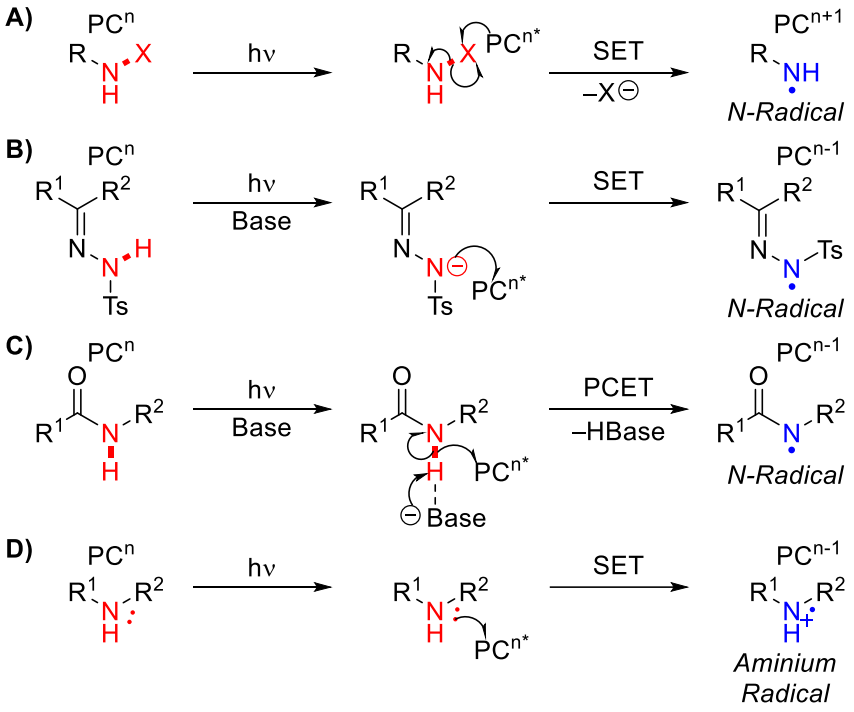

Figure 30. Common methods of *N*-radical generation by photoredox catalysis.

Mechanisms for C-H Amination Reactions of Nitrogen-Centered Radicals

The best starting point to discuss mechanisms of radical C-H amination is to consider the Hofmann−Löffler−Freytag (H-L-F) reaction, an early *N*-radical reaction containing steps observed in modern sp^3 radical C-H aminations.[110,111,216,217] Acidic treatment of a chloramine enables homolytic cleavage of the N-Cl bond in the protonated species under photolysis or thermolysis. The resulting aminium radical undergoes 1,5-hydrogen atom transfer to generate a carbon centered radical at the δ-position. Chloride abstraction from an equivalent of chloramine propagates the radical chain and basic treatment forms the pyrrolidine via an S_N2 reaction (**Scheme 15**).

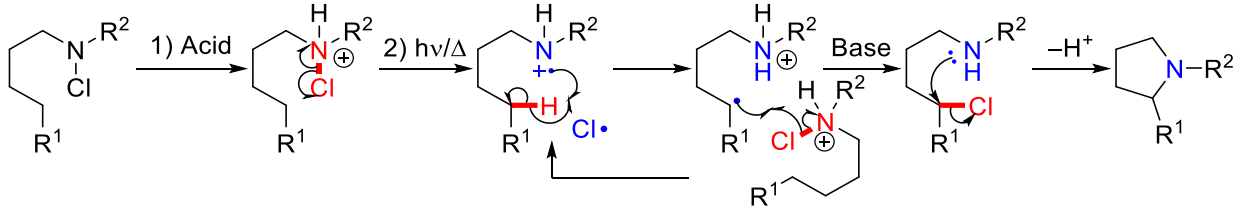

Scheme 15. Mechanism for classic Hofmann−Löffler−Freytag radical C-H amination reaction.

Aside from the stepwise reactivity of metal-nitrenes with triplet character, sp^3 C-H amination reactions with *N*-centered radicals are rare.[218–220] Most related reactions involve modified / interrupted H-L-F reactions,[213,221–225] but modern variants are often conducted using redox agents, [218–221,224] or through direct electrolysis in an electrolytic cell.[226,227] Thus, the reaction can be initiated by reductive cleavage of an N-X bond,[219,220] or oxidative aminium formation,[218] and the carbon radical generated through hydrogen atom transfer undergoes oxidation to the corresponding carbocation, which is then attacked by a nitrogen nucleophile (**Scheme 16**).

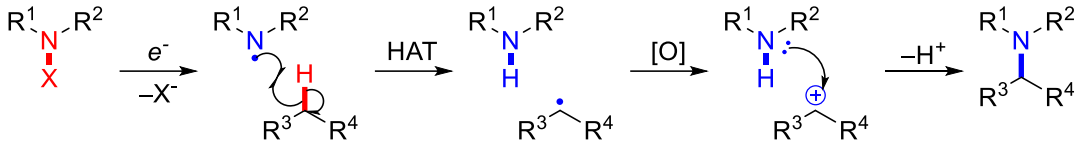

Scheme 16. General mechanism for sp^3 C-H amination by *N*-centered radicals.

Radical amination at sp^2 centers is much more common than sp^3 C-H amination.[106,109–111,214] The process is most often used for the amination of aromatic and heteroaromatic moieties. A radical electrophilic aromatic substitution forms the initial N-C bond, along with a resonance stabilized carbon-centered radical. Oxidation of the carbon radical forms an arenium ion, and aromaticity is restored through deprotonation, allowing for formation of the aminated arene (**Scheme 17**).

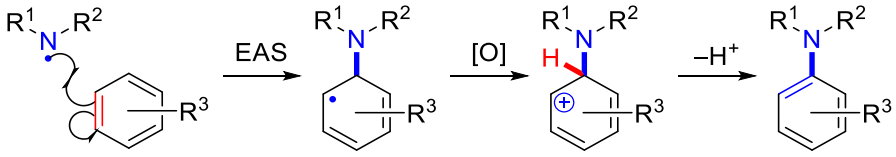

Scheme 17. Common mechanism for sp^2 C-H amination by *N*-centered radicals.

1.4.3 Transition Metal Catalyzed C-H Amination

As mentioned earlier, C-H amination can also be performed through transition-metal catalyzed C-H activation (**Figure 12, A**).[103,106] While important, this reactivity mode is less relevant to contextualize the results presented in this thesis, therefore this chapter will offer a brief overview.

One traditionally difficult objective associated with transition metal catalyzed amination reactions is the formation of a nitrogen-metal covalent bond.[228,229] While it is not the most common method, it is possible to introduce covalent nitrogen ligands in the same manner as for carbon, by oxidative addition of a weak N-X bond, commonly an N-O bond (**Figure 31**).[230–232]

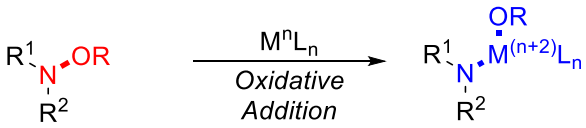

Figure 31. Oxidative addition as an activation mode to form nitrogen-metal covalent bonds.

In terms of the C-H activation step, many reactions involve a concerted-metalation-deprotonation (CMD) mechanism, where deprotonation and carbon-metal covalent bond formation occur concurrently through a six-membered transition state with the assistance of a carboxylate ligand. While its unlikely, because *N*-acyloxysulfonamide starting materials were used in this project, these mechanistic steps could theoretically be possible. For a generic catalytic cycle featuring covalent nitrogen ligand formation by N-O oxidative addition and C-H activation by concerted metalation deprotonation, see **Figure 32**.

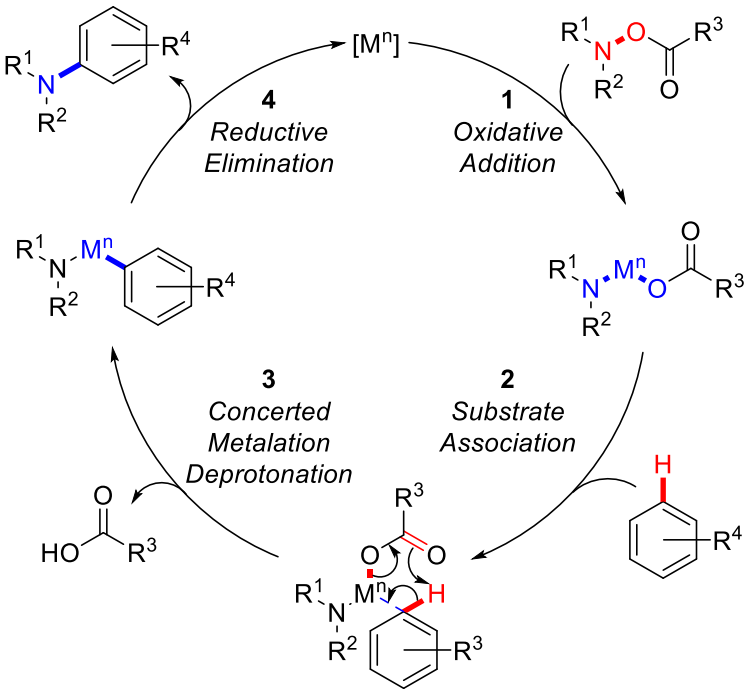

Figure 32. Catalytic cycle displaying N-O oxidative addition and CMD C-H activation.

1.4.4 C-H Amination in the Synthesis of γ-Sultams

γ-Benzosultam Synthesis Through Thermal C-H Amination

Rudolph Abramovitch was responsible for the earliest records of benzo[*d*]sultam synthesis through C-H amination. Three successive publications describe nitrene formation by the thermal decomposition of 2-methyl-benzenesulfonyl azides, thus enabling intramolecular C-H insertion into the *ortho*-methyl group.[129,132,133] A set of four sulfonyl azides were thermolyzed in *n*-dodecane to investigate this reactivity. The thermolysis of α-toluenesulfonyl azide generated no cyclized product, instead forming α-toluenesulfonamide and *N*-dodecyl α-toluenesulfonamide (**Figure 33, A**).[129] In contrast, the reaction of durenesulfonyl azide generated the benzo[*d*]sultam in low yield, along with durene and 2,3,4,6-tetramethylaniline (**Figure 33, B**).[129,132] The thermolysis of mesitylenesulfonyl azide again led to a low yield of the benzo[*d*]sultam, however, six byproducts were obtained, allowing the authors to gain insight about side-reactions (**Figure 33, C**).[132,133]

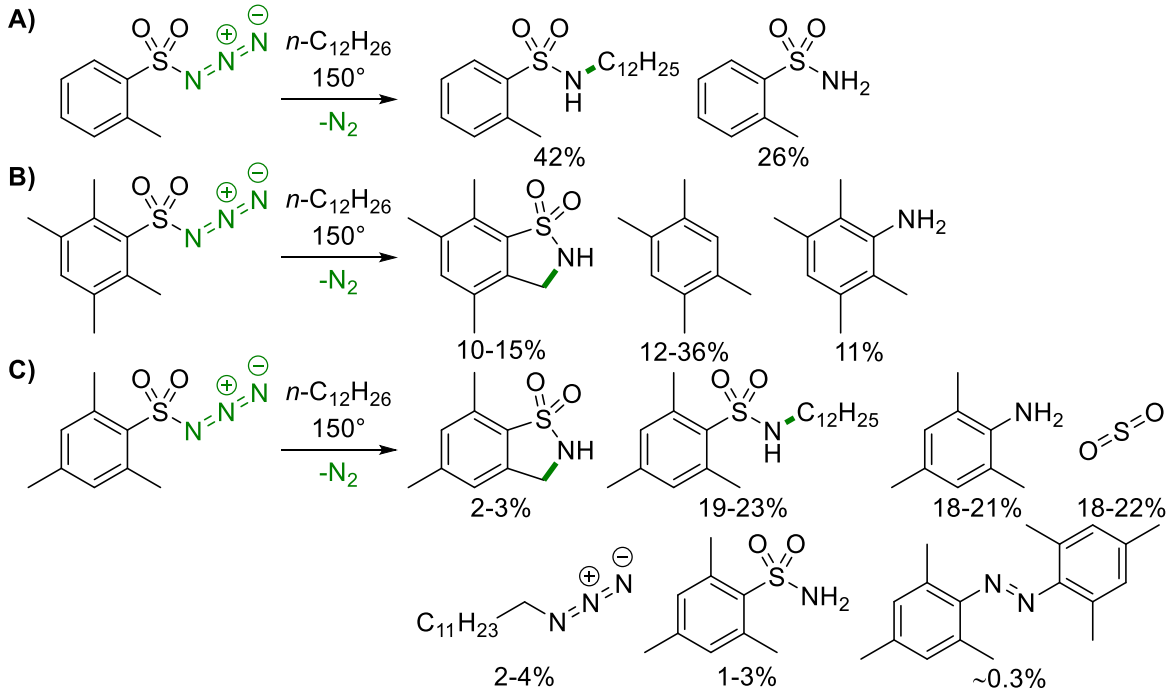

Figure 33. Nitrene formation/C-H insertion *via* thermal decomposition of sulfonyl azides

Similar to the reaction of α-toluenesulfonyl azide, the major product obtained for the mesitylene derivative was the *N*-dodecyl sulfonamide, likely derived from C-H insertion with the solvent (**Figure 33, A/C**). The authors reasoned that a steric "buttressing effect" imposed by the additional methyl group of the durene derivative both favoured a higher cyclization yield and decreased the rate of intermolecular C-H insertion compared to the other derivatives (**Figure 33, A-C**).[132] For α-toluenesulfonyl nitrene, steric interactions may have provoked C-S bond rotation, orienting the nitrene away from the *o*-methyl group, preventing cyclization (**Figure 33, A**).[129] They proposed that free sulfonamide formation was a result of nitrene intersystem crossing from the singlet to triplet state, followed by hydrogen abstraction from the solvent (**Figure 33, A/C**). The production of aniline derivatives in each case, along with SO_2 and the azomesitylene in **C** are evidence for a Curtius-type rearrangement. Dodecyl azide likely formed by a chain radical process involving the alkyl radical initially generated from solvent H-abstraction by the triplet nitrene (**Figure 33, C**).[132]

The final thermolysis reaction was conducted with 2,5-dicyclohexylbenzenesulfonyl azide. The intermolecular solvent insertion compound was again obtained as the major product, along with a mixture of intramolecular insertion products. Due to the presence of benzylic signals in the ^{1}H NMR spectrum, the authors concluded that the mixture consisted of trans and cis δ-sultams from amidation at the β-position of the cyclohexane ring, and no γ-sultam was formed (**Scheme 18**).[132]

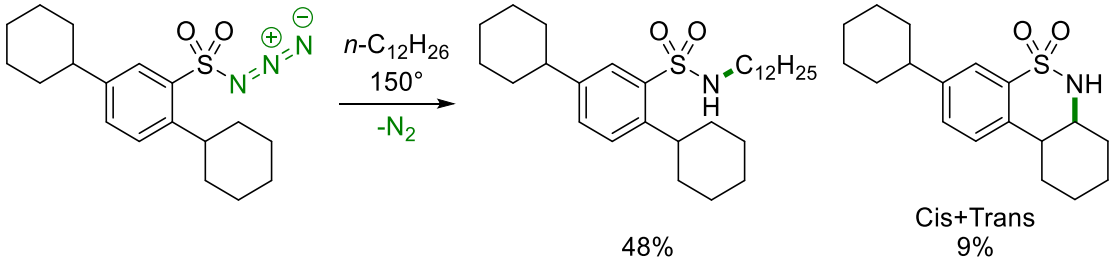

Scheme 18. Thermolysis of 2,5-dicyclohexylbenzenesulfonyl azide.

γ-Benzosultam Synthesis Through C-H Insertion with Imidoiodinanes / Hypervalent Iodine

Following Abramovitch, Breslow and Gellman published the earliest benzo[*d*]sultam synthesis through C-H insertion with an apparent nitrene intermediate.[151] Conversion of 2,5-diisopropyl-benzenesulfonamide to the corresponding iminoiodinane was achieved with phenyliodonium diacetate. Subsequent stirring in acetonitrile with the iron porphyrin catalyst, Fe^{III}(TPP)CI, or with dirhodium tetraacetate enabled intramolecular C-H insertion in 77% and 86% yield, respectively. The product also formed in 26% yield in dichloromethane in the absence of catalyst (**Scheme 19**).

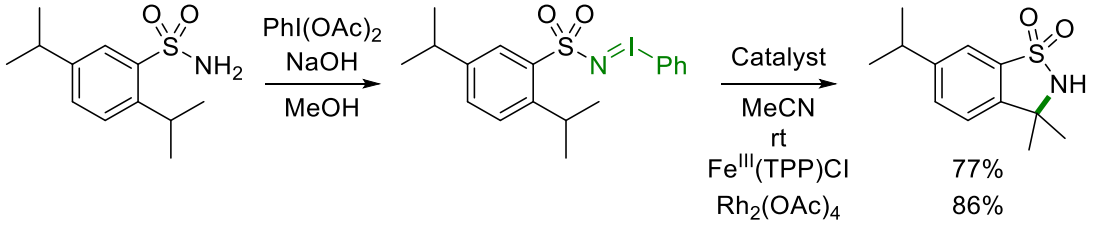

Scheme 19. Earliest example of benzo[*d*]sultam synthesis with an iminoiodinane.

Müller and co-workers later released three publications expanding this work (**Scheme 20**).[233–235] Dirhodium tetraacetate and various chiral carboxylatodirhodium(II) catalysts were found to catalyze the intramolecular secondary C-H amidation of [*N*-(arylsulfonyl)imino]phenyliodinanes to form γ-sultams in up to 65% yield and 20% ee (separate experiments). Evidence was also found for a concerted nitrene transfer mechanism using cyclopropane radical probes.

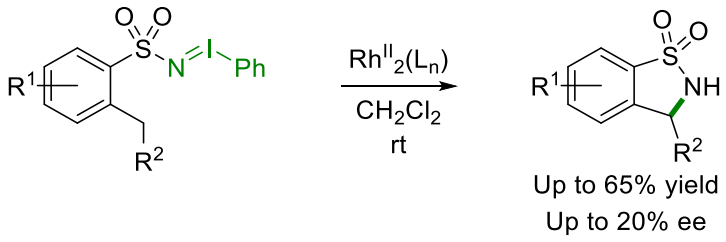

Scheme 20. Müller's initial work toward the synthesis of sultams from iminoiodinanes.

Schomaker's group recently published a synthesis of benzosultams from sulfonamides through intramolecular C-H insertion using silver catalysts and iodosobenzene.[236] In general, the catalysts

favoured δ-sultam formation by C-H amidation at the homobenzylic position, but the structure of both the catalyst and the substrate itself considerably influenced the reaction regioselectivity (**Scheme 21**). Using $[Ag(Py_5Me_2)OTf]_2$ as a catalyst, δ-sultam formation was consistent for sulfonamides with o*rtho*-propyl groups, but competitive insertion at more substituted benzylic carbons overrode catalyst regioselectivity for homobenzylic methyl and methylene groups, and γ-sultams formed from sulfonamides with o*rtho*-ethyl and (*sec*)butyl groups. When both the benzylic and homobenzylic positions were tertiary, selectivity was lost. It was also found that γ-sultams selectively formed when benzylic C-H amidation was sterically enforced by bulky substitution at the ε-carbon. When $[Ag(^tButpy)OTf]_2$ was instead employed as a catalyst, the poor regioselectivity imposed by the steric bulk was negated and homobenzylic amidation was again dominant.

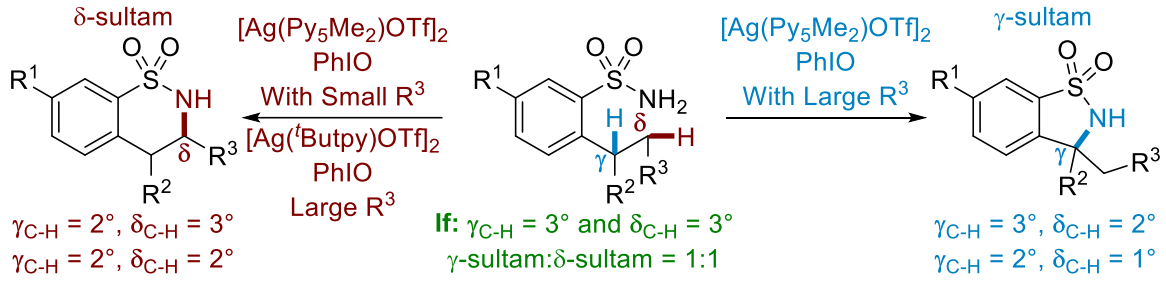

Scheme 21. Tunable regioselectivity for intramolecular silver catalyzed nitrene transfer.

Wen-Bo Liu developed a C-H amidation reaction with iron-nitrenoid intermediacy for sultam synthesis; in-situ catalyst generation was achieved using iron(II)perchlorate and an amino pyridine ligand (**Scheme 22**).[237] The reaction was limited for benzosultams, and more applicable to aliphatic sultam synthesis from 3-phenylpropane sulfonamides by benzylic C-H amidation, and from other precursors with activated γ-C-H bonds. Other aliphatic sulfonamides formed γ-sultams if the δ-carbon was primary, otherwise regioselectivity was poor and δ-sultam byproducts were observed.

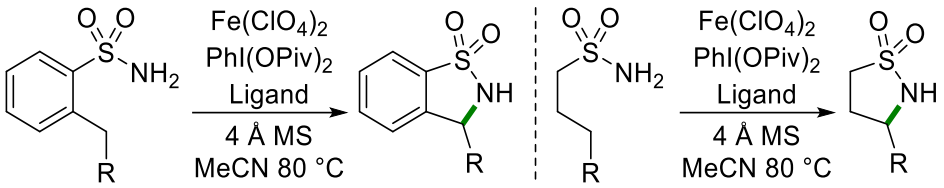

Scheme 22. Intramolecular C-H amidation by iron nitrenoids with in-situ generated catalyst.

Synthesis of γ-Benzosultams via Nitrene Aziridination Using Hypervalent Iodine Reagents

Aside from C-H insertion reactions, nitrene intermediates can also engage in intramolecular aziridination reactions when an olefin is present in the substrate, allowing for the synthesis of tricyclic benzo[*d*]sultams (**Scheme 23**). While the initial products of these reactions cannot be formed using the methodology developed in this thesis, or directly through C-H insertion reactions, the aziridine rings can be opened to afford formal C-H amination products.[238]

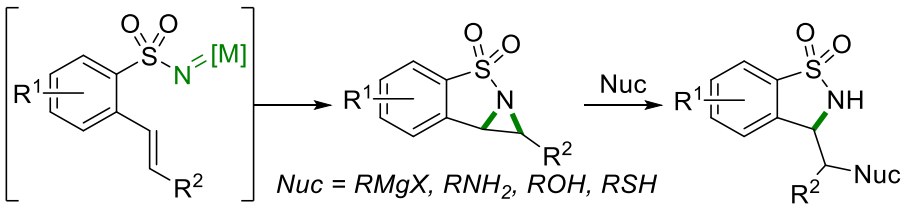

Scheme 23. Sultams as formal C-H insertion products from nitrene aziridination and ring opening.

Initially, metal catalysts derived from rhodium and copper enabled aziridination reactions with iminoiodinane precursors in low yield and with limited scope (**Figure 34, A**).[238,239] The tribromide salt, PTAB, was also found to catalyze aziridination with iminoiodinanes,[238] along with chloramine reagents generated in-situ from bleach (**Figure 34, B**).[240] Further advances in metal-catalyzed aziridination led to the development of one-pot protocols for the synthesis of sultams with various catalysts, including stereoselective variants (**Figure 34, C**).[241–245]

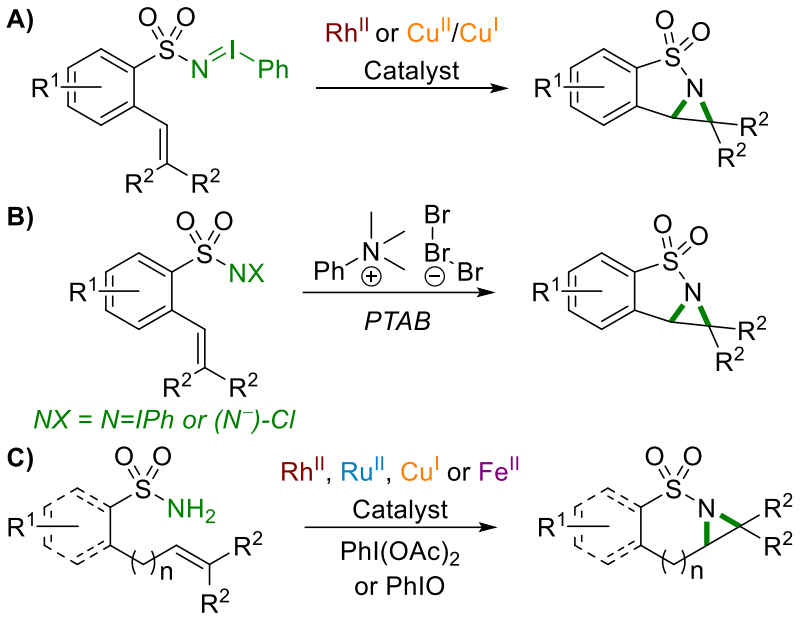

Figure 34. Progression of research into sultam synthesis via nitrene aziridination.

γ-Benzosultam Synthesis from Haloamines

The sole publication involving benzo[*d*]sultam synthesis from a chloramine derivative describes the generation of amidyl radicals from *N*-chlorosulfonamides under visible-light using an iridium photocatalyst for the intramolecular amidation of C(sp^3)-H bonds (**Scheme 24**).[221] A H-L-F-based mechanism (**Scheme 15**) is initiated by SET from the excited state photocatalyst. Sulfonamide deprotonation by sodium hydroxide allows cyclization. While the process involves a substitution reaction, it constitutes a formal C-H activation. A single tricyclic sultam has also been synthesized through a similar iodine-catalyzed H-L-F reaction,[222] and by a related anodic C-H amination.[227]

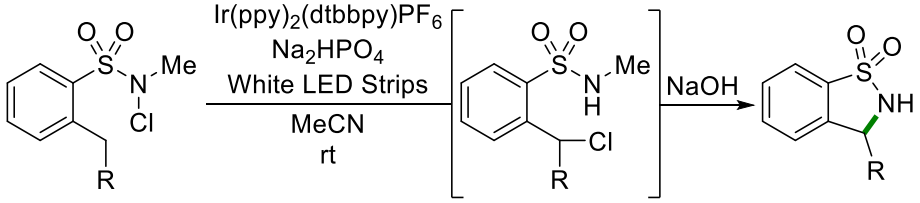

Scheme 24. Visible-light-promoted intramolecular C(sp^3)-H amidation of chloramines.

Catalytic Synthesis of γ-Sultams from Azides

Zhang designed a method for benzo[*d*]sultam synthesis in high yield using arylsulfonyl azides with a cobalt porphyrin catalyst, [Co(TPP)].[246] Intramolecular C-H amidation was possible with a range of *ortho*-alkyl-substituted azides, including those with reactive primary, secondary and tertiary C-H bonds (**Figure 35, A**). Exclusive γ-sultam formation was observed in the presence of multiple secondary C-H bonds for the benzylic C-H amidation of 2,5-dicyclohexylbenzenesulfonyl azide, but *o*-propyl and *o*-butyl substituted precursors gave mixtures of γ- and δ-sultams (**Figure 35, B**).

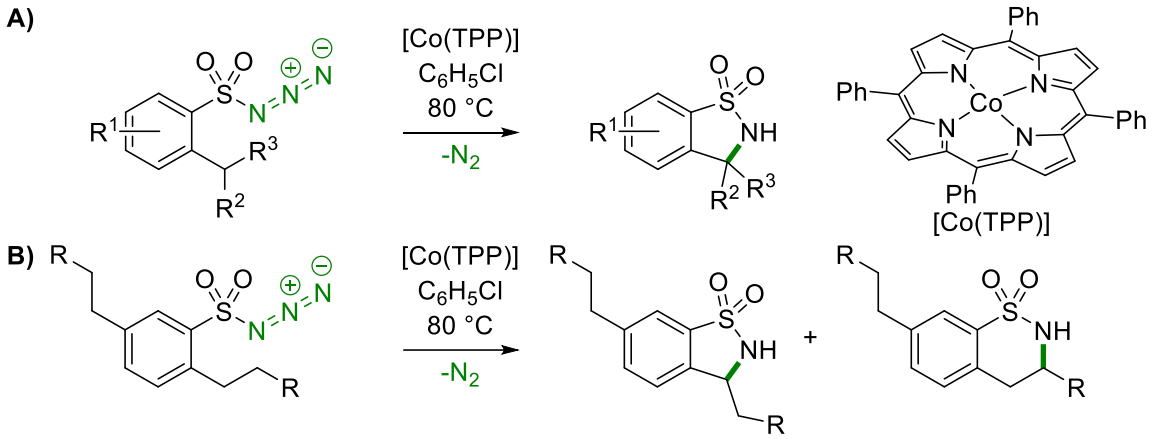

Figure 35. Intramolecular C-H amidation with sulfonyl azides catalyzed by cobalt-porphyrins.

Zhang's group later found that enantioselective cobalt catalyzed intramolecular C-H amidation of both arylsulfonyl and alkylsulfonyl azides was possible with D2-symmetric chiral amidoporphyrin ligands.[247] A range of *ortho*-substituted arylsulfonyl azides cyclized in an enantioselective manner using [Co(2,6-DiMeO-ZhuPhyrin)] as a catalyst and regioselective formation of γ-sultams was observed in the presence of multiple secondary C-H bonds (**Figure 36, A**). Using the ligand 2,6-DiMeO-Qing(4'-Me)Phyrin with alkylsulfonyl azides allowed for C-H amidation at benzylic and allylic positions with no aziridination byproducts (**Figure 36, B**).

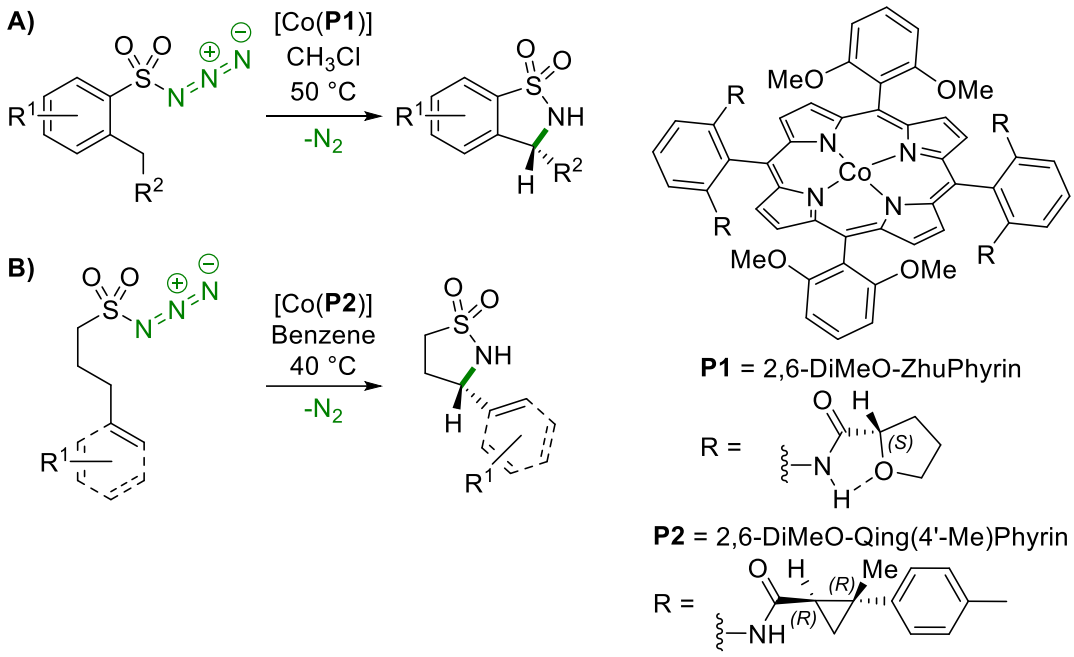

Figure 36. Enantioselective sultam synthesis by cobalt-porphyrin catalyzed C-H amidation.

Evidence for a stepwise metalloradical mechanism was found for the cobalt porphyrin-catalyzed processes; the intermediates undergo standard free-radical reactions while stabilized by cobalt. First, metalloradical activation of the azide generates an α-Co^{III}-aminyl radical **(1)**, which undergoes 1,5-hydrogen atom transfer to generate an ε-Co^{III}-alkyl radical **(2)**, followed by a 5-*exo*-*tet* radical cyclization to generate the product (**Figure 37**).

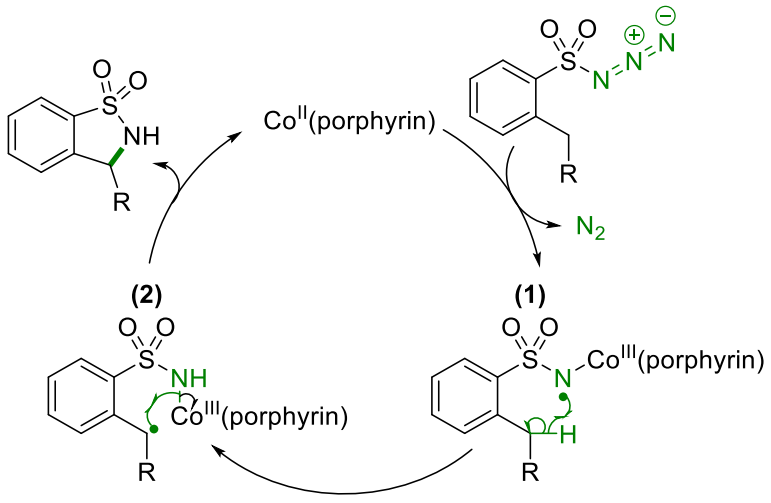

Figure 37. Mechanism for sultam synthesis by cobalt porphyrin catalyzed C-H amidation.

Katsuki published a reaction applying a chiral iridium-salen complex to achieve a similar enantioselective intramolecular C-H amidation with sulfonyl azides (**Figure 38**).[248] A fair scope was produced, but azides with multiple secondary C-H bonds again gave poor regioselectivity, forming δ-sultam side products, even from 2,5-dicyclohexylbenzenesulfonyl azide. The authors suggested that the selectivity of these reactions is dependent on the structure of both the substrate and catalyst and a certain conformation must be achieved for efficient orbital overlap of the C-H bond and the iridium-nitrenoid to achieve selectivity.

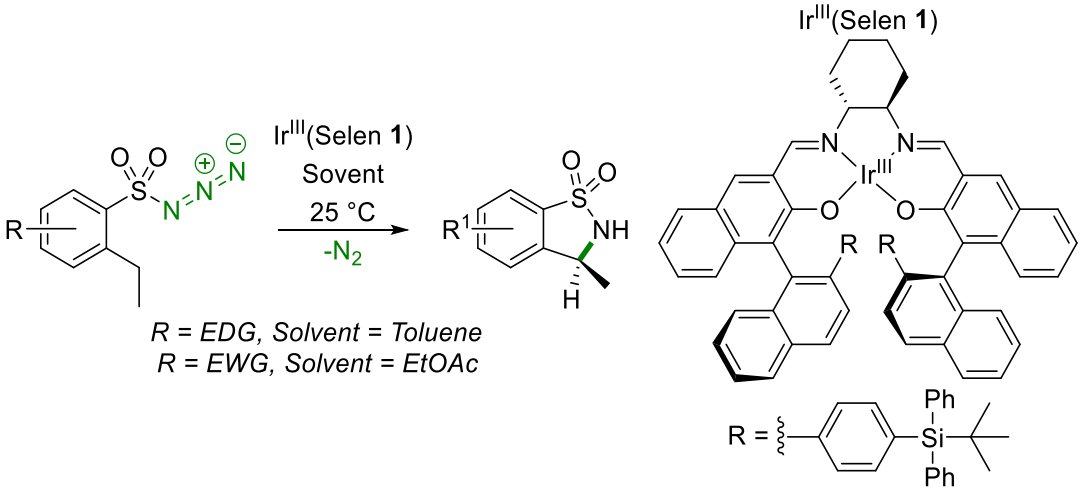

Figure 38. Enantioselective sultam synthesis by C-H amidation with Ir(III)-Salen complexes.

Enzymatic C-H Amination in the Synthesis of γ-Benzosultams

Cytochrome P450 enzymes have natural activity to catalyze oxygen transfer reactions through the activation of molecular oxygen.[249–251] Breslow harnessed this atom transfer capability using the cytochrome $P450_{LM3,4}$ variant from rabbit liver microsomes to catalyze the intramolecular C-H insertion of the iminoiodinane derived from 2,5-diisopropybenzenesulfonamide (**Scheme 25**).[252] While this was unprecedented, only 2.2 catalytic turnovers were possible, the reaction had poor atom economy and hydrolysis of the iron-imido complex introduced oxene transfer side reactions.

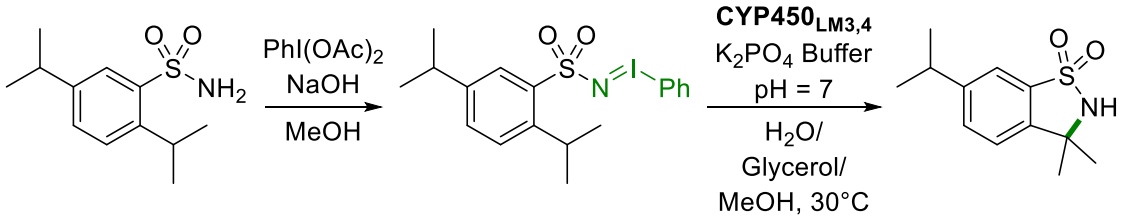

Scheme 25. First enzyme catalyzed intramolecular C-H amidation reaction by Breslow et al.

The main obstacle preventing enzyme engineering in recent years is the inherent difficulty screening the vast set of possible amino acid combinations for a given peptide length.[253,254] For this reason, modern research in biocatalysis has relied heavily on directed evolution, a process that creates novel enzymes by sequence modification through iterative cycles of artificial selection.[255] These mutants can display altered reactivity, increased selectivity and improved thermal stability.[255,256] The process of directed evolution consists of four main steps. First, a parent protein sequence is identified, often a mutant derived from a diverse enzyme family that displays the desired transformation as a side reaction.[255] Next, a library of enzymes is produced to contain a range of single and double mutations, particularly at residues with known involvement in structural elements, binding or reactivity.[255] This step makes use of the polymerase chain reaction and a host culture, such as *E. coli*, expressing the enzyme.[254] Third, high-throughput-screening is performed

to acquire mutants with improved properties.[255] The final step simply involves repeating the process, instead using the improved mutant enzyme from the previous generation as the mutagenesis template, rather than the parent enzyme. This process is repeated until the desired biocatalytic improvement, or a fair compromise, is met, which usually requires 5-10 cycles.[254,255]

Nearly thirty years after Breslow's discovery, Arnold's lab found that cytochrome P411 variants of the $CYP450_{BM3}$ enzyme, which contain a mutation at the 400th position from the axially coordinating cysteine residue to a serine, could catalyze intramolecular benzylic C-H amidation.[257] The mutant enzyme $CYP411_{BM3}$-CIS-T438S enabled enantioselective benzo[*d*]sultam formation on a preparative scale (50 mg) in vivo with *E. coli* cells (**Scheme 26**). Reactions run with 2,4,6-trimethyl- and 2,4,6-triisopropylbenzenesulfonyl azide formed product less efficiently (<40 TTN), despite typical trends in BDE, thus the steric confirmation of the active site plays a key role.

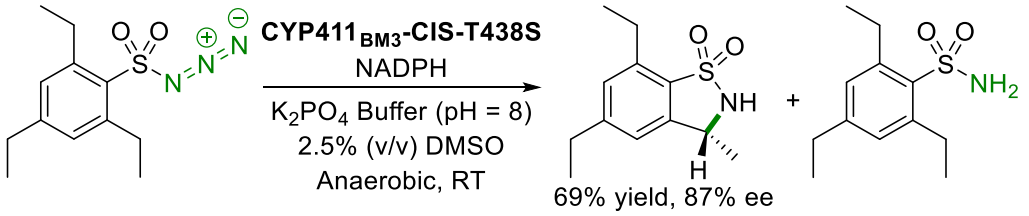

Scheme 26. First report of enzyme catalyzed intramolecular amidation of sulfonyl azides.

The following year, Fasan et al. found that cysteine ligated $CYP450_{BM3}$ enzymes themselves could catalyze benzylic C-H amidation.[258] The $CYP450_{BM3}$-FL#62 mutant enzyme formed benzo[*d*]sultams from 2,4,6-trimethyl-, triethyl- and triisopropyl- benzenesulfonylazides in 5, 47 and 388 TTN, respectively, with TTN inversely correlating to benzylic C-H BDE (**Scheme 27**, **A**). A small scope of sultams was generated, but TTN varied widely; substrates with bulky substituents gave higher TTN, corroborating that active site confirmation influences amination efficiency. Enantioselective reactions were also investigated with $CYP450_{BM3}$-193-3-T268A (**Scheme 27, B**).

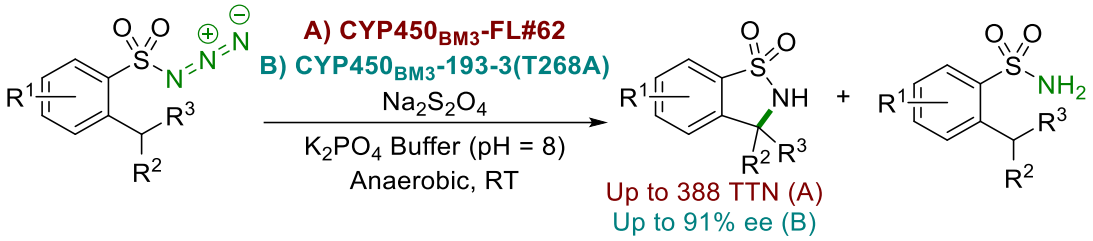

Scheme 27. Intramolecular amidation toward sultams catalyzed by cysteine ligated P450.

Other natural iron-based hemoproteins have also been found to catalyze C-H amidation with 2,4,6-triisopropylbenzene sulfonyl azide.[259] Sperm whale myoglobin (mb) and horse radish peroxidase, with axially coordinating histidine residues formed sultams with 181 and 311 TTN, respectively but efficiency with secondary and primary C-H bonds was comparatively low.[260–263] The Mb(H64V) mutant slightly increased turnover to 200 TTN. Myoglobin mutants with either Mn^{II} and Co^{II} co-factors also catalyzed C-H amidation in low turnover, 142 and 64 TTN, respectively.

Arnold's group engineered $CYP11_{BM3}$ enzymes that enabled regiodivergent γ- and δ-benzosultam synthesis (**Scheme 28**).[264] An I263F mutation in the $CYP411_{BM3}$-CIS-T438S from their previous study promoted homobenzylic amidation and $CYP411_{BM3}$-T268A-F87A formed γ-sultams.

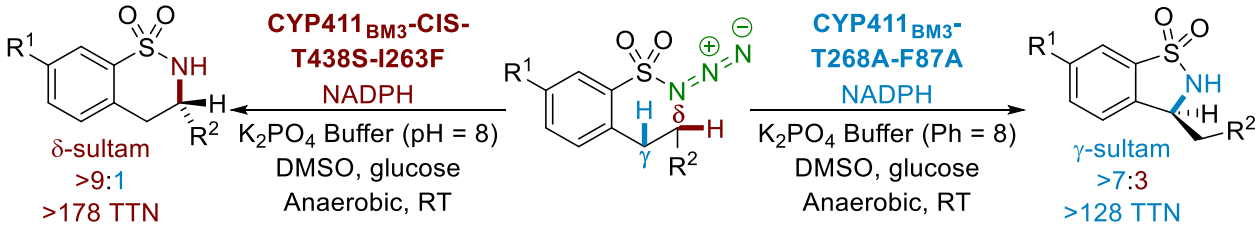

Scheme 28. Regiodivergent γ- and δ- benzosultam synthesis with mutant CYP411 enzymes.

Hartwig's group synthesized sultams using modified CYP450 enzymes with iridium-porphyrin co-factors.[265] Using several Ir(Me)-PIX-CYP119 enzyme variants, a small scope of sultams was synthesized with high yield though the C-H amidation of benzenesulfonyl azides with good turnover, enantioselectivity and chemoselectivity over reduction to the sulfonamide (**Scheme 29**).

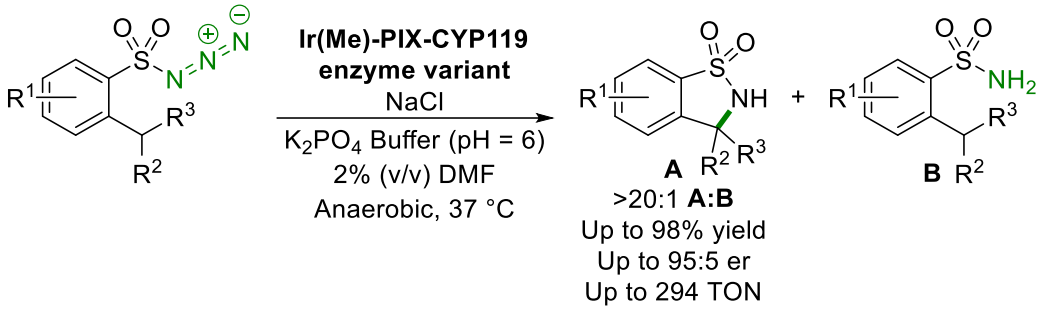

Scheme 29. C-H amidation by CYP119 enzymes with an Ir(Me)-PIX-porphyrin cofactor.

Arnold later designed the first C-H amination reactions catalyzed by non-heme iron enzymes (**Scheme 30**).[266] Mutant enzymes were derived from *Pseudomonas savastanoi* ethylene forming enzyme (*Ps*EFE), an *α*-ketoglutarate (*α*KG) dependent iron-dioxygenase enzyme that naturally catalyzes oxene transfer reactions. Swapping the natural iron coordinating ligand from *α*KG to *N*-oxalyl glycine enabled intramolecular amidation of 2-ethylbenzensulfonyl azide with the mutant *Ps*EFE VMM when expressed in whole *E coli* cells or in cell lysate.

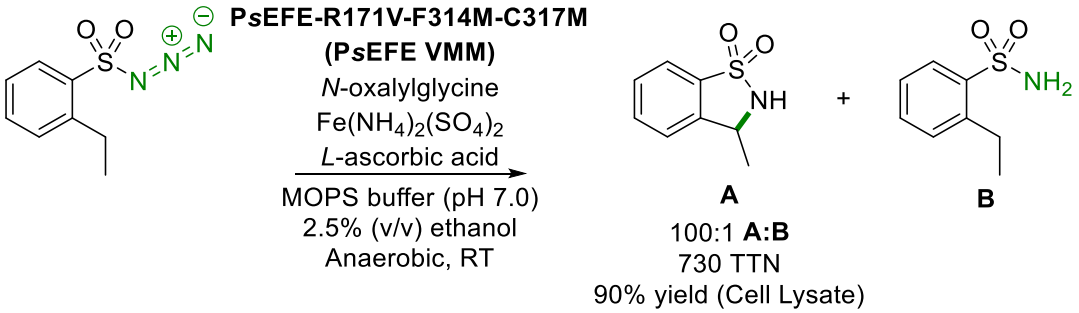

Scheme 30. C-H amidation with mutant *Pseudomonas savastanoi* ethylene forming enzymes.

Experimental evidence and allusion to natural CYP450 oxidation activity has led to a mechanistic proposal for enzymatic C-H amidation reactions (**Figure 39**).[258,259,264,267] The enzyme active state consists of the ferrous (Fe^{II}) heme center **(2)**, which is formed by reduction of the ferric (Fe^{III}) state **(1)** with the internal reductant (NADPH or $Na_2S_2O_4$). Sulfonyl azide coordination forms an Fe^{II}-azido complex **(3)**, which is oxidized to the Fe^{IV}-imido nitrene species **(4)** with concomitant loss

of nitrogen gas. The subsequent C-H insertion proceeds through a stepwise hydrogen abstraction/ radical rebound pathway, forming a C-N bond from the intermediate carbon centered radical **(5)**.

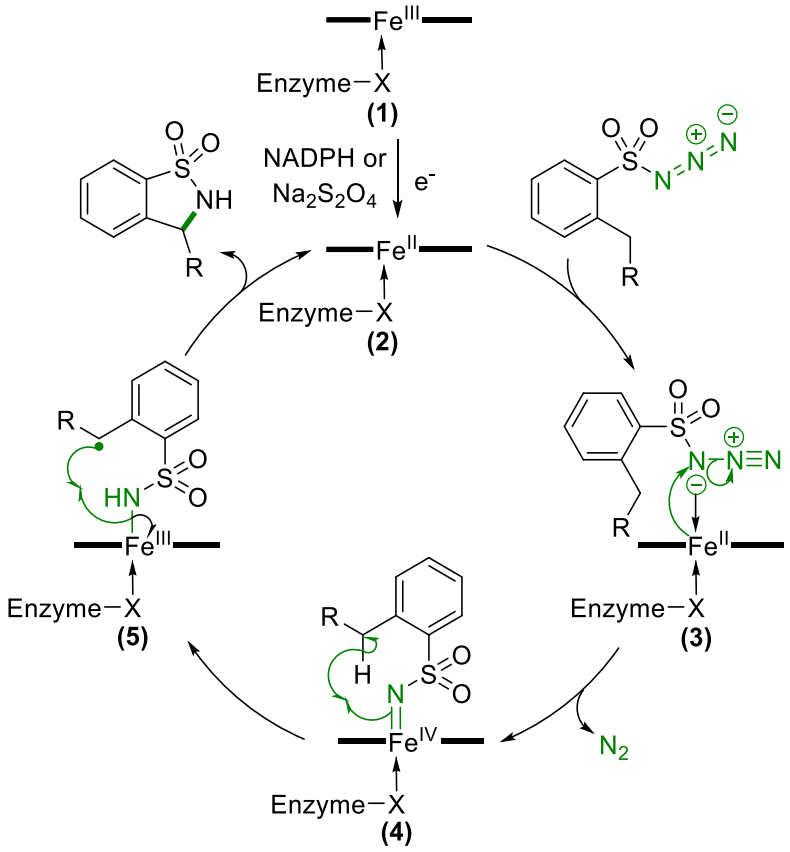

Figure 39. Catalytic cycle for sultam synthesis via C-H amidation with iron-heme enzymes.

Two competitive pathways can explain reduction to the sulfonamide byproduct; the Fe^{IV}-imido complex may be directly reduced or could be first hydrolyzed to the Fe^{IV}-oxo species, followed by reduction.[258] Kinetic isotope effect (KIE) studies have shown evidence for a rate limiting C-H insertion with both the CYP411 and myoglobin catalysts.[259,264,267] Quantum mechanical and molecular mechanical studies instead suggest that the rate is determined by the higher energy radical rebound transition state, thus dictating both regioselectivity and stereoselectivity.[267]

Further research into benzo[*d*]sultam synthesis with modified enzymes was conducted in 2019-2020 by Fasan's Group, earning them two publications.[268,269]

1.5 Project Initiation and Research Objectives

Prior to the initiation of research compiled in this Master's thesis, two PhD students from the Beauchemin group, Dr. Ryan Ivanovich and Dr. Dilan Polat, developed a new methodology for the intramolecular C-H amidation of hydroxamic acid derivatives via photoredox catalysis.[205–207] Irradiation of *N*-acyloxyureas with blue light in the presence of $Ru(Bpy)_3(PF_6)_2$ and triethylamine enabled the formation of imidazolidinones (5-membered cyclic ureas) through intramolecular aliphatic tertiary and secondary $C(sp^3)$-H amidation, aromatic $C(sp^2)$-H amidation and alkene aziridination (**Scheme 31**).[205–207] Lactams could also be synthesized from *N*-acyloxyamides by switching to a phosphate base, tetrabutylammonium dibutylphosphate ($[Bu_4N][OP(O)(OBu)_2]$).

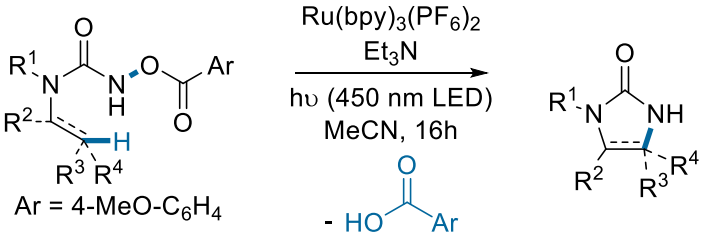

Scheme 31. Intramolecular C-H amidation of *N*-acyloxyureas via photoredox catalysis.

Mechanistic studies implied a unique C-H insertion reaction pathway with an intermediate triplet-state nitrene. Evidence suggested that the reaction involved a PCET[205–207,270–275] pathway, a process where an acid-base hydrogen-bond complex undergoes proton transfer with simultaneous single electron oxidation from the X-H σ-bond by the photocatalyst (**Scheme 32**). The process could enable the formation of amidyl radical (**D**) through oxidation of the *N*-acyloxyurea-base hydrogen-bond complex (**C**) by the excited state ruthenium catalyst (**B**). Single electron transfer from the reduced Ru(I) catalyst (**E**) to the carbon atom of the acyloxy carbonyl group regenerates the active catalyst (**A**) along with the corresponding triplet nitrene (**F**) by N-O bond cleavage.

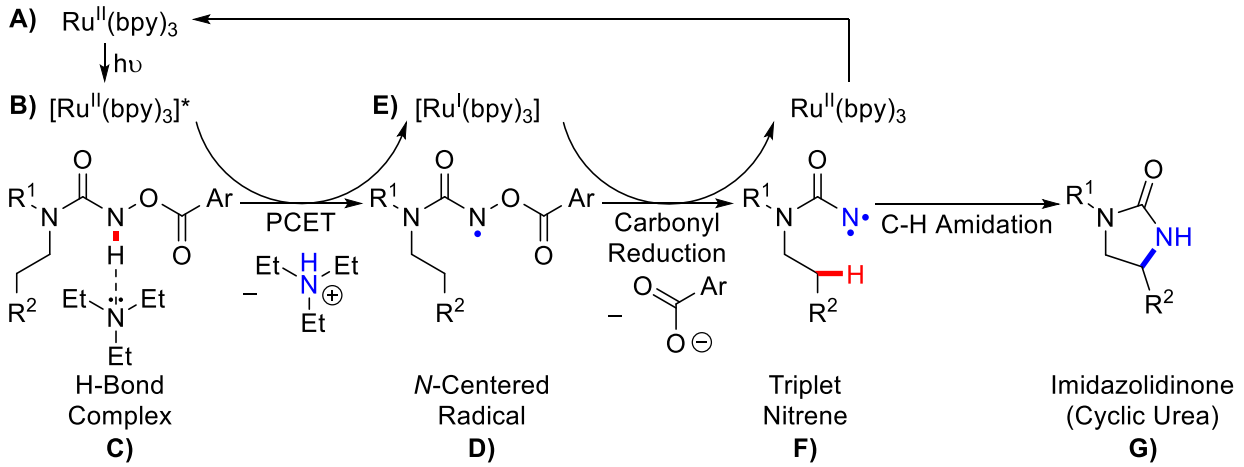

Scheme 32. Proposed mechanism for C-H amidation of *N*-acyloxyureas.

When 2,4,6-triisopropyl-*N*-((4-methoxybenzoyl)oxy) benzenesulfonamide (**1v**), was submitted to the reaction conditions for urea formation with CH_2Cl_2 as a solvent, an encouraging result was obtained (**Scheme 33**). The corresponding benzo[*d*]sultam (**1a**) was formed in 97% ^{1}H NMR yield, showing that the tertiary benzylic C(sp^3)-H amidation was indeed possible.

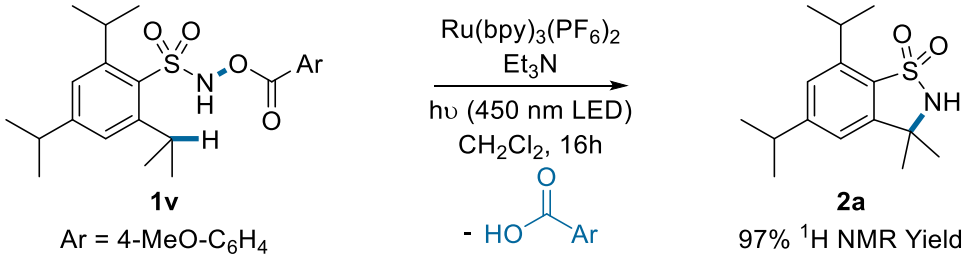

Scheme 33. Preliminary C-H amidation of an *N*-acyloxysulfonamide via photoredox catalysis.

This preliminary result led to further reaction exploration under photoredox conditions. The initial project objective was to design a general and robust method for sultam synthesis through intramolecular C-H amidation of *N*-acyloxysulfonamides. The conditions gradually evolved during the optimization, but the general objective was preserved. With the optimal conditions in hand, the next goal was to compile a broad and representative substrate scope. Thus, results from several iterations of reaction optimization and a scope of prepared sultams are presented herein.

Chapter 2: Results and Discussion

2.1 Substrate Synthesis

To study the reactivity of N-acyloxysulfonamides, the preparation of a variety of starting materials was needed to access gram quantities of substrates for reaction optimization, and to survey the applicability of the optimized reaction conditions. Overall, this was the most time-consuming aspect of this research project, as the synthetic route toward each benzo[*d*]sultam product involves a minimum of three steps. The synthesis first involves the conversion of a substituted benzene derivative to an arylsulfonyl chloride, which can be achieved through several procedures, often requiring multiple steps.[248,276–280] In this project, chlorosulfonic acid was adopted as a reagent to accomplish chlorosulfonylation via one-pot electrophilic aromatic substitution (**Scheme 34**).[246,281]

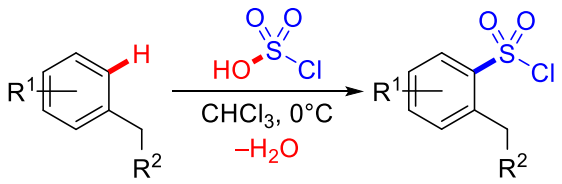

Scheme 34. Arylsulfonyl chloride synthesis via chlorosulfonylation of benzene derivatives.[246]

Sulfonyl chlorides are strong electrophiles suitable for the incorporation of nucleophilic hydroxylamine, a feature that was exploited here for the assembly of *N*-hydroxysulfonamides. The hydroxylamine later serves as the source of the electrophilic nitrogen atom that undergoes nitrene transfer following N-O bond cleavage. The transformation can be accomplished using magnesium oxide in a 3:2:30 methanol:water:THF solvent mixture (**Scheme 35**).[282]

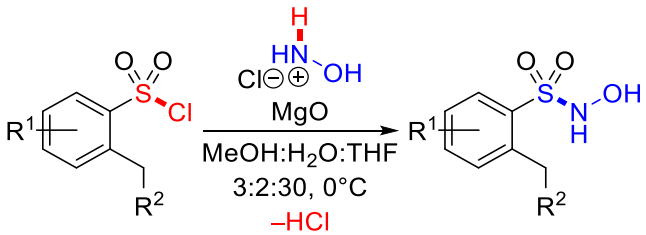

Scheme 35. Synthesis of *N*-hydroxysulfonamides via substitution of sulfonylchlorides.[282]

The final step in the synthesis of an *N*-acyloxysulfonamide nitrene precursor is the acylation of an *N*-hydroxysulfonamide. Previously, acyl chlorides have been used as acylating agents in the presence of an amine base, and this strategy was used to synthesize *N*-acyloxyureas in our previous publication.[207,283–286] When investigated here, the high electrophilicity of acyl chlorides gave side products that were acylated at both the oxygen and nitrogen atoms, and had similar retention factors to the desired compounds during column chromatography, thus making separation difficult. Anhydrides were adopted as alternative reagents to circumvent this problem (**Scheme 36**).[285]

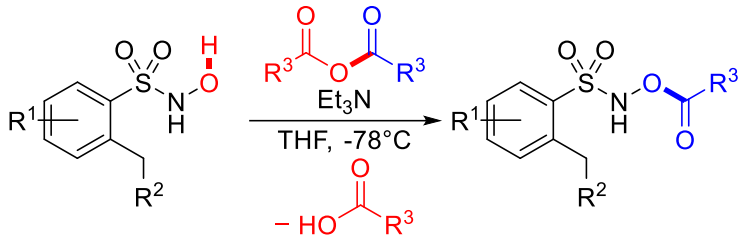

Scheme 36. Nitrene precursor synthesis via anhydride acylation of *N*-hydroxysulfonamides.

The set of reactions described above was used in the formation of *N*-(benzoyloxy)-2,4,6-triethylbenzenesulfonamide (**1b**), a key optimization substrate (**Chapters 2.3.2**, **2.4.1, 2.5.1**). The synthetic scheme for the formation of *N*-acyloxysulfonamide **1b** is shown below as a representative example (**Scheme 37**), affording the desired product in 12% total yield over three synthetic steps.

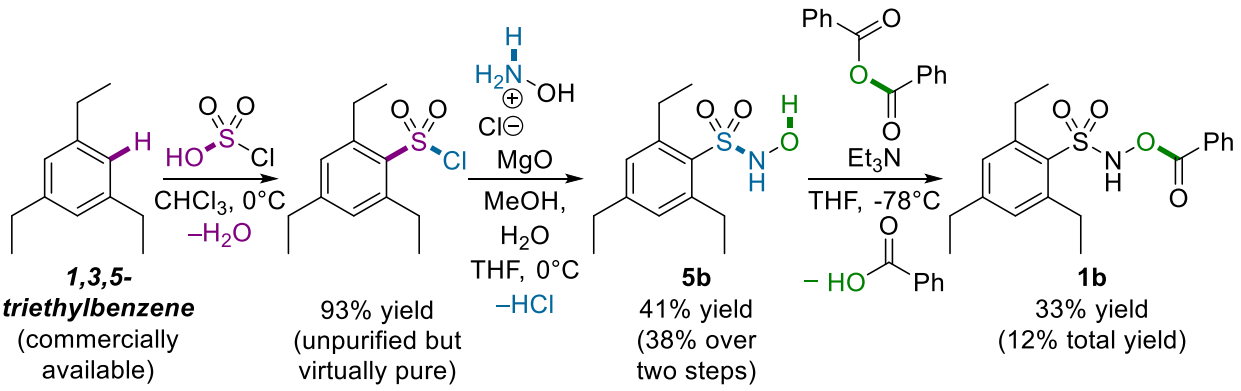

Scheme 37. Synthetic pathway toward *N*-acyloxysulfonamide nitrene precursor **1b**.

The synthetic scheme for *N*-acyloxysulfonamide **1m**, methyl 3-(N-(benzoyloxy)sulfamoyl)-4-ethylbenzoate, is shown below to represent an alternative synthetic route (**Scheme 38**). In order to synthesize the methyl ester containing sulfonyl chloride **4m**, the conversion of 4-ethylbenzoic acid to the chlorosulfonylated carboxylic acid **3m** was first required. A two-pot chlorodehydration-esterification sequence was then required to convert **3m** to the desired sulfonyl chloride **4m**. Overall the *N*-acyloxysulfonamide **1m** could be formed in 25% total yield over four steps.

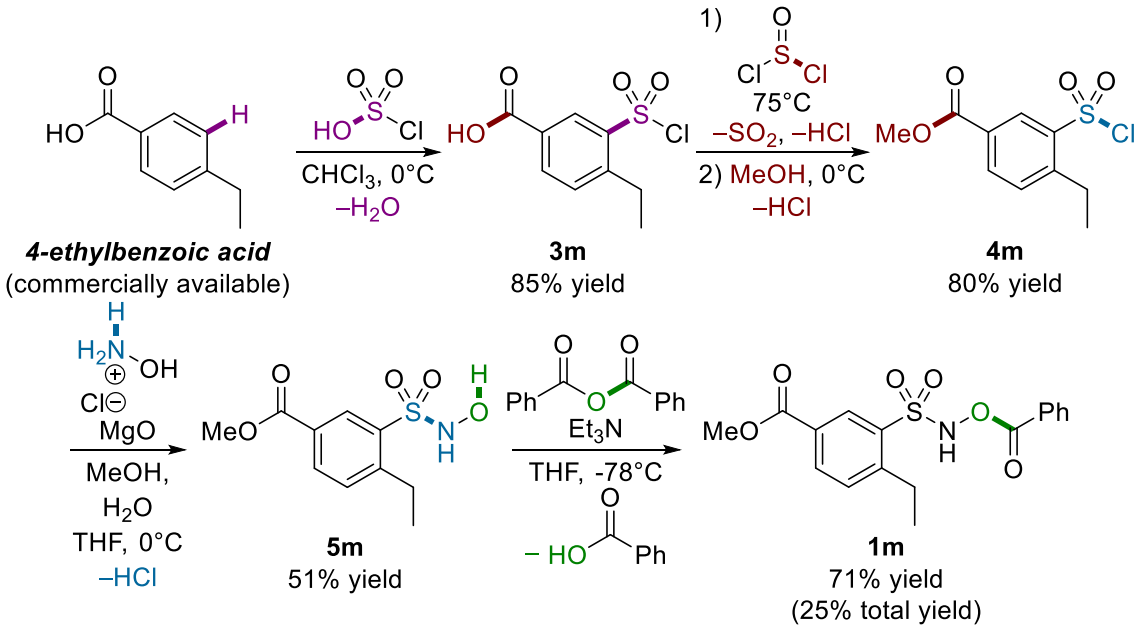

Scheme 38. Synthetic pathway toward *N*-acyloxysulfonamide nitrene precursor **1m**.

These examples show that improved methods are required to synthesize and purify *N*-hydroxysulfonamides and *N*-acyloxysulfonamides for these precursors to be widely applied to the synthesis of sultams, and to simplify extension of this reactivity to similar nitrene precursors.

2.2 oSultams from Photoredox Catalysed Aminative Cyclization

2.2.1 Initial Survey and Attempted Optimization of Photoredox Conditions

Following the successful cyclization reaction of **1v** (**Scheme 33**), the analogous primary benzylic C(sp^3)-H amination candidate, **1w** was subjected to the reaction conditions, attempting to form the corresponding benzo[*d*]sultam (**2c**). Unfortunately, the product formed in less than 5% yield (^{1}H NMR) and the reduced sulfonamide **3c** was the major product (**Table 1**, entry 1). Various bases and carboxylate leaving groups were then screened, attempting to improve reactivity (**Table 1**).

Table 1. Initial carboxylate leaving group and base optimization for photoredox conditions.[a,b]

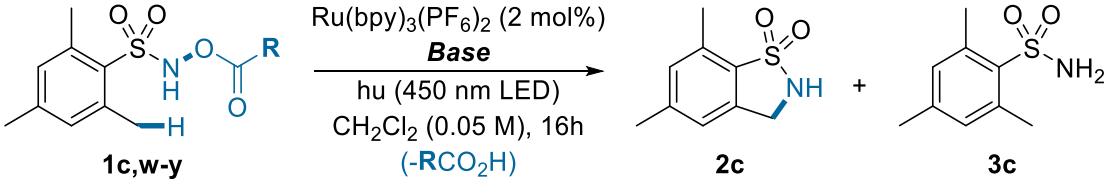

Entry	R	Base	1n (%)	2c (%)	3c (%)
1	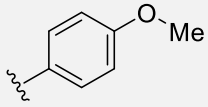 **1w**	Et_3N	<5	<5	41
2		$[Bu_4N][OP(O)(OBu)_2]$	5	<5	38
3	 **1x**	Et_3N	<5	<5	71
4		$[Bu_4N][OP(O)(OBu)_2]$	<5	23	≈ 70
5	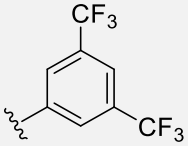 **1y**	Et_3N	7	14	43
6	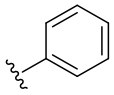 **1c**	Et_3N	6	30	28

[a]Conditions: **1c or 1w-y** (0.1 mmol), **Et_3N (1.1 equiv.) or $[Bu_4N][OP(O)(OBu)_2]$ (5.0 mol%)**, $Ru(Bpy)_3(PF_6)_2$ (2.0 mol %) and CH_2Cl_2 (0.05 M) were added to an 8 mL Kimax glass vial with a Teflon screw cap, purged with argon gas on ice and irradiated with 450 nm light using 12 V flexible blue LED strip lights for 16 h. [b]Yields determined by ^{1}H NMR analysis; integration of known peaks compared to combined integration of peaks from unreacted starting material and released carboxylate.

With our group's positive lactam synthesis results using tetrabutylammonium dibutylphosphate ($[Bu_4N][OP(O)(OBu)_2]$) as a base,[205–207] and the structural similarity of sultams and lactams, the reaction of **1w** was tested with this base, again forming **3c** as the major product. (**Table 1**, entry 2). At this point, the acyl substituent on the hydroxylamine oxygen atom was varied to establish an optimal leaving group (Entries 3-6) and three additional acyl groups were selected.

Acetate was first tested; the reaction of **1x** with triethylamine formed the sultam in low yield (Entry 3), however, $[Bu_4N][OP(O)(OBu)_2]$ gave a moderate product yield of 23% (**Table 1**, entries 3-4). Unfortunately, several similar side products were observed by ^{1}H NMR and TLC. The reaction of substrate **1y** containing electron withdrawing substituents (Entry 5) gave higher yield (14%) than with the electron rich substrate **1w**, opposing the trend observed with *N*-acyloxyureas. The simple benzoyl- derivative **1c** was the final substrate tested (Entry 6). The reaction gave the highest yield for **2c** (30%) and represented the first reaction to form the sulfonamide as the minor product (28%). This substrate was selected for further screening, starting with catalyst optimization (**Table 2**).

Table 2. Catalyst optimization for photoredox aminative cyclization of *N*-oxysulfonamides.[a,b]

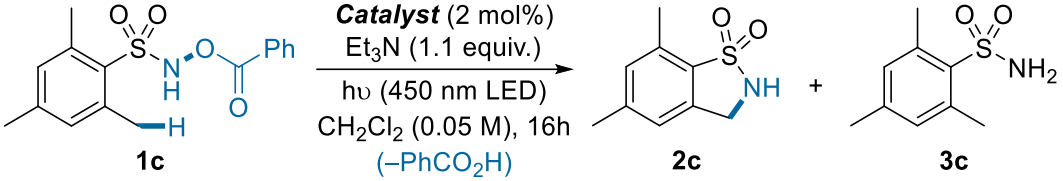

Entry	Catalyst	1c (%)	2c (%)	3c (%)
1	$Ir(dFppy)_3$	-	5	14
2	$[Ir(dF(CF_3)ppy)_2$-(5,5'-$d(CF_3)bpy)]PF_6$	-	8	12
3	$[Ir(dtbbpy)(ppy)_2]PF_6$	<5	10	18
4	$(Ir[dF(CF_3)ppy]_2(dtbpy))PF_6$	-	13	52
5	-	15	21	15
6[c]	$Ru(Bpy)_3(PF_6)_2$	7	<5	19

[a]Conditions: 1c (0.1 mmol), Et_3N (1.1 equiv.), **catalyst** (2.0 mol %) and CH_2Cl_2 (0.05 M) were added to an 8 mL Kimax glass vial with a Teflon screw cap, purged with argon gas on ice and irradiated with 450 nm light using 12 V flexible blue LED strip lights for 16 h. [b]Yields determined by ^{1}H NMR analysis; integration of known peaks compared to combined integration of peaks from unreacted starting material and released carboxylate. [c]Cooled with a stream of compressed air.

Several iridium photocatalysts previously employed by Knowles and colleagues for PCET C-H amination were screened for their ability to catalyze the reaction (**Table 2**, entries 1-4),[273,287–289] but all gave a lower sultam yield than $Ru(Bpy)_3(PF_6)_2$. At this point a control reaction was performed to test for background reactivity in the absence of a photocatalyst (Entry 5). Surprisingly, 21% yield was observed in the absence of $Ru(Bpy)_3(PF_6)_2$, with 15% unconverted starting material, indicating either that photoredox reactivity is possible in the absence of a photocatalyst, or that a thermal base-induced reaction pathway was accessible with mild heating by the LED lamp. An additional control with a photocatalyst was conducted while pointing a stream of cool air at the reaction vial to maintain low temperature (Entry 6). Without added heat, less than 5% product yield was observed with 19% yield of the sulfonamide byproduct, indicating that thermal energy was indeed required for the desired amination reaction to outcompete reduction. At this point, we decided to investigate the thermal base-induced C-H amination of *N*-acyloxysulfonamides as a candidate for novel amination methodology, and efforts were directed toward optimization for a robust thermal base-induced reaction, as described in **Chapter 2.3**.

The only successful C-H amidation reaction throughout this preliminary screen was the reaction of **1v** (**Scheme 33**). The photoredox conditions investigated here may only form sultams in high yield using *N*-acyloxyarylsulfonamides with weak tertiary benzylic C-H bonds. Improved conditions were required for amidation of stronger C-H bonds.

2.2.2 Miscellaneous Substrates Tested for Photoredox Conditions

During the initial photoredox optimization, two substrates (**1t** and **1u**) were tested to determine if non-benzylic amidation of aliphatic and aromatic C-H bonds can form sultams (**Table 3**).

Table 3. Failed scope entries for non-benzylic C-H amidation of *N*-acyloxysulfonamides.[a,b]

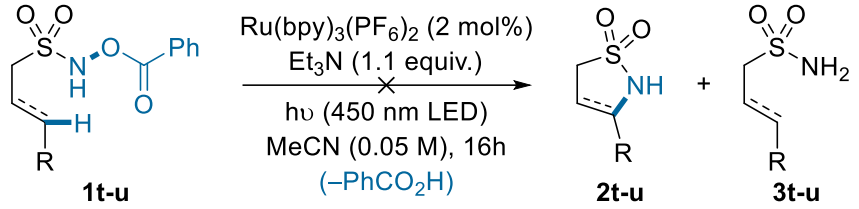

Starting Material	Expected Product	Side Product	Yield of 1t-u (%)	Yield of 2t-u (%)	Yield of 3t-u (%)
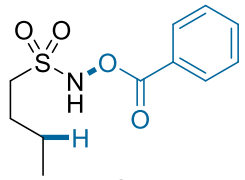 1t	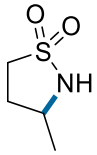 2t	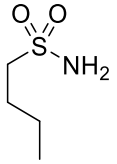 3t	-	0	86
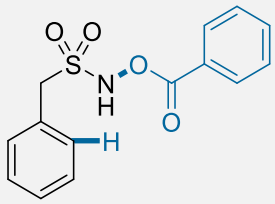 1u	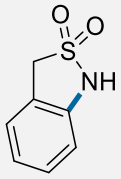 2u	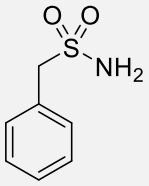 3u	-	<5	59

[a]Conditions: **1t-u** (0.1 mmol), Et_3N (1.1 equiv.), $Ru(Bpy)_3(PF_6)_2$ (2.0 mol %) and MeCN (0.05 M) were added to an 8 mL Kimax glass vial with a Teflon screw cap, purged with argon gas on ice and irradiated with 450 nm light using 12 V flexible blue LED strip lights for 16 h. [b]Yields determined by ^1H NMR analysis; integration of known peaks compared to combined integration of peaks from unreacted starting material and released carboxylate.

The reaction of linear aliphatic **1t** (**Table 3**, entry 1), intended for a secondary C-H amidation, allowed for full starting material conversion and the formation of sulfonamide **3t** as the major product (86%), with no trace of the desired sultam. The reaction of **1u** was attempted to test aromatic C-H bond amination efficiency (Entry 2). Complete substrate conversion allowed for the formation of benzylsulfonamide **3u** in 59% yield, with minimal yield of the desired sultam. Once again, the initial photoredox conditions were inefficient to promote the desired aminative cyclization, and base-induced thermal C-H amidation became the focus for future optimization.

2.3 Thermal Base-Induced Synthesis of Sultams

2.3.1 Background

Abramovitch's pioneering studies showed that the thermal decomposition of arylsulfonyl azides can generate free sulfonyl nitrenes, and a subsequent intramolecular C-H insertion is possible when using *ortho*-alkyl substituted azides, enabling the formation γ-benzo[*d*]sultams (**Chapter 1.4.4**, **Figure 33**, **Scheme 18**).[129,132,133] Unfortunately, the desired sultams were formed in low yield due to the high reactivity of nitrenes, and byproducts from other pathways were observed, namely intermolecular C-H insertion and C-H abstraction reactions with solvent, along with rearrangement reactions.[129,132,133] Hence, the field of C-H amidation using sulfonyl azides is dominated by nitrenes that are stabilized with metals and enzymes.[106,113,139,290] Similar to azides, most C-H amidation reactions using *N*-oxysulfonamide precursors involve metal complexes for nitrene stabilization.[156,162,167,194,195,291–293] Attempts toward thermal C-H amidation of *N*-oxysulfonamide derivatives are dominated by Lossen-Type rearrangement reactivity and give even lower yields of C-H amination products (**Chapter 1.4.1**, **Figure 23**, **Scheme 14**).[158,159,161]

2.3.2 Optimization of Thermal Base-Induced C-H Amidation Reactivity

Following the finding that thermal base-induced C-H amidation of *N*-acyloxysulfonamides is possible, the first optimization step taken was screening through temperatures with hopes that benzo[*d*]sultams could be selectively formed over sulfonamides (**Table 4**). Acetonitrile was selected over CH_2Cl_2 as a practical solvent for high temperature optimization, given its higher boiling point (82 vs. 40 °C) and lower vapour pressure (73 vs. 353 mm Hg at 20 °C) at ambient conditions.[205–207] Three temperatures were tested by heating under microwave irradiation.

Table 4. Temperature optimization for thermal C-H amidation of *N*-acyloxysulfonamides.[a,b]

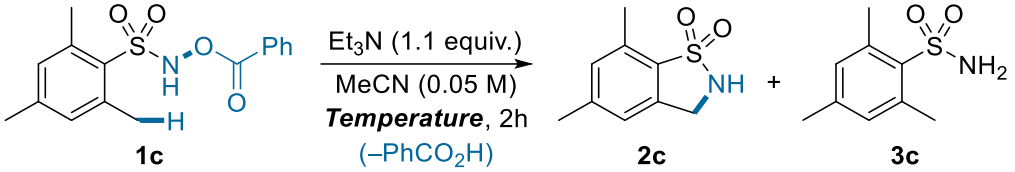

Entry	Temperature (°C)	1c (%)	2c (%)	3c (%)
1	90	8	46	24
2	120	-	50	28
3	150	-	55	21
4[c]	120	-	49	27

[a]Conditions: **1c** (0.1 mmol), Et_3N (1.1 equiv.) and MeCN (0.05 M) were added to a microwave vial, purged with argon gas on ice and heated at the indicated **temperature** through microwave irradiation for 2 h. [b]Yields determined by ^1H NMR analysis; integration of known peaks compared to combined integration of peaks from unreacted starting material and released carboxylate. [c]Heated for 16 h with an oil bath.

The reaction at 90 °C gave a modest sultam (**2c**) yield of 46% with 24% sulfonamide (**3c**) and some starting material remaining (**Table 4**, entry 1). At 120 °C, the starting material underwent full conversion and slight yield increases were observed for both the desired (50%) and undesired products (28%) (Entry 2). Finally, 150 °C gave 55% yield with a slight decrease in sulfonamide formation (Entry 3). In the end, 120 °C was chosen as the optimal temperature as reactions at 150 °C pose safety issues, especially on large scale. An additional reaction tested efficiency in an oil bath over 16 h (Entry 4); a similar yield to the two-hour microwave reaction was obtained and an oil bath was selected as the primary heat source. With the optimal temperature determined, several nitrogenous bases and a single inorganic base were screened for base optimization (**Table 5**).

Table 5. Optimization of base for thermal C-H amidation of *N*-acyloxysulfonamides.[a,b]

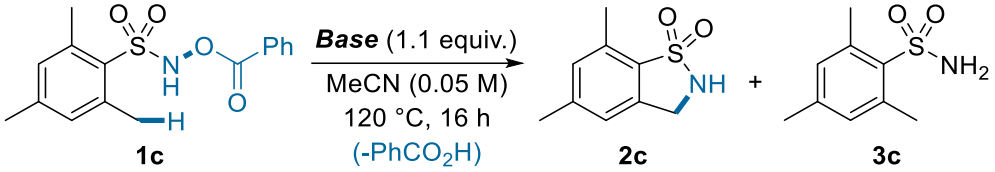

Entry	Base	1c (%)	2c (%)	3c (%)
1	DBU	5	43	53
2	TMG	9	43	16
3	Imidazole	<5	35	<5
4	DMAP	5	35	20
5	*N*-methyl-morpholine	<5	35	41
6	*i*-Pr_2NEt	<5	61	25
7[c]	K_2CO_3	6	53	6

[a]Conditions: 1c (0.1 mmol), **base** (1.1 equiv.) and MeCN (0.05 M) were added to a microwave vial, purged with argon gas on ice and heated to 120 °C in an oil bath for 16 h. [b]Yields were determined by ^{1}H NMR analysis; integration of known peaks compared to combined integration of peaks from unreacted starting material and released carboxylate. [c]Yield determined by ^{1}H NMR analysis following extraction using 1,3,5-trimethoxybenzene as an internal standard.

Overall, the nature of the base had a significant impact on the yield of the sulfonamide byproduct. DBU and TMG gave 43% yield of product, with DBU forming more of **3c** (**Table 5**, entries 1-2). DMAP, imidazole and *N*-methylmorpholine also enabled product formation, but with an appreciable yield decrease to 35% (Entries 3-5).

Ultimately, *N*,*N*-diisopropylethylamine (*i*-Pr_2NEt) proved to be the optimal base, forming **2c** in 61% yield with only 25% sulfonamide (**Table 5**, entry 6). The inorganic base, potassium carbonate gave the second highest yield (Entry 7). Poor solubility and difficulty analyzing crude ^{1}H NMR spectra without an extraction step led to the exclusion of this base from further optimization.

After establishing *i*-Pr_2NEt as the optimal base, solvent optimization was commenced. The results are presented in **Table 6**.

Table 6. Solvent optimization for thermal C-H amidation of *N*-acyloxysulfonamides.[a,b]

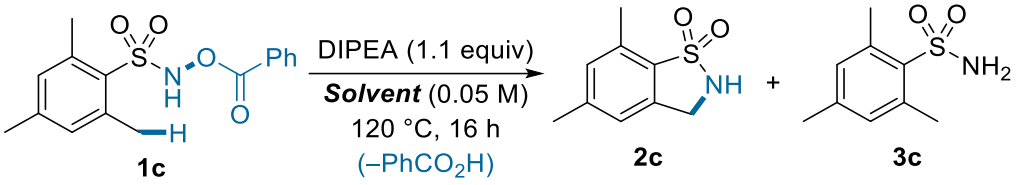

Entry	Solvent	1c (%)	2c (%)	3c (%)
1	1,2-Dichloroethane[c]	21	34	29
2	α,α,α-Trifluorotoluene[d]	25	17	43
3	Tetrahydrofuran	7	42	33
4	Dimethylsulfoxide-d_6[d]	-	47	48
5	Nitromethane	-	59	25
6	Dimethylformamide[d,e]	-	54	21
7	Pyridine[f]	7	37	21

[a]Conditions: 1c (0.1 mmol), *i*-Pr$_2$NEt (1.1 equiv.) and **Solvent** (0.05 M) were added to a microwave, purged with argon gas on ice and heated to 120 °C in an oil bath for 16 h. [b]Yields determined by ^{1}H NMR analysis; integration of known peaks compared to combined integration of peaks from unreacted starting material and released carboxylate. [c]Run using TMG as a base (1.1 equiv.). [d]Yields determined by ^{1}H NMR analysis using 1,3,5-trimethoxybenzene as an internal standard. [e]Extraction required. [f]Run in the absence of additional base.

All reactions tested formed product, but polar aprotic solvents with a high capacity for hydrogen bonding generally gave better yield and conversion. DMSO-d_6 enabled moderate sultam formation in equivalent yield to the sulfonamide (**Table 6**, entry 4). Nitromethane and DMF gave the best results, with sultam yields comparable to acetonitrile along with a significant amount of sulfonamide byproduct (Entries 5-6). The possible explosiveness of nitromethane and the low vapour pressure of DMF (3.87 mm Hg) deterred further investigation, and acetonitrile was conserved as the optimal solvent. Interestingly, conducting the reaction in pyridine without an additional base gave 37% yield of **2c** (Entry 7).

At this point, the next step required was to reoptimize the carboxylate leaving groups and determine if the electronic nature of the acyl group could be tuned to enable productive reactivity (**Table 7**).

Table 7. Optimization of carboxylate leaving group for thermal C-H amidation.[a,b]

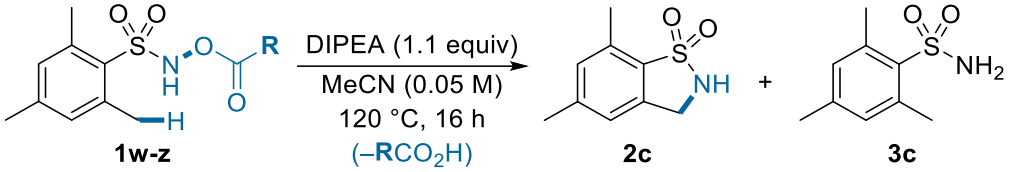

Entry	R	1n (%)	2c (%)	3c (%)
1	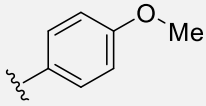 **1w**	5	61	24
2	 **1x**	-	65	26
3	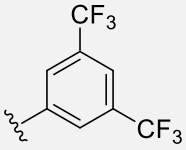 **1y**	<5	42	30
4	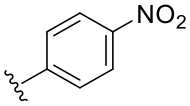 **1z**	<5	42	32

[a]Conditions: **1w-1z** (0.1 mmol), *i*-Pr_2NEt (1.1 equiv.) and MeCN (0.05 M) were added to a microwave vial, purged with argon gas on ice and heated to 120 °C in an oil bath for 16 h. [b]Yields determined by ^1H NMR analysis using 1,3,5-trimethoxybenzene as an internal standard.

The yields obtained were similar to those with **1c**, and sulfonamide byproduct formation continued to limit synthetic efficiency. Electron rich 4-methoxy benzoyl (**1w**) and acetyl (**1x**) groups (**Table 7**, entries 1-2) formed both **2c** and **3c** in comparable yields to **1c**, with slightly higher sultam yield (65%) from **1x**. These substrates were excluded from further investigation, in part due to complexity of starting material synthesis. Electron poor 3,5-Bis(trifluoromethyl)benzoyl (**1y**) and *p*-nitrobenzoyl groups (**1z**) gave lower sultam yields (42%) and higher reduction yields overall (Entries 3-4). While one may expect that a stabilized leaving group could accelerate the desired reaction through increased N-H bond acidity, promoting faster α-elimination, there is a possibility that the electron withdrawing nature is too strong and other pathways operate. The increased acidity may allow nitrenoid formation, and a Lossen-type rearrangement like that seen by Loïc

Pantaine et al. (**Scheme 14**).[159,160] Indeed, several additional singlet peaks were present in the benzylic C-H region of the ^{1}H NMR spectrum which may correspond to those of a 2,4,6-trimethyl aniline derivative.

Further optimization studies were performed to determine if increased substrate concentration was viable for the reaction (**Table 8**). Reactions run at 0.05 M do not represent green or economical processes and require a significant solvent volume relative to the mass of product formed.

Table 8. Substrate concentration studies for thermal C-H amidation.[a,b]

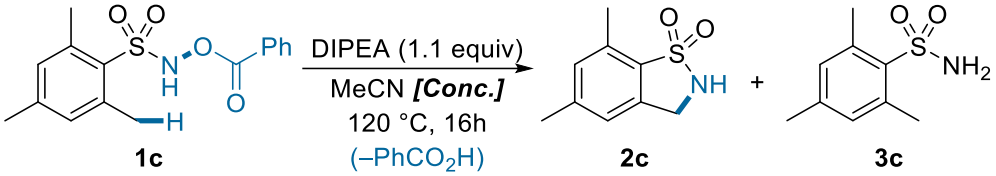

Entry	Substrate Concentration (M)	2c (%)	3c (%)
1	0.08	54	36
2	0.10	44	33
3	0.25	40	40
4	0.50	24	43
5[c]	0.02	70	21
6	0.01	70	17

[a]Conditions: 1c (0.1 mmol), *i*-Pr$_2$NEt (1.1 equiv.) and MeCN were added to a microwave vial to achieve the desired concentration, purged with argon gas on ice and heated to 120 °C in an oil bath for 16 h. [b]Yields determined by ^{1}H NMR analysis using 1,3,5-trimethoxybenzene as an internal standard. [c]Temporarily, 0.02 M was adopted as the optimal concentration but was reverted to the original 0.05 M for scope studies.

Unfortunately, the increased concentration was inversely correlated with product yield and directly correlated to higher reduction yields. The concentrated reaction mixtures were also progressively a darker red hue, thus, diazo benzene side products may have formed, as seen in Abramovitch's work (**Figure 33**, **C**),[132,133] a reasonable outcome as the nitrene intermediates would be in closer proximity in solution, allowing for a kinetically accessible dimerization pathway.

The next step taken was to determine if the base could act catalytically, and if an excess of base would negatively affect the reaction (**Table 9**).

Table 9. Base loading optimization studies for thermal C-H amidation.[a,b]

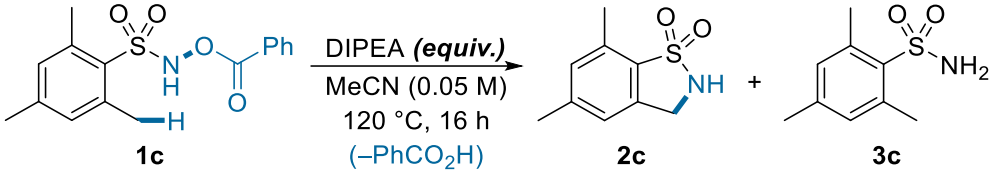

Entry	Base Loading (Equivalents)	1c (%)	2c (%)	3c (%)
1[c]	0.2	-	57	26
2	0.3	-	59	26
3	0.4	-	59	27
4	0.6	-	64	28
5	0.8	-	59	28
6[d]	1.0	<5	72	18
7[d]	2.0	-	65	20
8[d]	20	-	59	24

[a]Conditions: 1c (0.1 mmol), the **desired quantity of *i*-Pr$_2$NEt** and MeCN (0.05 M) were added to a microwave vial, purged with argon gas on ice and heated to 120 °C in an oil bath for 16 h. [b]Yields determined by ^{1}H NMR analysis using 1,3,5-trimethoxybenzene as an internal standard. [c]Yield determined by ^{1}H NMR analysis; integration of known peaks compared to combined integration of peaks from unreacted starting material and released carboxylate. [d]Concentration of 0.02 M.

Several iterations of catalytic base loading were investigated ranging from 20-80 mol % (**Table 9**, entries 1-5), all of which promoted product formation with similar yield to the reaction using 1.1 equivalents, confirming that the reaction is productive with catalytic base. Excess base, either 2.0 or 20 equivalents, did not significantly impact the reaction (Entries 7-8). Testing the reaction with an equimolar base loading (Entry 6), while attempting to interrupt reduction by excess base, gave the highest yield of sultam thus far (72%), with the lowest sulfonamide yield (18%). It should be noted that the yields observed were similar and most appear to be within experimental error. As such, the efficiency of the reaction was comparable using the base under catalytic and stoichiometric conditions. On the basis of these results, the optimal base loading was adjusted to 1.0 equivalents for further optimization and scope studies.

The final stage of the optimization studies was to determine an optimal reaction time (**Table 10**). While the entire optimization was conducted with sixteen-hour reactions, a shorter reaction time was desired, both for convenience and for cost efficiency.

Table 10. Optimization of reaction time for thermal C-H amidation.[a,b]

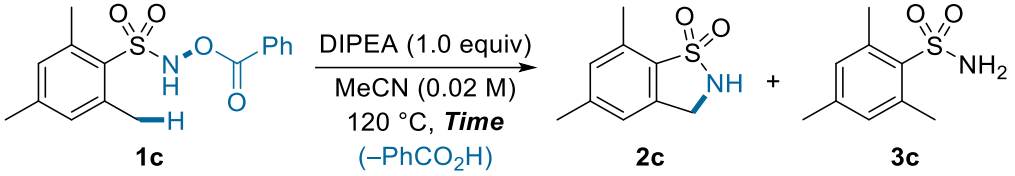

Entry	Reaction Time (h)	1c (%)	2c (%)	3c (%)
1	0.5	<5	73	21
2	2	<5	72	18
3	4	<5	71	18

[a]Conditions: 1c (0.1 mmol), *i*-Pr_2NEt (1.0 equiv.) and MeCN (0.02 M) were added to a microwave vial, purged with argon gas on ice and heated to 120 °C for the **indicated time** with an oil bath. [b]Yields determined by ^{1}H NMR analysis using 1,3,5-trimethoxybenzene as an internal standard.

Three shorter reaction times were chosen: thirty minutes, two hours and four hours. Overall, all three time points gave comparable yields to the 16-hour reaction, ranging from 71-73%. Two hours was then selected as optimal, leaving leeway for substrates that may require additional time, such as those with sterically inaccessible C-H insertion sites.

2.3.3 Scope of Benzo[*d*]sultams from Thermal Base-Induced C-H Amidation

After pinpointing the optimal conditions for the novel base-induced thermal C-H amidation reaction of *N*-acyloxysulfonamide derivatives, attempts were made to create a product scope using the reaction. The results of the scope studies are shown below in **Table 11**.

Table 11. Sultam scope for base-induced thermal C-H amidation of *N*-acyloxysulfonamides.[a]

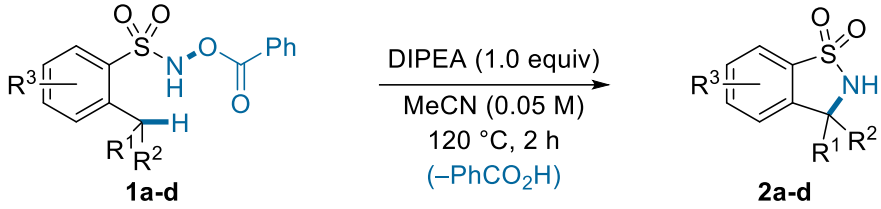

1a-d → **2a-d**

2a	**2b**	**2c**	**2d**
(63%)[b]	85%[e,f]	46%[e]	41%[e,h]
(77%)[b-d]	(92%)[b,g]	(61%)[b,g]	(75%)[b]

[a]Conditions: **1a-d** (1.0 mmol), *i*-Pr_2NEt (1.0 equiv.) and MeCN (0.05 M) were added to a microwave vial vial, purged with argon gas on ice and heated at 120 °C for 2 h with an oil bath. [b]Yields in parenthesis were determined by ^{1}H NMR analysis, by integration of known peaks compared to combined integration of peaks from unreacted starting material and released carboxylate. [c]Triethylamine used as a base. [d]Run on 0.1 mmol scale. [e]Isolated yields. [f]Run on 0.5 mmol scale. [g]Run with 1.1 equivalents of *i*-Pr_2NEt. [h]Required multiple isolation steps.

The first step to analyze the substrate scope was to reinvestigate the tertiary C-H amidation forming **2a**, as seen with **1v** under photoredox conditions (**Chapter 1.5**, **Scheme 33**). The reaction of *N*-(benzoyloxy)-2,4,6-triisopropylbenzenesulfonamide (**1a**) only formed 63% yield of product, a surprising result considering that nitrene insertion at a tertiary C-H bond, with the weakest bond strength of the 2,4,6-trisubstituted series, was expected to give the highest yield. The reaction was conducted again after replacing *i*-Pr_2NEt with Et_3N, the less sterically hindered, analogous base, and the yield increased to 77%. It seems that the C-H insertion success by the nitrene intermediate is not only dictated by the electronic nature of the C-H bond, and that steric hindrance of the N-H bond appears to warrant the use of a less hindered base.

Gratifyingly, the reaction of *N*-(benzoyloxy)-2,4,6-triethylbenzenesulfonamide (**1b**), containing a secondary benzylic C-H bond at the *ortho*- position, allowed for the isolation of sultam **2b** in 85% yield. The optimization substrate (**1c**) was investigated next; despite the numerous optimization attempts, the primary C-H insertion product **2c** was only isolated in a 46% yield.

The final scope entry involved another tertiary C-H insertion; the reaction of *N*-(benzoyloxy)-2,5-dicyclohexylbenzenesulfonamide (**1d**) gave an encouraging result, forming sultam **2d** in 74% ^{1}H NMR yield. The presence of impurities with similar polarity to the sultam made isolation difficult and column chromatography gave product with ~6% impurity; the yield based on mass was close to 68%. An additional recrystallization enabled isolation of the pure product in 41% yield.

Given that the likely pathway toward nitrene formation involves deprotonation / α-elimination,[158,294,295] the steric bulkiness of *i*-Pr_2NEt and **1a** may have interrupted the formation of the initial base-substrate hydrogen-bond complex, decreasing the efficiency of α-elimination and nitrene formation. The hydrogen-bond may form more efficiently with triethylamine. At the other end of the series, the hydrogen-bond complex of **1c** and *i*-Pr_2NEt would be more hindered than with Et_3N, possibly triggering a faster α-elimination pathway before complex dissociation. If the reaction is stepwise or more asynchronous in nature, the ion pair formed upon initial deprotonation of **1c** would be also more hindered with *i*-Pr_2NEt than with Et_3N, further forcing the elimination. Isolation was not attempted on either of the reactions forming **2a**; investigating the remainder of the scope and developing more efficient reaction conditions was adopted as a higher priority.

Notably, the isolated yields obtained for **2b** and **2c** were lower than those observed by ^{1}H NMR. The more dilute fractions containing compounds **2b** and **2c** were too faint to observe on TLC using UV light or a variety of stains during column chromatography, which may have reduced yield.

With the scope of benzo[*d*]sultams derived from base-induced thermal C-H amidation partially assembled, attempts were made to extend the scope to substrates that would require more difficult C-H insertion steps, especially *ortho*-monoalkyl-*N*-acyloxyarylsulfonamides, which do not benefit from the same conformational bias as the previous substrates with a 2,6-disubstitution pattern, along with substrates containing electron withdrawing groups to strengthen the benzylic C-H bond. Alas, all tested reactions returned negative results. The failed substrates are disclosed in **Table 12**.

Table 12. Synthetic limitations of the thermal base-induced benzylic C-H amidations.[a/b,c]

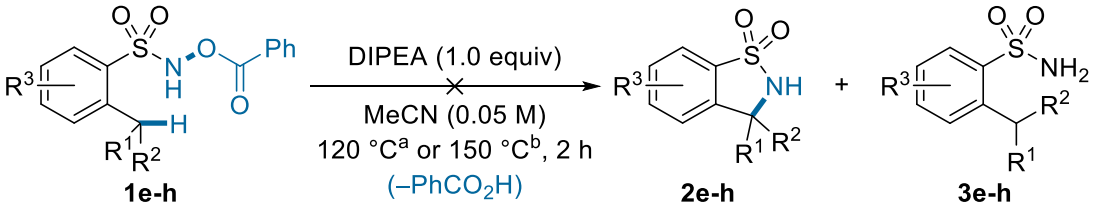

Starting Material	Expected Product	Yield of 1e-h (%)	Yield of 2e-h (%)	Yield of 3e-h (%)
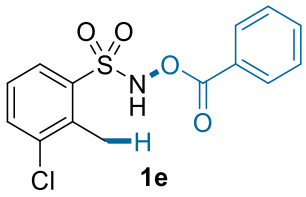 **1e**	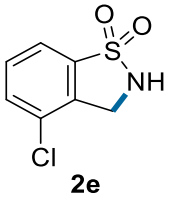 **2e**	<5[a] <5[b]	<5[a] <5[b]	75[a] 73[b]
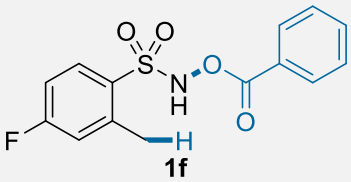 **1f**	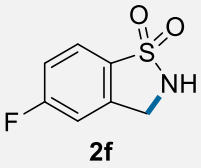 **2f**	<5[a] <5[b]	<5[a] <5[b]	86[a] 58[b]
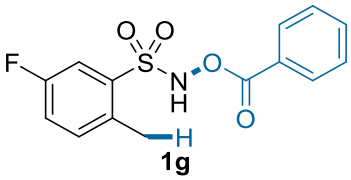 **1g**	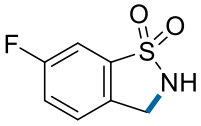 **2g**	-[b]	<5[b]	55[b]
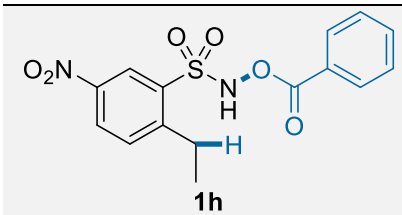 **1h**	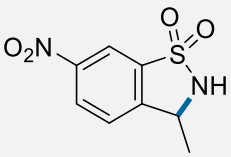 **2h**	<5	<5	33

[a]Conditions: **1e-h** (0.1 mmol), *i*-Pr$_2$NEt (1.0 equiv.) and MeCN (0.05 M) were added to a microwave vial, purged with argon gas on ice and heated at 120 °C for 2 h with an oil bath. [b]Heated to 150 °C for 2 h with an oil bath. [c]Yields determined by ^{1}H NMR analysis using 1,3,5-trimethoxy benzene as an internal standard.

The reaction of 3-choro (**1e**) and 4-fluoro (**1f**) substituted *ortho*-monomethyl substrates resulted in full starting material conversion with low product yield. Increasing the temperature to 150 °C gave similar results, an observation that extended to 5-fluoro substituted *ortho*-monomethyl substrate **1g**. All reactions in **Table 12** gave less than 5% yield of sultam with the sulfonamide formed as the major product in 55-86% yield. Even the secondary *ortho*-monoethyl substrate **1h** formed the desired benzo[*d*]sultam in less than 5% yield with the sulfonamide as the major product (33%).

Attempts were also made to to produce a larger scope by extending the reactivity to precursors with non-benzylic C-H bonds (**Table 13**).

Table 13. Failed scope entries for thermal base-induced non-benzylic C-H amidation.[a,b]

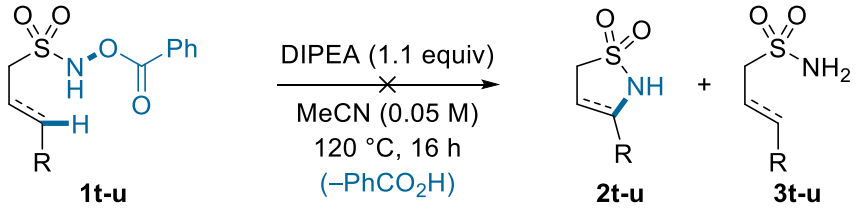

Starting Material	Expected Product	Side Product	Yield of 1t-u (%)	Yield of 2t-u (%)	Yield of 3t-u (%)
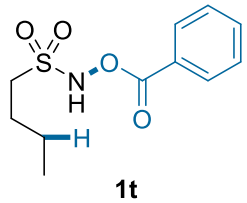 1t	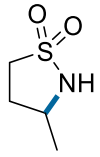 2t	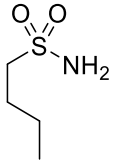 3t	-[e]	0[e]	83[e]
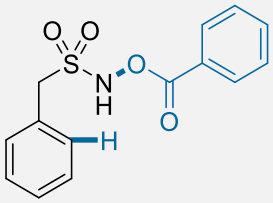 1u	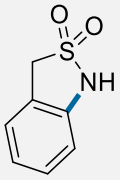 2u	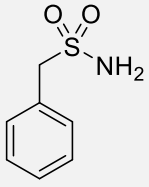 3u	<5[d]	<5[d]	66[d]

[a]Conditions: **1t-u** (0.1 mmol), **base** and MeCN (0.05 M) were added to a microwave vial, purged with argon gas on ice and heated at 120 °C for 2 h with an oil bath. [b]Yields determined by ^{1}H NMR analysis; integration of known peaks compared to combined integration of peaks from unreacted starting material and released carboxylate. [c]TMG (1.1 equiv.) used as a base. [d]Et_3N (1.1 equiv.) used as a base. [e]*i*-Pr_2NEt (1.1 equiv.) used as a base. [f]Yield determined by ^{1}H NMR analysis using 1,3,5-trimethoxy benzene as an internal standard. [g]*i*-Pr_2NEt (1.0 equiv.) used as a base.

Following the finding that thermal triethylamine-induced C-H amidation was possible, the aliphatic secondary C-H amidation of *N*-(benzoyloxy)butane-1-sulfonamide (**1t**) was tested. The reaction gave the sulfonamide **3t** in 83% yield with no trace of sultam **2t**. The reaction of *N*-(benzoyloxy)-1-phenylmethanesulfonamide (**1u**) was attempted after *i*-Pr_2NEt was adopted as the optimal base, forming the minimal product yield (**2u**) and 66% yield of the sulfonamide (**3u**).

Overall, it seems that the thermal base-induced C-H amidation reaction unveiled in this chapter is only applicable to *N*-acyloxyarylsulfonamide substrates with tertiary benzylic C-H bonds (**Table 11**, **2a**, **2d**) and 2,6-dialkyl-*N*-acyloxyarylsulfonamides (**Table 11**, **2a-2c**). For *ortho*-monoalkyl-*N*-acyloxyarylsulfonamides, the cyclization reaction is likely more challenging on conformational grounds. The steric repulsion of the *ortho* alkyl group likely forces the reactive nitrene intermediate to rotate away from the desired insertion site, making the benzylic C-H bond less kinetically accessible. While in this more favorable confirmation, the singlet nitrene may undergo intersystem crossing (ISC)[119,296] before the C-H insertion event can occur, allowing the resultant triplet nitrene to abstract hydrogen atoms from base or solvent (**Scheme 39**). [112,114,115,120,123,131,132,134] It may also simply be possible that the steric interactions imposed by the additional *ortho*-alkyl group in the 2,6-disubstituted substrates block the approach of base or solvent to decrease the reduction pathway, allowing for C-H amination even in the triplet state.

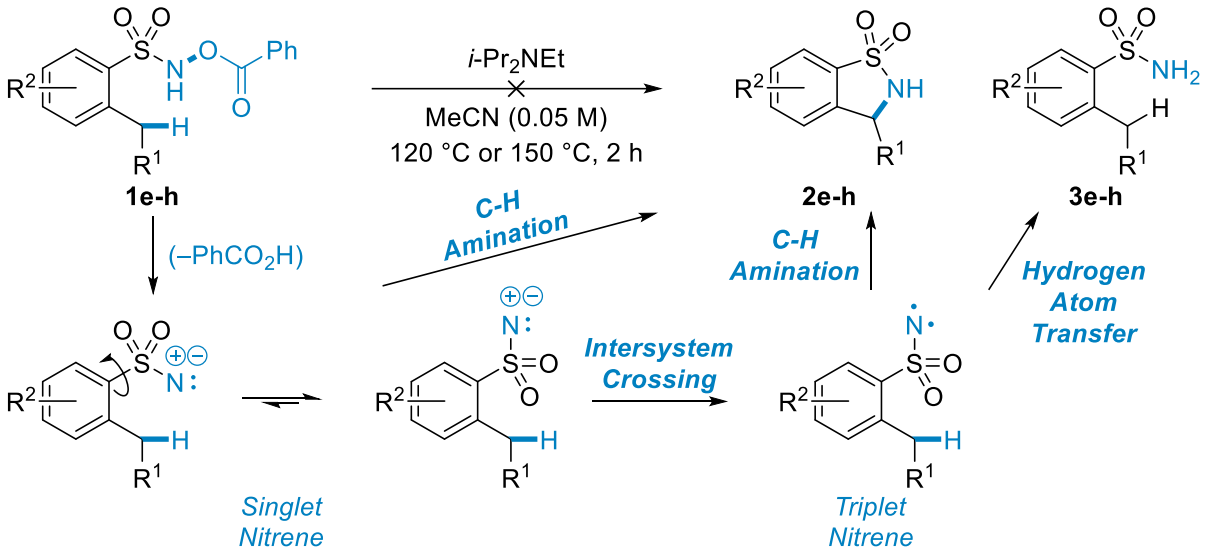

Scheme 39. Likely reaction mechanism to explain the formation of sulfonamide byproducts.

The poor fate in the reaction of substrate **1u** containing an aryl C(sp^2)-H bond insertion site was likely a result the high bond strength for an aryl C(sp^2)-H bond compared to that for a benzylic C-H (113 kcal/mol vs. 90 kcal/mol).[107] Even for substrate **1t**, the secondary C-H bond is still about 10 kcal/mol stronger (101 kcal/mol)[107] than a benzylic C-H bond. With **1t** an additional factor must be considered: arranging the bonds of the linear substrate into the envelope conformation for the desired reaction creates a large entropic penalty. Intersystem crossing may outcompete this process, and the major pathway may involve conversion to the triplet nitrene and hydrogen atom abstraction.

Due to the limited substrate scope and low yields obtained under thermal conditions, further investigation was taken to elucidate alternative conditions which could produce a larger scope and enable a more robust reaction (**Chapters 2.5** and **2.6**).

2.4 Return to Photoredox Catalysis for Sultam Synthesis

The limitations observed when compiling a scope for base-induced thermal C-H amidation of *N*-acyloxysulfonamides led to the need for further optimization to achieve robust reaction conditions. Returning to the photoredox conditions was the first direction to take, both because of the high yield obtained for the reaction of **1v** (**Chapter 1.5**, **Scheme 33**), and the previous success with *N*-acyloxyurea substrates.[205–207] Indeed, the mesitylene derived substrate **1x** formed sultam **2c** in 23% yield under partially optimized photoredox conditions (**Chapter 2.2.1, Table 1**, entry 4).

2.4.1 Attempted Optimization of Photoredox Conditions

At this point, the best course of action was to return to phosphate bases, as the second highest yield achieved in the initial photoredox survey was for the reaction of **1x** using $[Bu_4N][OP(O)(OBu)_2]$ (**Chapter 2.2.1**, **Table 1**, entry 4). Additionally, $[Bu_4N][OP(O)(OBu)_2]$ was used for lactam synthesis in our previous work,[207] and sultams are more structurally analogous to lactams than ureas. The efficiency of phosphate bases for photoredox C-H amination following a PCET mechanism has been demonstrated by Knowles' lab and other prominent groups.[273–275,287–289,297,298] This inspired further confidence, because the photoredox conditions investigated here were assumed to follow a PCET mechanism (**Chapter 1.5**, **Scheme 32**), akin to that proposed for the photoredox C-H amidation of *N*-acyloxyureas (**Chapter 1.5**, **Scheme 31**, **Scheme 32**).[205–207,270–275] Using the phosphate base, $[Bu_4N][OP(O)(OBu)_2]$, several catalytic base iterations were surveyed (**Table 14**).

Table 14. Attempted phosphate base loading optimization for photoredox conditions.

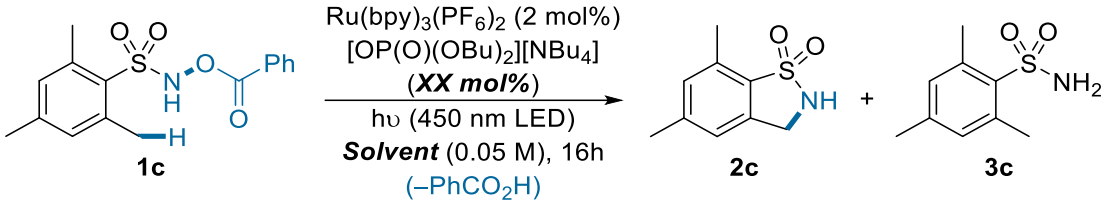

Entry	Solvent	Base Loading (mol %)	1c (%)	2c (%)	3c (%)
1	CH_2Cl_2	5[b]	-	13	45
2	CH_2Cl_2	80[b]	<5	<5	37
3	CH_2Cl_2	80[b,c]	65	5	<5
4	CH_2Cl_2	1[b]	-	68	7
5	CH_2Cl_2	1[b]	-	42	28
6	CH_2Cl_2	1[b]	<5	63	15
7	CH_2Cl_2	1[b]	-	47	23
8	CH_2Cl_2	0[d]	50	50	-
9	$(CH_2Cl)_2$	0[d,e]	-	95	-

[a]Conditions: 1c (0.1 mmol), $Ru(Bpy)_3(PF_6)_2$ (2.0 mol %) and **desired quantity of $[Bu_4N][OP(O)(OBu)_2]$** were solubilized in $(CH_2Cl)_2$ (0.05 M) within an 8 mL Kimax glass vial with a Teflon screw cap, purged with argon gas on ice and irradiated with 450 nm light using 12 V flexible blue LED strip lights for 16 h. [b]Yields determined by ^1H NMR analysis using 1,3,5-trimethoxybenzene as an internal standard. [c]Catalyst was omitted. [d]Yields determined by ^1H NMR analysis; integration of known peaks compared to combined integration of peaks from unreacted starting material and released carboxylate. [e]Run for 36 h.

The solvent was changed to CH_2Cl_2 at this point, in part due to the increased phosphate base solubility, but also because the initial photoredox conditions used CH_2Cl_2 (**Chapter 2.2.1**, **Table 1**), as do other methodologies reporting C-H amidation through a PCET mechanism.[287–289,297,298] It should also be noted that accurate mass measurements are difficult with phosphate bases of this nature without a glovebox, as their high hydrophilicity allows for rapid hydration upon contact with air. The initial goal was to run the reaction of **1c** with the conditions used for the reaction of **1x** (**Chapter 2.2.1**, **Table 1**, entry 4). The sultam formed in 13% yield using 5 mol% $[Bu_4N][OP(O)(OBu)_2]$, but the sulfonamide was the major product (**Table 14**, entry 1).

A reaction with 80% base loading was run to analyze reaction efficiency with base equivalency approaching the nitrene precursor (**Table 14**, entry 2). The yield decreased significantly while

giving a comparable reduction yield. Running the 80 mol% reaction again with the catalyst omitted surprisingly increased the product yield slightly (Entry 3) and about 2/3 of the starting material remained after the reaction time, indicating that catalyst is required for full substrate consumption. The base likely introduces side reactions that consume the starting material and base-induced α-elimination may generate some free nitrene that can cyclize to form the product in low yield.

When tested with 1 mol% base, the sultam was formed in the highest yield (68%) observed under photoredox conditions (**Table 14**, entry 4), with comparable yields (70% / 72%) to thermal base-induced C-H amidation (**Chapter 2.3.2**, **Table 8**, entries 5-6 / **Table 9**, entry 6). Unfortunately, repeating the reaction in triplicate gave inconsistent yields of 42%, 63% and 47% (Entries 5-7).

With the apparent finding that lower base loadings gave higher, yet inconsistent yields, the next step was to conduct a control reaction in the absence of base (**Table 14**, entry 8). After sixteen-hours, the desired product was formed in 50% yield with 50% remaining starting material, with no traces of sulfonamide byproduct. A similar solvent compatible with photoredox conditions was then sought and a control reaction was run in DCE; the starting material was completely consumed, forming desired sultam in 95% yield, again with no traces of **3c** (Entry 9). DCE was then selected as the optimal solvent, and phosphate bases were excluded from further photoredox optimization.

With DCE established as a uniquely effective solvent for the amination reaction, the prospect of running an entirely metal-free reaction with an organic photocatalyst was explored (**Scheme 40**).

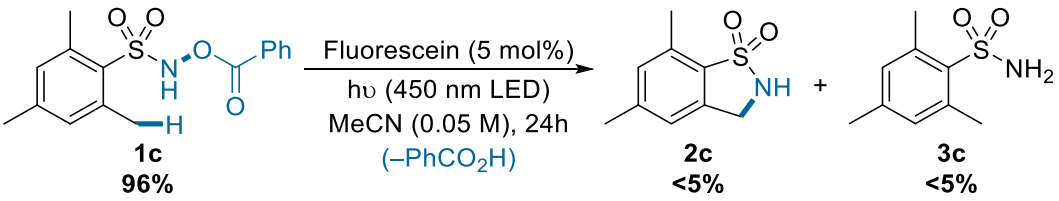

Scheme 40. Attempted metal-free sultam synthesis with Fluorescein as a photocatalyst.

Fluorescein was selected based on its similar excited state reduction potential to $Ru(Bpy)_3$ (0.78 V vs. 0.77 V). Fluorescein was an ineffective catalyst which gave less than 5% yield each of the sultam and sulfonamide, leaving 96% of the starting material unreacted. With this observation, $Ru(Bpy)_3(PF_6)_2$ was retained as the optimal photocatalyst.

A quick round of concentration optimization was performed to determine if the reaction could proceed using a lower solvent volume, in an effort to decrease the environmental impact and toxicity concerns associated with DCE (**Table 15**). Entry 1 is equivalent to **Table 14**, entry 9.

Table 15. Viability of photoredox conditions at higher concentrations.[a,b]

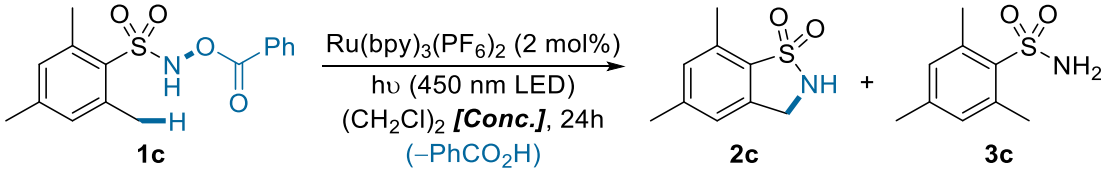

Entry	Concentration (M)	1c (%)	2c (%)	3c (%)
1	0.05[c,d]	-	95	-
2	0.5	-	91	<5
3	1.0	-	94	<5

[a]Conditions: 1c (0.1 mmol) and $Ru(Bpy)_3(PF_6)_2$ (2.0 mol%) were solubilized in $(CH_2Cl)_2$ at the desired **concentration** within an 8 mL Kimax glass vial with a Teflon screw cap, purged with argon gas on ice and irradiated with 450 nm light using 12 V flexible blue LED strip lights for 24 h. [b]Yields determined by ^{1}H NMR analysis using 1,3,5-trimethoxybenzene as an internal standard. [c]Yield determined by ^{1}H NMR analysis; integration of known peaks compared to combined integration of peaks from unreacted starting material and released carboxylate. [d]Run for 36 h.

Running the reaction at higher concentrations of 0.5 M and 1.0 M gave the product in 91% and 94% yield, respectively (Entries 2-3), thus the reaction of substrate **1c** is possible with less solvent.

Given the apparent evidence that photoredox reactions are possible with lower solvent volume, several reactions were prepared to test the current conditions for substrates bearing a single *ortho*-methyl group (**Table 16**). As described in **Chapter 2.3.3**, these substrates only have one primary C-H amination site, and steric interactions imposed by the *ortho*-methyl group may introduce a confirmational bias, orienting the free nitrene away from the desired amidation position (**Scheme 39**), thus explaining the lack of product formation and the high yields observed for reduction.

Table 16. Attempted optimization to enable cyclization of *ortho*-monomethyl substrates.[a,b]

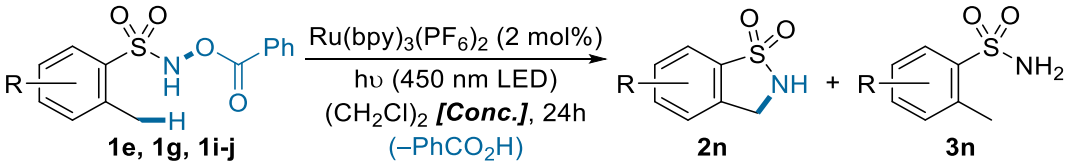

1e: R = 3-Cl, **1g**: R = 5-F, **1i**: R = 5-NO_2, **1j**: R = 4-Me

Entry	Substrate	Concentration (M)	1n (%)	2n (%)	3n (%)
1	**1e**	0.5	87	<5	5
2	**1g**	0.5	96	<5	<5
3	**1i**	0.5	86	<5	7
4	**1j**	0.5	80	<5	6
5	**1g**[c]	0.5	84	<5	7
6	**1g**	0.2	77	5	8
7	**1g**	0.1	85	6	6
8	**1g**[d]	0.05	62	18	9
9	**1g**	0.05	78	12	8

[a]Conditions: **1e, 1f, 1i or 1j** (0.1 mmol) and $Ru(Bpy)_3(PF_6)_2$ (2.0 mol%) were solubilized in $(CH_2Cl)_2$ at the desired concentration within an 8 mL Kimax glass vial with a Teflon screw cap, purged with argon gas on ice and irradiated with 450 nm light using 12 V flexible blue LED strip lights for 24 h. [b]Yields determined by ^{1}H NMR analysis using 1,3,5-trimethoxybenzene as an internal standard. [c]Purged with three freeze-pump-thaw cycles under vacuum to remove excess water and oxygen. [d]Yield determined by ^{1}H NMR analysis; integration of known peaks compared to combined integration of peaks from unreacted starting material and released carboxylate.

The *ortho*-monomethyl-*N*-acyloxysulfonamide substrates bearing 3-chloro (**1e**), 5-fluoro (**1g**), 5-nitro (**1i**) and 4-methyl (**1j**) substituents were left largely unconverted when were subjected to the reaction conditions (**Table 16**, entries 1-4). Considering the need for removal of water and oxygen in our publication concerning *N*-acyloxyureas,[207] and the fact that all reactions tested thus far were purged with argon, a reaction was run with substrate **1g** after purging the solution with three cycles of a freeze-pump-thaw degassing protocol under vacuum (Entry 5). The product yield improvement was negligible and excessive degassing was deemed unnecessary.

The previous optimization studies regarding base-induced thermal C-H amidation (**Chapter 2.3.2**) indicated that the reaction was more efficient under dilute conditions (**Table 8**). It was speculated that reaction dilution may also improve photoredox yields, and three concentration iterations were investigated for **1g**. Running the reaction at either 0.2 M or 0.1 M did not improve the reactivity

(**Table 16**, entries 6-7). Conducting the reaction at 0.05 M gave an encouraging result; the desired product was formed in 18% yield with only 9% reduction (Entry 8). Unfortunately, a second trial of the reaction at 0.05 M indicated that the result was not reproducible (Entry 9).

The poor reactivity with *ortho*-monomethyl-*N*-acyloxysulfonamides led to the consideration that 12 V flexible blue LED strips were too weak a light source to release significant photons and promote nitrene formation. A Kessil 40 W Tuna blue LED lamp was instead adopted for further optimization, with hopes that an increase in photon emission / absorption could give significant catalyst photoexcitation and allow efficient conversion of the *N*-acyloxysulfonamides (**Table 17**).

Table 17. Optimization for *ortho*-monomethyl substrates with Kessil 40 W Tuna LED lamp.[a,b]

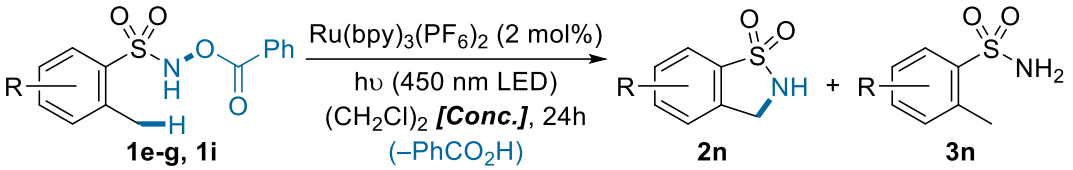

1e: R = 3-Cl, **1f**: R = 4-F, **1g**: R = 5-F, **1i**: R = 5-NO_2

Entry	Substrate	Concentration (M)	1n (%)	2n (%)	3n (%)
1	**1e**	0.05	<5	93	<5
2	**1e**[c]	0.05	94	<5	<5
3	**1g**	0.05	<5	93	-
4	**1g**[c]	0.05	92	<5	<5
5	**1f**	0.05	<5	28	23
6	**1i**	0.05	<5	69	27
7	**1e**	0.1	6	88	12
8	**1e**[d]	0.2	9	72	19
9	**1e**[e]	0.05	46	19	35

[a]Conditions: **1e, 1f, 1g or 1i** (0.1 mmol) and $Ru(Bpy)_3(PF_6)_2$ (2.0 mol%) were solubilized in $(CH_2Cl)_2$ at the desired **concentration** within an 8 mL Kimax glass vial with a Teflon screw cap, purged with argon gas on ice and irradiated with 450 nm light using a Kessil 40 W Tuna blue LED lamp for 24 h. [b]Yields determined by ^{1}H NMR analysis using 1,3,5-trimethoxybenzene as an internal standard. [c]Catalyst was omitted. [d]Run for 16 h. [e]Cooled using a stream of compressed air.

Substrates **1e** and **1g** were first resubmitted to the optimal conditions from the previous round (**Table 16**, entries 8-9) using the new light source (**Table 17**, entries 1,3), and an additional catalyst-free control reaction was prepared with each substrate (Entries 2,4). Both substrates reacted efficiently with the new light source to form the product in 93% yield and generated less than 5% product when the catalyst was omitted, verifying the necessity of the catalyst for reactivity (Entries 1-4). Substrates **1f** and **1i** bearing 4-fluoro and 5-nitro substituents reacted much less efficiently to form the products in 28% and 69% yield with the sulfonamide forming in 23% and 27% yield, respectively (Entries 5-6). Using the Kessil 40 W Tuna blue LED lamp enabled successful conversion with the largest number of *N*-acyloxysulfonamides up to this point.

Two concentration iterations were investigated with **1e**, again to see if reaction volume could be decreased. Running the reaction at 0.1 M decreased the yield slightly (**Table 17**, entry 7) with the

reduction yield tripling, and at 0.2 M, the product only formed in 72% yield (Entry 8) with 19% sulfonamide yield, clearly indicating that concentration increases made the reaction less selective.

After running reactions with the Kessil LED lamp the reaction vial became warm, and the solvent was visibly boiling. A control reaction was prepared to determine the degree that thermal energy from the LED lamp influenced the observed results (**Table 17**, entry 9). A reaction was prepared with substrate **1e** with a stream of compressed air aimed at the vial for continuous cooling. A massive yield plummet of 74% percent was observed for the cooled reaction, with the sulfonamide yield increasing to 35% and over half the starting material remaining. Thus, photoredox conditions at low temperature lack selectivity and fail to efficiently convert the starting materials.

With the finding that thermal energy was required to promote the reaction of certain substrates, the next goal was to determine if a catalytic reaction was possible in the absence of light when supplied with only thermal energy. A reaction with **1e** was prepared in an aluminum foil wrapped microwave vial and heated for 24 h in an oil bath at 85 °C, just over the DCE boiling point (**Scheme 41**). The previous concentration analysis showed that 0.1 M and 0.05 M were similarly effective for the reaction (**Table 17**, entry 7 vs. entry 1), thus 0.1 M was elected for the thermal reaction.

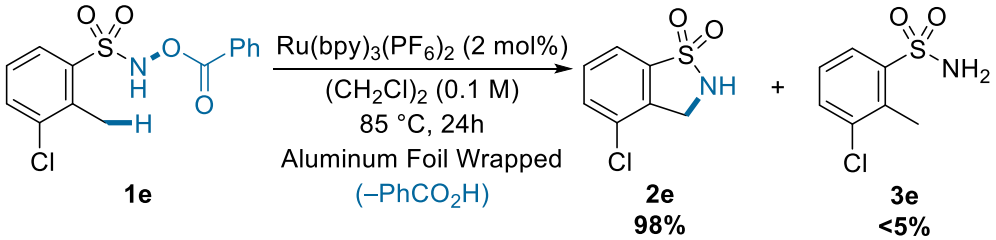

Scheme 41. Thermal $Ru(Bpy)_3(PF_6)_2$ catalyzed aminative cyclization in the absence of light.

Gratifyingly, the ruthenium catalyzed reaction run in the dark gave **2e** in 98% yield, the highest yield observed for the reaction of **1e** under any conditions. This control reaction placed the project at crossroads; the identification of $Ru(Bpy)_3(PF_6)_2$ as a superior catalyst suggested a new

mechanism, and further reaction development. On the other hand, this control was performed in parallel to several cyclization attempts under photoredox conditions, allowing for the successful synthesis of a small selection of benzo[*d*]sultams which are presented in **Chaper 2.4.2**. From this point, all further optimization and scope studies for the C-H amidation of *N*-acyloxysulfonamides were conducted under thermal $Ru(Bpy)_3(PF_6)_2$ catalysis conditions (**Chapter 2.5**).

2.4.2 Scope of Benzo[*d*]sultams from Photoredox Conditions

Throughout the second optimization round for photoredox amidation of *N*-acyloxysulfonamides, some substrates did in fact cyclize to form the corresponding benzo[*d*]sultam in high yield while using 12 V flexible blue LED strips as a light source. The ^{1}H NMR yields were recorded, but the products were not isolated (**Table 18**).

Table 18. Summary of successful benzo[*d*]sultam synthesis via photoredox C-H amination.[a,b]

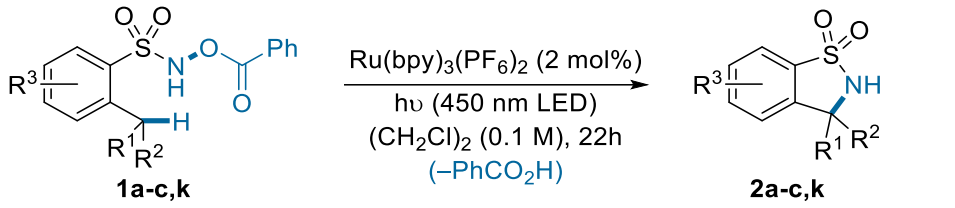

1a-c,k → **2a-c,k**

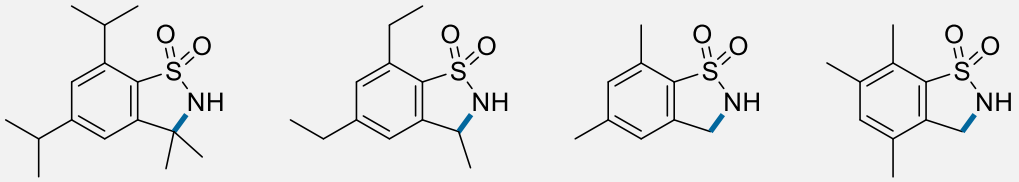

2a	**2b**	**2c**	**2k**
99%	99%	95%[c,d]	67%[e,f]

[a]Conditions: **1a-c, k** (0.1 mmol), $Ru(Bpy)_3(PF_6)_2$ (2.0 mol%) and $(CH_2Cl)_2$ (0.1 M) were added to an 8 mL Kimax glass vial with a Teflon screw cap, purged with argon gas on ice and irradiated with 450 nm light using 12 V flexible blue LED strip lights for 22 h. [b]Yields determined by ^{1}H NMR analysis using 1,3,5-trimethoxybenzene as an internal standard. [c]Run at 0.05 M. [d]Run for 36 h. [e]Run at 0.5 M. [f]Run for 24 h.

The reaction of both tertiary and secondary 2,4,6-trialkyl-*N*-acyloxyarylsulfonamides **1a** and **1b** at 0.1 M in DCE formed the corresponding benzo[*d*]sultams quantitatively. The initial control optimization reaction of **1c**, run for 36 h at 0.05 M in DCE, gave the product in 95% yield (**Table 14**, entry 9 / **Table 15**, entry 1). The reaction of durene derived substrate **1k** was tested at 0.5 M, which was temporarily viewed as optimal throughout the concentration optimization confirmation studies (**Table 15**, entry 2 / **Table 16**, entries 1-5), and the product **2k** was formed in 67% yield.

Overall, the photoredox conditions are only applicable for the formation of benzo[*d*]sultams from 2,6-disubstituted-*N*-acyloxysulfonamides. While some product did form throughout reactions of

*ortho*monomethyl-*N*-acyloxyarylsulfonamides, the yields were low without added thermal energy and often inconsistent (**Table 16**). Oddly, these reactions also led to minimal starting material conversion, in stark contrast to the failed reactions of *ortho*monomethyl-*N*-acyloxyaryl-sulfonamides under thermal base-induced conditions, which gave full starting material conversion and minimal product yield (**Table 12**). It is possible that the thermal ruthenium catalyzed reaction of 2,6-dialkyl-*N*-acyloxyarylsulfonamides is efficient enough to form product at room temperature, or that some thermal energy is required to initiate photoredox reactivity when using unbiased precursors. The formation of the reactive intermediate *N*-species may be reversible under either photoredox or low temperature ruthenium catalysis conditions, and either thermal energy or steric repulsion are required to overcome an initial energy barrier. While the product scope with these conditions was limited, the reaction is useful for the formation of specific 6-alkyl benzo[*d*]sultams from *N*-acyloxysulfonamides. The novel thermal ruthenium catalyzed conditions, however, represented a much more robust reaction, and it was applied to compile a substrate scope of benzo[*d*]sultams, as seen in the **Chapter 2.5**.

2.5 Ruthenium Catalyzed Sultam Synthesis

The optimization survey conducted to reveal reaction conditions for the synthesis benzo[*d*]sultams from *N*-acyloxysulfonamides through C-H amidation screened a variety of photoredox and thermal conditions. The majority of photoredox conditions investigated included a catalyst alone, or with base at room temperature, and the thermal conditions involved heating in the presence of a base. In the end, the most effective method for sultam synthesis through C-H amidation simply involved heating with $Ru(Bpy)_3$ as a catalyst. The presence of light and a base generally decreased the reaction efficiency and chemoselectivity. **Chapter 2.5** describes the final rounds of optimization (**Chapter 2.5.1**), which uncovered robust reaction conditions and enabled the successful formation benzo[*d*]sultams from *N*-acyloxysulfonamides, along with the compiled scope of thirteen benzo[*d*]sultams that were synthesized according to this method (**Chapter 2.5.2**).

2.5.1 Optimization of Ruthenium Catalyzed C-H Amidation

With the newly optimized reaction conditions for thermal ruthenium catalyzed C-H amidation, the next goal was to either verify optimality or find a better iteration of reaction conditions. **Table 19** tabulates the final optimization studies, with Entry 1 representing the current optimal conditions (**Chapter 2.4.1**, **Scheme 41**).

Table 19. Confirmation of optimal conditions for ruthenium catalyzed C-H amidation.[a,b]

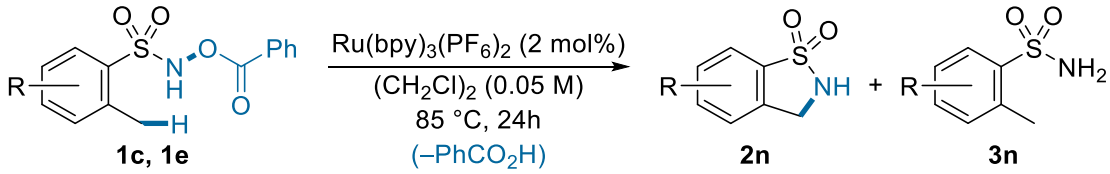

1c: R = 4,6-Me, **1e:** R = 3-Cl

Entry	Substrate	Solvent	Temperature (°C)	Time (h)	1 (%)	2 (%)	3 (%)
1	**1e**	$(CH_2Cl)_2$	85	24	-	98	<5
2	**1e**[c]	$(CH_2Cl)_2$	85	24	99	<5	-
3	**1c**	$(CH_2Cl)_2$	85	24	-	99	-
4	**1c**	CH_2Cl_2	60	22	-	97	<5
5	**1c**	$(CH_2Cl)_2$	60	22	-	95	<5
6	**1c**	$CHCl_3$	60	22	3	77	<5
7	**1c**	$CHCl_3$	85	22	-	78	6
8	**1c**	MeCN	85	22	97	<5	<5
9	**1e**	CH_2Cl_2	60	22	62	35	<5
10	**1e**	$CHCl_3$	85	24	95	<5	<5
11	**1e**	MeCN	85	24	99	<5	<5

[a]Conditions: **1c or 1e** (0.1 mmol), $Ru(Bpy)_3(PF_6)_2$ (2.0 mol%) and **solvent** (0.1 M) were added to a microwave vial, purged with argon gas on ice and heated at the **temperature** indicated for the **time** shown. [b]Yields determined by ^1H NMR analysis using 1,3,5-trimethoxybenzene as an internal standard. [c]Catalyst was omitted.

A control reaction was first prepared to test if product formation was possible in the absence of catalyst (**Table 19**, entry 2). As expected, minimal conversion of **1e** was observed and the product was formed in low yield. The reaction of 2,4,6-trimethyl-*N*-acyloxysulfonamide **1c** formed the product in 99% yield, a result that supports the optimality of the current conditions (Entry 3).

The next goal was to determine if a less toxic, more environmentally benign solvent could be used with similar efficiency. Acetonitrile, chloroform ($CHCl_3$) and CH_2Cl_2 were chosen as a result of the positive results with acetonitrile under previous conditions (**Chapters 2.3.2**, **2.3.3**) and the similarity of the chloroalkane solvents with DCE. The reaction of **1c** was investigated at 60 °C in CH_2Cl_2, $CHCl_3$ and DCE to compare organochlorine solvents at a temperature above the boiling point of CH_2Cl_2 (**Table 19**, entries 4-6). Interestingly, the reaction of **1c** in both CH_2Cl_2 and DCE at 60 °C gave high product yields of 97% and 95%, respectively (Entries 4-5). Using $CHCl_3$ at 60

°C enabled sultam formation in a moderate yield of 77% (Entry 6). Raising the temperature for the $CHCl_3$ reaction to the optimized 85 °C did not significantly improve the yield (Entry 7).

In contrast to the base-induced thermal reaction conditions (**Chapter 2.3**), the reaction of **1c** in acetonitrile with catalyst at 85 °C resulted in a lack of starting material conversion and less than 5% product yield (**Table 19**, entry 8). From these results it was deduced that the organochlorine solvents tested, particularly CH_2Cl_2, were similarly effective to DCE, but this was not actually the case. The reaction of *ortho*-monomethyl-*N*-acyloxysulfonamide substrate **1e**–which lacks the confirmational bias present for 2,6-dialkyl-*N*-acyloxysulfonamides–in CH_2Cl_2 at 60 °C only enabled product formation in 35% yield, leaving 62% starting material (Entry 9). Using either $CHCl_3$ or acetonitrile as the solvent for the reaction of **1e** at 85 °C essentially left the starting material unreacted (Entries 10-11). Overall, DCE acted as a uniquely effective solvent for the C-H amidation of *ortho*-monomethyl-*N*-acyloxysulfonamides, whereas the more facile C-H amidation of 2,6-dialkyl-*N*-acyloxyarylsulfonamides was possible in several organochlorine solvents.

2.5.2 Scope of Sultams from Thermal Ruthenium Catalyzed C-H Amidation

With the conditions uncovered that effectively enabled intramolecular C-H amidation of *N*-acyloxysulfonamides, the remainder of the study was met with optimism. The next goal was to expand the novel reaction and produce a representative scope, demonstrating that the reaction is general and robust. Several benzo[*d*]sultams were synthesized successfully by this method (**Table 20**) but efficient non-benzylic C-H amination was not achieved (**Table 21**).

The first action taken to survey the reaction scope was the investigation of the three substrates in the 2,4,6-trisubstituted-*N*-acyloxybenzenesulfonamide series (**1a**-**1c**). Encouragingly, cyclization products (**2a**-**2c**) of the tertiary, secondary and primary C-H amidation reactions were isolated in high yields of 80%, 97% and 89%, respectively. While the yields did not follow the typical reactivity trends that correlate with C-H bond dissociation energy, the steric interactions imposed by the isopropyl group in **1a** could have influenced the efficiency of the tertiary C-H amidation.

Returning to the previously studied 2,5-dicyclohexyl substituted starting material **1d** (**Chapter 2.3.3**), the optimal conditions formed the spirocyclic sultam product (**2d**) in 74% yield. Sultam **2e** was isolated in 85% yield following the reaction of 3-chloro substituted optimization substrate **1e**. Two additional halogenated *ortho*-monomethyl-*N*-acyloxysulfonamides were next investigated; benzo[*d*]sultams **2f** and **2g** substituted with fluorine atoms at the 4- and 5- positions were isolated in 50% and 71% yield, respectively. Analysis of the ^{1}H NMR spectra for 0.1 mmol test reactions of **1f** and **1g** showed that the sultams had formed in 86% and 87% yield, despite the increased BDE of the methyl C-H resulting from the high electronegativity of the fluorine atom. The lower yield obtained was again likely a result of isolation issues; fractions containing impurities were collected both before and after the purified sultam during column chromatography in each case.

Table 20. Benzo[*d*]sultam scope from ruthenium catalyzed intramolecular C-H amidation.[a]

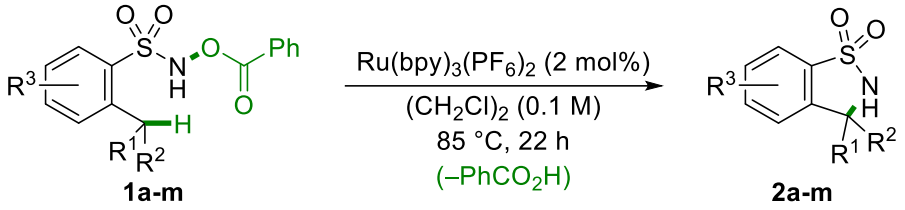

1a-m **2a-m**

2a
80%

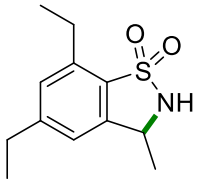

2b
97%[b]

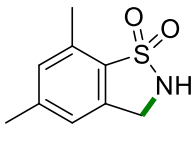

2c
89%[b]

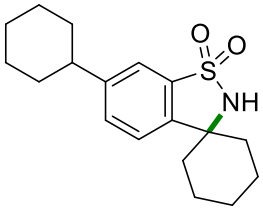

2d
74%

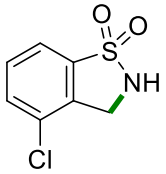

2e
85%

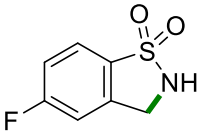

2f
50%
(86%)[c,d]

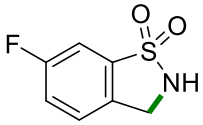

2g
71%
(87%)[c,d]

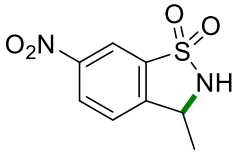

2h
98%

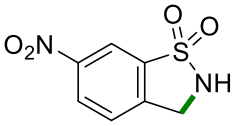

2i
(40%)[c,d]

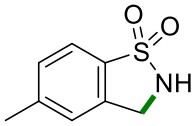

2j
66%[e]
(90%)[c,d,e]

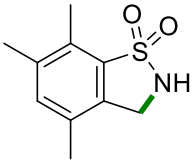

2k
80%

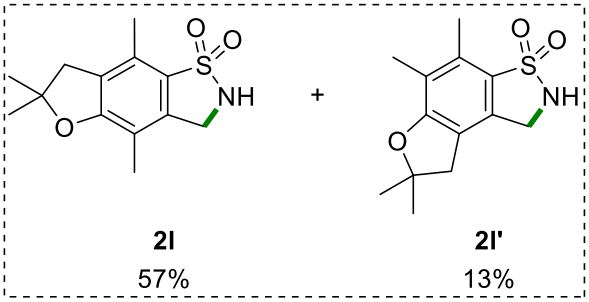

2l **2l'**
57% 13%

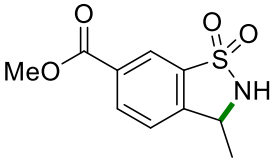

2m
90%

[a]Conditions: **1a-m** (0.5 mmol), $Ru(bpy)_3(PF_6)_2$ (2.0 mol %), $(CH_2Cl)_2$ (0.1 M) and a magnetic stir bar were added to a microwave vial, purged with argon gas on ice and heated to 85 °C in an oil bath for 22 h. [b]1.0 mmol scale. [c]Yields in parenthesis were determined by ^1H NMR analysis using 1,3,5-trimethoxybenzene as an internal standard. [d]0.1 mmol scale. [e]Reaction run at 100 °C.

Ortho-monoethyl substrate **1h** bearing the strong electron withdrawing nitro group as next submitted to the reaction conditions, allowing for isolation of the product sultam **2h** in 98% yield. Running the reaction with the analogous nitro substituted *ortho*-monomethyl substrate **1i** gave a less positive result, forming the desired sultam in 40% ^{1}H NHR yield with 8% of the sulfonamide. The reaction mixture was difficult to separate, and isolation attempts gave a mixture of the two compounds with additional impurities.

The 2,4-dimethyl substituted *N*-acyloxysulfonamide **1j** underwent C-H amidation in 90% ^{1}H NMR yield on a 0.1 mmol scale. When rerun on a 0.5 mmol scale, the product was isolated in a mixture by chromatography with a mass of 0.073 g and ~7 mol% ^{1}H NMR impurity. Assuming the sultam represents 93% of the "0.398 mmol" isolated (~0.371 mmol), a 74% yield could be possible. A second chromatography round allowed for isolation of the pure sultam in 66% yield.

Two additional 2,6-dimethyl-*N*-acyloxysulfonamides were then investigated for comparison to the 2,4,6-trimethyl substrate **1c**. Tetramethyl durene-derived *N*-acyloxysulfonamide **1k** reacted to form sultam **2k** in 80% yield. The reaction of unsymmetrical 2,3-dihydrobenzofuran derived substrate **1l**, containing two distinct *ortho*- methyl groups, led to isolation of the tricyclic benzo[*d*]sultam **2l** in 57% yield along with 13% yield of the opposite regioisomer (**2l'**) derived from the other possible C-H insertion. Finally, the electron poor substrate **1m** containing a methyl ester and a secondary C-H bond reacted to form the corresponding sultam (**2m**) in 90% yield.

The same non-benzylic C-H insertion precursors (**1t**-**1u**) investigated with previous conditions (**Chapters 2.2.2**, **2.3.3**), were also tested under thermal $Ru(Bpy)_3(PF_6)_2$ catalysis (**Table 21**).

Table 21. Limitations of ruthenium catalyzed non-benzylic C-H amidation.[a,b]

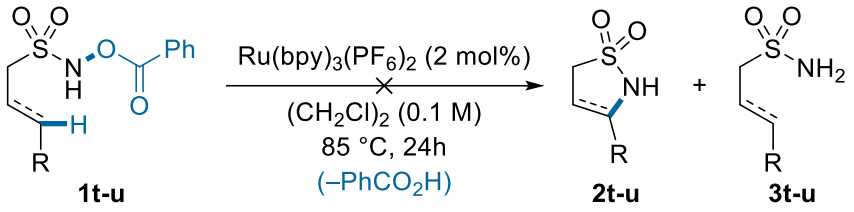

Starting Material	Expected Product	Side Product	Yield of 1t-u (%)	Yield of 2t-u (%)	Yield of 3t-u (%)
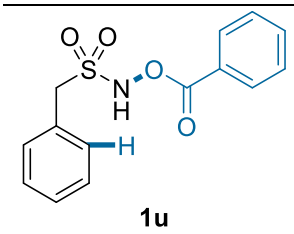 1u	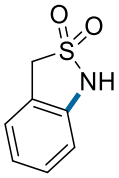 2u	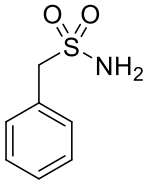 3u	93	0	<5
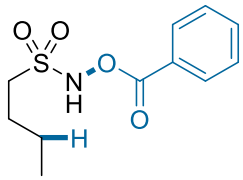 1t	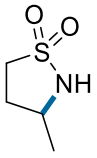 2t	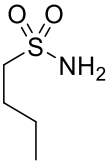 3t	53	40	0

[a]Conditions: **1t-u** (0.1 mmol), $Ru(bpy)_3(PF_6)_2$ (2.0 mol %), $(CH_2Cl)_2$ (0.1 M) and a magnetic stir bar were added to a microwave vial, purged with argon gas on ice and heated to 85 °C in an oil bath for 24 h. [b]Yields determined by ^1H NMR analysis using 1,3,5-trimethoxybenzene as an internal standard.

The investigation of substrate **1u** led to minimal starting material conversion, less than 5% yield of the reduced sulfonamide byproduct and no trace of the desired sultam. The reaction of *N*-(benzoyloxy)butane-1-sulfonamide (**1t**), however, resulted in approximately half of the starting material being converted to form the desired sultam in 40% yield. While the yield was not very synthetically useful, it shows promise for future studies toward the intramolecular C-H amidation of aliphatic *N*-acyloxysulfonamides. The formation of a stable ruthenium-nitrene intermediate from aliphatic *N*-acyloxysulfonamides may be more difficult with this catalyst than for *N*-acyloxyarylsulfonamides, thus explaining the lack of conversion for these starting materials.

2.6 *N*-Acyloxysulfonamide C-H Amidation: Mechanistic Discussion

Determination of the reaction mechanism for all C-H amidation conditions surveyed would be valuable to understand the variations in reaction efficiency. Mechanistic studies could give insights toward the future of this chemistry and the possibility of extension to accommodate other substrate classes. While mechanistic studies were not conducted here, other researchers have published data related to the reactivity of *N*-hydroxysulfonamides and analogous azides under similar conditions, allowing for the formulation of a mechanistic hypotheses consistent with the results obtained.

2.6.1 Potential Mechanisms for Photoredox C-H Amidation

The best way to discuss possible mechanisms under photoredox conditions is to start with the project initiation. As described in **Chapter 1.5**, mechanistic studies for the previous C-H amidation of *N*-acyloxyureas gave evidence that the reaction was initiated through PCET (**Scheme 32**).[205–207] This project was initially planned as an extension of the previous research, and thus a similar mechanism (**Figure 40**) was expected during the project design and optimization (**Chapter 2.2**). Two additional mechanisms are also described (**Figure 41**, **Figure 42**).

For the PCET-based mechanism (**Figure 40**), the initial absorption of blue light forms the excited state photocatalyst that undergoes the putative PCET mechanism upon formation of hydrogen-bond complex **II** with *N*-acyloxysulfonamide **I** and triethylamine. This gives a Ru(I) complex along with amidyl radical **III**. Carbonyl reduction by Ru(I) enables N-O bond cleavage and loss of the benzoate anion to form triplet nitrene **IV**, with concurrent regeneration of the active catalyst. Computational studies with *N*-acyloxyureas showed that reduction of the analogous amidyl radical (**III**) is favourable, whereas direct reduction of the carbonyl by Ru(II)* or Ru(I) is not (**Figure 41**, **Figure 42**), a convincing argument for the PCET mechanism. A singlet nitrene was ruled out

because optically pure *N*-acyloxyureas gave full racemization, and radical clock probes led to cyclopropane ring-opening. Thus, the triplet nitrene **IV** undergoes stepwise C-H amidation.

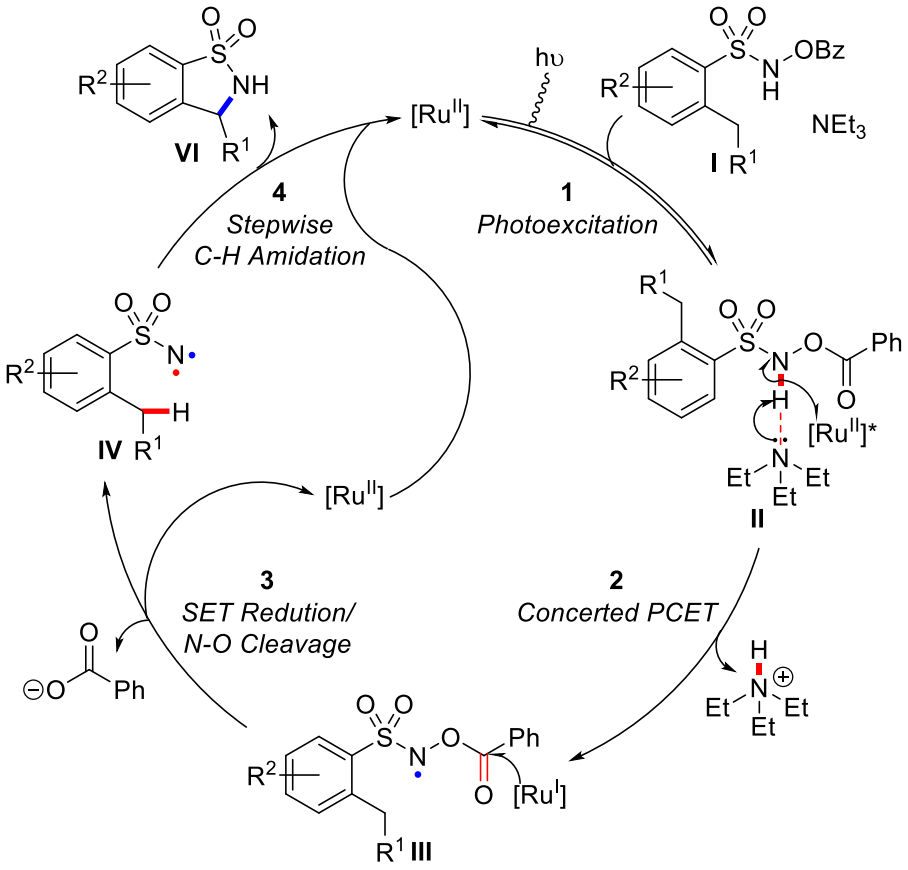

Figure 40. Initial expected PCET mechanism for photoredox C-H amidation.

While mechanisms of the following nature are rarely seen in the literature,[218–220] two additional photoredox mechanisms (**Figure 41**, **Figure 42**) with standard steps from the H-L-F reaction (**Chapter 1.4.2**, **Scheme 15**, **Scheme 16**) were considered.[213,216,217,221–225] First, an oxidative quench manifold can be visualized (**Figure 41**): initial reduction of *N*-acyloxysulfonamide **I** at the carbonyl would generate ketyl radical **II**.[299–301] Alas, this step is unfavored, and can be easily ruled out; Ru(II)* is too weak a reductant ($E[Ru^{III}/ Ru^{II}*] = -0.81$ V vs SCE) to engage in electron transfer with an ester-type carbonyl ($E_{1/2} \approx -2.24$ V vs SCE). The following steps, however, are more plausible.

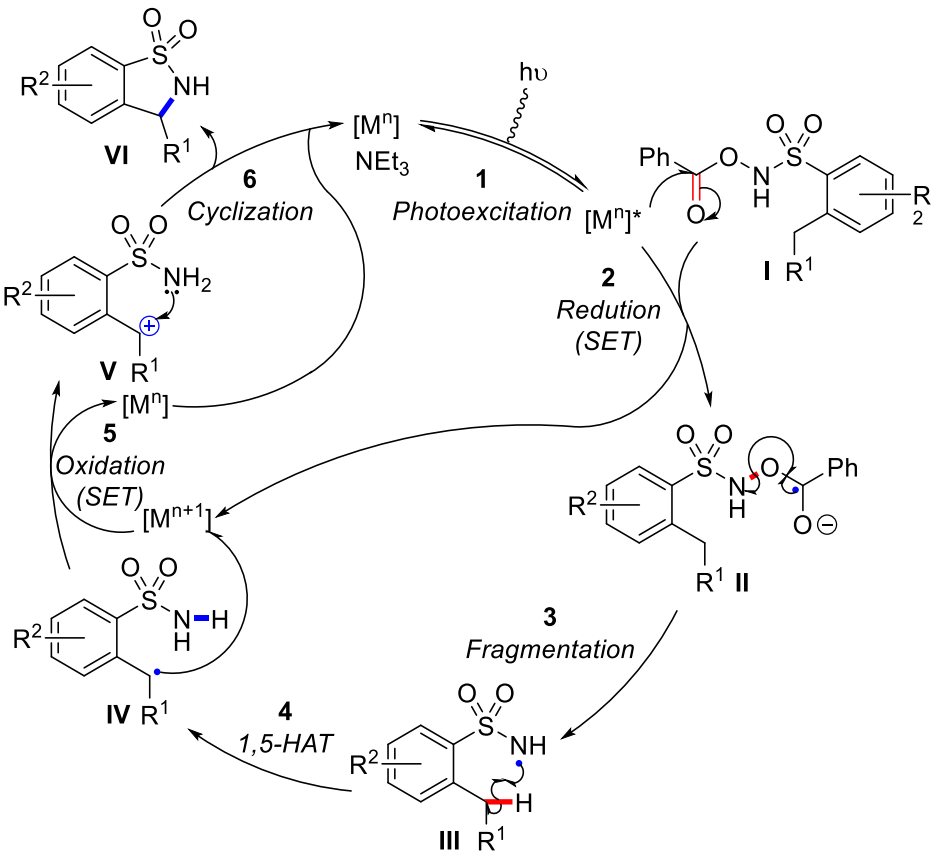

Figure 41. Unlikely oxidative quench mechanism for C-H amination with *N*-oxy precursors.

Fragmentation of **II** would generate amidyl radical **III** and subsequent 1,5-HAT would give benzylic radical **IV**. Ru(III) could theoretically oxidize (E[Ru(III)/ Ru(II)] = 1.29 V vs SCE) the radical to benzylic carbocation **V**, akin to other photocatalysts,[220,300–304] but this step is unlikely as the reduction potential for benzylic cations [$E_{1/2}$ = 0.16 V (3°) – 0.73 V (1°) vs SCE] falls outside the +/- 0.5 V range typically required for effective electron transfer from a photocatalyst.[121,206] Finally, cyclization by nucleophilic attack of the sulfonamide generates sultam **VI**. Photoredox C-H amination reactions with this type of oxidation are rare,[218–220] and interrupted H-L-F cascades that harness intermediate carbon radicals (**IV**) for intermolecular reactions are more common.[213]

An alternative H-L-F based mechanism for C-H amidation is next worth discussing (**Figure 42**). Following photocatalyst excitation, the reductive quench of the Ru(II)* complex by an equivalent

of triethylamine [$E_{1/2}$ = 0.96 V vs SCE] could generate Ru(I). One would expect that the carbonyl of *N*-acyloxysulfonamide **I** could be reduced by Ru(I) to generate ketyl radical **II**, but Ru(I) is again not reducing enough ($E[Ru^{II}/ Ru^{I}]$ = −1.33 V vs SCE) to efficiently transfer electrons to the desired carbonyl ($E_{1/2}$ ≈ −2.24 V vs SCE). It is possible, however, that the electron withdrawing nature of the sulfonamide group increases the carbonyl reduction potential. In a similar fashion to the reaction in **Figure 41**, fragmentation of **III** and subsequent 1,5-HAT generates benzylic radical **V**, which is oxidized to carbocation **VI**, in this case, using the triethylammonium radical cation.

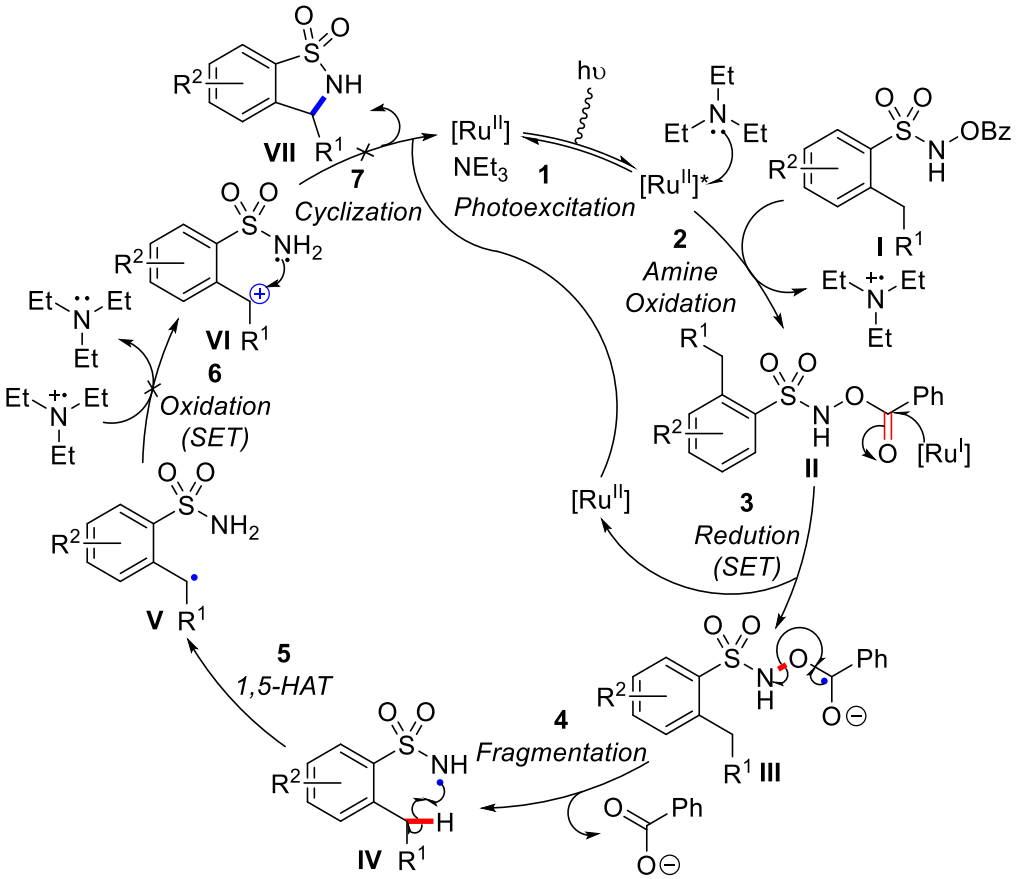

Figure 42. Possible oxidative quench mechanism for C-H amination with *N*-oxy precursors.

The free reduced sulfonamide byproduct could form by intermolecular hydrogen atom transfer with solvent or base from similar radical intermediates that would be produced through the stepwise C-H amination reactions in any of the three proposed mechanisms above (**Figure 43**).

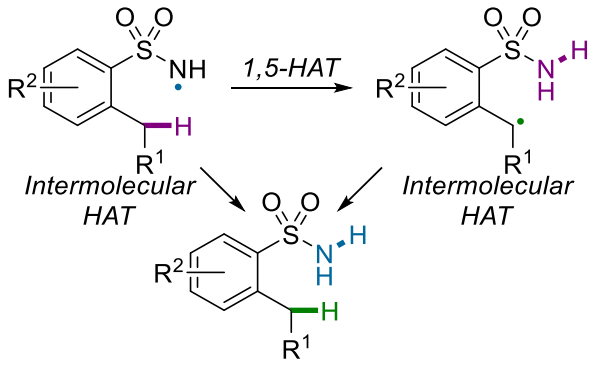

Figure 43. Potential side reactions to form the sulfonamide byproduct in photoredox reactions.

While most photoredox reactions are dominated by SET, energy transfer can also occur.[121] Chang published C-H amidation methodology with *N*-acyloxy nitrene precursors using $Ru(bpy)_3(PF_6)_2$ as a triplet sensitizer.[175] The substrates required full deprotonation for energy transfer to occur. While some *N*-acyloxysulfonamide may be deprotonated here (Piloty's acid p*K*a = 15.4, Et_3N^+H p*K*a = 9), energy transfer could also occur with neutral substrates. Alternatively, PCEnT mechanisms analogous to PCET are possible but rare (**Scheme 42**).[305,306] These mechanisms both allow direct access to a triplet nitrene, the mechanistically supported intermediate for *N*-acyloxyureas.[205–207]

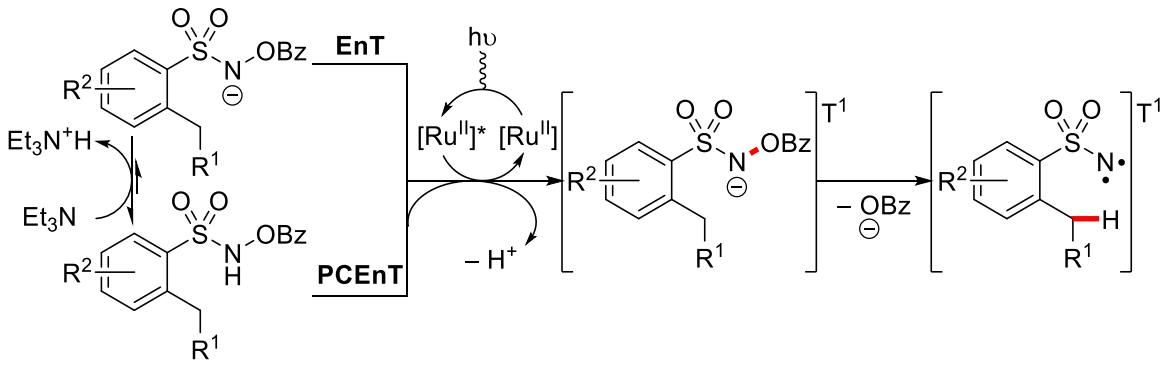

Scheme 42. Photoredox initiation through triplet-triplet energy transfer to form a triplet nitrene.

Other than **Figure 41**, any of the proposed mechanisms could theoretically be responsible for the formation of sultam **2a** though tertiary C-H amidation under the initial photoredox conditions with base, along with the minimal product formation of **2c**. For the latter unbiased substrate, reduction

to the sulfonamide may be the major pathway and the base-induced side reaction that occurs in the absence of catalyst may have simultaneously allowed for the sultam to form in comparable yield.

Overall, the photoredox conditions used to produce a small scope appear to be consistent with an EnT mechanism. The reactions were conducted without a basic additive, which essentially rules out the PCET mechanism, the H-L-F mechanism initiated by the oxidation of triethylamine, and the EnT mechanism requiring prior deprotonation, as all three options require a base. Species capable of acting as hydrogen bond acceptors, or sacrificial oxidants could be present in the reaction mixture to enable PCET or H-L-F mechanisms, but an EnT mechanism from the neutral substrate is more likely. The lack of substrate conversion with *ortho*-monoalkyl-substrates thus may be a result of insufficient steric forces; the initial energy transfer may be reversible, and the N-O bond cleavage may only occur if enough steric repulsion is present to effectively lengthen the N-O bond in the triplet state, preventing reverse energy transfer or another triplet decay pathway. The bulkiness of 2,6-dialkyl-*N*-acyloxyarylsulfonamides may also increase the rate of dissociation for the intermolecular collision complex to prevent reverse energy transfer.

It is worth noting that the excitation of $Ru(bpy)_3$ with light significantly increases its oxidation potential and that absorption of light by certain *N*-acyloxysulfonamides may decrease their reduction potential. There may simply be a chance that photoexcitation of either component increases the likelihood of an N-O bond oxidative addition mechanism, allowing for subsequent C-H insertion or C-H activation reactivity (**Figure 48**).

2.6.2 Potential Mechanisms for Thermal Base-Induced C-H Amidation

The mechanism for the base-induced thermal C-H amidation of *N*-acyloxysulfonamides is likely similar to that for the thermolysis of analogous azides,[119,129,131–133,307] which give products derived from free nitrenes in both the singlet and triplet state, including products of rearrangement, aziridination, and C-H insertion with aliphatic and aromatic solvents.[123,124,129–132] Most importantly these reactions form sultams and sulfonamides, likely via intramolecular C-H insertion by a singlet state nitrene and hydrogen abstraction from solvent molecules by a triplet nitrene, respectively. Moreover, the triplet nitrene could potentially engage in C-H insertion.[119,129,131–133,307] While rearrangement reactivity dominates the thermolysis of *N*-oxysulfonamides,[158–160] free nitrene products are observed from other *N*-oxy precursors.[158,294,295,308–312] In alignment with these reports of *N*-oxy precursors, the reaction is likely initiated through sulfonamide N-H deprotonation by *i*-Pr_2NEt, accompanied by ejection of the carboxylate, a process that overall constitutes an α-elimination (**Scheme 43**).[112,116,313]

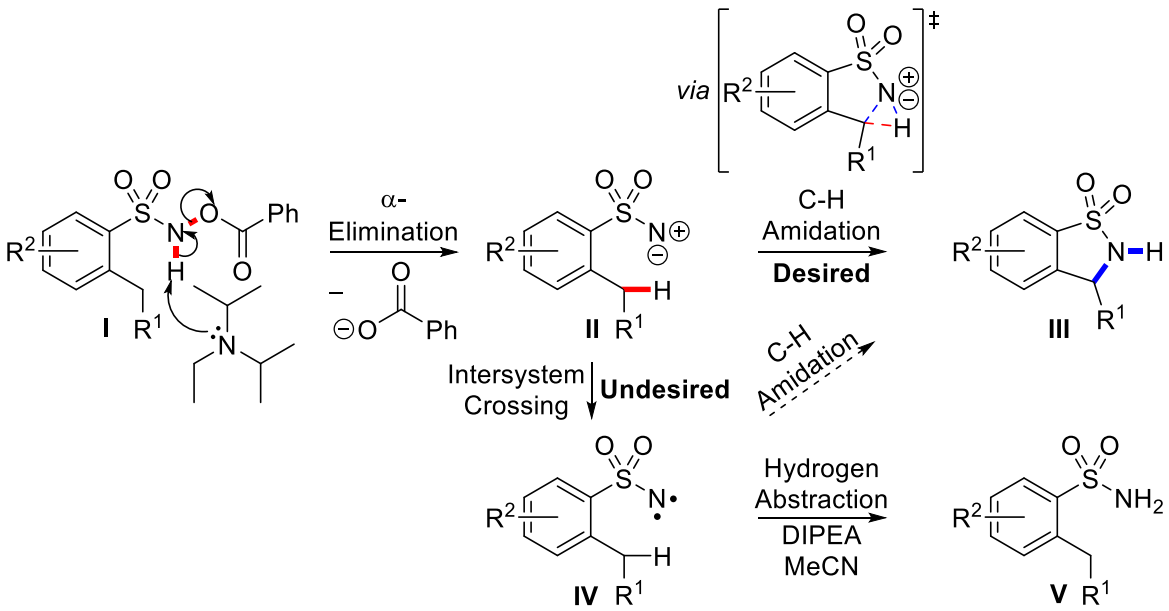

Scheme 43. Mechanism of sultam and sulfonamide formation by base-induced thermolysis.

The α-elimination results in the formation of free nitrene **II**, which can undergo a concerted C-H amidation reaction, likely via a three-centered transition state to afford the benzo[*d*]sultam product **III**. The rate of C-H insertion competes with the rate of intersystem crossing from the singlet state nitrene **II** to the more stable triplet ground state **IV**. Following intersystem crossing, the triplet nitrene can also undergo C-H amination, but its diradical nature introduces side reactivity such as hydrogen atom abstraction from molecules of solvent or base to form the free sulfonamide **V**.

While the mechanism for the α-elimination reaction is likely concerted, there is a possibility that a stepwise α-elimination could occur (**Scheme 44**). Because the p*K*a for Piloty's acid is 15.4, and that for triethylamine (or analogous tertiary amines) is 9, there is a possibility that the electron withdrawing nature of the benzoyl group lowers the p*K*a sufficiently so that a small concentration of the corresponding anion can form, allowing for the carboxylate to leave in a second step.

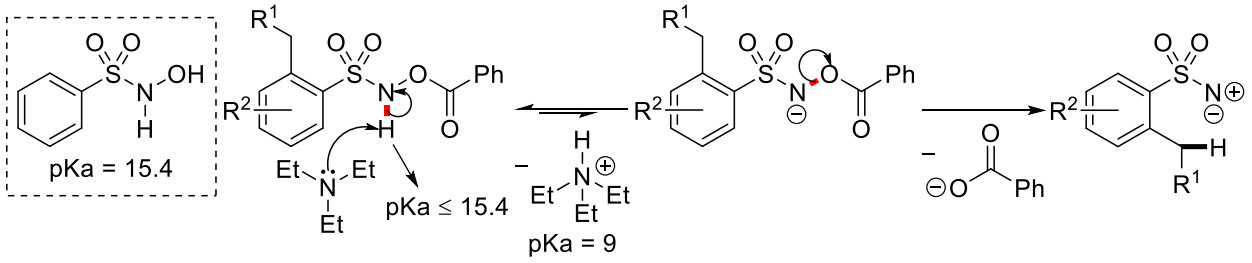

Scheme 44. Potential stepwise mechanism for α-elimination of *N*-acyloxysulfonamide.

As described, an α-elimination mechanism is most consistent with the results (**Table 11**). The reaction of 2,6-dialkyl-*N*-acyloxyarylsulfonamides with secondary or tertiary C-H bonds at the benzylic position formed sultams in moderate to high yield, consistent with a rapid C-H insertion. The analogous *ortho*-disubstituted substrates with primary C-H bonds only gave modest yield, suggesting that ISC and hydrogen atom abstraction compete with C-H insertion, a phenomenon that is even more pronounced with *ortho*-monoalkyl-substrates, for which bond rotation may further separate the nitrene intermediate and the desired C-H bond, favouring ISC with minimal

C-H amination. Conducting a reaction with an enantiopure substrate could give insight about the spin state of the reactive nitrene and help quantify the relative proportion of nitrene in the singlet vs triplet state. While these reactions produced sultams in the highest yields from apparent free nitrene intermediates, these unstabilized synthetic intermediates are not viable for robust C-H amidation conditions due to the competing C-H abstraction process, regardless of the method for nitrene formation.

2.6.3 Potential Mechanisms for Ruthenium Catalyzed C-H Amidation

The final set of reaction conditions for benzo[*d*]sultam synthesis through C-H amidation relied on ruthenium catalysis at elevated temperature in the absence of light and a base. The reaction likely follows a mechanism involving a ruthenium stabilized nitrene, as seen in studies by Meggers group with *N*-oxy nitrene precursors[194–196,314,315] and azides,[315–318] where ruthenium complexes analogous to $Ru(bpy)_3$ were used for C-H amination. Meggers' catalysts feature weakly coordinated acetonitrile ligands that easily dissociate and open coordination sites for substrate binding. Indeed, the reaction of *N*-acyloxysulfonamide **1c** in CH_2Cl_2 at 40 °C with $RuCl_2(bpy)_3$ containing weakly coordinated chloride ligands formed the desired sultam in 60% ^1H NMR yield (**Scheme 45**). While this yield is lower than at 60 °C with $Ru(bpy)_3(PF_6)_2$ (**Chapter 2.5.1**, **Table 19**,entry 5), it shows that ruthenium catalyzed C-H amidation pursues with weakly coordinating ligands.

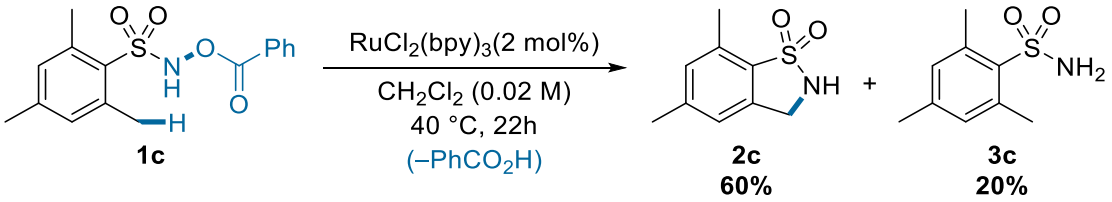

Scheme 45. C-H amidation using a Ru(II) catalyst with weakly coordinated chloride ligands.

The final optimal conditions for this reaction made use of DCE, a solvent which can act as an electrophile for S_N2 reactions.[319–321] With the nucleophilicity of pyridine, *N*-alkylation could occur on the bipyridine ligand, generating an *N*-alkyl pyridinium ring that can no longer chelate to the ruthenium center, allowing facile ligand substitution with the desired substrate (**Scheme 46**).

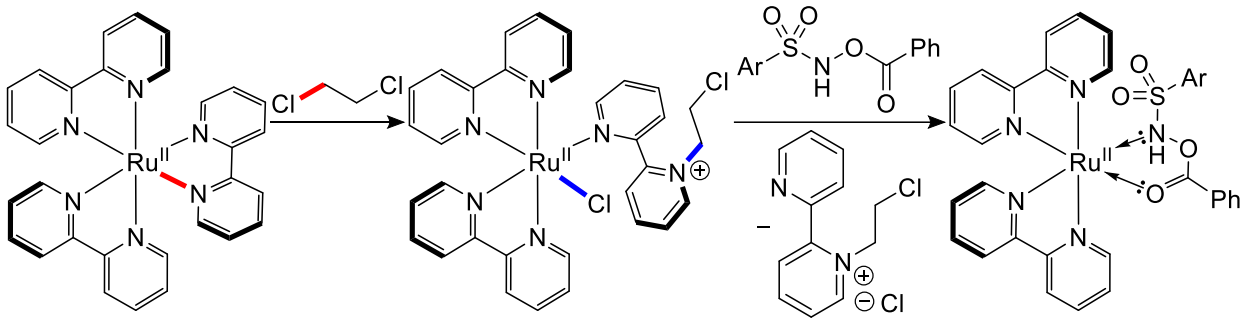

Scheme 46. Potential role of DCE: *N*-alkylation of pyridine ligands opens coordination sites.

Unfortunately, the bipyridine *N*-alkylation theory does not account for sultam formation from 2,6-dialkyl-*N*-acyloxyarylsulfonamides in less electrophilic chloroalkane solvents. Since bipyridine ligands can freely dissociate, the substrate may bind to some degree in the absence of chloroalkane electrophiles, likely by initial ligation of the Lewis basic carbonyl. The strength of chelation, however, is inevitably lower than that of 2,2′-bipyridine, which contains two strong Lewis basic sites. The ligand binding equilibrium should therefore favour association of 2,2′-bipyridine (**Figure 44**, k_1). Upon carbonyl ligation with 2,6-dialkyl substrates, the steric bulk may prevent reapproach of the bipyridine ligand (lower k_1), allowing time for the substrate to chelate and form a nitrene (**Figure 44**, k_3). Alternatively, the bulky precursors could increase the rate for carboxylate leaving group extrusion to a point where it is comparable to the dissociation rate, allowing nitrene formation (higher k_3). It is also possible that pyridine *N*-alkylation occurs to some degree with less electrophilic chloroalkane solvents[321] to produce a low concentration of active catalyst that can catalyze C-H amidation with biased 2,6-dialkyl substrates but is too minimal to react with

*ortho*monomethyl substrates, a phenomenon which could also be influenced if steric interactions indeed increased the rate of carboxylate extrusion (**Figure 44**, k_3).

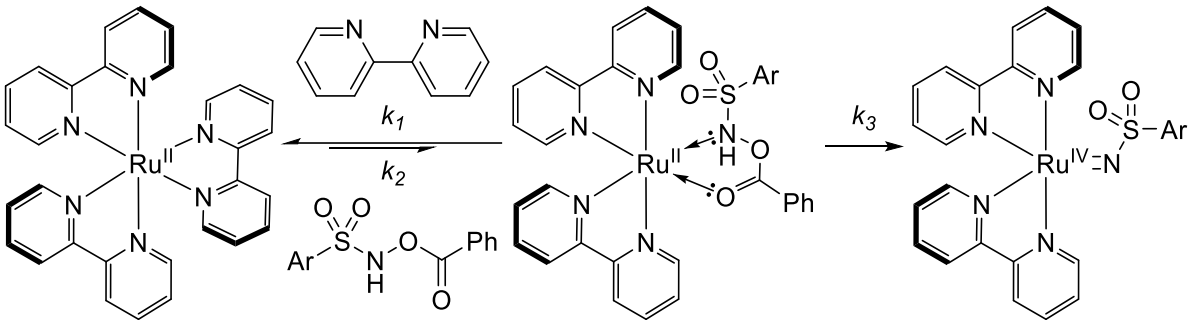

Figure 44. Ruthenium nitrenes without pyridine *N*-alkylation: k_1 may decrease with substrate bulk, approaching k_2. Steric bulk of 2,6-dialkyl substrates may increase k_3 to compete with k_1.

The carboxylate expulsion / nitrene formation step of initiation presents another mechanistic uncertainty, especially because most C-H amination reactions of *N*-acyloxy nitrene precursors involve a base.[156,162,174,194,196,197,291,322] Some reactions of *N*-acyloxy compounds, however, perform comparably without a base.[194,197,203,285] While *N*-acyloxysulfonamides are unable to be deprotonated by anything in the reaction vessel (Piloty's acid p*K*a = 15.4),[323] metal coordination of the nitrogen lone pair decreases the N-H p*K*a. Additionally, chelation through the carbonyl would weaken the N-O bond, further decreasing the p*K*a and accelerating the N-O bond cleavage (**Figure 45**). There is also evidence that the N-O bond cleavage mechanism with a Ru(II) species follows an S_N2-type oxidative mechanism.[324,325]

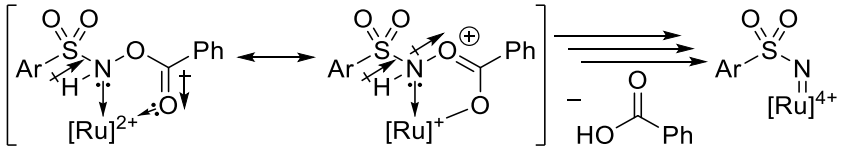

Figure 45. Chelation of *N*-acyloxysulfonamides lowers N-H p*K*a and weakens the N-O bond.

C-H amination and aziridination reactions of metal stabilized nitrenes follow two mechanistic regimes: concerted from a stabilized nitrene with singlet character, or stepwise from a diradical

nitrene with triplet character (**Chapter 1.4.1**). Meggers' group has found evidence for stepwise mechanisms in the formation of ureas[194] and carbamates[196] from *N*-oxy nitrene precursors using Ru(II) catalysts containing pyridyl-substituted NHC ligands. Their studies also pointed to a stepwise mechanism for sulfamide synthesis with azide precursors using Ru-pybox catalysts.[318] Additionally, radical intermediates were implicated for intermolecular Ru-porphyrin catalyzed C-H tosylamidation reactions,[326,327] and intramolecular C-H amidation reactions to form sulfamate esters with ruthenium paddlewheel complexes.[328] Based on these reports, the current reaction with the analogous *N*-oxysulfonamide group most likely also involves a stepwise mechanism from a triplet sulfonyl nitrene. On the other hand, Meggers' group found evidence that lactam formation from dioxazolone nitrene precursors follows a concerted mechanism,[314] as do the ruthenium-catalyzed C-H amination reactions of 2-azidoacetamides[113] and aliphatic azides.[317] They also found that carbocation intermediacy is likely in the aziridination of *N*-acyloxycarbamates, suggesting π-electron addition to a singlet state nitrene.[195] With the lack of experimental evidence for a specific mechanism, both pathways are outlined below (**Figure 46**, **Figure 47**).

The first potential C-H amidation mechanism described involves the stepwise pathway from a ruthenium stabilized triplet diradical nitrene that is commonly observed with ruthenium stabilized sulfonyl and acyl nitrenes as described above (**Figure 46**).[194,196,318,326–328] First, interaction of $[Ru(bpy)_3]^{2+}$ with the *N*-acyloxysulfonamide substrate **I** allows for the formation of nitrene **II** through N-O bond cleavage and expulsion of the carboxylate/ carboxylic acid leaving group. The details for this mechanistic step are unclear, but the N-O cleavage may involve an S_N2-type oxidative mechanism.[324,325] This process may lead to direct formation of a ruthenium stabilized nitrene in the triplet state, but initial formation of a singlet nitrene followed by intersystem crossing is more likely.[119,296,329] The ruthenium atom is likely in the Ru(IV) oxidation state, but evidence

has been found for active Ru(VI)bisimido complexes in nitrene transfer reactions with porphyrin ligands.[244,326,327,330,331] The triplet nitrene **II** can undergo 1,5-hydrogen atom transfer to form benzylic radical **III**, still containing a ruthenium-nitrogen bond. Radical homolytic substitution affords the final desired benzo[*d*]sultam product **IV** with simultaneous catalyst regeneration.

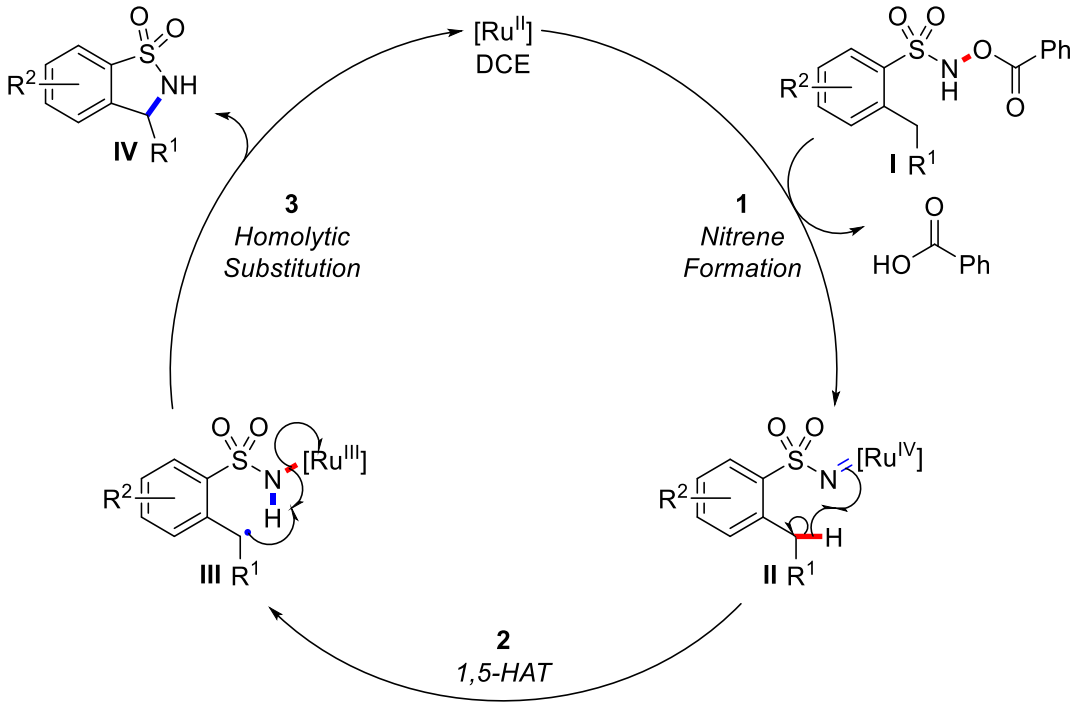

Figure 46. Potential stepwise mechanism for sultam synthesis by Ru-catalyzed C-H amidation.

The mechanisms for Ru-catalyzed C-H amidation with aliphatic nitrenes[316,317] and lactam-derived acyl nitrenes[314] were shown to be concerted and some studies attempting to identify the active spin state for ruthenium stabilized acyl[195] and sulfonyl[244,332] nitrenes were inconclusive. Additionally, C-H amidation reactions involving rhodium stabilized sulfonyl nitrenes tend to follow a concerted mechanism.[153,333–336] The possible concerted mechanism for sultam formation through C-H amidation of *N*-acyloxysulfonamides is shown in **Figure 47**. Once again, nitrene **II** can form by N-O bond cleavage of *N*-acyloxysulfonamide **I** with $[Ru(bpy)_3]^{2+}$ through an oxidative mechanism such as an S_N2-type addition.[324,325] The ruthenium-nitrene **II** can undergo concerted C-H insertion

through a stereo-controlled 3-centered transition state (**III**) to afford the desired benzo[*d*]sultam **IV**.

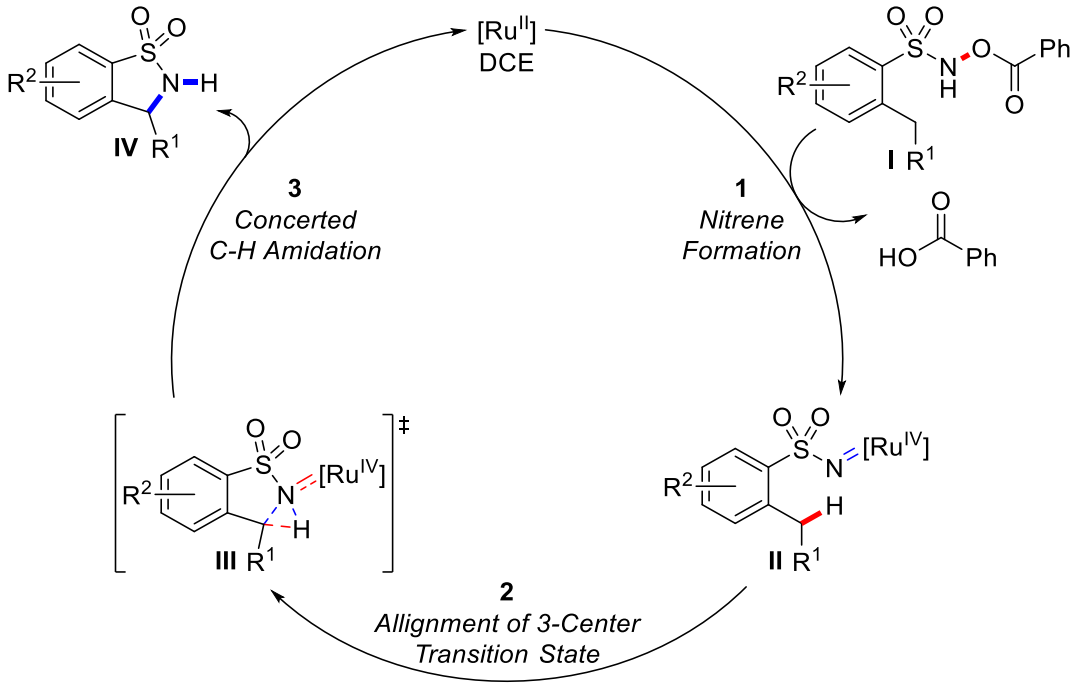

Figure 47. Potential concerted mechanism for sultam synthesis by Ru-catalyzed C-H amidation.

While less likely, another mechanism can be considered for the ruthenium catalyzed reaction. There is a possibility that a ruthenium-nitrene complex does not form through the course of the reaction, and that the reaction instead follows a C-H activation mechanism (**Figure 48**).[106] In this case, the activated hydrogen atom would have proton character rather than acting as a hydride, as seen in C-H insertion reactions. Following coordination of *N*-acyloxysulfonamide **I** to the ruthenium center, an oxidative N-O bond cleavage could occur, potentially through an S_N2 type mechanism as described, to form complex **III**.[324,325] Indeed, the oxidation of N-O bonds has played a key role in the mechanism of several ruthenium catalyzed C-H activation reactions.[324,325,337–340] Because Ru(II) catalysts have been applied previously for directed sp^3 C-H activation[341–345], and concerted metalation deprotonation (CMD) pathways have been observed for sp^2 C-H activation

with Ru(II),[346–348] a CMD-type mechanism can be visualized, employing the ruthenium carboxylate for the benzylic C-H activation. The C-H activation would allow for the formation of ruthenacycle **IV**, which could furnish the desired sultam **V** through reductive elimination.

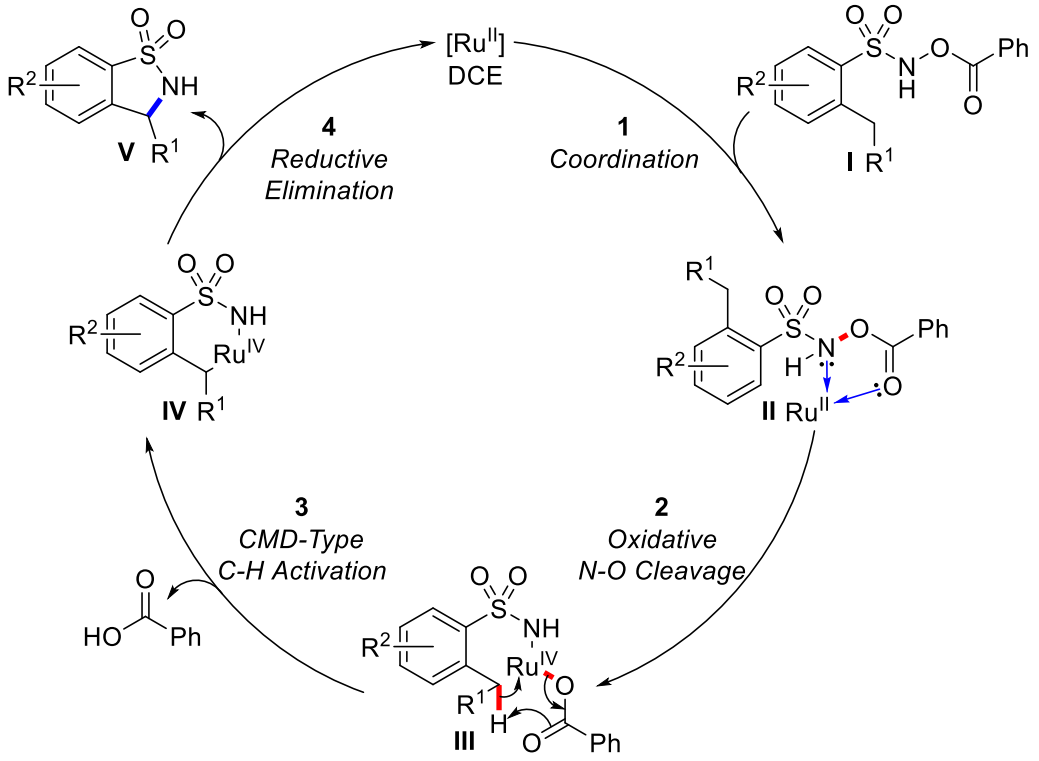

Figure 48. C-H activation mechanism to describe C-H amination without nitrene intermediacy.

As stated, the reaction likely follows a stepwise C-H amidation mechanism, similar to previous reports for C-H amination with ruthenium complexes.[194,196,318,326–328] Regardless of the mechanism, however, the use of $Ru(bpy)_3$ in the absence of base and light effectively supressed the formation of the sulfonamide byproduct in the final conditions. Overall, the mechanistic hypothesis outlined, the promising result for linear substrate **1t**, and recent advances in Ru-catalyzed C-H amination collectively suggest that the catalytic efficiency of the system could be improved to further advance this chemistry. The overall conclusion and future work will be presented in the following chapter.

2.7 Conclusions and Future Work

The results presented in this thesis describe the attempted optimization of three sets of reaction conditions—photoredox, thermal base-induced, and thermal ruthenium catalyzed—to enable the intramolecular C-H amidation of hydroxylamine-based nitrene precursors in the synthesis of sultams. Following exhaustive optimization attempts for photoredox or metal-free base-induced reactions, efficient conditions were established for the thermal ruthenium catalyzed C-H amidation reaction of *N*-acyloxysulfonamides, allowing for the synthesis of a representative scope of 12 benzo[*d*]sultams. While several iterations of reaction conditions were surveyed, the results obtained align with the project goal of expanding the applicability of hydroxylamine reagents in C-H amination reactions, and a general reaction was developed for the synthesis of benzo[*d*]sultams via the intramolecular C-H amidation of *N*-acyloxysulfonamides.

The project was initiated from our previous photoredox C-H amidation conditions; the reaction of a triisopropyl- substituted substrate under blue light irradiation with $Ru(bpy)_3(PF_6)_2$ and Et_3N and gave the sultam in high yield via tertiary C-H amidation, but the analogous primary C-H amidation was not achieved. Control reactions also indicated that a base-induced cyclization occurred in the absence of catalyst.

Thorough screening of the thermal base-induced conditions enabled the synthesis of four benzo[*d*]sultams in moderate yield; the reaction was restricted to *N*-acyloxyarylsulfonamides with tertiary benzylic C-H bonds and those with a 2,6-dialkyl-substitution pattern. While limited, this represents the highest yielding benzosultam synthesis through thermal decomposition of N-X precursors and C-H amination by an apparent free nitrene intermediate. Given the limits in thermal base-induced reactivity, photoredox conditions were further developed. A key control showed that

the reaction improved without a base in 1,2-dichloroethane. Again, only 2,6-disubstituted-*N*-acyloxysulfonamides reacted productively, and *ortho*-monoalkyl-substrates failed to cyclize. In contrast to the base-induced reaction, the lack of product yield corresponded to minimal substrate conversion, rather than sulfonamide side product formation.

Test reactions with a stronger light source improved yield for *ortho*-monoalkyl-substrates, but a cooled control suggested that a thermal ruthenium catalyzed reaction was operating. Optimization verified that heating with $Ru(bpy)_3(PF_6)_2$ in the absence of light and base allowed for C-H amidation in high yield, enabling the synthesis of a representative scope with 12 benzo[*d*]sultams. Additional control reactions further illustrated the reactivity bias of 2,6-dialkyl-*N*-acyloxyarylsulfonamides, which react in several organochlorine solvents, but 1,2-dichloroethane was specifically required for the C-H amidation of *ortho*monomethyl-*N*-acyloxyarylsulfonamides.

While the conditions evolved for photoredox and base-induced C-H amidation were limited to certain substrates, they represent the highest yielding examples of sultam synthesis from hydroxylamine-based nitrene precursors. Additionally, these reactions represent the first successful synthesis of a benzo[*d*]sultam scope under photoredox conditions, and the highest yielding sultam synthesis through an apparent free nitrene intermediate, respectively. In the end, the ruthenium catalyzed process accommodates the largest substrate scope and is arguably simpler than the initial photoredox conditions, which not only required $Ru(Bpy)_3$, but also base and light, which often requires an expensive apparatus for industrial applications. The major drawback of the final reaction involves the use of DCE as a solvent, but there may be potential to further optimize the reaction to perform efficiently in alternate solvents, particularly upon elucidation of the mechanism and identification of an alternative catalyst.

In terms of future work for this chemistry, the first clear extension would be to investigate the intramolecular C-H amidation of *N*-acyloxy alkylsulfonamides (**Figure 49**), especially with the encouraging preliminary 40% yield obtained from the reaction of *N*-(benzoyloxy)butane-1-sulfonamide, **1t** (**Chapter 2.3.3**, **Table 21**).

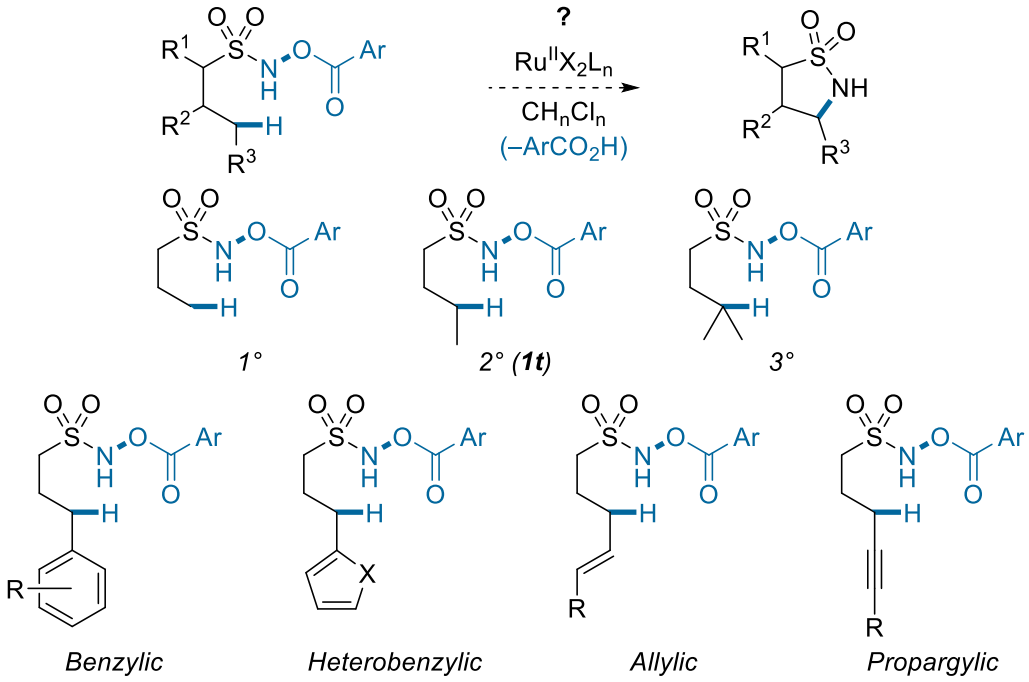

Figure 49. Future goal: C-H amidation of *N*-acyloxy alkylsulfonamides and potential substrates.

Based on this initial result, **1t** could be used as an optimization substrate to screen various catalysts, solvents, and temperatures. Ideally, the optimized reaction could also accommodate linear *N*-acyloxy alkylsulfonamides with tertiary and primary carbons at the distal C-H insertion site (See examples in **Figure 49**). Precursors with a decreased C-H bond strength at the distal position could be investigated to enable more facile scope compilation. These substrates could include those with benzylic C-H insertion sites (aromatic or heteroaromatic) or even propargylic or allylic substrates. Indeed, ruthenium has previously been more proficient than other second-row transition metals at catalyzing allylic C-H amination over the competing aziridination.[244,326,328,331,349–354] Substrates

containing heteroatoms adjacent to the insertion site could also be tested. It may also be worth introducing substrates with a Thorpe-Ingold bias to promote a more efficient cyclization.

Simultaneous with this synthetic extension study, mechanistic studies must be conducted to truly understand the nature of the reaction. With more knowledge of how the reaction operates, further research extensions can be planned. The main mechanistic inquiry for this reaction relates to the active spin state for the proposed ruthenium-nitrene intermediate. Several studies could be performed to elucidate the mechanism and distinguish between stepwise and concerted pathways, including kinetic isotope effect studies, stereospecificity testing with enantioenriched substrate probes, nitrene traps, radical traps, radical clock probes and DFT calculations.

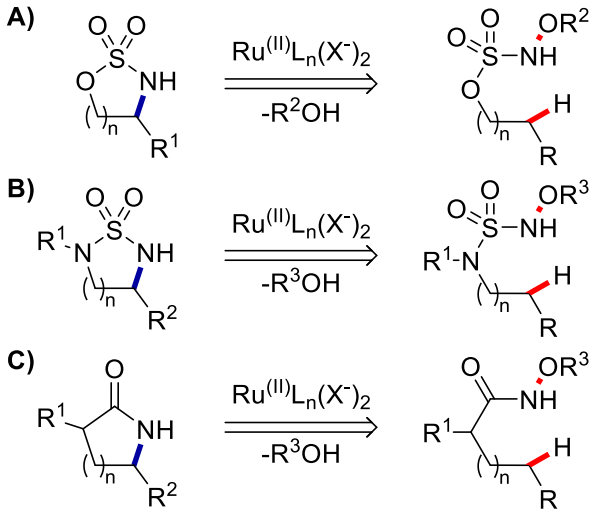

Figure 50. Heterocycle retrosynthesis for Ru-catalyzed C-H amidation with *N*-oxy precursors.

While several publications describe the intramolecular cyclization of sulfonyl nitrenes to form sulfamates[244,352,355–361] and sulfamides[315,318,362–365], these reactions make use of potentially explosive azides and wasteful iodonium oxidants. Additionally, the catalysts used are often synthetically complex and a general catalyst has not been designed to catalyze the C-H amination of sulfonyl nitrenes with varying electronic properties. It would be ideal to design a ruthenium-

based C-H amination catalyst that could encompass several classes of sulfonyl nitrenes with varying electronic properties (**Figure 50, A-B**). So far, the C-H amidation of *N*-oxysulfamate and *N*-oxysulfamide nitrene precursors has yet to be investigated, but *N*-hydroxysulfamates and sulfamides are difficult to synthesize.[366–370] Aside from sulfonyl nitrenes, examples of the intramolecular C-H amidation of acyl nitrenes to form lactams remain scarce in the literature and need further development (**Figure 50, C**).[174,175,371–374] This extension could be met with optimism as sultams are the sulfur-based structural analogues of lactams, and ruthenium catalysts have been successful for some of the few methodologies involving these acyl nitrene intermediates.[175,207,314,371]

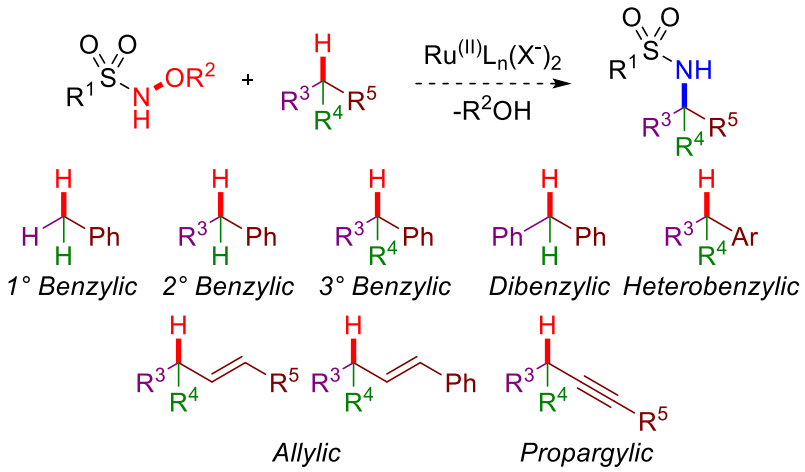

Figure 51. Future potential for intermolecular C-H amidation reactions with *N*-oxysulfonamides.

It may be a more difficult task, but performing intermolecular C-H amidation reactions with *N*-oxysulfonamides would be a significant achievement (**Figure 51**). The research could be particularly impactful if a range of aryl/alkyl substitution patterns on the nitrene precursor could be tolerated, as most intermolecular C-H sulfonamination reactions require specialized precursors.[152,153,291,353,375–378] It would be best to first aim for a realistic goal, and attempt to form products from biased reaction partners containing weak C-H bonds. Reaction partners with

activated benzylic, allylic and α-heteroatom substituted C-H bonds could be applied, including those with primary, secondary and tertiary insertion sites. Ideally, catalyst optimization could achieve a highly chemoselective reaction, and competitive C-H insertion reactions would be avoided.

One of the most valuable future contributions would be the development of a stereoselective method for sultam synthesis (**Scheme 47**). With a better understanding of the reaction mechanism, one could better predict the effect of catalyst modifications, and strategically screen catalysts to enable this goal. The most obvious modification involves the introduction of bipyridine ligands with chiral substituents. Catalysts could be first prepared with the three bidentate bipyridine ligands and weakly coordinating anions. Alternatively, some could contain two coordinated x-type ligands, such as halogens or acetonitrile molecules. The application of chiral-at-metal catalysts with achiral ligands, as developed by Meggers group, is also worth considering.[194,196,314,316,317]

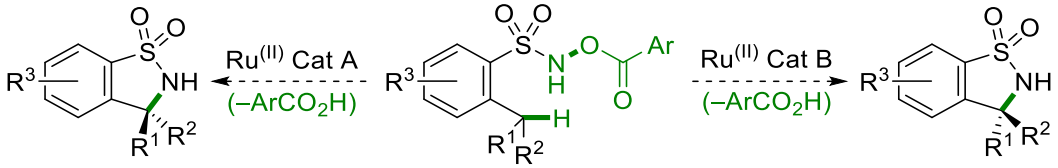

Scheme 47. Potential for ruthenium catalyzed stereoselective sultam synthesis.

Chapter 3: References

1 R. W. Dugger, J. A. Ragan and D. H. Brown Ripin, *Org. Process Res. Dev.*, 2005, **9**, 253–258.

2 J. S. Carey, D. Laffan, C. Thomson and M. T. Williams, *Org. Biomol. Chem.*, 2006, **4**, 2337–2347.

3 E. Vitaku, D. T. Smith and J. T. Njardarson, *J. Med. Chem.*, 2014, **57**, 10257–10274.

4 A. Bryskier, in *Antimicrobial Agents: Antibacterials and Antifungals*, ed. A. Bryskier, ASM Press, Washington, DC, 2005, pp. 1–50.

5 C. Hubschwerlen, in *Comprehensive Medicinal Chemistry II*, eds. J. B. Taylor, D. J. Triggle, J. J. Plattner and M. C. Desai, Elselvier Ltd, Allschwil, Switzerland, 2nd edn., 2007, vol. 7, pp. 479–518.

6 D. R. Mager, *Home Healthc. Now*, 2015, **33**, 139–141.

7 Y. Bedoui, X. Guillot, J. Sélambarom, P. Guiraud, C. Giry, M. C. Jaffar-Bandjee, S. Ralandison and P. Gasque, *Int. J. Mol. Sci.*, 2019, **20**, 5023–5055.

8 B. N. Cronstein and T. M. Aune, *Nat. Rev. Rheumatol.*, 2020, **16**, 145–154.

9 E. M. Kaplan and R. L. DuPont, *Curr. Med. Res. Opin.*, 2005, **21**, 941–950.

10 C. J. L. La Porte, *Expert Opin. Drug Metab. Toxicol.*, 2009, **5**, 1313–1322.

11 S. I van Leuven and J. J. P. Kastelein, *Expert Opin. Pharmacother.*, 2005, **6**, 1191–1203.

12 T. B. Horwich and W. R. MacLellan, *Expert Opin. Pharmacother.*, 2007, **8**, 3061–3068.

13 J. D. Wilden, *J. Chem. Res.*, 2010, **34**, 541–548.

14 G. Domagk, *Angew. Chem. Int. Ed.*, 1935, **48**, 657–667.

15 A. H. Mhemeed, *Int. J. Res. Pharm. Sci.*, 2019, **10**, 241–244.

16 R. A. G. Sheeja, G. R. Prasobh, V. M. Nishad, A. . Athira and C. S. Visal, *Indo. Am. J. Pharm. Sci.*, 2020, **07**, 20–27.

17 *World Health Organization Model List of Essential Medicines*, Geneva: World Health Organization, 2019, vol. 21.

18 F. Carta, A. Scozzafava and C. T. Supuran, *Expert Opin. Ther. Pat.*, 2012, **22**, 747–758.

19 İ. Gulçin and P. Taslimi, *Expert Opin. Ther. Pat.*, 2018, **28**, 541–549.

20 P. A. Masters, T. A. O'Bryan, J. Zurlo, D. Q. Miller and N. Joshi, *JAMA Intern. Med.*, 2003, **163**, 402–410.

21 I. P. Kaur, R. Smitha, D. Aggarwal and M. Kapil, *Int. J. Pharm.*, 2002, **248**, 1–14.

22 M. Y. Neufeld, in *The Treatment of Epilepsy*, eds. S. Shorvon, E. Perucca and J. Engel, John

Wiley & Sons, Ltd, Southern Gate, Chichester, West Sussex, 4th edn., 2016, pp. 376–387.

23 J. Prandota, *Am. J. Ther.*, 2002, **9**, 317–328.

24 L. Carone, S. G. Oxberry, R. Twycross, S. Charlesworth, M. Mihalyo and A. Wilcock, *J. Pain Symptom Manage.*, 2016, **52**, 144–150.

25 L. Tive, *Rheumatology*, 2000, **39**, 21–28.

26 P. G. Shete, N. G. Shete, D. N. Kumbhakaran, N. S. Mane, V. S. Padole and R. P. Kalsait, *Int. J. Res. Pharm. Chem.*, 2020, **10**, 382–389.

27 A. Salonia, P. Rigatti and F. Montorsi, *Curr. Med. Res. Opin.*, 2003, **19**, 241–262.

28 M. Ala, R. Mohammad Jafari and A. R. Dehpour, *Fundam. Clin. Pharmacol.*, 2021, **35**, 235–259.

29 S. Noble and K. L. Goa, *Drugs*, 2000, **60**, 1383–1410.

30 H. B. Fung, H. L. Kirschenbaum and R. Hameed, *Clin. Ther.*, 2000, **22**, 549–572.

31 S. D. Silberstein and D. A. Marcus, *Expert Opin. Pharmacother.*, 2013, **14**, 1659–1667.

32 F. Napoletano, L. Lionetto and P. Martelletti, *Expert Opin. Pharmacother.*, 2014, **15**, 303–305.

33 G. W. Bemis and M. A. Murcko, *J. Med. Chem.*, 1996, **39**, 2887–2893.

34 G. W. Bemis and M. A. Murcko, *J. Med. Chem.*, 1999, **42**, 5095–5099.

35 A. Vicente-Blázquez, M. González, R. Álvarez, S. del Mazo, M. Medarde and R. Peláez, *Med. Res. Rev.*, 2019, **39**, 775–830.

36 T. Owa and T. Nagasu, *Expert Opin. Ther. Pat.*, 2000, **10**, 1725–1740.

37 T. Cohen, D. A. Bennett, A. J. Mura and P. M. C. Chchsph, *J. Org. Chem.*, 1976, **41**, 2507–2508.

38 F. G. Bordwell, J. E. Bartmess and J. A. Hautala, *J. Org. Chem.*, 1978, **43**, 3095–3101.

39 Z. Liu and Y. Takeuchi, *Heterocycles*, 2009, **78**, 1387–1412.

40 J. Y. Winum, A. Scozzafava, J. L. Montero and C. T. Supuran, *Med. Res. Rev.*, 2006, **26**, 767–792.

41 S. Shoaib Ahmad Shah, G. Rivera and M. Ashfaq, *Mini-Rev. Med. Chem.*, 2012, **13**, 70–86.

42 A. Scozzafava, F. Carta and C. T. Supuran, *Expert Opin. Ther. Pat.*, 2013, **23**, 203–213.

43 Zajdel, Pawel, Marciniec, Bojarski, Pawlowski and Wesolowska, *Future Med. Chem.*, 2014, **6**, 57–75.

44 F. Carta, C. T. Supuran and A. Scozzafava, *Future Med. Chem.*, 2014, **6**, 1149–1165.

45 S. Apaydın and M. Török, *Bioorg. Med. Chem. Lett.*, 2019, **29**, 2042–2050.

46 H. Yang and R. G. Carter, *Synlett*, 2010, 2827–2838.

47 Y. Gu and S. K. Tian, *Synlett*, 2013, **24**, 1170–1185.

48 Y. Takeuchi and Z. Liu, *Heterocycles*, 2002, **56**, 693.

49 K. C. Majumdar and S. Mondal, *Chem. Rev.*, 2011, **111**, 7749–7773.

50 V. A. Rassadin, D. S. Grosheva, A. A. Tomashevskii and V. V. Sokolov, *Chem. Heterocycl. Compd.*, 2013, **49**, 39–65.

51 E. Differding and R. W. Lang, *Helv. Chim. Acta*, 1989, **72**, 1248–1252.

52 J. G. Lombardino and E. H. Wiseman, *Med. Res. Rev.*, 1982, **2**, 127–152.

53 S. Noble and J. A. Balfour, *Drugs*, 1996, **51**, 424–430.

54 R. Fleischmann, I. Iqbal and G. Slobodin, *Expert Opin. Pharmacother.*, 2002, **3**, 1501–1512.

55 J. R. Green, A. S. Troupin, L. M. Halpern, P. Friel and P. Kanarek, *Epilepsia*, 1974, **15**, 329–349.

56 B. Ben-Zeev, N. Watemberg, P. Lerman, I. Barash, N. Brand and T. Lerman-Sagie, *Pediatr. Int.*, 2004, **46**, 521–524.

57 N. Fejerman, R. Caraballo, R. Cersõsimo, S. M. Ferraro, S. Galicchio and H. Amartino, *Epilepsia*, 2012, **53**, 1156–1161.

58 M. Iester, *Expert Opin. Pharmacother.*, 2008, **9**, 653–662.

59 J. A. Lusthaus and I. Goldberg, *Expert Opin. Drug Saf.*, 2017, **16**, 1071–1078.

60 K. M. Neff and J. J. Nawarskas, *Cardiol. Rev.*, 2010, **18**, 51–56.

61 H. Sternlicht and G. L. Bakris, *J. Am. Coll. Cardiol.*, 2016, **67**, 390–391.

62 WO2020092187, 2020, 1–186.

63 WO2021003157, 2021, 1–536.

64 S. Debnath and S. Mondal, *Eur J. Org. Chem.*, 2018, **2018**, 933–956.

65 A. Mustafa, *Chem. Rev.*, 1954, **54**, 195–223.

66 K. Wojciechowski, *Heterocycles*, 2002, **57**, 1717–1740.

67 P. H. Cobb and G. P. Fuller, *Am. Chem. J.*, 1911, **45**, 605.

68 H. Watanabe, R. L. Gay and C. L. Hauser, *J. Org. Chem.*, 1968, **33**, 900–903.

69 Z. Liu, N. Shibata and Y. Takeuchi, *J. Org. Chem.*, 2000, **65**, 7583–7587.

70 Z. Liu, N. Shibata and Y. Takeuchi, *J. Chem. Soc., Perkin Trans. 1.*, 2002, **2**, 302–303.

71 Y. H. Dong, Q. W. Ni, S. T. Ma and Z. P. Liu, *Heterocycles*, 2010, **81**, 637–648.

72 Kyo Han Ahn, H. H. Baek, Seok Jong Lee and C. W. Cho, *J. Org. Chem.*, 2000, **65**, 7690–7696.

73 Y. Gao, K. B. Sharpless, J. M. Klunder, R. M. Hanson, S. Y. Ko and H. Masamune, *J. Am. Chem. Soc.*, 1987, **109**, 5765–5780.

74 D. Chiarino and A. M. Contri, *J. Heterocycl. Chem.*, 1986, **23**, 1645–1649.

75 B. Li, J. Chen, Z. Zhang, I. D. Gridnev and W. Zhang, *Angew. Chem. Int. Ed.*, 2019, **58**, 7329–7334.

76 Y. Li, K. Zhou, Z. Wen, S. Cao, X. Shen, M. Lei and L. Gong, *J. Am. Chem. Soc.*, 2018, **140**, 15850–15858.

77 G. Yang and W. Zhang, *Angew. Chem. Int. Ed.*, 2013, **52**, 7540–7544.

78 K. Morisaki, M. Sawa, R. Yonesaki, H. Morimoto, K. Mashima and T. Ohshima, *J. Am. Chem. Soc.*, 2016, **138**, 6194–6203.

79 S. T. Mei, H. W. Liang, B. Teng, N. J. Wang, L. Shuai, Y. Yuan, Y. C. Chen and Y. Wei, *Org. Lett.*, 2016, **18**, 1088–1091.

80 P. Wonneberger, N. König, F. B. Kraft, M. B. Sárosi and E. Hey-Hawkins, *Angew. Chem. Int. Ed.*, 2019, **58**, 3208–3211.

81 J. Pan, J. H. Wu, H. Zhang, X. Ren, J. P. Tan, L. Zhu, H. S. Zhang, C. Jiang and T. Wang, *Angew. Chem. Int. Ed.*, 2019, **58**, 7425–7430.

82 M. Rommel, T. Fukuzumi and J. W. Bode, *J. Am. Chem. Soc.*, 2008, **130**, 17266–17267.

83 K. Wojciechowski, *Pol. J. Chem.*, 1992, **66**, 1121–1124.

84 M. Mąkosza and K. Wojciechowski, *Tetrahedron Lett.*, 1984, **25**, 4791–4792.

85 M. Mąkosza and K. Wojciechowski, *Synthesis (Stuttg).*, 1992, 571–576.

86 J. F. Bunnett, T. Kato, R. R. Flynn and J. A. Skorcz, *J. Org. Chem.*, 1963, **28**, 1–6.

87 J. A. Skorez, J. T. Suh and R. L. Germershausen, *J. Heterocycl. Chem.*, 1973, **11**, 73–75.

88 R. A. Abramovitch, R. R. Harder and W. D. Lialcom, *Heterocycles*, 1987, **26**, 2327–2330.

89 M. Penso, D. Albanese, D. Landini, V. Lupi and A. Tagliabue, *J. Org. Chem.*, 2008, **73**, 6686–6690.

90 F. Foschi, A. Tagliabue, V. Mihali, T. Pilati, I. Pecnikaj and M. Penso, *Org. Lett.*, 2013, **15**, 3686–3689.

91 Y. Tao and S. R. Gilbertson, *Chem. Commun.*, 2018, **54**, 11292–11295.

92 P. Evans, T. McCabe, B. S. Morgan and S. Reau, *Org. Lett.*, 2005, **7**, 43–46.

93 A. Rolfe, K. Young and P. R. Hanson, *Eur J. Org. Chem.*, 2008, 5254–5262.

94 W. Xie, J. Yang, B. Wang and B. Li, *J. Org. Chem.*, 2014, **79**, 8278–8287.

95 Q. Ding, T. Liu, Q. Zheng, Y. Zhang, L. Long and Y. Peng, *RSC Adv.*, 2014, **4**, 51309–51314.

96 X. Li, Y. Dong, F. Qu and G. Liu, *J. Org. Chem.*, 2015, **80**, 790–798.

97 X. Li, X. Hu, Z. Liu, J. Yang, B. Mei, Y. Dong and G. Liu, *J. Org. Chem.*, 2020, **85**, 5916–1926.

98 Z. Pan, S. Wang, J. T. Brethorst and C. J. Douglas, *J. Am. Chem. Soc.*, 2018, **140**, 3331–3338.

99 S. Rousseaux, S. I. Gorelsky, B. K. W. Chung and K. Fagnou, *J. Am. Chem. Soc.*, 2010, **132**, 10692–10705.

100 J. K. Laha, N. Dayal, K. P. Jethava and D. V. Prajapati, *Org. Lett.*, 2015, **17**, 1296–1299.

101 Z. Yang and J. Xu, *Chem. Commun.*, 2014, **50**, 3616–3618.

102 P. Huang, Z. Yang and J. Xu, *Tetrahedron*, 2017, **73**, 3255–3265.

103 F. Collet, R. H. Dodd and P. Dauban, *Chem. Commun.*, 2009, 5061–5074.

104 H. M. L. Davies and J. R. Manning, *Nature*, 2008, **451**, 417–424.

105 D. N. Zalatan and J. Du Bois, in *C-H Activation Topics in Current Chemistry*, eds. J.-Q. Yu and Z. Shi, Springer, Berlin, Heidelberg, Volume 292., 2009, pp. 347–378.

106 Y. Park, Y. Kim and S. Chang, *Chem. Rev.*, 2017, **117**, 9247–9301.

107 Y.-R. Luo, *Comprehensive Handbook of Chemical Bond Energies*, CRC Press, Taylor & Francis Group, LLC, Boca Raton, 1st edn., 2007.

108 M. M. Díaz-Requejo and P. J. Pérez, *Chem. Rev.*, 2008, **108**, 3379–3394.

109 J.-R. Chen, X.-Q. Hu, L.-Q. Lu and W.-J. Xiao, *Chem. Soc. Rev.*, 2016, **45**, 2044–2056.

110 T. Xiong and Q. Zhang, *Chem. Soc. Rev.*, 2016, **45**, 3069–3087.

111 M. D. Kärkäs, *ACS Catal.*, 2017, **7**, 4999–5022.

112 G. L'Abbé, *Chem. Rev.*, 1969, **69**, 345–363.

113 G. Dequirez, V. Pons and P. Dauban, *Angew. Chem. Int. Ed.*, 2012, 7384–7395.

114 D. E. Falvey and A. D. Gudmundsdottir, *NITRENES AND NITRENIUM IONS*, John Wiley & Sons, Inc., Hoboken, New Jersey, 2013.

115 E. F. V. Scriven, *Azides and Nitrenes: Reactivity and Utility*, ACADEMIC PRESS, INC. (Harcourt Brace Jovanovich, Publishers), Orlando, Florida, 1984.

116 G. Boche and J. C. W. Lohrenz, *Chem. Rev.*, 2001, **101**, 697–756.

117 D. Hazelard, P. A. Nocquet and P. Compain, *Org. Chem. Front.*, 2017, **4**, 2500–2521.

118 P. Müller and C. Fruit, *Chem. Rev.*, 2003, **103**, 2905–2919.

119 W. Lwowski, *Trans. N. Y. Acad. Sci.*, 1971, **33**, 259–266.

120 N. P. Gritsan and M. S. Platz, *Chem. Rev.*, 2006, **106**, 3844–3867.

121 F. Strieth-Kalthoff, M. J. James, M. Teders, L. Pitzer and F. Glorius, *Chem. Soc. Rev.*, 2018, **47**, 7190–7202.

122 R. A. Abramovitch and V. Uma, *Chem. Commun.*, 1968, **39**, 797–798.

123 R. A. Abramovitch, G. N. Knaus and V. Uma, *J. Org. Chem.*, 1974, **39**, 1101–1106.

124 R. A. Abramovitch, T. D. Bailey, T. Takaya and V. Uma, *J. Org. Chem.*, 1974, **39**, 340–345.

125 T. Curtius, *Ber. Dtsch. Chem. Ges*, 1890, **23**, 3023–3033.

126 T. Curtius, *J. für Prakt. Chemie*, 1894, **50**, 275–294.

127 C. Wentrup, *Acc. Chem. Res.*, 2011, **44**, 393–404.

128 C. Wentrup, *Angew. Chem. Int. Ed.*, 2018, **57**, 11508–11521.

129 R. A. Abramovitch, C. I. Azogu and I. T. McMaster, *J. Am. Chem. Soc.*, 1969, **91**, 1219–1220.

130 D. S. Breslow, E. I. Edwards, E. C. Linsay and H. Omura, *J. Am. Chem. Soc.*, 1976, **98**, 4268–4275.

131 D. S. Breslow, M. F. Sloan, N. R. Newburg and W. B. Renfrow, *J. Am. Chem. Soc.*, 1969, **91**, 2273–2279.

132 R. A. Abramovitch, T. Chellathurai, W. D. Holcomb, I. T. McMaster and D. P. Vanderpool, *J. Org. Chem.*, 1977, **42**, 2920–2926.

133 R. A. Abramovitch and W. D. Holcomb, *J. Chem. Soc. D*, 1969, 1298–1299.

134 B. A. Shainyan and A. V. Kuzmin, *J. Phys. Org. Chem.*, 2014, **27**, 156–162.

135 H. E. Simmons and R. D. Smith, *J. Am. Chem. Soc.*, 1958, **80**, 5323–5324.

136 H. E. Simmons and R. D. Smith, *J. Am. Chem. Soc.*, 1959, **81**, 4256–4264.

137 J. M. Denis, C. Girard and J. M. Conia, *Synthesis (Stuttg).*, 1972, 549–551.

138 P. F. Kuijpers, J. I. van der Vlugt, S. Schneider and B. de Bruin, *Chem. Eur. J.*, 2017, **23**, 13819–13829.

139 T. A. Ramirez, B. Zhao and Y. Shi, *Chem. Soc. Rev.*, 2012, **41**, 931–942.

140 H. Hayashi and T. Uchida, *Eur J. Org. Chem.*, 2020, **2020**, 909–916.

141 F. Collet, C. Lescot and P. Dauban, *Chem. Soc. Rev.*, 2011, **40**, 1926–1936.

142 J. M. Alderson, J. R. Corbin and J. M. Schomaker, *Acc. Chem. Res.*, 2017, **50**, 2147–2158.

143 J. Wang, K. Zheng, B. Lin and Y. Weng, *RSC Adv.*, 2017, **7**, 34783–34794.

144 S. Cenini and G. La Monica, *Inorg. Chim. Acta*, 1976, **18**, 279–293.

145 D. A. Bamford and C. H. Bamford, *J. Chem. Soc. B*, 1941, **0**, 30–34.

146 J. H. Boyer, W. E. Krueger and G. J. Mikol, *J. Am. Chem. Soc.*, 1967, **89**, 5504–5505.

147 J. H. Boyer and G. J. Mikol, *J. Heterocycl. Chem.*, 1972, **9**, 1325–1330.

148 S. K. Nag and S. N. Bose, *Tetrahedron*, 1989, **30**, 2855–2856.

149 G. Hajos and Z. Riedl, *Curr. Org. Chem.*, 2009, **13**, 791–809.

150 X. Dong, Q. Liu, Y. Dong and H. Liu, *Chem. Eur. J.*, 2017, **23**, 2481–2511.

151 R. Breslow and S. H. Gellman, *J. Am. Chem. Soc.*, 1983, **105**, 6728–6729.

152 J. L. Roizen, M. E. Harvey and J. Du Bois, *Acc. Chem. Res.*, 2012, **45**, 911–922.

153 J. L. Roizen, D. N. Zalatan and J. Du Bois, *Angew. Chem. Int. Ed.*, 2013, **52**, 11343–11346.

154 N. D. Chiappini, J. B. C. Mack and J. Du Bois, *Angew. Chem. Int. Ed.*, 2018, **57**, 4956–4959.

155 K. Huard and H. Lebel, *Chem. Eur. J.*, 2008, **14**, 6222–6230.

156 H. Lebel, C. Spitz, O. Leogane, C. Trudel and M. Parmentier, *Org. Lett.*, 2011, **13**, 5460–5463.

157 H. Lebel, C. Trudel and C. Spitz, *Chem. Commun.*, 2012, **48**, 7799–7801.

158 W. Lwowski and E. Scheiffele, *J. Am. Chem. Soc.*, 1965, **87**, 4359–4365.

159 L. Pantaine, F. Richard, J. Marrot, X. Moreau, V. Coeffard and C. Greck, *Adv. Synth. Catal.*, 2016, **358**, 2012–2016.

160 L. Pantaine, V. Humblot, V. Coeffard and A. Vallée, *Beilstein J. Org. Chem.*, 2017, **13**, 648–658.

161 D. E. Polat, D. D. Brzezinski and A. M. Beauchemin, *Org. Lett.*, 2019, **21**, 4849–4852.

162 H. Lebel, K. Huard and S. Lectard, *J. Am. Chem. Soc.*, 2005, **127**, 14198–14199.

163 H. Lebel and H. Kim, *Org. Lett.*, 2007, **9**, 639–642.

164 H. Lebel, L. Mamani Laparra, M. Khalifa, C. Trudel, C. Audubert, M. Szponarski, C. Dicaire Leduc, E. Azek and M. Ernzerhof, *Org. Biomol. Chem.*, 2017, **15**, 4144–4158.

165 E. Azek, M. Khalifa, J. Bartholoméüs, M. Ernzerhof and H. Lebel, *Chem. Sci.*, 2019, **10**, 718–729.

166 E. Azek, C. Spitz, M. Ernzerhof and H. Lebel, *Adv. Synth. Catal.*, 2020, **362**, 384–397.

167 H. Lebel, S. Lectard and M. Parmentier, *Org. Lett.*, 2007, **9**, 4797–4800.

168 H. Lebel and M. Parmentier, *Pure Appl. Chem.*, 2010, **82**, 1827–1833.

169 H. Lebel, M. Parmentier, O. Leogane, K. Ross and C. Spitz, *Tetrahedron*, 2012, **68**, 3396–3409.

170 C. Grohmann, H. Wang and F. Glorius, *Org. Lett.*, 2013, **15**, 3014–3017.

171 X. Wang, T. Gensch, A. Lerchen, C. G. Daniliuc and F. Glorius, *J. Am. Chem. Soc.*, 2017, **139**, 6506–6512.

172 P. Patel and S. Chang, *Org. Lett.*, 2014, **16**, 3328–3331.

173 P. Patel and S. Chang, *ACS Catal.*, 2015, **5**, 853–858.

174 S. Huh, S. Y. Hong and S. Chang, *Org. Lett.*, 2019, **21**, 2808–2812.

175 H. Jung, H. Keum, J. Kweon and S. Chang, *J. Am. Chem. Soc.*, 2020, **142**, 5811–5818.

176 B. Zhou, J. Du, Y. Yang, H. Feng and Y. Li, *Org. Lett.*, 2014, **16**, 592–595.

177 J. Du, Y. Yang, H. Feng, Y. Li and B. Zhou, *Chem. Eur. J.*, 2014, **20**, 5727–5731.

178 S. Yu, G. Tang, Y. Li, X. Zhou, Y. Lan and X. Li, *Angew. Chem. Int. Ed.*, 2016, **55**, 8696–8700.

179 M. Wang, L. Kong, F. Wang and X. Li, *Adv. Synth. Catal.*, 2017, **359**, 4411–4416.

180 M. Zou, J. Liu, C. Tang and N. Jiao, *Org. Lett.*, 2016, **18**, 3030–3033.

181 C. Tang, M. Zou, J. Liu, X. Wen, X. Sun, Y. Zhang and N. Jiao, *Chem. Eur. J.*, 2016, **22**, 11165–11169.

182 J. Liu, K. Wu, T. Shen, Y. Liang, M. Zou, Y. Zhu, X. Li, X. Li and N. Jiao, *Chem. Eur. J.*, 2017, **23**, 563–567.

183 M. P. Paudyal, A. M. Adebesin, S. R. Burt, D. H. Ess, Z. Ma, L. Kürti and J. R. Falck, *Science*, 2016, **353**, 1144–1147.

184 S. Munnuri, A. M. Adebesin, M. P. Paudyal, M. Yousufuddin, A. Dalipe and J. R. Falck, *J. Am. Chem. Soc.*, 2017, **139**, 18288–18294.

185 S. Munnuri, R. R. Anugu and J. R. Falck, *Org. Lett.*, 2019, **21**, 1926–1929.

186 R. R. Anugu, S. Munnuri and J. R. Falck, *J. Am. Chem. Soc.*, 2020, **142**, 5266–5271.

187 L. Legnani, G. P. Cerai and B. Morandi, *ACS Catal.*, 2016, **6**, 8162–8165.

188 E. Falk, V. C. M. Gasser and B. Morandi, *Org. Lett.*, 2021, **23**, 1422–1426.

189 K. Arai, Y. Ueda, K. Morisaki, T. Furuta, T. Sasamori, N. Tokitoh and T. Kawabata, *Chem. Commun.*, 2018, **54**, 2264–2267.

190 R. Ninomiya, K. Arai, G. Chen, K. Morisaki, T. Kawabata and Y. Ueda, *Chem. Commun.*, 2020, **56**, 5759–5762.

191 G. Chen, K. Arai, K. Morisaki, T. Kawabata and Y. Ueda, *Synlett*, 2021, **32**, 728–732.

192 G. Ju, G. Li, G. Qian, J. Zhang and Y. Zhao, *Org. Lett.*, 2019, **21**, 7333–7336.

193 G. Ju, C. Yuan, D. Wang, J. Zhang and Y. Zhao, *Org. Lett.*, 2019, **21**, 9852–9855.

194 Z. Zhou, Y. Tan, T. Yamahira, S. Ivlev, X. Xie, R. Riedel, M. Hemming, M. Kimura and E. Meggers, *Chem*, 2020, **6**, 2024–2034.

195 Y. Tan, F. Han, M. Hemming, J. Wang, K. Harms, X. Xie and E. Meggers, *Org. Lett.*, 2020, **22**, 6653–6656.

196 Z. Zhou, Y. Tan, X. Shen, S. Ivlev and E. Meggers, *Sci. China Chem.*, 2021, **64**, 452–458.

197 L. Jarrige, Z. Zhou, M. Hemming and E. Meggers, *Angew. Chem. Int. Ed.*, 2021, **60**, 6314–6319.

198 E. J. Yoo, S. Ma, T.-S. Mei, K. S. L. Chan and J.-Q. Yu, *J. Am. Chem. Soc.*, 2011, **133**, 7652–7655.

199 K. Wu, Z. Fan, Y. Xue, Q. Yao and A. Zhang, *Org. Lett.*, 2014, **16**, 42–45.

200 J. Shi, G. Zhao, X. Wang, H. E. Xu and W. Yi, *Org. Biomol. Chem.*, 2014, **12**, 6831–6836.

201 Y. Xue, Z. Fan, X. Jiang, K. Wu, M. Wang, C. Ding, Q. Yao and A. Zhang, *Eur J. Org. Chem.*, 2014, **2014**, 7481–7488.

202 Y. Zhang, J. Huang, Z. Deng, X. Mao and Y. Peng, *Tetrahedron*, 2018, **74**, 2330–2337.

203 H. Noda, Y. Asada and M. Shibasaki, *Org. Lett.*, 2020, **22**, 8769–8773.

204 D. Zhong, L. Y. Wu, X. Z. Wang and W. B. Liu, *Chin J. Chem.*, 2021, **39**, 855–858.

205 D. E. Polat, University of Ottawa - Ottawa, 2019.

206 R. A. Ivanovich, University of Ottawa, Ottawa, ON, 2020.

207 R. A. Ivanovich, D. E. Polat and A. M. Beauchemin, *Org. Lett.*, 2020, **22**, 6360–6364.

208 S. Y. Hong, Y. Park, Y. Hwang, Y. B. Kim, M. H. Baik and S. Chang, *Science*, 2018, **359**, 1016–1021.

209 T. Shimbayashi, K. Sasakura, A. Eguchi, K. Okamoto and K. Ohe, *Chem. Eur. J.*, 2019, **25**, 3156–3180.

210 K. M. Van Vliet and B. De Bruin, *ACS Catal.*, 2020, **10**, 4751–4769.

211 Y. Gao, *Org. Chem. Front.*, 2020, **7**, 1177–1196.

212 S. Z. Zard, *Chem. Soc. Rev.*, 2008, **37**, 1603–1618.

213 W. Li, W. Xu, J. Xie, S. Yu and C. Zhu, *Chem. Soc. Rev.*, 2018, **47**, 654–667.

214 J. M. Ganley, P. R. D. Murray and R. R. Knowles, *ACS Catal.*, 2020, **10**, 11712–11738.

215 X. Q. Hu, J. R. Chen, Q. Wei, F. L. Liu, Q. H. Deng, A. M. Beauchemin and W. J. Xiao, *Angew. Chem. Int. Ed.*, 2014, **53**, 12163–12167.

216 H. W. Hofman, *Chem. Ber.*, 1883, **16**, 558–560.

217 C. Freytag and K. Loffler, *Chem. Ber.*, 1909, **42**, 3427–3431.

218 G. Pandey and R. Laha, *Angew. Chem. Int. Ed.*, 2015, **54**, 14875–14879.

219 W. Shu and C. Nevado, *Angew. Chem. Int. Ed.*, 2017, **56**, 1881–1884.

220 Q. Guo, X. Ren and Z. Lu, *Org. Lett.*, 2019, **21**, 880–884.

221 Q. Qin and S. Yu, *Org. Lett.*, 2015, **17**, 1894–1897.

222 C. Martínez and K. Muniz, *Angew. Chem. Int. Ed.*, 2015, **54**, 8287–8291.

223 C. Q. O'Broin, P. Fernandez, C. Martinez and K. Muniz, *Org. Lett.*, 2016, **18**, 436–439.

224 P. Becker, T. Duhamel, C. J. Stein, M. Reiher and K. Muniz, *Angew. Chem. Int. Ed.*, 2017, **56**, 8004–8008.

225 P. Becker, T. Duhamel, C. Martinez and K. Muniz, *Angew. Chem. Int. Ed.*, 2018, **57**, 5166–5170.

226 P. Xiong and H. Xu, *Acc. Chem. Res.*, 2019, **52**, 3339–3350.

227 S. Herold, D. Bafaluy and K. Muñiz, *Green Chem.*, 2018, **20**, 3191–3196.

228 R. Dorel, C. P. Grugel and A. M. Haydl, *Angew. Chem. Int. Ed.*, 2019, **58**, 17118–17129.

229 A. Ribaucourt and J. Cossy, *ACS Catal.*, 2020, **10**, 10127–10148.

230 Y. Tan and J. F. Hartwig, *J. Am. Chem. Soc.*, 2010, **132**, 3676–3677.

231 Y. N. Timsina, B. F. Gupton and K. C. Ellis, *ACS Catal.*, 2018, **8**, 5732–5776.

232 K. M. Korch and D. A. Watson, *Chem. Rev.*, 2019, **119**, 8192–8228.

233 I. Nägeli, C. Baud, G. Bernardinelli, Y. Jacquier, M. Moran and P. Müller, *Helv. Chim. Acta*, 1997, **80**, 1087–1105.

234 P. Mueller, C. Baud and I. Naegeli, *J. Phys. Org. Chem.*, 1998, **11**, 597–601.

235 C. Fruit and P. Müller, *Helv. Chim. Acta*, 2004, **87**, 1607–1615.

236 R. J. Scamp, B. Scheffer and J. M. Schomaker, *Chem. Commun.*, 2019, **55**, 7362–7365.

237 D. Zhong, D. Wu, Y. Zhang, Z. Lu, M. Usman, W. Liu, X. Lu and W. B. Liu, *Org. Lett.*, 2019, **21**, 5808–5812.

238 P. Dauban and R. H. Dodd, *Org. Lett.*, 2000, **2**, 2327–2329.

239 P. Müller, C. Baud and Y. Jacquier, *Can. J. Chem.*, 1998, **76**, 738–750.

240 P. Dauban and R. H. Dodd, *Tetrahedron Lett.*, 2001, **42**, 1037–1040.

241 P. Dauban, L. Sanière, A. Tarrade and R. H. Dodd, *J. Am. Chem. Soc.*, 2001, **123**, 7707–7708.

242 J. L. Liang, S. X. Yuan, P. W. H. Chan and C. M. Che, *Org. Lett.*, 2002, **4**, 4507–4510.

243 J. L. Liang, S. X. Yuan, P. W. H. Chan and C. M. Che, *Tetrahedron Lett.*, 2003, **44**, 5917–5920.

244 J. L. Liang, S. X. Yuan, J. S. Huang and C. M. Che, *J. Org. Chem.*, 2004, **69**, 3610–3619.

245 P. Liu, E. L. M. Wong, A. W. H. Yuen and C. M. Che, *Org. Lett.*, 2008, **10**, 3275–3278.

246 J. V. Ruppel, R. M. Kamble and X. P. Zhang, *Org. Lett.*, 2007, **9**, 4889–4892.

247 Y. Hu, K. Lang, C. Li, J. B. Gill, I. Kim, H. Lu, K. B. Fields, M. Marshall, Q. Cheng, X. Cui, L. Wojtas and X. P. Zhang, *J. Am. Chem. Soc.*, 2019, **141**, 18160–18169.

248 M. Ichinose, H. Suematsu, Y. Yasutomi, Y. Nishioka, T. Uchida and T. Katsuki, *Angew. Chem. Int. Ed.*, 2011, **50**, 9884–9887.

249 R. E. White and M. J. Coon, *Annu. Rev. Biochem.*, 1980, **49**, 315–356.

250 V. Guallar, B. F. Gherman, S. J. Lippard and R. A. Friesner, *Curr. Opin. Chem. Biol.*, 2002, **6**, 236–242.

251 M. Newcomb, P. F. Hollenberg and M. J. Coon, *Arch. Biochem. Biophys.*, 2003, **409**, 72–79.

252 E. W. Svastits, J. H. Dawson, R. Breslow and S. H. Gellman, *J. Am. Chem. Soc.*, 1985, **107**, 6427–6428.

253 C. Jäckel, P. Kast and D. Hilvert, *Annu. Rev. Biophys.*, 2008, **37**, 153–173.

254 M. T. Reetz, *Angew. Chem. Int. Ed.*, 2011, **50**, 138–174.

255 P. A. Romero and F. H. Arnold, *Nat. Rev. Mol. Cell Biol.*, 2009, **10**, 866–876.

256 T. K. Hyster and T. R. Ward, *Angew. Chem. Int. Ed.*, 2016, **55**, 7344–7357.

257 J. A. McIntosh, P. S. Coelho, C. C. Farwell, Z. J. Wang, J. C. Lewis, T. R. Brown and F. H. Arnold, *Angew. Chem. Int. Ed.*, 2013, **52**, 9309–9312.

258 R. Singh, M. Bordeaux and R. Fasan, *ACS Catal.*, 2014, **4**, 546–552.

259 M. Bordeaux, R. Singh and R. Fasan, *Bioorg. Med. Chem.*, 2014, **22**, 5697–5704.

260 B. C. Finzel, T. L. Poulos and J. Kraut, *J. Biol. Chem.*, 1984, **259**, 13027–13036.

261 F. Yang and G. N. J. Phillips, *J. Mol. Biol.*, 1996, **256**, 762–774.

262 J. Vojtěchovský, K. Chu, J. Berendzen, R. M. Sweet and I. Schlichting, *Biophys. J.*, 1999, **77**, 2153–2174.

263 G. I. Berglund, G. H. Carlsson, A. T. Smith, H. Szöke, A. Henriksen and J. Hajdu, *Nature*, 2002, **417**, 463–468.

264 T. K. Hyster, C. C. Farwell, A. R. Buller, J. A. McIntosh and F. H. Arnold, *J. Am. Chem. Soc.*, 2014, **136**, 15505–15508.

265 P. Dydio, H. M. Key, H. Hayashi, D. S. Clark and J. F. Hartwig, *J. Am. Chem. Soc.*, 2017, **139**, 1750–1753.

266 N. W. Goldberg, A. M. Knight, R. K. Zhang and F. H. Arnold, *J. Am. Chem. Soc.*, 2019, **141**, 19585–19588.

267 Z. Li, D. J. Burnell and R. J. Boyd, *J. Phys. Chem. B*, 2017, **121**, 10859–10868.

268 V. Steck, J. N. Kolev, X. Ren and R. Fasan, *J. Am. Chem. Soc.*, 2020, **142**, 10343–10357.

269 M. A. Vila, V. Steck, S. Rodriguez Giordano, I. Carrera and R. Fasan, *ChemBioChem*, 2020, **21**, 1981–1987.

270 M. H. V Huynh and T. J. Meyer, *Chem. Rev.*, 2007, **107**, 5004–5064.

271 D. R. Weinberg, C. J. Gagliardi, J. F. Hull, C. F. Murphy, C. A. Kent, B. C. Westlake, A. Paul, D. H. Ess, D. G. McCaffery and T. J. Meyer, *Chem. Rev.*, 2012, **112**, 4016–4093.

272 E. C. Gentry and R. R. Knowles, *Acc. Chem. Res.*, 2016, **49**, 1546–1556.

273 Q. Zhu, D. E. Graff and R. R. Knowles, *J. Am. Chem. Soc.*, 2018, **140**, 741–747.

274 C. B. Roos, J. Demaerel, D. E. Graff and R. R. Knowles, *J. Am. Chem. Soc.*, 2020, **142**, 5974–5979.

275 S. Zheng, S. Zhang, B. Saeednia, J. Zhou, J. M. Anna, X. Hong and G. A. Molander, *Chem. Sci.*, 2020, **11**, 4131–4137.

276 G. Blotny, *Tetrahedron Lett.*, 2003, **44**, 1499–1501.

277 G. K. S. Prakash, T. Mathew, C. Panja and G. A. Olah, *J. Org. Chem.*, 2007, **72**, 5847–5850.

278 C. Wang, C. Hamilton, P. Meister and C. Menning, *Org. Process Res. Dev.*, 2007, **11**, 52–55.

279 K. Bahrami, M. M. Khodaei and M. Soheilizad, *Synlett*, 2009, 2773–2776.

280 K. Bahrami, M. M. Khodaei and M. Soheilizad, *J. Org. Chem.*, 2009, **74**, 9287–9291.

281 C. Hansch, B. Schmidhalter, F. Reiter and W. Saltonstall, *J. Org. Chem.*, 1956, **21**, 265–270.

282 A. Porcheddu, L. De Luca and G. Giacomelli, *Synlett*, 2009, 2149–2153.

283 L. A. Carpino, C. A. Giza and B. A. Carpino, *J. Am. Chem. Soc.*, 1959, **81**, 955–957.

284 H. M. D. Bandara, D. Jin, M. A. Mantell, K. D. Field, A. Wang, R. P. Narayanan, N. A. Deskins and M. H. Emmert, *Catal. Sci. Technol.*, 2016, **6**, 5304–5310.

285 A. Wang, N. J. Venditto, J. W. Darcy and M. H. Emmert, *Organometallics*, 2017, **36**, 1259–1268.

286 M. A. Allen, R. A. Ivanovich, D. E. Polat and A. M. Beauchemin, *Org. Lett.*, 2017, **19**, 6574–6577.

287 G. J. Choi and R. R. Knowles, *J. Am. Chem. Soc.*, 2015, **137**, 9226–9229.

288 D. C. Miller, G. J. Choi, H. S. Orbe and R. R. Knowles, *J. Am. Chem. Soc.*, 2015, **137**, 13492–13495.

289 G. J. Choi, Q. Zhu, D. C. Miller, C. J. Gu and R. R. Knowles, *Nature*, 2016, **539**, 268–271.

290 D. Hazelard, P.-A. Nocquet and P. Compain, *Org. Chem. Front.*, 2017, **4**, 2500–2521.

291 R. P. Reddy and H. M. L. Davies, *Org. Lett.*, 2006, **8**, 5013–5016.

292 G. S. Liu, Y. Q. Zhang, Y. A. Yuan and H. Xu, *J. Am. Chem. Soc.*, 2013, **135**, 3343–3346.

293 X. Ren, Q. Guo, J. Chen, H. Xie, Q. Xu and Z. Lu, *Chem. Eur. J.*, 2016, **22**, 18695–18699.

294 W. Lwowski, T. J. Maricich and T. W. Mattingly, *J. Am. Chem. Soc.*, 1963, **85**, 1200–1202.

295 W. Lwowski and T. J. Maricich, *J. Am. Chem. Soc.*, 1965, **87**, 3630–3637.

296 J. Kubicki, Y. Zhang, J. Xue, H. Ling Luk and M. Platz, *Phys. Chem. Chem. Phys.*, 2012, **14**, 10377–10390.

297 C. M. Morton, Q. Zhu, H. Ripberger, L. Troian-gautier, Z. S. D. Toa, R. R. Knowles and E. J. Alexanian, *J. Am. Chem. Soc.*, 2019, **141**, 13253–13260.

298 W. Yuan, Z. Zhou, L. Gong and E. Meggers, *Chem. Commun.*, 2017, **53**, 8964–8967.

299 X. De An, Y. Y. Jiao, H. Zhang, Y. Gao and S. Yu, *Org. Lett.*, 2018, **20**, 401–404.

300 X. De An, H. Zhang, Q. Xu, L. Yu and S. Yu, *Chin J. Chem.*, 2018, **36**, 1147–1150.

301 H. Chen, L. Guo and S. Yu, *Org. Lett.*, 2018, **20**, 6255–6259.

302 K. Miyazawa, T. Koike and M. Akita, *Chem. Eur. J.*, 2015, **21**, 11677–11680.

303 W. D. Liu, G. Q. Xu, X. Q. Hu and P. F. Xu, *Org. Lett.*, 2017, **19**, 6288–6291.

304 J. N. Mo, W. L. Yu, J. Q. Chen, X.-Q. Hu and P.-F. Xu, *Org. Lett.*, 2018, **20**, 4471–4474.

305 E. R. Young, J. Rosenthal and D. G. Nocera, *Chem. Sci.*, 2012, **3**, 455–459.

306 C. Drolen, E. Conklin, S. J. Hetterich, A. Krishnamurthy, G. A. Andrade, J. L. Dimeglio, M. I. Martin, L. K. Tran, G. P. A. Yap, J. Rosenthal and E. R. Young, *J. Am. Chem. Soc.*, 2018, **140**, 10169–10178.

307 M. F. Sloan, W. B. Renfrow and D. S. Breslow, *Tetrahedron*, 1964, **5**, 2905–2909.

308 W. Lwowski, *Angew. Chem. Int. Ed.*, 1967, **6**, 897–906.

309 M. Okahara and D. Swern, *Tetrahedron Lett.*, 1969, **38**, 3301–3304.

310 M. A. Loreto, P. A. Tardella and D. Tofani, *Tetrahedron Lett.*, 1995, **36**, 8295–8298.

311 M. Carducci, S. Fioravanti, M. A. Loreto, L. Pellacani and P. A. Tardella, *Tetrahedron Lett.*, 1996, **37**, 3777–3778.

312 T. Feng, Z. Tang, X. Luo and J. Mo, *Org. Biomol. Chem.*, 2020, **18**, 6497–6501.

313 R. A. Abramovitch and B. A. Davis, *Chem. Rev.*, 1964, **64**, 149–185.

314 Z. Zhou, S. Chen, Y. Hong, E. Winterling, Y. Tan, M. Hemming, K. Harms, K. N. Houk and E. Meggers, *J. Am. Chem. Soc.*, 2019, **141**, 19048–19057.

315 L. Li, F. Han, X. Nie, Y. Hong, S. Ivlev and E. Meggers, *Angew. Chem. Int. Ed.*, 2020, **59**, 12392–12395.

316 Z. Zhou, S. Chen, J. Qin, X. Nie, X. Zheng, K. Harms, R. Riedel, K. N. Houk and E. Meggers, *Angew. Chem. Int. Ed.*, 2019, **58**, 1088–1093.

317 J. Qin, Z. Zhou, T. Cui, M. Hemming and E. Meggers, *Chem. Sci.*, 2019, **10**, 3202–3207.

318 X. Nie, Z. Yan, S. Ivlev and E. Meggers, *J. Org. Chem.*, 2021, **86**, 750–761.

319 S. H. Hansen and L. Nordholm, *J. Chromatogr. A*, 1981, **204**, 97–101.

320 Z. Wang, J. Yin, F. Zhou, Y. Liu and J. You, *Angew. Chem. Int. Ed.*, 2019, **58**, 254–258.

321 A. B. Rudine, M. G. Walter and C. C. Wamser, *J. Org. Chem.*, 2010, **75**, 4292–4295.

322 A. V. G. Prasanthi, S. Begum, H. K. Srivastava, S. K. Tiwari and R. Singh, *ACS Catal.*, 2018, **8**, 8369–8375.

323 F. G. Bordwell, J. A. Harrelson and T. Y. Lynch, *J. Org. Chem.*, 1990, **55**, 3337–3341.

324 M. Shang, S. H. Zeng, S. Z. Sun, H. X. Dai and J. Q. Yu, *Org. Lett.*, 2013, **15**, 5286–5289.

325 Y. Yu, G. Luo, J. Yang and Y. Luo, *Catal. Sci. Technol.*, 2020, **10**, 1914–1924.

326 S. M. Au, J. S. Huang, W. Y. Yu, W. H. Fung and C. M. Che, *J. Am. Chem. Soc.*, 1999, **121**, 9120–9132.

327 S. K. Y. Leung, W. M. Tsui, J. S. Huang, C. M. Che, J. L. Liang and N. Zhu, *J. Am. Chem. Soc.*, 2005, **127**, 16629–16640.

328 M. E. Harvey, D. G. Musaev and J. Du Bois, *J. Am. Chem. Soc.*, 2011, **133**, 17207–17216.

329 G. Manca, E. Gallo, D. Intrieri and C. Mealli, *ACS Catal.*, 2014, **4**, 823–832.

330 J. Liang, S.-X. Yuan, J.-S. Huang, W.-Y. Yu and C.-M. Che, *Angew. Chem. Int. Ed.*, 2002, **41**, 3465–3468.

331 S. Fantauzzi, E. Gallo, A. Caselli, F. Ragaini, N. Casati, P. MacChi and S. Cenini, *Chem. Commun.*, 2009, 3952–3954.

332 X. Lin, C. M. Che and D. L. Phillips, *J. Org. Chem.*, 2008, **73**, 529–537.

333 X. Lin, C. Zhao, C. M. Che, Z. Ke and D. L. Phillips, *Chem. Asian J.*, 2007, **2**, 1101–1108.

334 K. W. Fiori, C. G. Espino, B. H. Brodsky and J. Du Bois, *Tetrahedron*, 2009, **65**, 3042–3051.

335 R. H. Perry, T. J. Cahill, J. L. Roizen, J. Du Bois and R. N. Zare, *Proc. Natl. Acad. Sci. U. S. A.*, 2012, **109**, 18295–18299.

336 A. Varela-Álvarez, T. Yang, H. Jennings, K. P. Kornecki, S. N. Macmillan, K. M. Lancaster, J. B. C. Mack, J. Du Bois, J. F. Berry and D. G. Musaev, *J. Am. Chem. Soc.*, 2016, **138**, 2327–2341.

337 M. R. Yadav, M. Shankar, E. Ramesh, K. Ghosh and A. K. Sahoo, *Org. Lett.*, 2015, **17**, 1886–1889.

338 K. Raghuvanshi, D. Zell, K. Rauch and L. Ackermann, *ACS Catal.*, 2016, **6**, 3172–3175.

339 K. Okamoto, K. Sasakura, T. Shimbayashi and K. Ohe, *Chem. Lett.*, 2016, **45**, 988–990.

340 A. A. G. Fernandes, M. L. Stivanin and I. D. Jurberg, *Chem. Sel.*, 2019, **4**, 3360–3365.

341 C. Bruneau, *Ruthenium in catalysis*, Springer International Publishing, Rennes, France, 2014, vol. 48.

342 N. Dastbaravardeh, M. Schnürch and M. D. Mihovilovic, *Org. Lett.*, 2012, **14**, 3792–3795.

343 N. Dastbaravardeh, M. Schnürch and M. D. Mihovilovic, *Eur J. Org. Chem.*, 2013, 2878–2890.

344 N. Y. P. Kumar, R. Jeyachandran and L. Ackermann, *J. Org. Chem.*, 2013, **78**, 4145–4152.

345 M. Schinkel, L. Wang, K. Bielefeld and L. Ackermann, *Org. Lett.*, 2014, **16**, 1876–1879.

346 I. Fabre, N. Von Wolff, G. Le Duc, E. F. Flegeau, C. Bruneau, P. H. Dixneuf and A. Jutand, *Chem. Eur. J.*, 2013, **19**, 7595–7604.

347 M. Simonetti, G. J. P. Perry, X. C. Cambeiro, F. Juliá-Hernández, J. N. Arokianathar and I. Larrosa, *J. Am. Chem. Soc.*, 2016, **138**, 3596–3606.

348 R. A. Alharis, C. L. McMullin, D. L. Davies, K. Singh and S. A. MacGregor, *Faraday Discuss.*, 2019, **220**, 386–403.

349 S. M. Au, S. B. Zhang, W. H. Fung, W. Y. Yu, C. M. Che and K. K. Cheung, *Chem. Commun.*, 1998, 2677–2678.

350 X.-Q. Yu, J.-S. Huang, X.-G. Zhou and C.-M. Che, *Org. Lett.*, 2000, **2**, 2233–2236.

351 S. M. Au, J. S. Huang, C. M. Che and W. Y. Yu, *J. Org. Chem.*, 2000, **65**, 7858–7864.

352 E. Milczek, N. Boudet and S. Blakey, *Angew. Chem. Int. Ed.*, 2008, **47**, 6825–6828.

353 Y. Nishioka, T. Uchida and T. Katsuki, *Angew. Chem. Int. Ed.*, 2013, **52**, 1739–1742.

354 Q. Xing, C. M. Chan, Y. W. Yeung and W. Y. Yu, *J. Am. Chem. Soc.*, 2019, **141**, 3849–3853.

355 J. Liang, S.-X. Yuan, J.-S. Huang, W.-Y. Yu and C.-M. Che, *Angew. Chem. Int. Ed.*, 2002, **41**, 3465–3468.

356 D. N. Barman and K. M. Nicholas, *Eur J. Org. Chem.*, 2011, 908–911.

357 Y. Liu, X. Guan, E. L. M. Wong, P. Liu, J. S. Huang and C. M. Che, *J. Am. Chem. Soc.*, 2013, **135**, 7194–7204.

358 J. D. St. Denis, C. F. Lee and A. K. Yudin, *Org. Lett.*, 2015, **17**, 5764–5767.

359 S. M. Paradine, J. R. Griffin, J. Zhao, A. L. Petronico, S. M. Miller and M. Christina White, *Nat. Chem.*, 2015, **7**, 987–994.

360 W. Liu, D. Zhong, C. L. Yu, Y. Zhang, D. Wu, Y. L. Feng, H. Cong, X. Lu and W. B. Liu, *Org. Lett.*, 2019, **21**, 2673–2678.

361 G. Pandey, R. Laha and P. K. Mondal, *Chem. Commun.*, 2019, **55**, 9689–9692.

362 M. Ichinose, H. Suematsu, Y. Yasutomi, Y. Nishioka, T. Uchida and T. Katsuki, *Angew. Chem. Int. Ed.*, 2011, **50**, 9884–9887.

363 H. Lu, K. Lang, H. Jiang, L. Wojtas and X. P. Zhang, *Chem. Sci.*, 2016, **7**, 6934–6939.

364 K. Lang, S. Torker, L. Wojtas and X. P. Zhang, *J. Am. Chem. Soc.*, 2019, **141**, 12388–12396.

365 Y. Yang, I. Cho, X. Qi, P. Liu and F. H. Arnold, *Nat. Chem.*, 2019, **11**, 987–993.

366 L. Sreerama, G. K. Rekha and N. E. Sladek, *Biochem. Pharmacol.*, 1995, **49**, 669–675.

367 A.-H. Hajri, G. Dewynter, M. Criton, P. Dilda and J.-L. Montero, *Heteroat. Chem.*, 2001, **12**, 1–5.

368 WO03097656, 2003.

369 J. D. Park and D. H. Kim, *Bioorg. Med. Chem.*, 2004, **12**, 2349–2356.

370 J. Winum, A. Innocenti, J. Nasr, J. Montero, A. Scozzafava, D. Vullo and C. T. Supuran, *Bioorg. Med. Chem. Lett.*, 2005, **15**, 2353–2358.

371 H. Jung, M. Schrader, D. Kim, M. H. Baik, Y. Park and S. Chang, *J. Am. Chem. Soc.*, 2019, **141**, 15356–15366.

372 J. Liu, W. Ye, S. Wang, J. Zheng, W. Tang and X. Li, *J. Org. Chem.*, 2020, **85**, 4430–4440.

373 X. Tian, X. Li, S. Duan, Y. Du, T. Liu, Y. Fang, W. Chen, H. Zhang, M. Li and X. Yang, *Adv. Synth. Catal.*, 2021, **363**, 1050–1058.

374 J. Kweon and S. Chang, *Angew. Chem. Int. Ed.*, 2021, **60**, 2909–2914.

375 C. G. Espino, K. W. Fiori, M. Kim and J. Du Bois, *J. Am. Chem. Soc.*, 2004, **126**, 15378–15379.

376 K. W. Fiori and J. Du Bois, *J. Am. Chem. Soc.*, 2007, **129**, 562–568.

377 A. Nörder, P. Herrmann, E. Herdtweck and T. Bach, *Org. Lett.*, 2010, **12**, 3690–3692.

378 J. R. Suárez and J. L. Chiara, *Chem. Commun.*, 2013, **49**, 9194–9196.

379 U. Hermann, M. Yaktapour and C. Bliefert, *Zeitschrift für Naturforsch. B*, 1978, **33**, 574–

574.

380 F. Mincione, L. Menabuoni, F. Briganti, G. Mincione, A. Scozzafava and C. T. Supuran, *J. Enzyme Inhib.*, 1998, **13**, 267–284.

381 A. Scozzafava and C. T. Supuran, *J. Med. Chem.*, 2000, **43**, 3677–3687.

382 J. Cheng, Z. Yang, Y. Li, Y. Xi, Q. Sun and L. He, *Synth.*, 2018, **50**, 2385–2393.

Chapter 4: Supporting Information

General Procedure A: Synthesis of Substituted Benzenesulfonyl Chloride Derivatives. The synthesis of arenesulfonyl chlorides was achieved through electrophilic aromatic substitution following a literature procedure.[246] In this synthetic protocol, chlorosulfonylation was achieved using chlorosulfonic acid, an extremely corrosive reagent for which safe handling is a major concern. It is imperative that only glass labware is used to transfer and contain the chlorosulfonic acid throughout the procedure and that contact with water is avoided to prevent its violent reactivity. All glassware used should be quenched immediately after use, first with slow addition of water, followed by *aq.* saturated $NaHCO_3$ solution. A substituted benzene derivative (1.0 equiv.) was first solubilized in $CHCl_3$ (0.5 M) within a round bottom flask containing a magnetic stir bar, and the solution was cooled to 0 °C using a water-ice bath. At the same time two clean Erlenmeyer flasks were prepared for the purpose of quenching acid, with one containing water for a first quench, and the other *aq.* saturated $NaHCO_3$ solution for further neutralization. After cooling the reaction solution, the water-ice bath was removed and set aside. While wearing acid resistant gloves, an appropriate volume of chlorosulfonic acid (4.5 equiv.) was measured in a clamp-secured glass graduated cylinder using a glass pipette for transfer. The glass pipette was again used to transfer the volume from the graduated cylinder to a glass drip funnel secured above the round bottom flask containing the reaction solution. Following the transfer, the reaction flask was submerged back into the water-ice bath and the reaction apparatus was purged with argon for 10 minutes. The acid was added to the reaction flask dropwise, and the reaction was run for 4 hours while warming to room temperature, after which the consumption of substituted benzene derivative was analyzed by TLC. After completion, the reaction mixture was slowly poured onto crushed ice and the resulting solution was extracted in triplicate with $CHCl_3$ and washed with *aq.* saturated NaCl solution. The organic phase was dried with sodium sulphate and concentrated under reduced pressure. The reaction gives a product with reasonable purity which can be carried to the next step without further purification.

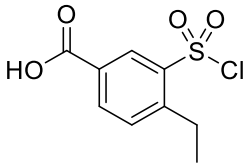

4m

*3-(Chlorosulfonyl)-4-ethylbenzoic acid. (**4m**).* The title compound was synthesized following an altered chlorosulfonylation procedure found in the literature.[281] Chlorosulfonic acid (30 mL, 53 g, 0.45 mol, 4.5 equiv.) was prepared in a round bottom flask following the necessary precautions outlined above (glass labware for transfer only, acid resistant gloves, avoiding water). *p*-Ethyl benzoic acid (15.0 g, 0.100 mol, 1.00 eqiuv.) was solubilized directly in the sulfonylating agent in preparation for a neat reaction, and the round bottom flask was fitted with a reflux condenser. An argon balloon was then used to purge the reaction apparatus for 10 minutes, and the reaction mixture was heated to 100 °C for 30 minutes, which was followed by 10 minutes of heating at 135 °C. The mixture was cooled to room temperature then slowly poured onto crushed ice. The resulting suspension was filtered and washed with distilled water to obtain the pure product as a white solid (*m* = 21.2 g, 85% yield). M. p. 199.7-203.4 °C; ^{1}H NMR (X00 MHz, DMSO-d_6) δ ^{1}H NMR (300 MHz, DMSO-d_6) δ 8.34 (d, *J* = 1.9 Hz, 1H), 7.80 (dd, *J* = 7.9, 1.9 Hz, 1H), 7.30 (d, *J* = 8.0 Hz, 1H), 3.07 (q, *J* = 7.5 Hz, 2H), 1.18 (t, *J* = 7.5 Hz, 3H); ^{13}C{^{1}H} NMR (101 MHz, $CDCl_3$) δ 169.5 (C), 150.2 (C), 143.3 (C), 136.4 (CH), 132.3 (CH), 131.0 (CH), 128.2 (C), 26.3 (CH_2), 14.9 (CH_3); IR (FTIR): 3084, 2981, 2887, 2824 (br), 2669, 1689, 1604, 1418, 1395, 1363, 1263, 1176, 1133 cm^{-1}; HRMS [EI]: Exact mass calcd for $C_9H_9ClO_4S^+$ [M]$^+$ 247.9910. Found: 247.9913.

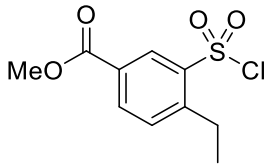

5m

*Methyl 3-(Chlorosulfonyl)-4-ethylbenzoate. (**5m**).* The title compound was synthesized following a procedure found in the literature.[247] 3-(Chlorosulfonyl)-4-ethylbenzoic acid (7.00 g, 28.1 mmol, 1.00 equiv.) was solubilized in thionyl chloride (29 mL, 48 g, 0.40 mol, 14 equiv.) and refluxed at 75 °C for 1 h. The thionyl chloride was evaporated using ***a rotary evaporator in a fumehood*** and quenched after collection in the solvent trap by slow drop-wise addition of water. The rotary evaporator was thoroughly rinsed with water and acetone to ensure removal or remaining thionyl chloride. The dry crude product was cooled to 0 °C in a water-ice bath and pre-cooled methanol (145 mL, 115 g, 3.58 mol, 127 equiv.) was added and the reaction was monitored by TLC to test the consumption of acyl chloride and prevent the further reaction to the methyl sulfone. The product was isolated by column chromatography (10% EtOAc/Hexanes). The product was obtained as an off-white solid (*m* = 0.084 g, 80% yield). TLC R_F = 0.33 in 10% EtOAc/Hexanes; ^{1}H NMR (400 MHz, $CDCl_3$) δ 8.68 (d, *J* = 1.8 Hz, 1H), 8.27 (dd, *J* = 8.0, 1.8 Hz, 1H), 7.57 (d, *J* = 8.0 Hz, 1H), 3.95 (s, 3H), 3.23 (q, *J* = 7.5 Hz, 2H), 1.36 (t, *J* = 7.5 Hz, 3H); ^{13}C{^{1}H} NMR (101 MHz, $CDCl_3$) δ 164.9 (C), 149.0 (C), 142.9 (C), 135.9 (CH), 132.1 (CH), 130.2 (CH), 129.1 (C), 52.8 (CH_3), 26.1 (CH_2), 14.8 (CH_3); IR (FTIR): 1726, 1604, 1436, 1363, 1285, 1266, 1177, 1124 cm^{-1}; HRMS [ESI]: Exact mass calcd for $C_{10}H_{11}ClO_4SNa^+$ [M+Na]$^+$ 262.0067. Found: 262.0087.

General Procedure B: Synthesis of Piloty's Acid Derivatives (*N*-Hydroxy Sulfonamides). (Scheme 35). The synthesis *N*-Hydroxy Sulfonamides was achieved through the sulfonylation of hydroxylamine with arenesulfonyl chlorides based on a literature procedure.[282] The reaction was performed in a methanol-water-tetrahydrofuran solvent mixture with a 3:2:30 (v:v:v) ratio, where the final concentration of the arenesulfonyl chloride was 0.143 M in THF (omitting MeOH and H_2O for the concentration determination). Hydroxylamine hydrochloride (2.3 equiv.) was first dissolved in a methanol-water mixture in a round bottom flask containing a magnetic stir bar and cooled to 0 °C using a water-ice bath, followed by the addition of magnesium oxide (2.3 equiv.). A volume of THF corresponding to the ratio stated above (10 times that of methanol) was divided into two parts: two thirds was added to the reaction mixture, which was allowed to cool for an additional 10 minutes, and the remaining third was used to solubilize the arenesulfonyl chloride (1.0 equiv.) in a drip-funnel. The solubilized arenesulfonyl chloride was added slowly to the cooled

reaction mixture followed by addition of magnesium oxide (0.7 equiv.). The reaction was monitored for completion by TLC over the course of 30 minutes to 3 hours. After consumption of the arenesulfonyl chloride, the solvent was evaporated under reduced pressure. The solid obtained was dissolved/ suspended in methanol and filtered through a pad of Celite. The solvent of the filtrate was again removed under reduced pressure and the new solid was dissolved/ suspended in diethyl ether and filtered through a pad of silica. The solvent was removed under reduced pressure to give pure *N*-Hydroxy Sulfonamide, or a semi-pure mixture which could be further purified by column chromatography or by recrystallization with ether/hexanes or CH_2Cl_2/hexanes if absolutely necessary (several Piloty's Acid derivatives decompose readily upon heating).

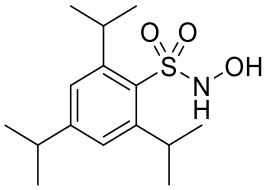

6a

*N-Hydroxy-2,4,6-triisopropylbenzenesulfonamide (**6a**).* The title compound was synthesized according to general procedure **B** through the sulfonylation of hydroxylamine hydrochloride (1.47 g, 22.8 mmol) with 2,4,6-triisopropylbenzenesulfonyl chloride (3.00 g, 9.90 mmol) using magnesium oxide as a base (0.918 g, 22.8 mmol; 0.279 g, 6.93 mmol). The reaction was carried out in a 3:2:30 (v:v:v) mixture of MeOH:H_2O:THF (7 mL : 4.7 mL : 70 mL) at 0 °C using a water-ice bath until TLC analysis indicated the consumption of 2,4,6-triisopropylbenzenesulfonyl chloride. The solvent was evaporated and the solid was washed through a Celite pad with methanol. The methanol was again evaporated to give a new solid that was washed through a silica pad with diethyl ether. The solvent was removed under reduced pressure to give the pure product as a white powder (*m* = 1.25 g, 42% yield). ^{1}H NMR (400 MHz, DMSO-d_6) δ 9.32 (s, 1H), 9.27 (s, 1H), 7.24 (s, 2H), 4.13 (hept, *J* = 6.7 Hz, 2H), 2.92 (hept, *J* = 6.8 Hz, 1H), 1.20 (t, *J* = 7.1 Hz, 18H); ^{13}C{^{1}H} NMR (101 MHz, DMSO-d_6) δ 152.7 (C), 151.3 (C), 130.9 (C), 123.5 (CH), 33.4 (CH), 29.3 (CH), 24.8 (CH_3), 23.4 (CH_3). ^{1}H and ^{13}C{^{1}H} NMR are in accordance with those reported in the literature.[282]

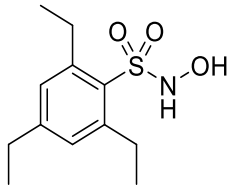

6b

*2,4,6-Triethyl-N-hydroxybenzenesulfonamide (**6b**).* The title compound was synthesized through the sulfonylation of hydroxylamine hydrochloride with 2,4,6-triethylbenzenesulfonyl chloride. Following general procedure **A**, the chlorosulfonylation of 1,3,5-triethylbenzene (1.88 mL, 1.62 g, 9.99 mmol, 1.00 equiv.) with chlorosulfonic acid (2.3 mL, 4.0 g, 35 mmol, 3.5 equiv.) was achieved in chloroform (20 mL) at 0 °C. The intermediate sulfonyl chloride was obtained as a yellow oil (2.42 g, 9.30 mmol, 93% yield). ^{1}H spectrum is in accordance with those reported in the literature. The 2,4,6-triethyl-*N*-hydroxybenzenesulfonyl chloride obtained was then carried to the next step without further purification. Thus, hydroxylamine hydrochloride (1.49 g, 23.0 mmol) was sulfonylated with the 2,4,6-triethylbenzenesulfonyl chloride obtained (2.42 g, 9.30 mmol) according to general procedure **B** using magnesium oxide as a base (0.862 g, 21.4 mmol; 0.262 g, 6.50 mmol). The reaction was carried out in a 3:2:30 (v:v:v) mixture of MeOH:H_2O:THF (7 mL : 4.7 mL : 70 mL) at 0 °C using a water-ice bath until TLC analysis indicated the consumption of 2,4,6-triethylbenzenesulfonyl chloride. The solvent was evaporated and the solid was washed through a Celite pad with methanol. The methanol was again evaporated to give a new solid that was washed through a silica pad with diethyl ether. The solvent was removed under reduced pressure to give a semi-pure solid which was further purified by recrystallization in CH_2Cl_2/hexanes. ***Note:** these compounds are very sensitive to heat and decompose readily, care must be taken if recrystallization is the desired method of purification. The product was obtained as a white fluffy powder (*m* = 0.989 g, 41% {38% yield over two steps}). M. p. 114.2-116.1 °C; ^{1}H NMR (300 MHz, DMSO-d_6) δ 9.36 (d, *J* = 2.7 Hz, 1H), 9.21 (d, *J* = 3.0 Hz, 1H), 7.09 (s, 2H), 2.99 (q, *J* = 7.4 Hz, 4H), 2.60 (q, *J* = 7.6 Hz, 2H), 1.19 (t, *J* = 7.4 Hz, 6H), 1.18 (t, *J* = 7.6 Hz, 3H); ^{13}C{^{1}H} NMR (101 MHz, DMSO-d_6) δ 148.4 (C), 146.5 (C), 131.1 (C), 129.1 (CH), 28.1(CH_2), 27.6 (CH_2), 17.1 (CH_3), 14.9 (CH_3); IR (FTIR): 3409 (br), 3236, 2970, 2933, 2872, 1598, 1559, 1525, 1459, 1417, 1349, 1307, 1263, 1154 1043, 901, 879 cm^{-1}; HRMS [ESI]: Exact mass calcd for $C_{12}H_{19}NO_3SNa^+$ $[M+Na]^+$ 280.0983. Found: 280.0999.

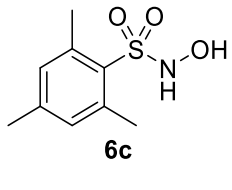

6c

*N-Hydroxy-2,4,6-trimethylbenzenesulfonamide (**6c**).* The title compound was synthesized according to general procedure **B** through the sulfonylation of hydroxylamine hydrochloride (3.20 g, 46.0 mmol) with 2,4,6-trimethylbenzenesulfonyl chloride (4.37 g, 20.0 mmol) using magnesium oxide as a base (1.85 g, 46.0 mmol; 0.564 g, 14.0 mmol). The reaction was carried out in a 3:2:30 (v:v:v) mixture of MeOH:H_2O:THF (14 mL : 9.3 mL : 140 mL) at 0 °C using a water-ice bath until TLC analysis indicated the consumption of 2,4,6-trimethylbenzenesulfonyl chloride. The solvent was evaporated and the solid was washed through a Celite pad with methanol. The methanol was again evaporated to give a new solid that was washed through a silica pad with diethyl ether. The solvent was removed under reduced pressure to give the pure product as a white powder

(*m* = 3.24 g, 75% yield). ^{1}H NMR (400 MHz, DMSO-d_6) δ 9.42 (d, *J* = 2.6 Hz, 1H), 9.25 (d, *J* = 2.4 Hz, 1H), 7.04 (s, 2H), 2.57 (s, 6H), 2.27 (s, 3H); ^{13}C{^{1}H} NMR (101 MHz, DMSO-d_6) δ 142.4 (C), 140.2 (C), 131.7 (C), 131.6 (CH), 23.0 (CH_3), 20.5 (CH_3). ^{1}H and ^{13}C{^{1}H} NMR are in accordance with those reported in the literature.[282]

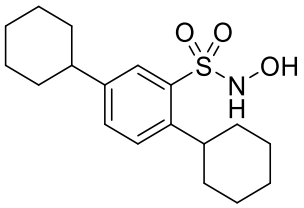

6d

*2,5-Dicyclohexyl-N-hydroxybenzenesulfonamide (**6d**).* The title compound was synthesized through the sulfonylation of hydroxylamine hydrochloride with 2,5-dicyclohexylbenzenesulfonyl chloride. Following general procedure **A**, the chlorosulfonylation of 1,4-dicyclohexylbenzene (4.85 g, 20.0 mmol, 1.00 equiv.) with chlorosulfonic acid (6.0 mL, 10 g, 90 mmol, 4.5 equiv.) was achieved in chloroform (40 mL) at 0 °C. The semi-pure product was obtained as a white solid which was carried to the next step without further purification. Thus, hydroxylamine hydrochloride (3.20 g, 49.6 mmol) was sulfonylated with 2,5-dicyclohexylbenzenesulfonyl chloride carried forward from the previous chlorosulfonylation ("6.82 g, 20.0 mmol") according to general procedure **B** using magnesium oxide as a base (1.85 g, 46.0 mmol; 0.564 g, 14.0 mmol). The reaction was carried out in a 3:2:30 (v:v:v) mixture of MeOH:H_2O:THF (14 mL : 9.3 mL : 140 mL) at 0 °C using a water-ice bath until TLC analysis indicated the consumption of 2,5-dicyclohexylbenzenesulfonyl chloride. The solvent was evaporated and the solid was washed through a Celite pad with methanol. The methanol was again evaporated to give a new solid that was washed through a silica pad with diethyl ether. The solvent was removed under reduced pressure to give a semi-pure solid which was further purified by recrystallization in Et_2O/hexanes ***Note:** these compounds are very sensitive to heat and decompose readily, care must be taken if recrystallization is the desired method of purification. The pure product was obtained as an off-white foam-like solid. (*m* = 2.95 g, 44% yield over two steps). M. p. 102.2-105.7 °C; ^{1}H NMR (400 MHz, DMSO-d_6) δ 9.59 (d, *J* = 3.1 Hz, 1H), 9.54 (d, *J* = 3.1 Hz, 1H), 7.68 (d, *J* = 1.5 Hz, 1H), 7.49 – 7.42 (m, 2H), 3.54 (t, *J* = 10.2 Hz, 1H), 2.54 (t, *J* = 7.7 Hz, 1H), 1.88 – 1.63 (m, 10H), 1.49 – 1.14 (m, 10H); ^{13}C{^{1}H} NMR (101 MHz, DMSO-d_6) δ 145.5 (C), 145.0 (C), 135.5 (C), 131.3 (CH), 128.4 (CH), 127.3 (CH), 43.1 (CH), 39.0 (CH), 33.9 (CH_2), 33.7 (CH_2), 26.4 (CH_2), 26.2 (CH_2), 25.6 (CH_2), 25.5 (CH_2); IR (FTIR): 3285 (br), 3057, 2921, 2849, 1484, 1446, 1353, 1318, 1265, 1161, 1117, 1077, 1020, 995, 827 cm^{-1}; HRMS [ESI]: Exact mass calcd for $C_{18}H_{27}NO_3SNa^+$ [M+Na]$^+$ 360.1609. Found: 360.1596.

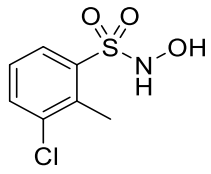

6e

*3-Chloro-N-hydroxy-2-methylbenzenesulfonamide (**6e**).* The title compound was synthesized according to general procedure **B** through the sulfonylation of hydroxylamine hydrochloride (1.32 g, 20.4 mmol) with 3-chloro-2-methylbenzenesulfonyl chloride (2.00 g, 8.88 mmol) using magnesium oxide as a base (0.824 g, 20.4 mmol; 0.251 g, 6.22 mmol). The reaction was carried out in a 3:2:30 (v:v:v) mixture of MeOH:H_2O:THF (6 mL : 4 mL : 60 mL) at 0 °C using a water-ice bath until TLC analysis indicated the consumption of 3-chloro-2-methylbenzenesulfonyl chloride. The solvent was evaporated and the solid was washed through a Celite pad with methanol. The methanol was again evaporated to give a new solid that was washed through a silica pad with diethyl ether. The solvent was removed under reduced pressure to give the pure product as an off-white powder (*m* = 1.36 g, 69% yield). ^{1}H NMR (500 MHz, DMSO-d_6) δ 9.80 (s, 1H), 9.66 (s, 1H), 7.86 (dd, *J* = 8.0, 1.3 Hz, 1H), 7.78 (dd, *J* = 8.0, 1.3 Hz, 1H), 7.46 (td, *J* = 8.0, 0.8 Hz, 1H), 2.64 (s, 3H); ^{13}C{^{1}H} NMR (101 MHz, DMSO-d_6) δ 138.2 (C), 135.7 (C), 135.4 (C), 133.8 (CH), 129.2 (CH), 127.3 (CH), 17.0 (CH_3); IR (FTIR): 3357 (br), 3248, 1453, 1433, 1376, 1314, 1272, 1167, 1152, 1088, 1003, 803, 785, 772 cm^{-1}; HRMS [ESI]: Exact mass calcd for $C_7H_7ClNO_3S^-$ [M]$^-$ 219.9835. Found: 219.9813.

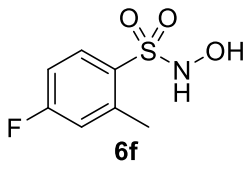

6f

*4-Fluoro-N-hydroxy-2-methylbenzenesulfonamide (**6f**).* The title compound was synthesized according to general procedure **B** through the sulfonylation of hydroxylamine hydrochloride (1.42 g, 22.0 mmol) with 4-fluoro-2-methylbenzenesulfonyl chloride (2.00 g, 9.59 mmol) using magnesium oxide as a base (0.889 g, 22.0 mmol; 0.270 g, 6.71 mmol). The reaction was carried out in a 3:2:30 (v:v:v) mixture of MeOH:H_2O:THF (6.7 mL : 4.5 mL : 67 mL) at 0 °C using a water-ice bath until TLC analysis indicated the consumption of 4-fluoro-2-methylbenzenesulfonyl chloride. The solvent was evaporated and the solid was washed through a Celite pad with methanol. The methanol was again evaporated to give a new solid that was washed through a silica pad with diethyl ether. The solvent was removed under reduced pressure to give the pure product as an off-white powder (*m* = 1.46 g, 74% yield). ^{1}H NMR (500 MHz, DMSO-d_6) δ 9.58 (s, 2H), 7.89 (dd, *J* = 8.8, 5.9 Hz, 1H), 7.32 (dd, *J* = 10.0, 2.7 Hz, 1H), 7.27 (td, *J* = 8.6, 2.8 Hz, 1H), 2.61 (s, 3H); ^{13}C{^{1}H} NMR (101 MHz, DMSO-d_6) δ 164.2 (d, *J* = 251.5 Hz, C), 141.9 (d, *J* = 9.5 Hz, C), 133.4 (d, *J* = 9.9 Hz, CH), 132.1 (d, *J* = 2.9 Hz, C), 119.0 (d, *J* = 22.3 Hz, CH), 113.2 (d, *J* = 22.0 Hz, CH), 20.39 (CH_3); IR (FTIR): 3406 (br),

3229, 3111, 3084, 2920, 2818, 1602, 1578, 1478, 1441, 1404, 1367, 1313, 1230, 1155, 1119, 1059, 1002, 951, 861, 831 cm^{-1}; HRMS [ESI]: Exact mass calcd for $C_7H_7FNO_3S^-$ $[M]^-$ 204.0131. Found: 204.0102.

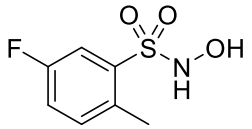

6g

*5-Fluoro-N-hydroxy-2-methylbenzenesulfonamide (**6g**).* The title compound was synthesized according to general procedure **B** through the sulfonylation of hydroxylamine hydrochloride (1.42 g, 22.0 mmol) with 5-fluoro-2-methylbenzenesulfonyl chloride (2.00 g, 9.59 mmol) using magnesium oxide as a base (0.889 g, 22.0 mmol; 0.270 g, 6.71 mmol). The reaction was carried out in a 3:2:30 (v:v:v) mixture of MeOH:H_2O:THF (6.7 mL : 4.5 mL : 67 mL) at 0 °C using a water-ice bath until TLC analysis indicated the consumption of 5-fluoro-2-methylbenzenesulfonyl chloride. The solvent was evaporated and the solid was washed through a Celite pad with methanol. The methanol was again evaporated to give a new solid that was washed through a silica pad with diethyl ether. The solvent was removed under reduced pressure to give the pure product as an off-white powder (m = 1.42 g, 72% yield). ^{1}H NMR (400 MHz, DMSO-d_6) δ 9.76 (d, J = 3.0 Hz, 1H), 9.72 (d, J = 3.0 Hz, 1H), 7.58 (dd, J = 8.7, 2.3 Hz, 1H), 7.50 – 7.42 (m, 2H), 2.57 (s, 3H); ^{13}C{^{1}H} NMR (101 MHz, DMSO-d_6) δ 159.6 (d, J = 245.0 Hz, C), 137.3 (d, J = 6.5 Hz, C), 134.5 (d, J = 7.3 Hz, CH), 134.1 (d, J = 3.4 Hz, C), 120.0 (d, J = 20.6 Hz, CH), 116.6 (d, J = 24.8 Hz, CH) 19.5 (CH_3); IR (FTIR): 3393 (br), 3207, 3080, 2928, 2820, 1603, 1487, 1390, 1348, 1320, 1225, 1161, 1051, 994, 904, 872, 838 cm^{-1}; HRMS [ESI]: Exact mass calcd for $C_7H_7FNO_3S^-$ $[M]^-$ 204.0131. Found: 204.0131.

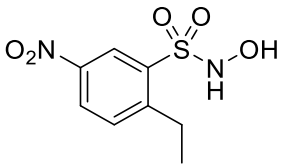

6h

*2-Ethyl-N-hydroxy-5-nitrobenzenesulfonamide (**6h**).* The title compound was synthesized through the sulfonylation of hydroxylamine hydrochloride with 2-ethyl-5-nitrobenzenesulfonyl chloride, which was synthesized following an altered chlorosulfonylation procedure found in the literature.[ref] *p*-Ethylnitrobenzene (6.76 mL, 7.56 g, 50.0 mmol, 1.00 equiv.) was added to a round bottom flask containing a magnetic stir bar. Chlorosulfonic acid (12 mL, 21 g, 0.18 mol, 3.5 equiv.) was measured in a clamp-secured glass graduated cylinder and transferred to the reaction flask, allowing for solubilization of *p*-ethylnitrobenzene. The reaction flask was equipped with a reflux condenser and purged with argon for 10 minutes. The neat reaction mixture was heated to 100 °C in an oil bath for 4 hours. An additional 10 minutes of heat was applied at 130 °C before being cooled to room temperature. The reaction mixture was then slowly poured onto crushed ice. The resulting solution was extracted in triplicate with $CHCl_3$ and washed with *aq.* saturated NaCl solution. The organic phase was dried with sodium sulphate and concentrated under reduced pressure. The semi-pure product was obtained as a yellow oil which was carried to the next step without further purification. Thus, hydroxylamine hydrochloride (7.42 g, 115 mmol) was sulfonylated with 2-ethyl-5-nitrobenzenesulfonyl chloride carried forward from the previous chlorosulfonylation ("12.5 g, 50.0 mmol") according to general procedure **B** using magnesium oxide as a base (4.63 g, 115 mmol; 1.41 g, 35.0 mmol). The reaction was carried out in a 3:2:30 (v:v:v) mixture of MeOH:H_2O:THF (36 mL : 24 mL : 360 mL) at 0 °C using a water-ice bath until TLC analysis indicated the consumption of 2-ethyl-5-nitrobenzenesulfonyl chloride. The solvent was evaporated and the solid was washed through a Celite pad with methanol. The methanol was again evaporated to give a new solid that was washed through a silica pad with diethyl ether. The solvent was removed under reduced pressure to give the pure product as a yellow chunky powder (m = 5.81 g, 47% yield over two steps). ^{1}H NMR (500 MHz, DMSO-d_6) δ 10.04 (d, J = 2.8 Hz, 1H), 9.88 (d, J = 2.6 Hz, 1H), 8.62 (d, J = 2.5 Hz, 1H), 8.43 (dd, J = 8.6, 2.5 Hz, 1H), 7.79 (d, J = 8.6 Hz, 1H), 3.13 (q, J = 7.5 Hz, 2H), 1.25 (t, J = 7.5 Hz, 3H); ^{13}C{^{1}H} NMR (126 MHz, DMSO-d_6) δ 151.9 (C), 145.3 (C), 137.0 (C), 132.8 (CH), 127.5 (CH), 124.7 (CH), 26.1 (CH_2), 15.5 (CH_3); IR (FTIR): 3419 (br), 3354, 3230, 3109, 3085, 2984, 2946, 2891, 1602, 1581, 1523, 1468, 1345, 1323, 1162, 1123, 1054, 993, 910, 884, 854 cm^{-1}; HRMS [ESI]: Exact mass calcd for $C_8H_{10}N_2O_5SNa^+$ $[M+Na]^+$ 269.0208. Found: 269.0190.

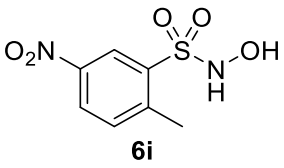

6i

*N-Hydroxy-2-methyl-5-nitrobenzenesulfonamide (**6i**).* The title compound was synthesized according to general procedure **B** through the sulfonylation of hydroxylamine hydrochloride (1.26 g, 19.5 mmol) with 2-methyl-5-nitrobenzenesulfonyl chloride (2.00 g, 8.49 mmol) using magnesium oxide as a base (0.787 g, 19.5 mmol; 0.239 g, 5.94 mmol). The reaction was carried out in a 3:2:30 (v:v:v) mixture of MeOH:H_2O:THF (5.9 mL : 4 mL : 59 mL) at 0 °C using a water-ice bath until TLC analysis indicated the consumption of 2-methyl-5-nitrobenzenesulfonyl chloride. The solvent was evaporated and the solid was washed through a Celite pad with methanol. The methanol was again evaporated to give a new solid that was washed through a silica pad with diethyl ether. The solvent was removed under reduced pressure to give the pure product as an orange solid (m = 0.697 g, 35% yield). ^{1}H NMR (400 MHz, DMSO-d_6) δ 10.00 (d, J = 3.0 Hz, 1H), 9.87 (d, J = 2.9 Hz, 1H), 8.59 (d, J = 2.5 Hz, 1H), 8.41 (dd, J = 8.4, 2.5 Hz, 1H), 7.74 (d, J = 8.5 Hz, 1H), 2.73 (s, 3H); ^{13}C{^{1}H} NMR (101 MHz, DMSO-d_6) δ 146.1 (C), 145.5 (C), 137.1 (C), 134.2

(CH), 127.4 (CH), 124.9 (CH), 20.5 (CH_3); IR (FTIR): 3374 (br), 3261, 3090, 2959, 2924, 2864, 1603, 1583, 1520, 1473, 1349, 1331, 1266, 1169, 1149, 1124, 987, 883, 859 cm^{-1}; HRMS [ESI]: Exact mass calcd for $C_7H_8N_2O_5SNa^+$ $[M+Na]^+$ 255.0052. Found: 255.0051.

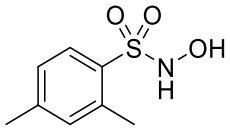

6j

*N-Hydroxy-2,4-dimethylbenzenesulfonamide (**6j**).* The title compound was synthesized according to general procedure **B** through the sulfonylation of hydroxylamine hydrochloride (1.16 g, 18.0 mmol) with 2,4-dimethylbenzenesulfonyl chloride (1.60 g, 7.82 mmol) using magnesium oxide as a base (0.725 g, 18.0 mmol; 0.220 g, 5.47 mmol). The reaction was carried out in a 3:2:30 (v:v:v) mixture of MeOH:H_2O:THF (5.6 mL : 3.7 mL : 56 mL) at 0 °C using a water-ice bath until TLC analysis indicated the consumption of 2,4-dimethylbenzenesulfonyl chloride. The solvent was evaporated and the solid was washed through a Celite pad with methanol. The methanol was again evaporated to give a new solid that was washed through a silica pad with diethyl ether. The solvent was removed under reduced pressure to give the pure product as a white powder (*m* = 1.20 g, 76% yield). ^{1}H NMR (400 MHz, DMSO-d_6) δ 9.49 (d, *J* = 3.0 Hz, 1H), 9.45 (d, *J* = 3.0 Hz, 1H), 7.72 (d, *J* = 8.0 Hz, 1H), 7.22 (s, 1H), 7.21 (d, *J* = 8.0 Hz, 1H), 2.55 (s, 3H), 2.33 (s, 3H); ^{13}C{^{1}H} NMR (101 MHz, DMSO-d_6) δ 143.4 (C), 137.9 (C), 132.94 (CH), 132.90 (C), 130.5 (CH), 126.7 (CH), 20.8 (CH_3), 20.3 (CH_3); IR (FTIR): 3378 (br), 3228, 2925, 1599, 1563, 1476, 1438, 1361, 1308, 1159, 1057, 995, 830 cm^{-1}; HRMS [ESI]: Exact mass calcd for $C_8H_{10}NO_3S^-$ $[M]^-$ 200.0381. Found: 200.0366.

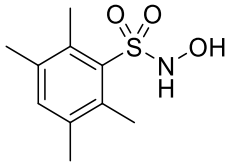

6k

*N-Hydroxy-2,3,5,6-tetramethylbenzenesulfonamide (**6k**).* The title compound was synthesized according to general procedure **B** through the sulfonylation of hydroxylamine hydrochloride (1.27 g, 19.8 mmol) with 2,3,5,6-tetramethylbenzenesulfonyl chloride (2.00 g, 8.59 mmol) using magnesium oxide as a base (0.797 g, 19.8 mmol; 0.242 g, 6.01 mmol). The reaction was carried out in a 3:2:30 (v:v:v) mixture of MeOH:H_2O:THF (6 mL : 4 mL : 60 mL) at 0 °C using a water-ice bath until TLC analysis indicated the consumption of 2,3,5,6-tetramethylbenzenesulfonyl chloride. The solvent was evaporated and the solid was washed through a Celite pad with methanol. The methanol was again evaporated to give a new solid that was washed through a silica pad with diethyl ether. The solvent was removed under reduced pressure to give the pure product as a white powder (*m* = 1.10 g, 56% yield). ^{1}H NMR (400 MHz, DMSO-d_6) δ 9.44 (d, *J* = 3.0 Hz, 1H), 9.34 (d, *J* = 3.1 Hz, 1H), 7.27 (s, 1H), 2.47 (s, 6H), 2.23 (s, 6H); ^{13}C{^{1}H} NMR (101 MHz, DMSO-d_6) δ 136.3 (C), 136.1 (C), 135.7 (CH), 135.4 (C), 20.5 (CH_3), 18.2 (CH_3); IR (FTIR): 3407 (br), 3238, 2974, 2957, 2924, 2868, 1463, 1425, 1351, 1303, 1249, 1203, 1145, 1010, 993, 940, 830 cm^{-1}; HRMS [ESI]: Exact mass calcd for $C_{10}H_{15}NO_3SNa^+$ $[M+Na]^+$ 252.0670. Found: 252.0681.

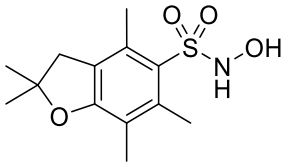

6l

*N-Hydroxy-2,2,4,6,7-pentamethyl-2,3-dihydrobenzofuran-5-sulfonamide (**6l**).* The title compound was synthesized according to general procedure **B** through the sulfonylation of hydroxylamine hydrochloride (1.03 g, 15.9 mmol) with 2,2,4,6,7-pentamethyl-2,3-dihydrobenzofuran-5-sulfonyl chloride (2.00 g, 6.92 mmol) using magnesium oxide as a base (0.642 g, 15.9 mmol; 0.195 g, 4.85 mmol). The reaction was carried out in a 3:2:30 (v:v:v) mixture of MeOH:H_2O:THF (4.8 mL : 3.2 mL : 48 mL) at 0 °C using a water-ice bath until TLC analysis indicated the consumption of 2,2,4,6,7-pentamethyl-2,3-dihydrobenzofuran-5-sulfonyl chloride. The solvent was evaporated and the solid was washed through a Celite pad with methanol. The methanol was again evaporated to give a new solid that was washed through a silica pad with diethyl ether. The solvent was removed under reduced pressure to give the pure product as an off-white powder (*m* = 0.933 g, 47% yield). ^{1}H NMR (400 MHz, DMSO-d_6) δ 9.30 (d, *J* = 3.0 Hz, 1H), 9.11 (d, *J* = 3.2 Hz, 1H), 3.01 (s, 2H), 2.45 (s, 3H), 2.41 (s, 3H), 2.04 (s, 3H), 1.43 (s, 6H); ^{13}C{^{1}H} NMR (101 MHz, DMSO-d_6) δ 159.2 (C), 140.4 (C), 135.1 (C), 126.6 (C), 125.2 (C), 116.8 (C), 87.1 (C), 42.3 (CH_2), 28.3 (CH_3), 19.4 (CH_3), 18.0 (CH_3), 12.4 (CH_3); IR (FTIR): 3389 (br), 3240, 2983, 2967, 2928, 2862, 1603, 1573, 1457, 1409, 1358, 1301, 1237, 1207, 1158, 1137, 1093, 994, 906, 850, 802 cm^{-1}; HRMS [ESI]: Exact mass calcd for $C_{13}H_{19}NO_4SNa^+$ $[M+Na]^+$ 308.0932. Found: 308.0943.

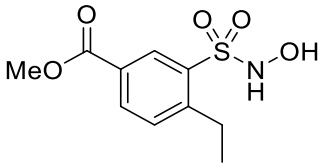

6m

*Methyl 4-Ethyl-3-(N-hydroxysulfamoyl)benzoate (**6m**).* The title compound was synthesized according to general procedure **B** through the sulfonylation of hydroxylamine hydrochloride (1.69 g, 26.3 mmol) with methyl 3-(chlorosulfonyl)-4-ethylbenzoate **5m** (3.00 g, 11.4 mmol) using magnesium oxide as a base (1.06 g, 26.3 mmol; 0.322 g, 8.00 mmol). The reaction was carried out in a 3:2:30 (v:v:v) mixture of MeOH:H_2O:THF (8.0 mL : 5.3 mL : 80 mL) at 0 °C using a water-ice bath until TLC analysis indicated the consumption of methyl 3-(chlorosulfonyl)-4-ethylbenzoate. The solvent was evaporated and the solid was washed through a Celite pad with methanol. The methanol was again evaporated to give a new solid that was washed through a silica pad with diethyl ether. The solvent was removed under reduced pressure and the crude product was purified by column chromatography (35% EtOAc/hexanes). The pure product was obtained as a white powder (m = 1.52 g, 51% yield). TLC R_F = 0.23 in 35% EtOAc/hexanes; ^{1}H NMR (400 MHz, DMSO-d_6) δ 9.82 (d, J = 3.1 Hz, 1H), 9.71 (d, J = 3.0 Hz, 1H), 8.44 (d, J = 1.8 Hz, 1H), 8.13 (dd, J = 8.0, 1.9 Hz, 1H), 7.63 (d, J = 8.1 Hz, 1H), 3.89 (s, 3H), 3.08 (q, J = 7.4 Hz, 2H), 1.22 (t, J = 7.4 Hz, 3H); ^{13}C{^{1}H} NMR (101 MHz, DMSO-d_6) δ 165.1 (C), 149.7 (C), 136.2 (C), 133.3 (CH), 131.7 (CH), 130.9 (CH), 127.6 (C), 52.5 (CH_3), 26.1 (CH_2), 15.5 (CH_3); IR (FTIR): 3272 (br), 2979, 2926, 2870, 1597, 1456, 1409, 1373, 1317, 1270, 1250, 1133, 1090 cm^{-1}; HRMS [ESI]: Exact mass calcd for $C_{10}H_{13}NO_5SNa^+$ [M+Na]$^+$ 282.0412. Found: 282.0384.

6t

*N-hydroxybutane-1-sulfonamide (**6t**).* The synthesis of the title compound has been previously reported[282,379] and was included in the scope for the referenced paper for general procedure **B**,[282] however, full characterization data has never been published.[379] The NMR spectra included here were taken after partial compound degradation but the important peaks indicating the presence of **6t** are shown. Despite the impaired characterization data taken with the degraded sample, the pure product **6t** was carried forward earlier to synthesize *N*-(benzoyloxy)butane-1-sulfonamide **1t**, which was fully characterized. *N*-hydroxybutane-1-sulfonamide was synthesized according to procedure **B**, a variant derived from the protocol previously used for its synthesis. The sulfonylation of hydroxylamine hydrochloride (1.60 g, 23.0 mmol) was achieved with 1-butanesulfonyl chloride (1.57 g, 10.0 mmol) using magnesium oxide as a base (1.21 g, 30.0 mmol). The reaction was carried out in a 3:2:30 (v:v:v) mixture of MeOH:H_2O:THF (7.5 mL : 5.0 mL : 75 mL) at 0 °C using a water-ice bath until TLC analysis indicated the consumption of 1-butanesulfonyl chloride. The solvent was evaporated and the solid was washed through a Celite pad with methanol. The methanol was again evaporated to give a new solid that was washed through a silica pad with diethyl ether. The solvent was removed under reduced pressure to give the pure product as a clear oil (m = 1.36 g, 89% yield) ^{1}H NMR (400 MHz, DMSO-d_6) δ 9.49 (d, J = 3.0 Hz, 1H), 9.11 (s, 1H), 3.06 (t, J = 7.8 Hz, 3H), 1.63 (p, J = 7.6 Hz, 3H), 1.38 (h, J = 7.6 Hz, 3H), 0.87 (t, J = 7.3 Hz, 4H); ^{13}C{^{1}H} NMR (101 MHz, DMSO-d_6) δ 47.0 (CH_2), 24.6 (CH_2), 21.2 (CH_2), 13.7 (CH_3); IR (FTIR): 3402 (br), 3238 (br), 2961, 2937, 2876, 1635, 1466, 1362, 1318, 1304, 1146 cm^{-1}.

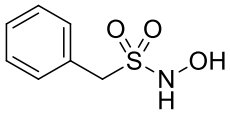

6u

*N-hydroxy-1-phenylmethanesulfonamide (**6u**).* The synthesis of the title compound has been previously reported[380–382] and was used as the primary starting material while synthesizing a scope for a certain paper,[382] however, only partial characterization data for the compound has been published.[380] The NMR spectra included here were taken after partial compound degradation but the important peaks indicating the presence of **6u** are shown. Despite the impaired characterization data taken with the degraded sample, the pure product **6u** was carried forward to synthesize *N*-(benzoyloxy)-1-phenylmethanesulfonamide **1u**, which was fully characterized. *N*-hydroxy-1-phenylmethanesulfonamide was synthesized according to general procedure **B** through the sulfonylation of hydroxylamine hydrochloride (1.60 g, 23.0 mmol) with phenylmethanesulfonyl chloride (1.91 g, 10.0 mmol) using magnesium oxide as a base (1.21 g, 30.0 mmol). The reaction was carried out in a 3:2:30 (v:v:v) mixture of MeOH:H_2O:THF (7.5 mL : 5.0 mL : 75 mL) at 0 °C using a water-ice bath until TLC analysis indicated the consumption of phenylmethanesulfonyl chloride. The solvent was evaporated and the solid was washed through a Celite pad with methanol. The methanol was again evaporated to give a new solid that was washed through a silica pad with diethyl ether. The solvent was removed under reduced pressure to give the pure product as a white powder (m = 1.35 g, 72% yield). ^{1}H NMR (400 MHz, DMSO-d_6) δ 9.68 (d, J = 3.3 Hz, 1H), 9.21 (d, J = 3.0 Hz, 1H), 7.38 (s, 5H), 4.40 (s, 2H); ^{13}C{^{1}H} NMR (101 MHz, DMSO-d_6) δ 131.0 (CH), 129.0 (C), 128.5 (CH), 128.2 (CH), 53.0 (CH_2); IR (FTIR): 3331, 3229, 1456, 1379, 1318, 1253, 1202, 1163, 1155, 1128 cm^{-1}; HRMS [ESI]: Exact mass calcd for $C_7H_9NO_3SNa^+$ [M+Na]$^+$ 210.0201. Found: 210.0186. ^{1}H NMR is in accordance with that reported in the literature.

General Procedure C: Synthesis of Acyloxy Sulfonamides. (**Scheme 36**). This procedure is based on a modified literature procedure.[285] A round bottom flask containing a magnetic stir bar was charged with an *N*-hydroxy arenesulfonamide derivative (1.0-1.25 equiv.) * A volume of tetrahydrofuran was measured for a 0.2 M reaction (concentration in *N*-hydroxy arenesulfonamide) and divided into two parts. Approximately two thirds of the THF volume was used to solubilize the *N*-hydroxy arenesulfonamide in the reaction flask, and the solution was cooled to -78 °C in a

dry ice-acetone bath for 15 minutes, followed by the addition of triethylamine (1.0-1.25 equiv.).* The remaining volume of THF was used to solubilize benzoic anhydride (1.0 equiv.) and the solution was added to the reaction mixture dropwise using a drip-funnel. Cooling at -78 °C was maintained for 4 hours and the reaction was continued while warming to ambient temperature over an additional 12 hours. the solvent was removed under reduced pressure and the crude oil obtained was solubilized in ethyl acetate and transferred to a separatory funnel. The solution was washed in triplicate with *aq.* saturated $NaHCO_3$ solution to remove triethylamine and benzoate salts followed by a final wash with *aq.* saturated NaCl solution. The resulting organic phase was dried with sodium sulphate and concentrated under reduced pressure. The desired acyloxysulfonamide was purified via recrystallization with Et_2O hexanes, unless otherwise noted. ***Note:** an equimolar quantity of Piloty's acid derivative, triethylamine and benzoic anhydride were used in earlier experiments but the possibility of di-addition (*N*-acylation) led to later reactions being performed with either 1.1 or 1.25 equivalents of both the Piloty's acid derivative and triethylamine.

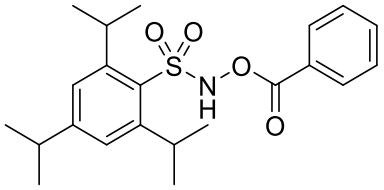

1a

*N-(Benzoyloxy)-2,4,6-triisopropylbenzenesulfonamide (**1a**).* (**Table 11**, **Table 18**, **Table 20**). The title compound was synthesized according to general procedure **C** through the acylation of *N*-hydroxy-2,4,6-triisopropylbenzenesulfonamide **6a** (1.43 g, 4.76 mmol, 1.00 equiv.) using benzoic anhydride (1.08 g, 4.76 mmol, 1.00 equiv.) with triethylamine (0.66 mL, 0.48 g, 4.7 mmol, 0.99 equiv.) in THF (24 mL) at -78 °C for 4 hours, then -78 °C – r.t. for 12h. After the total 16 hours the reaction mixture was concentrated under reduced pressure and recrystallized in Et_2O/hexanes. The title compound was obtained as a fluffy white powder (*m* = 0.689 g, 36% yield). M. p. 146.2-149.1 °C; ^{1}H NMR (400 MHz, $CDCl_3$) δ 9.34 (s, 1H), 7.97 (dd, *J* = 8.2, 1.5 Hz, 2H), 7.62 (t, *J* = 7.4 Hz, 1H), 7.44 (t, *J* = 7.8 Hz, 2H), 7.18 (s, 2H), 4.11 (hept, *J* = 6.7 Hz, 2H), 2.91 (hept, *J* = Hz, 1H), 1.25 (d, *J* = 6.5 Hz, 18H); ^{13}C{^{1}H} NMR (101 MHz, $CDCl_3$) δ 165.4 (C), 154.8 (C), 152.7 (C), 134.6 (CH), 130.0 (CH), 128.8 (C, overlapped), 128.8 (CH, overlapped), 126.1 (C), 124.3 (CH), 34.4 (CH), 30.5 (CH), 25.0 (CH_3), 23.6 (CH_3); IR (FTIR): 3172 (br), 2955, 2869, 1766, 1560, 1544, 1450, 1364, 1322, 1254, 1232, 1156, 1039, 1020, 966, 880 cm^{-1}; HRMS [ESI]: Exact mass calcd for $C_{22}H_{29}NO_4SNa^+$ $[M+Na]^+$ 426.1715. Found: 426.1704.

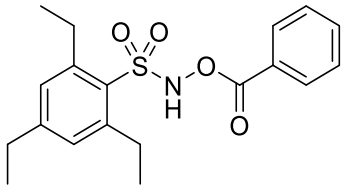

1b

*N-(Benzoyloxy)-2,4,6-triethylbenzenesulfonamide (**1b**).* (**Table 11**, **Table 18**, **Table 20**). The title compound was synthesized according to general procedure **C** through the acylation of 2,4,6-triethyl-*N*-hydroxy-benzenesulfonamide **6b** (0.772 g, 3.00 mmol, 1.25 equiv.) using benzoic anhydride (0.543 g, 2.40 mmol, 1.00 equiv.) with triethylamine (0.42 mL, 0.30 g, 3.0 mmol, 1.2 equiv.) in THF (15 mL) at -78 °C for 4 hours, then -78 °C – r.t. for 12h. After the total 16 hours the reaction mixture was concentrated under reduced pressure and recrystallized in Et_2O/hexanes. The title compound was obtained as a translucent white crystalline solid (*m* = 0.290 g, 33% yield). M. p. 131.6-132.2 °C; ^{1}H NMR (400 MHz, $CDCl_3$) δ 9.30 (s, 1H), 7.90 (dd, *J* = 8.4, 1.2 Hz, 3H), 7.61 (tt, *J* = 7.5, 1.4 Hz, 1H), 7.43 (t, *J* = 7.8 Hz, 2H), 3.08 (q, *J* = 7.4 Hz, 4H), 2.61 (q, *J* = 7.6 Hz, 2H), 1.28 (t, *J* = 7.4 Hz, 6H), 1.21 (t, *J* = 7.6 Hz, 3H); ^{13}C{^{1}H} (101 MHz, $CDCl_3$) δ 165.4 (C), 150.6 (C), 147.9 (C), 134.6 (CH), 129.8 (CH), 129.7 (CH), 128.8 (CH, overlapped), 128.8 (C, overlapped), 126.0 (C), 28.9 (CH_2), 28.6 (CH_2), 17.0 (CH_3), 14.9 (CH_3); IR (FTIR): 3207 (br), 2970, 2931, 2872, 1746, 1594, 1558, 1448, 1398, 1349, 1252, 1231, 1182, 1167, 1043, 1021, 964, 877 cm^{-1}; HRMS [ESI]: Exact mass calcd for $C_{19}H_{23}NO_4SNa^+$ $[M+Na]^+$ 384.1245. Found: 384.1252.

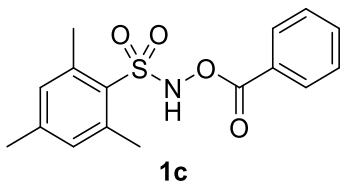

1c

*N-(Benzoyloxy)-2,4,6-trimethylbenzenesulfonamide (**1c**).* (**Table 1**, **Table 2**, **Table 4**, **Table 5**, **Table 6**, **Table 7**, **Table 8**, **Table 9**, **Table 10**, **Table 11**, **Scheme 40**, **Table 15**, **Table 18**, **Table 19**, **Table 20**). The title compound was synthesized according to general procedure **C** through the acylation of *N*-hydroxy-2,4,6-trimethylbenzenesulfonamide **6c** (1.51 g, 7.00 mmol, 1.00 equiv.) using benzoic anhydride (1.58 g, 7.00 mmol, 1.00 equiv.) with triethylamine (0.98 mL, 0.71 g, 7.0 mmol, 1.0 equiv.) in THF (35 mL) at -78 °C for 4 hours, then -78 °C – r.t. for 12h. After the total 16 hours the reaction mixture was concentrated under reduced pressure and recrystallized in CH_2Cl_2/hexanes. The title compound was obtained as a fluffy white powder (*m* = 0.748 g, 33% yield). M. p. 120.3-121.4 °C; ^{1}H NMR (500 MHz, $CDCl_3$) δ 9.28 (s, 1H), 7.92 (dd, *J* = 8.4, 1.3 Hz, 2H), 7.62 (tt, *J* = 7.5, 1.4 Hz, 1H), 7.48 – 7.41 (m, 2H), 6.95 (s, 3H), 2.68 (s, 6H), 2.29 (s, 3H); ^{13}C{^{1}H} (101 MHz, $CDCl_3$) δ 165.3 (C), 144.5 (C), 141.5 (C), 134.6 (CH), 132.3 (CH), 129.8 (CH), 129.4 (C), 128.9 (CH), 125.9 (C), 23.2 (CH_3), 21.2 (CH_3); IR (FTIR): 3138 (br), 2974, 2939, 1740,

1598, 1561, 1453, 1389, 1338, 1257, 1182, 1156, 1050, 1025, 918, 843 cm^{-1}; HRMS [ESI]: Exact mass calcd for $C_{16}H_{17}NO_4SNa^+$ $[M+Na]^+$ 342.0776. Found: 342.0774.

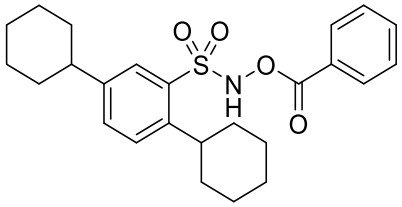

1d

*N-(Benzoyloxy)-2,5-dicyclohexylbenzenesulfonamide (**1d**).* (**Table 11**, **Table 20**). The title compound was synthesized according to general procedure **C** through the acylation of 2,5-dicyclohexyl-*N*-hydroxybenzenesulfonamide **6d** (2.83 g, 8.39 mmol, 1.00 equiv.) using benzoic anhydride (1.90 g, 8.39 mmol, 1.00 equiv.) with triethylamine (1.17 mL, 0.849 g, 8.39 mmol, 1.00 equiv.) in THF (42 mL) at -78 °C for 4 hours, then -78 °C – r.t. for 12h. After the total 16 hours the reaction mixture was concentrated under reduced pressure and recrystallized in Et_2O/hexanes. The title compound was obtained as a beige foam-like solid (*m* = 0.882 g, 24% yield). M. p. 131.6-133.5; ^1H NMR (400 MHz, $CDCl_3$) δ 9.29 (s, 1H), 7.92 – 7.82 (m, 3H), 7.60 (t, *J* = 7.5 Hz, 1H), 7.48 – 7.32 (m, 4H), 3.57 – 3.36 (m, 1H), 2.55 – 2.33 (m, 1H), 1.93 (d, *J* = 11.0 Hz, 2H), 1.88 – 1.58 (m, 8H), 1.45 (h, *J* = 12.9 Hz, 4H), 1.37 – 1.10 (m, 6H); $^{13}C\{^1H\}$ NMR (101 MHz, $CDCl_3$) δ 165.2 (C), 146.6 (C), 146.1 (C), 134.6 (CH), 133.3 (CH), 132.3 (C), 129.9 (CH, overlapped), 129.9 (CH, overlapped), 128.9 (CH), 128.8 (CH), 126.0 (C), 43.8 (CH), 40.4 (CH), 34.6 (CH_2), 34.1 (CH_2), 26.9 (CH_2), 26.7 (CH_2), 26.2 (CH_2), 26.0 (CH_2); IR (FTIR): 3153 (br), 3065, 2922, 2850, 1743, 1487, 1447, 1375, 1352, 1244, 1170, 1050, 1022, 999, 831 cm^{-1}; HRMS [ESI]: Exact mass calcd for $C_{25}H_{31}NO_4SNa^+$ $[M+Na]^+$ 464.1872. Found: 464.1860.

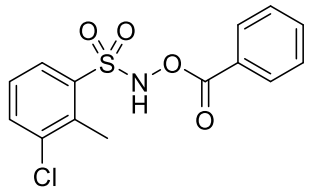

1e

*N-(Benzoyloxy)-3-chloro-2-methylbenzenesulfonamide (**1e**).* (**Table 12**, **Table 16**, **Table 17**, **Scheme 41**, **Table 19**, **Table 20**). The title compound was synthesized according to general procedure **C** through the acylation of 3-chloro-*N*-hydroxy-2-methylbenzenesulfonamide **6e** (0.724 g, 3.26 mmol, 1.10 equiv.) using benzoic anhydride (0.671 g, 2.97 mmol, 1.00 equiv.) with triethylamine (0.46 mL, 0.33 g, 3.3 mmol, 1.1 equiv.) in THF (16 mL) at -78 °C for 4 hours, then -78 °C – r.t. for 12h. After the total 16 hours the reaction mixture was concentrated under reduced pressure and recrystallized in Et_2O/hexanes. The title compound was obtained as a white crystalline solid (*m* = 0.468 g, 48% yield). M. p. 111.1-114.9 °C; ^1H NMR (400 MHz, $CDCl_3$) δ 9.29 (s, 1H), 8.01 (dd, *J* = 8.0, 1.3 Hz, 1H), 7.90 (dd, *J* = 8.4, 1.4 Hz, 2H), 7.67 – 7.59 (m, 2H), 7.45 (t, *J* = 7.9 Hz, 2H), 7.26 (d, *J* = 8.0 Hz, 1H), 2.81 (s, 3H); $^{13}C\{^1H\}$ NMR (101 MHz, $CDCl_3$) δ 165.4 (C), 137.5 (C), 137.5 (C), 136.0 (C), 135.5 (CH), 134.8 (CH), 130.2 (CH), 129.9 (CH), 129.0 (CH), 126.9 (CH), 125.7 (C), 17.4 (CH_3); IR (FTIR): 3138 (br), 2979, 2813, 1737, 1596, 1434, 1413, 1345, 1254, 1238, 1163, 1149, 1089, 1043, 1024, 935, 841, 783, 765 cm^{-1}; HRMS [ESI]: Exact mass calcd for $C_{14}H_{12}ClNO_4SNa^+$ $[M+Na]^+$ 348.0073. Found: 348.0095.

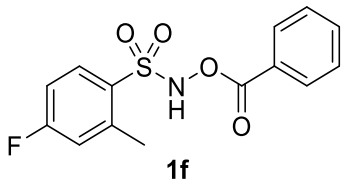

1f

*N-(Benzoyloxy)-4-fluoro-2-methylbenzenesulfonamide (**1f**).* (**Table 12**, **Table 16**, **Table 17**, **Table 5****Table 20**). The title compound was synthesized according to general procedure **C** through the acylation of 4-fluoro-*N*-hydroxy-2-methylbenzenesulfonamide **6f** (0.999 g, 4.87 mmol, 1.10 equiv.) using benzoic anhydride (1.00 g, 4.42 mmol, 1.00 equiv.) with triethylamine (0.68 mL, 0.49 g, 4.9 mmol, 1.1 equiv.) in THF (24 mL) at -78 °C for 4 hours, then -78 °C – r.t. for 12h. After the total 16 hours the reaction mixture was concentrated under reduced pressure and recrystallized in Et_2O/hexanes. The title compound was obtained as a fibrous, paper-like white solid (*m* = 0.713 g, 52% yield). M. p. 98.5-100.8 °C; ^1H NMR (500 MHz, $CDCl_3$) δ 9.23 (s, 1H), 8.05 (dd, *J* = 8.9, 5.6 Hz, 1H), 7.90 (dd, *J* = 8.4, 1.3 Hz, 1H), 7.63 (tt, *J* = 7.5, 1.4 Hz, 1H), 7.48 – 7.42 (m, 2H), 7.05 (dd, *J* = 9.1, 2.5 Hz, 1H), 6.98 (td, *J* = 8.6, 2.6 Hz, 1H), 2.75 (s, 3H); $^{13}C\{^1H\}$ (126 MHz, $CDCl_3$) δ 166.1 (d, *J* = 257.5 Hz, C), 165.4 (C), 143.3 (d, *J* = 9.6 Hz, C), 134.8 (CH), 134.5 (d, *J* = 10.1 Hz, CH), 129.9 (CH), 129.7 (d, *J* = 3.0 Hz, C), 129.0 (CH), 125.8 (C), 120.0 (d, *J* = 22.3 Hz, CH), 113.7 (d, *J* = 22.1 Hz, CH), 20.9 (d, *J* = 1.1 Hz, CH_3); IR (FTIR): 3117 (br), 2974, 2932, 1742, 1602, 1579, 1482, 1451, 1413, 1350, 1234, 1167, 1084, 1058, 1025, 997, 954, 862, 813 cm^{-1}; HRMS [ESI]: Exact mass calcd for $C_{14}H_{12}FNO_4SNa^+$ $[M+Na]^+$ 332.0369. Found: 332.0365.

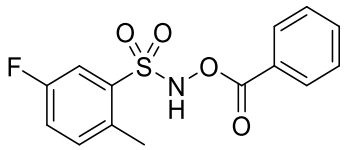

1g

*N-(Benzoyloxy)-5-fluoro-2-methylbenzenesulfonamide (**1g**).* (**Table 12**, **Table 16**, **Table 17**, **Table 20**). The title compound was synthesized according to general procedure **C** through the acylation of 5-fluoro-*N*-hydroxy-2-methylbenzenesulfonamide **6g** (1.57 g, 7.64 mmol, 1.10 equiv.) using benzoic anhydride (1.57 g, 6.94 mmol, 1.00 equiv.) with triethylamine (1.06 mL, 0.770 g, 7.60 mmol, 1.10 equiv.) in THF (38 mL) at -78 °C for 4 hours, then -78 °C – r.t. for 12h. After the total 16 hours the reaction mixture was concentrated under reduced pressure and recrystallized in Et_2O/hexanes. The title compound was obtained as a fine needle-like white solid (*m* = 0.875 g, 41% yield). M. p. 106.2-108.0 °C; ^{1}H NMR (500 MHz, $CDCl_3$) δ 9.28 (s, 1H), 7.91 (dd, *J* = 8.4, 1.4 Hz, 2H), 7.76 (dd, *J* = 8.3, 2.8 Hz, 1H), 7.64 (tt, *J* = 7.5, 1.4 Hz, 1H), 7.49 – 7.43 (m, 2H), 7.32 (dd, *J* = 8.5, 5.2 Hz, 1H), 7.22 (td, *J* = 8.1, 2.8 Hz, 1H), 2.71 (s, 2H); ^{13}C{^{1}H} (101 MHz, $CDCl_3$) δ 165.4, 160.4 (d, *J* = 249.4 Hz), 135.2 (d, *J* = 3.8 Hz, C, overlapped), 135.1 (d, *J* = 6.9 Hz, C, overlapped), 134.9 (CH), 134.6 (d, *J* = 7.0 Hz, CH), 129.9 (CH), 129.0 (CH), 125.7, 121.7 (d, *J* = 20.8 Hz, CH), 118.5 (d, *J* = 25.3 Hz, CH), 19.9 (CH_3); IR (FTIR): 3106 (br), 2932, 1743, 1598, 1488, 1452, 1405, 1353, 1229, 1163, 1061, 1028, 999, 871, 824 cm^{-1}; HRMS [ESI]: Exact mass calcd for $C_{14}H_{12}FNO_4SNa^+$ [M+Na]$^+$ 332.0369. Found: 332.0392.

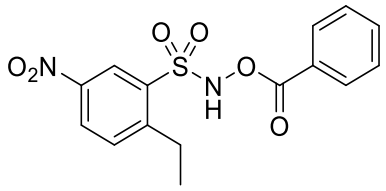

1h

*N-(Benzoyloxy)-2-ethyl-5-nitrobenzenesulfonamide (**1h**).* (**Table 12**, **Table 16**, **Table 20**). The title compound was synthesized according to general procedure **C** through the acylation of 2-ethyl-*N*-hydroxy-5-nitrobenzenesulfonamide **6h** (5.65 g, 23.0 mmol, 1.00 equiv.) using benzoic anhydride (5.19 g, 23.0 mmol, 1.00 equiv.) with triethylamine (3.20 mL, 2.32 g, 23.0 mmol, 1.00 equiv.) in THF (115 mL) at -78 °C for 4 hours, then -78 °C – r.t. for 12h. After the total 16 hours the reaction mixture was concentrated under reduced pressure. The crude product mixture was washed with warm Et_2O to afford the pure product as a light yellow/white solid (*m* = 4.33 g, 54% yield). M. p. 125.8-128.0; ^{1}H NMR (400 MHz, $CDCl_3$) δ 9.30 (s, br, 1H), 8.90 (d, *J* = 2.4 Hz, 1H), 8.40 (dd, *J* = 8.5, 2.5 Hz, 1H), 7.90 (dd, *J* = 8.4, 1.3 Hz, 2H), 7.67 – 7.60 (m, 2H), 7.50 – 7.42 (m, 3H), 3.25 (q, *J* = 7.5 Hz, 2H), 1.39 (t, *J* = 7.5 Hz, 3H); ^{13}C{^{1}H} (101 MHz, $CDCl_3$) δ 165.4 (C), 152.8 (C), 146.0 (C), 135.5 (C), 135.1 (CH), 132.6 (CH), 129.9 (CH), 129.1 (CH), 128.8 (CH), 126.8 (CH), 125.4 (C), 26.9 (CH_2), 15.2 (CH_3); IR (FTIR): 3110 (br), 2964, 2932, 1749, 1601, 1583, 1519, 1452, 1413, 1364, 1348, 1240, 1175, 1053, 1025, 885 cm^{-1}; HRMS [ESI]: Exact mass calcd for $C_{15}H_{14}N_2O_6SNa^+$ [M+Na]$^+$ 373.0470. Found: 373.0479.

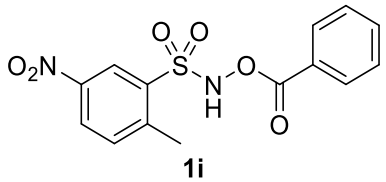

1i

*N-(Benzoyloxy)-2-methyl-5-nitrobenzenesulfonamide (**1i**).* (**Table 16**, **Table 17**, **Table 20**). The title compound was synthesized according to general procedure **C** through the acylation of *N*-hydroxy-2-methyl-5-nitrobenzenesulfonamide **6i** (0.655 g, 2.82 mmol, 1.10 equiv.) using benzoic anhydride (0.580 g, 2.56 mmol, 1.00 equiv.) with triethylamine (0.39 mL, 0.28 g, 2.8 mmol, 1.1 equiv.) in THF (12.5 mL) at -78 °C for 4 hours, then -78 °C – r.t. for 12h. After the total 16 hours the reaction mixture was concentrated under reduced pressure. The crude product mixture was washed with Et_2O to afford the pure product as a yellow-white solid (*m* = 0.502 g, 58% yield). M. p. 132.2-133.6; ^{1}H NMR (400 MHz, $CDCl_3$) δ 9.28 (s, 1H), 8.90 (d, *J* = 2.4 Hz, 1H), 8.35 (dd, *J* = 8.4, 2.5 Hz, 1H), 7.90 (dd, *J* = 8.4, 1.4 Hz, 2H), 7.64 (tt, *J* = 7.5, 1.4 Hz, 1H), 7.57 (d, *J* = 8.4 Hz, 1H), 7.50 – 7.42 (m, 2H), 2.88 (s, 3H); ^{13}C{^{1}H} NMR (101 MHz, $CDCl_3$) δ 165.4 (C), 146.9 (C), 146.2 (C), 135.7 (C), 135.2 (CH), 134.3 (CH), 130.0 (CH), 129.1 (CH), 128.7 (CH), 126.7 (CH), 125.3 (C), 21.1 (CH_3); IR (FTIR): 3081 (br), 2943, 1740, 1583, 1517, 1474, 1407, 1350, 1244, 1170, 1054, 999, 888 cm^{-1}; HRMS [ESI]: Exact mass calcd for $C_{14}H_{12}N_2O_6SNa^+$ [M+Na]$^+$ 359.0314. Found: 359.0310.

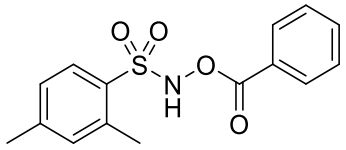

1j

*N-(Benzoyloxy)-2,4-dimethylbenzenesulfonamide (**1j**).* (**Table 16**, **Table 20**). The title compound was synthesized according to general procedure **C** through the acylation of *N*-hydroxy-2,4-dimethylbenzenesulfonamide **6j** (1.12 g, 5.56 mmol, 1.10 equiv.) using benzoic anhydride (1.14 g, 5.06 mmol, 1.00 equiv.) with triethylamine (0.78 mL, 0.57 g, 5.6 mmol, 1.1 equiv.) in THF (28 mL) at -78 °C for 4 hours, then -78 °C – r.t. for 12h. After the total 16 hours the reaction mixture was concentrated under reduced pressure and recrystallized in Et_2O/hexanes. The title compound was obtained as a white crystalline solid (*m* = 1.04 g, 67% yield). M. p. 93.8-95.2; ^{1}H NMR (500 MHz, $CDCl_3$) δ 9.23 (s, 1H), 7.92 – 7.87 (m, 5H), 7.64 – 7.59 (m, 1H), 7.46 – 7.41 (m, 2H), 7.14 (s, 1H), 7.08 (d, *J* = 8.2 Hz, 1H), 2.71 (s, 3H), 2.36 (s, 3H); ^{13}C{^{1}H} NMR (126 MHz, $CDCl_3$) δ 165.4 (C), 145.8 (C), 139.4 (C), 134.6 (CH), 133.8 (CH), 131.7 (CH), 130.6 (C), 129.9 (CH), 128.9 (CH), 127.2 (CH), 126.0 (C), 21.6 (CH_3), 20.6 (CH_3); IR (FTIR): 3132 (br), 1739, 1600, 1452, 1381, 1337, 1452, 1381, 1337, 1257, 1169, 1147, 1050, 930, 842 cm^{-1}; HRMS [ESI]: Exact mass calcd for $C_{15}H_{15}NO_4SNa^+$ [M+Na]$^+$ 328.0619. Found: 328.0626.

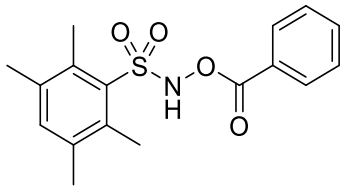

1k

*N-(Benzoyloxy)-2,3,5,6-tetramethylbenzenesulfonamide (**1k**).* (**Table 18**, **Table 20**) The title compound was synthesized according to general procedure **C** through the acylation of *N*-hydroxy-2,3,5,6-tetramethylbenzenesulfonamide **6k** (1.13 g, 4.94 mmol, 1.10 equiv.) using benzoic anhydride (1.02 g, 4.49 mmol, 1.00 equiv.) with triethylamine (0.69 mL, 0.50 g, 5.0 mmol, 1.1 equiv.) in THF (25 mL) at -78 °C for 4 hours, then -78 °C – r.t. for 12h. After the total 16 hours the reaction mixture was concentrated under reduced pressure and recrystallized in Et_2O/hexanes. The title compound was obtained as a white crystalline solid (*m* = 0.856 g, 57% yield). M. p. 91.9-93.9 °C; ^{1}H NMR (500 MHz, $CDCl_3$) δ 9.35 (s, 1H), 7.93 (dd, *J* = 8.4, 1.3 Hz, 2H), 7.62 (tt, *J* = 7.5, 1.4 Hz, 1H), 7.48 – 7.41 (m, 2H), 7.19 (s, 1H), 2.59 (s, 6H), 2.24 (s, 6H); ^{13}C{^{1}H} (101 MHz, $CDCl_3$) δ 165.4 (C), 137.6 (C), 137.5 (CH), 136.4 (C), 134.6 (CH), 133.7 (C), 129.9 (CH), 128.9 (CH), 126.0 (C), 21.1 (CH_3), 18.3 (CH_3); IR (FTIR): 3171 (br), 2980, 2920, 1746, 1599, 1571, 1450, 1356, 1241, 1208, 1159, 1044, 1020, 990, 826 cm^{-1}; HRMS [ESI]: Exact mass calcd for $C_{17}H_{19}NO_4SNa^+$ [M+Na]$^+$ 356.0932. Found: 356.0934.

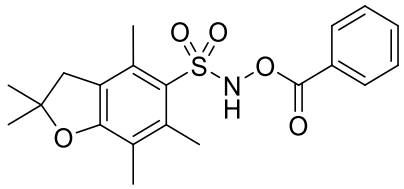

1l

*N-(Benzoyloxy)-2,2,4,6,7-pentamethyl-2,3-dihydrobenzofuran-5-sulfonamide (**1l**).* (**Table 20**). The title compound was synthesized according to general procedure **C** through the acylation of *N*-hydroxy-2,2,4,6,7-pentamethyl-2,3-dihydrobenzofuran-5-sulfonamide **6l** (0.643 g, 2.25 mmol, 1.10 equiv.) using benzoic anhydride (0.464 g, 2.05 mmol, 1.00 equiv.) with triethylamine (0.31 mL, 0.22 g, 2.2 mmol, 1.1 equiv.) in THF (12 mL) at -78 °C for 4 hours, then -78 °C – r.t. for 12h. After the total 16 hours the reaction mixture was concentrated under reduced pressure to afford a crude product mixture. The pure product was isolated by column chromatography (15% EtOAc/hexanes). The title compound was obtained as a yellow solid (*m* = 0.686 g, 86% yield). TLC R_F = 0.26 in 15% EtOAc/hexanes; ^{1}H NMR (500 MHz, $CDCl_3$) δ 9.27 (s, 1H), 7.93 (dd, *J* = 8.4, 1.4 Hz, 2H), 7.61 (tt, *J* = 7.5, 1.3 Hz, 1H), 7.49 – 7.40 (m, 3H), 2.91 (s, 2H), 2.59 (s, 3H), 2.49 (s, 3H), 2.07 (s, 3H), 1.44 (s, 6H); ^{13}C{^{1}H} NMR (101 MHz, $CDCl_3$) δ 165.5 (C), 161.3 (C), 142.3 (C), 136.4 (C), 134.5 (CH), 129.8 (CH), 128.8 (CH), 126.2 (C), 125.8 (C), 123.4 (C), 118.6 (C), 87.5 (C), 43.0 (CH_2), 28.6 (CH_3), 19.6 (CH_3), 18.2 (CH_3), 12.6 (CH_3); IR (FTIR): 3207 (br), 2982, 2935, 1777, 1571, 1450, 1405, 1326, 1233, 1162, 1139, 1093, 1044, 967, 848 cm^{-1}; HRMS [ESI]: Exact mass calcd for $C_{20}H_{23}NO_5SNa^+$ [M+Na]$^+$ 412.1195. Found: 412.1184.

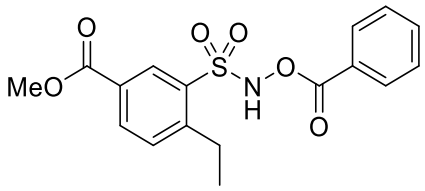

1m

*Methyl 3-(N-(Benzoyloxy)sulfamoyl)-4-ethylbenzoate (**1m**).* (**Table 20**). The title compound was synthesized according to general procedure **C** through the acylation of methyl 4-ethyl-3-(N-hydroxysulfamoyl)benzoate **6m** (1.30 g, 5.01 mmol, 1.10 equiv.) using benzoic anhydride (1.03 g, 4.56 mmol, 1.00 equiv.) with triethylamine (0.70 mL, 0.51 g, 5.0 mmol, 1.1 equiv.) in THF (25 mL) at -78 °C for 4 hours, then -78 °C – r.t. for 12h. After the total 16 hours the reaction mixture was concentrated under reduced pressure. Chloroform was used as the organic solvent for the extraction in this case. The pure product was isolated by column chromatography (25% EtOAc/hexanes). The title compound was obtained as a white solid (*m* = 1.29 g, 71% yield). TLC R_F = 0.26 in 25% EtOAc/Hexanes; ^{1}H NMR (400 MHz, $CDCl_3$) δ 9.30 (s, 1H), 8.67 (d, *J* = 1.8 Hz, 1H), 8.19 (dd, *J* = 8.0, 1.8 Hz, 1H), 7.87 (dd, *J* = 8.4, 1.3 Hz, 2H), 7.64 – 7.57 (m, 1H), 7.49 (d, *J* = 8.1 Hz, 1H), 7.46 – 7.39 (m, 2H), 3.88 (s, 3H), 3.18

(q, J = 7.5 Hz, 2H), 1.34 (t, J = 7.5 Hz, 3H); $^{13}C\{^1H\}$ NMR (101 MHz, $CDCl_3$) δ 165.33 (C), 165.28 (C), 150.6 (C), 135.3 (CH), 134.7 (CH), 134.0 (C), 132.7 (CH), 131.6 (CH), 129.9 (CH), 128.9 (CH), 128.7 (C), 125.7 (C), 52.6 (CH_3), 26.8 (CH_2), 15.3 (CH_3); IR (FTIR): 3296 (br), 3240, 1701, 1604, 1457, 1431, 1391, 1301, 1269, 1161, 1126 cm^{-1}; HRMS [ESI]: Exact mass calcd for $C_{17}H_{17}NO_6SNa^+$ $[M+Na]^+$ 386.0674. Found: 386.0670.

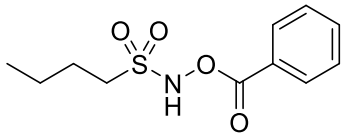

1t

*N-(benzoyloxy)butane-1-sulfonamide (**1t**).* (**Table 3**,**Table 13**,**Table 21**). The title compound was synthesized according to general procedure **C** through the acylation of *N*-hydroxybutane-1-sulfonamide **6t** (0.766 g, 5.00 mmol, 1.25 equiv.) using benzoic anhydride (0.905 g, 4.00 mmol, 1.00 equiv.) with triethylamine (0.70 mL, 0.51 g, 5.02 mmol, 1.26 equiv.) in THF (25 mL) at -78 °C for 4 hours, then -78 °C – r.t. for 12h. After the total 16 hours the reaction mixture was concentrated under reduced pressure. The pure product was isolated by column chromatography (15% EtOAc/hexanes). The title compound was obtained as a white flakey solid (m = 1.24 g, 89% yield). TLC R_F = 0.24 in 15% EtOAc/hexanes; The title compound was obtained as a white crystalline solid (m = 0.582 g, 57% yield). ^1H NMR (400 MHz, $CDCl_3$) δ 8.90 (s, 1H), 8.11 – 8.05 (m, 3H), 7.68 (tt, J = 7.5, 1.4 Hz, 1H), 7.56 – 7.48 (m, 4H), 3.28 – 3.21 (m, 2H), 1.99 – 1.88 (m, 2H), 1.51 (h, J = 7.4 Hz, 2H), 0.98 (t, J = 7.4 Hz, 3H); $^{13}C\{^1H\}$ NMR (101 MHz, $CDCl_3$) δ 165.7 (C), 134.9 (CH), 130.1 (CH), 129.1 (CH), 126.0 (C), 51.5 (CH_2), 25.0 (CH_2), 21.6 (CH_2), 13.6 (CH_3); IR (FTIR): 3107 (br), 2968, 2960, 2935, 2874, 1739, 1600, 1452, 1398, 1346, 1281, 1240, 1160 cm^{-1}; HRMS [ESI]: Exact mass calcd for $C_{11}H_{15}NO_4SNa^+$ $[M+Na]^+$ 280.0619. Found: 280.0630.

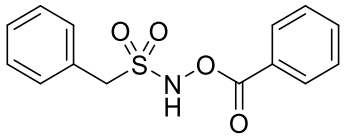

1u

*N-(benzoyloxy)-1-phenylmethanesulfonamide (**1u**).* (**Table 3**,**Table 13**,**Table 21**). The title compound was synthesized according to general procedure **C** through the acylation of *N*-hydroxy-1-phenylmethanesulfonamide **6u** (0.936 g, 5.00 mmol, 1.25 equiv.) using benzoic anhydride (0.905 g, 4.00 mmol, 1.00 equiv.) with triethylamine (0.70 mL, 0.51 g, 5.02 mmol, 1.26 equiv.) in THF (25 mL) at -78 °C for 4 hours, then -78 °C – r.t. for 12h. After the total 16 hours the reaction mixture was concentrated under reduced pressure. The pure product was isolated by column chromatography (20% EtOAc/hexanes), followed by recrystallization with Et_2O/hexanes. The title compound was obtained as a white solid (m = 0.419 g, 36% yield). TLC R_F = 0.17 in 20% EtOAc/hexanes; M. p. 122.9-126.2 °C; ^1H NMR (400 MHz, $CDCl_3$) δ 8.83 (s, 1H), 7.91 (dd, J = 8.3, 1.4 Hz, 2H), 7.66 (tt, J = 7.5, 1.4 Hz, 1H), 7.53 – 7.39 (m, 7H), 4.51 (s, 2H); $^{13}C\{^1H\}$ NMR (101 MHz, $CDCl_3$) δ 165.3 (C), 134.8 (C), 131.1 (CH), 130.1 (CH), 129.4 (CH), 129.2 (CH), 129.0 (CH), 127.1 (C), 126.0 (C), 58.1 (CH_2); IR (FTIR): 3082 (br), 1740, 1600, 1496, 1456, 1394, 1344, 1242, 1156 cm^{-1}; HRMS [ESI]: Exact mass calcd for $C_{14}H_{13}NO_4SNa^+$ $[M+Na]^+$ 314.0463. Found: 314.0455.

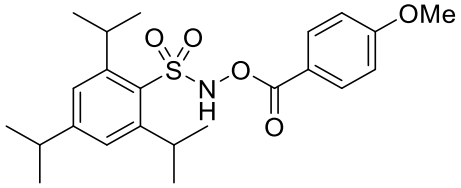

1v

*2,4,6-triisopropyl-N-((4-methoxybenzoyl)oxy)benzenesulfonamide (**1v**).* (**Scheme 33**). The title compound was synthesized according to general procedure **C** through the acylation of *N*-Hydroxy-2,4,6-trimethylbenzenesulfonamide **6c** (0.362 g, 1.21 mmol, 1.10 equiv.) using 4-methoxybenzoyl chloride (0.188 g, 1.10 mmol, 1.00 equiv.) with triethylamine (0.17 mL, 0.12 g, 1.2 mmol, 1.1 equiv.) in THF (6.0 mL) at -78 °C for 4 hours, then -78 °C – r.t. for 12h. After the total 16 hours the reaction mixture was concentrated under reduced pressure. The pure product was isolated by column chromatography (15% EtOAc/hexanes). The title compound was obtained as a white crystalline solid (m = 0.312 g, 67% yield). TLC R_F = 0.15 in 15% EtOAc/hexanes; ^1H NMR (400 MHz, Chloroform-*d*) δ 9.33 (s, 1H), 7.97 – 7.88 (m, 2H), 7.17 (s, 2H), 6.94 – 6.86 (m, 2H), 4.11 (hept, J = 6.7 Hz, 2H), 3.86 (s, 3H), 2.90 (hept, J = 7.0 Hz, 1H), 1.28 – 1.20 (m, 18H); $^{13}C\{^1H\}$ NMR (101 MHz, $CDCl_3$) δ 165.1 (C), 164.7 (C), 154.7 (C), 152.6 (C), 132.2 (CH), 129.0 (C), 124.2 (CH), 118.1 (C), 114.2 (CH), 55.7 (CH_3), 34.4 (CH), 30.5 (CH), 25.0 (CH_3), 23.6 (CH_3); IR (FTIR): 3268 (br), 2959, 2929, 2869, 1772, 1601, 1510, 1457, 1363, 1278, 1245, 1168, 1152, 1128 cm^{-1}; HRMS [ESI]: Exact mass calcd for $C_{23}H_{31}NO_5SNa^+$ $[M+Na]^+$ 456.1821. Found: 456.1820.

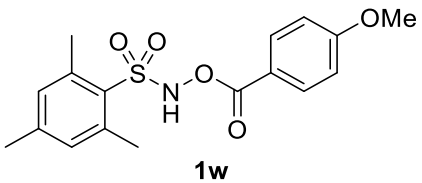

1w

*N-((4-methoxybenzoyl)oxy)-2,4,6-trimethylbenzenesulfonamide (**1w**).* (**Table 1**,**Table 7**). The title compound was synthesized according to general procedure **C** through the acylation of *N*-Hydroxy-2,4,6-trimethylbenzenesulfonamide **6c** (5.00 g, 1.08 mmol, 1.25 equiv.) using 4-methoxybenzoyl

chloride (0.682 g, 4.00 mmol, 1.00 equiv.) with triethylamine (0.70 mL, 0.51 g, 5.02 mmol, 1.26 equiv.) in THF (25 mL) at -78 °C for 4 hours, then -78 °C – r.t. for 12h. After the total 16 hours the reaction mixture was concentrated under reduced pressure. The pure product was isolated by column chromatography (10% EtOAc/hexanes). The title compound was obtained as an off-white solid (m = 1.24 g, 89% yield). TLC R_F = 0.11 in 10% EtOAc/hexanes; ^{1}H NMR (400 MHz, $CDCl_3$) δ 9.30 (s, 1H), 7.89 – 7.84 (m, 2H), 6.94 (d, J = 0.6 Hz, 1H), 6.93 – 6.88 (m, 2H), 3.86 (s, 3H), 2.67 (s, 6H), 2.28 (s, 3H); ^{13}C{^{1}H} NMR (101 MHz, $CDCl_3$) δ 165.0 (C), 164.7 (C), 144.4 (C), 141.5 (C), 132.3 (CH), 132.0 (CH), 129.5 (C), 117.9 (C), 114.2(CH), 55.7 (CH_3), 23.2 (CH_3), 21.2 (CH_3); IR (FTIR): 3156 (br), 1723, 1604, 1575, 1511, 1400, 1341, 1264, 1171, 1158 cm^{-1}; HRMS [ESI]: Exact mass calcd for $C_{17}H_{19}NO_5SNa^+$ [M+Na]$^+$ 372.0882. Found: 372.0875.

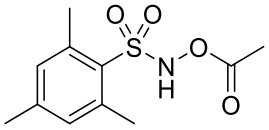

1x

*N-acetoxy-2,4,6-trimethylbenzenesulfonamide (**1x**).* (**Table 1**,**Table 7**). The title compound was synthesized according to general procedure **C** through the acylation of *N*-Hydroxy-2,4,6-trimethylbenzenesulfonamide **6c** (0.477 g, 2.22 mmol, 1.1 equiv.) using acetic anhydride (0.19 mL, 0.21 g, 2.0 mmol, 1.0 equiv.) with triethylamine (0.31 mL, 0.22 g, 2.2 mmol, 1.1 equiv.) in THF (11 mL) at -78 °C for 4 hours, then -78 °C – r.t. for 12h. After the total 16 hours the reaction mixture was concentrated under reduced pressure. The pure product was isolated by column chromatography (15% EtOAc/hexanes). The title compound was obtained as a white powder (m = 0.296 g, 57% yield). TLC R_F = 0.19 in 15% EtOAc/hexanes; ^{1}H NMR (400 MHz, $CDCl_3$) δ 8.97 (s, 1H), 6.98 (s, 2H), 2.65 (s, 6H), 2.31 (s, 3H), 2.04 (s, 3H); ^{13}C{^{1}H} NMR (101 MHz, $CDCl_3$) δ 169.2 (C), 144.5 (C), 141.4 (C), 132.2 (CH), 129.4 (C), 23.0 (CH_3), 21.2 (CH_3), 18.1 (CH_3); IR (FTIR): 3178 (br), 2981, 2942, 1776, 1600, 1374, 1362, 1341, 1191, 1166 cm^{-1}; HRMS [ESI]: Exact mass calcd for $C_{11}H_{15}NO_4SNa^+$ [M+Na]$^+$ 280.0619. Found: 280.0640.

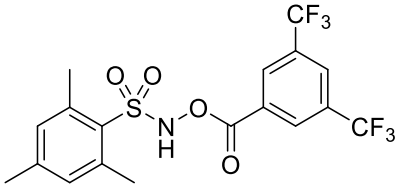

1y

*N-((3,5-bis(trifluoromethyl)benzoyl)oxy)-2,4,6-trimethylbenzenesulfonamide (**1y**).* (**Table 1**,**Table 7**). The title compound was synthesized according to general procedure **C** through the acylation of *N*-Hydroxy-2,4,6-trimethylbenzenesulfonamide **6c** (0.215 g, 1.00 mmol, 1.00 equiv.) using 3,5-bis(trifluoromethyl)benzoic anhydride (0.498 g, 1.00 mmol, 1.00 equiv.) with triethylamine (0.14 mL, 0.10 g, 1.00 mmol, 1.00 equiv.) in THF (5.0 mL) at -78 °C for 4 hours, then -78 °C – r.t. for 12h. After the total 16 hours the reaction mixture was concentrated under reduced pressure and recrystallized in Et_2O/hexanes. The title compound was obtained as a white crystalline solid (m = 0.375 g, 82% yield). M. p. 137.8-140.4 °C; ^{1}H NMR (400 MHz, $CDCl_3$) δ 9.15 (s, 1H), 8.35 (s, 2H), 8.13 (s, 1H), 6.99 (s, 2H), 2.67 (s, 6H), 2.31 (s, 3H); ^{13}C{^{1}H} NMR (101 MHz, $CDCl_3$) δ 163.0 (C), 145.1 (C), 141.7 (C), 132.9 (q, J = 34.5 Hz), 132.5 (CH), 130.0 – 129.7 (m, CH), 129.1 (C), 128.5 (C), 128.1 – 127.7 (m, CH), 122.6 (q, J = 273.2 Hz), 23.1 (CH_3), 21.2 (CH_3); IR (FTIR): 3167 (br), 1755, 1606, 1383, 1361, 1280, 1229, 1181, 1167, 1129, 1118 cm^{-1}; HRMS [EI]: Exact mass calcd for $C_{18}H_{15}F_6NO_4S^+$ [M]$^+$ 455.0626. Found: 455.0651.

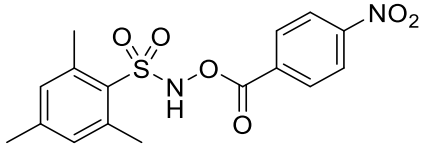

1z

*2,4,6-trimethyl-N-((4-nitrobenzoyl)oxy)benzenesulfonamide (**1z**).* (**Table 7**). The title compound was synthesized according to general procedure **C** through the acylation of *N*-Hydroxy-2,4,6-trimethylbenzenesulfonamide **6c** (0.215 g, 1.00 mmol, 1.00 equiv.) using 4-nitrobenzoic anhydride (0.316 g, 1.00 mmol, 1.00 equiv.) with triethylamine (0.14 mL, 0.10 g, 1.00 mmol, 1.00 equiv.) in THF (5.0 mL) at -78 °C for 4 hours, then -78 °C – r.t. for 12h. After the total 16 hours the reaction mixture was concentrated under reduced pressure and recrystallized in Et_2O/hexanes. The title compound was obtained as a white crystalline solid (m = 0.175 g, 48% yield). M. p. 132.1-133.9 °C; ^{1}H NMR (400 MHz, $CDCl_3$) δ 9.19 (s, 1H), 8.34 – 8.28 (m, 2H), 8.15 – 8.08 (m, 2H), 6.98 (s, 2H), 2.67 (s, 6H), 2.31 (s, 3H); ^{13}C{^{1}H} NMR (101 MHz, $CDCl_3$) δ 163.6 (C), 151.4 (C), 144.9 (C), 141.6 (C), 132.4 (CH), 131.4 (CH), 131.0 (C), 129.2 (C), 124.2 (CH), 23.2 (CH_3), 21.3 (CH_3); IR (FTIR): 3187 (br), 1741, 1603, 1385, 1347, 1319, 1238, 1163 cm^{-1}; HRMS [ESI]: Exact mass calcd for $C_{16}H_{16}N_2O_6SNa^+$ [M+Na]$^+$ 387.0627. Found: 387.0638.

General Procedure D: Synthesis of Substituted Benzosultams (Initial photoredox conditions). (**Scheme 33**). A substituted acyloxysulfonamide (1.0 equiv.) was placed in an 8 mL Kimax glass vial with a Teflon screw cap containing a stir bar and dissolved in dichloromethane (0.05 M), followed by the addition of $Ru(bpy)_3(PF_6)_2$ (2.0 mol%) and either Et_3N (1.1 equiv.) or $[Bu_4N][OP(O)(OBu)_2]$ (5.0 mol%) as a base. After the vial was sealed, the solution was cooled in a water-ice bath for 10 minutes and purged with argon for an additional 10 minutes while being held in the water-ice bath. The reaction vial was irradiated with 450 nm light using 12 V flexible blue LED strip lights for 16 hours. After the reaction time had completed, the solvent was removed under reduced pressure and the resulting crude mixture was solubilized in ethyl acetate and transferred to a separatory funnel. The solution was washed in triplicate with *aq.* saturated $NaHCO_3$ solution followed by a final wash with *aq.* saturated NaCl

solution. The resulting organic phase was dried with sodium sulphate and concentrated under reduced pressure. The desired sultam was isolated via silica gel column chromatography using a solvent system consisting of ethyl acetate/ hexanes.

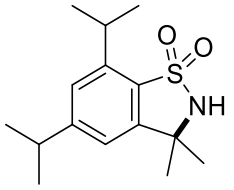

2a

*5,7-Diisopropyl-3,3-dimethyl-2,3-dihydrobenzo[d]isothiazole 1,1-dioxide (**2a**).* (**Scheme 33**). The title compound was synthesized according to general procedure **D**. 2,4,6-triisopropyl-*N*-((4-methoxybenzoyl)oxy)benzenesulfonamide **1v** (0.130 g, 0.300 mmol, 1.00 equiv.) was solubilized in dichloromethane (6.0 mL) in a microwave vial followed by the addition of $Ru(bpy)_3(PF_6)_2$ (0.0051 g, 0.0060 mmol, 2.0 mol%) and Et_3N (0.08 mL, 0.06 g, 0.6 mmol, , 2.0 equiv.) as a base. The solution was cooled to 0 °C and purged with argon for 10 minutes, after which the reaction was irradiated with 450 nm light using 12 V flexible blue LED strip lights for 16 hours. The product was isolated by column chromatography (15% EtOAc/hexanes). The product was obtained as an off-white solid (*m* = 0.0752 g, 89% yield). TLC R_F = 0.31 in 15% EtOAc/hexanes; ^{1}H NMR (400 MHz, $CDCl_3$) δ 7.21 (d, *J* = 1.4 Hz, 1H), 6.98 (d, *J* = 1.4 Hz, 1H), 4.74 (s, br, 1H), 3.60 (hept, *J* = 6.8 Hz, 1H), 2.97 (hept, *J* = 6.9 Hz, 1H), 1.62 (s, 6H), 1.33 (d, *J* = 6.8 Hz, 6H), 1.26 (d, *J* = 6.9 Hz, 6H); ^{13}C{^{1}H} NMR (101 MHz, $CDCl_3$) δ 155.6 (C), 146.9 (C), 145.3 (C), 130.9 (C), 124.4 (CH), 117.9 (CH), 59.9 (C), 34.7 (CH), 29.9 (CH_3), 29.5 (CH), 24.0 (CH_3), 23.7 (CH_3). ^{1}H and ^{13}C{^{1}H} NMR are in accordance with those reported in the literature.[246,257]

General Procedure E: Synthesis of Substituted Benzosultams (Thermal base-induced conditions). (**Table 11**). A substituted acyloxysulfonamide (1.0 equiv.) was placed in a microwave vial containing a stir bar and dissolved in acetonitrile (0.05 M), followed by the addition of *N,N*-diisopropylethylamine (1.0 equiv.). After the vial was sealed, the solution was cooled in a water-ice bath for 10 minutes and purged with argon for an additional 10 minutes while being held in the water-ice bath. The reaction vial was heated at 120 °C in an oil bath for 2 hours. After the reaction time had completed, the solvent was removed under reduced pressure and the resulting crude mixture was solubilized in ethyl acetate and transferred to a separatory funnel. The solution was washed in triplicate with *aq.* saturated $NaHCO_3$ solution followed by a final wash with *aq.* saturated NaCl solution. The resulting organic phase was dried with sodium sulphate and concentrated under reduced pressure. The desired sultam was isolated via silica gel column chromatography using a solvent system consisting of various ratios of ethyl acetate/ hexanes, unless otherwise specified.

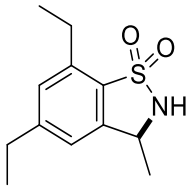

2b

*5,7-Diethyl-3-methyl-2,3-dihydrobenzo[d]isothiazole 1,1-dioxide (**2b**).* (**Table 11**). The title compound was synthesized according to general procedure **E**. *N*-(benzoyloxy)-2,4,6-triethylbenzenesulfonamide **1b** (0.181 g, 0.500, 1.00 equiv.) and *i*-pr_2Net (0.09 mL, 0.07 g, 0.5 mmol, 1 equiv.) were solubilized in acetonitrile (10.0 mL) in a microwave vial. The solution was cooled to 0 °C and purged with argon for 10 minutes, after which the reaction was heated at 120 °C in an oil bath for 2 hours. The product was isolated by column chromatography (15% EtOAc/hexanes). The product was obtained as an off-white solid (*m* = 0.101 g, 85% yield). TLC R_F = 0.325 in 15% EtOAc/hexanes; ^{1}H NMR (400 MHz, $CDCl_3$) δ 7.12 (d, *J* = 0.7 Hz, 1H), 6.98 (d, *J* = 0.6 Hz, 1H), 4.72 (s, br, 1H, overlapped), 4.68 (q, *J* = 6.7 Hz, 1H, overlapped), 2.99 (q, *J* = 7.6 Hz, 2H), 2.71 (q, *J* = 7.6 Hz, 2H), 1.58 (d, *J* = 6.5 Hz, 3H), 1.34 (t, *J* = 7.6 Hz, 3H), 1.25 (t, *J* = 7.6 Hz, 3H); ^{13}C{^{1}H} NMR (101 MHz, $CDCl_3$) δ 150.8 (C), 142.6 (C), 140.4 (C), 131.5 (C), 128.8 (CH), 120.4 (CH), 52.8 (CH), 29.2 (CH_2), 24.4 (CH_2), 21.7 (CH_3), 15.5 (CH_3), 14.8 (CH_3). ^{1}H and ^{13}C{^{1}H} NMR are in accordance with those reported in the literature.[246,248,257]

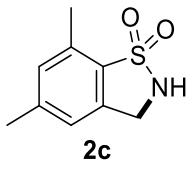

2c

*5,7-Dimethyl-2,3-dihydrobenzo[d]isothiazole 1,1-dioxide (**2c**).* (**Table 11**). The title compound was synthesized according to general procedure **E**. *N*-(benzoyloxy)-2,4,6-trimethylbenzenesulfonamide **1c** (0.319 g, 1.00 mmol, 1.00 equiv.) and *i*-pr_2Net (0.17 mL, 0.13 g, 0.98 mmol, 0.98 equiv.) were solubilized in acetonitrile (20.0 mL) in a microwave vial. The solution was cooled to 0 °C and purged with argon for 10 minutes, after which the reaction was heated at 120 °C in an oil bath for 2 hours. The product was isolated by column chromatography (15% EtOAc/hexanes). The product was obtained as an off-white solid (*m* = 0.176 g, 89% yield). TLC R_F = 0.04 in 15% EtOAc/hexanes; ^{1}H NMR (400 MHz, $CDCl_3$) δ 7.06 (s, 1H), 6.96 (s, 1H), 4.78 (s, br, 1H), 4.43 (s, 2H), 2.58 (s, 3H), 2.39 (s, 3H); ^{13}C{^{1}H} NMR (101 MHz, $CDCl_3$) δ 144.3 (C), 137.4 (C), 134.1 (C),

131.7 (CH), 131.5 (C), 122.4 (CH), 45.2 (CH_2), 21.6 (CH_3), 17.0 (CH_3). ^1H and $^{13}C\{^1H\}$ NMR are in accordance with those reported in the literature.[246,257]

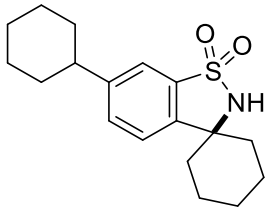

2d

6-Cyclohexyl-2H-spiro[benzo[d]isothiazole-3,1'-cyclohexane] 1,1-dioxide ***(2d)****.* (**Table 11**). The title compound was synthesized according to general procedure **E**. *N*-(benzoyloxy)-2,5-dicyclohexylbenzenesulfonamide **1d** (0.442 g, 1.000 mmol, 1.00 equiv.) and *i*-pr_2Net (0.17 mL, 0.13 g, 0.98 mmol, 0.98 equiv.) were solubilized in acetonitrile (20.0 mL) in a microwave vial. The solution was cooled to 0 °C and purged with argon for 10 minutes, after which the reaction was heated at 120 °C in an oil bath for 2 hours. The product was purified by recrystallization in CH_2Cl_2/hexanes. The product was obtained as a white fluffy powder (*m* = 0.132 g, 41% yield). M. p. 213.3-216.9 °C; ^1H NMR (400 MHz, $CDCl_3$) δ 7.55 (d, *J* = 1.5 Hz, 1H), 7.44 (dd, *J* = 8.0, 1.6 Hz, 1H), 7.28 (d, *J* = 8.1 Hz, 1H), 4.77 (s, 1H), 2.67 – 2.50 (m, 1H), 1.93 – 1.72 (m, 12H), 1.60 (qt, *J* = 14.3, 4.7 Hz, 2H), 1.48 – 1.33 (m, 5H), 1.32 – 1.15 (m, 1H); $^{13}C\{^1H\}$ NMR (101 MHz, $CDCl_3$) δ 150.0 (C), 143.8 (C), 135.4 (C), 132.5 (CH), 122.9 (CH), 119.1 (CH), 63.6 (C), 44.4 (CH), 37.9 (CH_2), 34.4 (CH_2), 26.8 (CH_2), 26.0 (CH_2), 24.9 (CH_2), 22.7 (CH_2); ^1H and $^{13}C\{^1H\}$ NMR are in accordance with those reported in the literature.[246]

General Procedure F: Synthesis of Substituted Benzosultams (Improved photoredox conditions). A substituted acyloxysulfonamide (1.0 equiv.) and $Ru(bpy)_3(PF_6)_2$ (2.0 mol%) were placed in a microwave vial containing a stir bar and dissolved in 1,2-dichloroethane (0.1 M). After the vial was sealed, the solution was cooled in a water-ice bath for 10 minutes and purged with argon for an additional 10 minutes while being held in the water-ice bath. was irradiated with 450 nm light using 12 V flexible blue LED strip lights for 16 hours, unless otherwise specified. After the reaction time had completed, the solvent was removed under reduced pressure and the resulting crude mixture analyzed by ^1H NMR; yields were determined using 1,3,5-trimethoxybenzene as an internal standard. While several high ^1H NMR yields were obtained with this method, isolation was not attempted with any of the sultams synthesized due to the limits in product scope.

General Procedure G: Synthesis of Substituted Benzosultams. (**Table 20**). A substituted acyloxysulfonamide (1.0 equiv.) and $Ru(bpy)_3(PF_6)_2$ (2.0 mol%) were placed in a microwave vial containing a stir bar and dissolved in 1,2-dichloroethane (0.1 M). After the vial was sealed, the solution was cooled in a water-ice bath for 10 minutes and purged with argon for an additional 10 minutes while being held in the water-ice bath. The reaction vial was heated at 85 °C in an oil bath for 22 hours. After the reaction time had completed, the solvent was removed under reduced pressure and the resulting crude mixture was solubilized in ethyl acetate and transferred to a separatory funnel. The solution was washed in triplicate with *aq.* saturated $NaHCO_3$ solution followed by a final wash with *aq.* saturated NaCl solution. The resulting organic phase was dried with sodium sulphate and concentrated under reduced pressure. ***Note:** in some cases an extraction was not performed; the crude product mixture was instead directly added to a column containing silica treated with 1% triethylamine. The desired sultam was isolated via silica gel column chromatography using a solvent system consisting of various ratios of ethyl acetate/ hexanes, unless otherwise specified.

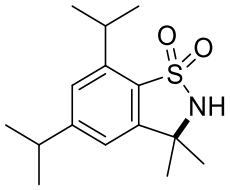

2a

5,7-Diisopropyl-3,3-dimethyl-2,3-dihydrobenzo[d]isothiazole 1,1-dioxide ***(2a)****.* (**Table 20**). The title compound was synthesized according to general procedure **G**. *N*-(benzoyloxy)-2,4,6-triisopropylbenzenesulfonamide **1a** (0.202 g, 0.500 mmol, 1.00 equiv.) and $Ru(bpy)_3(PF_6)_2$ (0.0086 g, 0.010 mmol, 2.0 mol%) were solubilized in 1,2-dichloroethane (5.0 mL) in a microwave vial. The solution was cooled to 0 °C and purged with argon for 10 minutes, after which the reaction was heated at 85 °C in an oil bath for 22 hours. The product was isolated by column chromatography (33% EtOAc/hexanes). The product was obtained as an off-white solid (*m* = 0.112 g, 80% yield). TLC R_F = 0.45 in 33% EtOAc/hexanes; ^1H NMR (400 MHz, $CDCl_3$) δ 7.21 (d, *J* = 1.4 Hz, 1H), 6.98 (d, *J* = 1.4 Hz, 1H), 4.74 (s, br, 1H), 3.60 (hept, *J* = 6.8 Hz, 1H), 2.97 (hept, *J* = 6.9 Hz, 1H), 1.62 (s, 6H), 1.33 (d, *J* = 6.8 Hz, 6H), 1.26 (d, *J* = 6.9 Hz, 6H); $^{13}C\{^1H\}$ NMR (101 MHz, $CDCl_3$) δ 155.6 (C), 146.9 (C), 145.3 (C), 130.9 (C), 124.4 (CH), 117.9 (CH), 59.9 (C), 34.7 (CH), 29.9 (CH_3), 29.5 (CH), 24.0 (CH_3), 23.7 (CH_3). ^1H and $^{13}C\{^1H\}$ NMR are in accordance with those reported in the literature.[246,257]

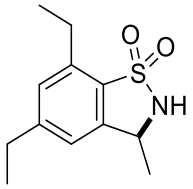

2b

*5,7-Diethyl-3-methyl-2,3-dihydrobenzo[d]isothiazole 1,1-dioxide (**2b**).* (**Table 20**). The title compound was synthesized according to general procedure **G**. *N*-(benzoyloxy)-2,4,6-triethylbenzenesulfonamide **1b** (0.362 g, 1.00 mmol, 1.00 equiv.) and $Ru(bpy)_3(PF_6)_2$ (0.017 g, 0.020 mmol, 2.0 mol%) were solubilized in 1,2-dichloroethane (10.0 mL) in a microwave vial. The solution was cooled to 0 °C and purged with argon for 10 minutes, after which the reaction was heated at 85 °C in an oil bath for 22 hours. The product was isolated by column chromatography (25% EtOAc/hexanes). The product was obtained as an off-white solid (*m* = 0.234 g, 97% yield). TLC R_F = 0.25 in 25% EtOAc/hexanes; ^{1}H NMR (400 MHz, $CDCl_3$) δ 7.12 (d, *J* = 0.7 Hz, 1H), 6.98 (d, *J* = 0.6 Hz, 1H), 4.72 (s, br, 1H, overlapped), 4.68 (q, *J* = 6.7 Hz, 1H, overlapped), 2.99 (q, *J* = 7.6 Hz, 2H), 2.71 (q, *J* = 7.6 Hz, 2H), 1.58 (d, *J* = 6.5 Hz, 3H), 1.34 (t, *J* = 7.6 Hz, 3H), 1.25 (t, *J* = 7.6 Hz, 3H); $^{13}C\{^1H\}$ NMR (101 MHz, $CDCl_3$) δ 150.8 (C), 142.6 (C), 140.4 (C), 131.5 (C), 128.8 (CH), 120.4 (CH), 52.8 (CH), 29.2 (CH_2), 24.4 (CH_2), 21.7 (CH_3), 15.5 (CH_3), 14.8 (CH_3). ^{1}H and $^{13}C\{^1H\}$ NMR are in accordance with those reported in the literature.[246,248,257]

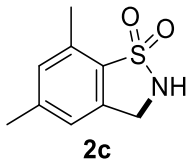

2c

*5,7-Dimethyl-2,3-dihydrobenzo[d]isothiazole 1,1-dioxide (**2c**).* (**Table 20**). The title compound was synthesized according to general procedure **G**. *N*-(benzoyloxy)-2,4,6-trimethylbenzenesulfonamide **1c** (0.319 g, 1.00 mmol, 1.00 equiv.) and $Ru(bpy)_3(PF_6)_2$ (0.017 g, 0.020 mmol, 2.0 mol%) were solubilized in 1,2-dichloroethane (10.0 mL) in a microwave vial. The solution was cooled to 0 °C and purged with argon for 10 minutes, after which the reaction was heated at 85 °C in an oil bath for 22 hours. The product was isolated by column chromatography (gradient column with 15% EtOAc/hexanes to 33% EtOAc/hexanes) The product was obtained as an off-white solid (*m* = 0.176 g, 89% yield). TLC R_F = 0.3 in 33% EtOAc/hexanes; ^{1}H NMR (400 MHz, $CDCl_3$) δ 7.06 (s, 1H), 6.96 (s, 1H), 4.78 (s, br, 1H), 4.43 (s, 2H), 2.58 (s, 3H), 2.39 (s, 3H); $^{13}C\{^1H\}$ NMR (101 MHz, $CDCl_3$) δ 144.3 (C), 137.4 (C), 134.1 (C), 131.7 (CH), 131.5 (C), 122.4 (CH), 45.2 (CH_2), 21.6 (CH_3), 17.0 (CH_3). ^{1}H and $^{13}C\{^1H\}$ NMR are in accordance with those reported in the literature.[246,257]

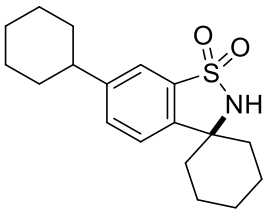

2d

*6-Cyclohexyl-2H-spiro[benzo[d]isothiazole-3,1'-cyclohexane] 1,1-dioxide (**2d**).* (**Table 20**). The title compound was synthesized according to general procedure **G**. *N*-(benzoyloxy)-2,5-dicyclohexylbenzenesulfonamide **1d** (0.221 g, 0.500 mmol, 1.00 equiv.) and $Ru(bpy)_3(PF_6)_2$ (0.0086 g, 0.010 mmol, 2.0 mol%) were solubilized in 1,2-dichloroethane (5.0 mL) in a microwave vial. The solution was cooled to 0 °C and purged with argon for 10 minutes, after which the reaction was heated at 85 °C in an oil bath for 22 hours. The product was isolated by column chromatography (gradient column with 10% Et_2O/pentanes to 50% Et_2O/pentanes). The product was obtained as a white fluffy powder (*m* = 0.119 g, 74% yield). TLC R_F = 0.26 in 30% Et_2O/pentanes; ^{1}H NMR (400 MHz, $CDCl_3$) δ 7.55 (d, *J* = 1.5 Hz, 1H), 7.44 (dd, *J* = 8.0, 1.6 Hz, 1H), 7.28 (d, *J* = 8.1 Hz, 1H), 4.77 (s, 1H), 2.67 – 2.50 (m, 1H), 1.93 – 1.72 (m, 12H), 1.60 (qt, *J* = 14.3, 4.7 Hz, 2H), 1.48 – 1.33 (m, 5H), 1.32 – 1.15 (m, 1H); $^{13}C\{^1H\}$ NMR (101 MHz, $CDCl_3$) δ 150.0 (C), 143.8 (C), 135.4 (C), 132.5 (CH), 122.9 (CH), 119.1 (CH), 63.6 (C), 44.4 (CH), 37.9 (CH_2), 34.4 (CH_2), 26.8 (CH_2), 26.0 (CH_2), 24.9 (CH_2), 22.7 (CH_2); ^{1}H and $^{13}C\{^1H\}$ NMR are in accordance with those reported in the literature.[246]

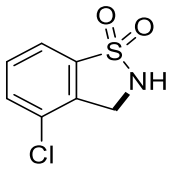

2e

*4-Chloro-2,3-dihydrobenzo[d]isothiazole 1,1-dioxide (**2e**).* (**Table 20**). The title compound was synthesized according to general procedure **G**. *N-(benzoyloxy)-3-chloro-2-methylbenzenesulfonamide* **1e** (0.163 g, 0.500 mmol, 1.00 equiv.) and $Ru(bpy)_3(PF_6)_2$ (0.0086 g, 0.010 mmol, 2.0 mol%) were solubilized in 1,2-dichloroethane (5.0 mL) in a microwave vial. The solution was cooled to 0 °C and purged with argon for 10 minutes, after which the reaction was heated at 85 °C in an oil bath for 22 hours. The product was isolated by column chromatography (20% EtOAc/hexanes). The product was obtained as a white solid (*m* = 0.0864 g, 85% yield). TLC R_F = 0.12 in 20% EtOAc/hexanes; ^{1}H NMR (400 MHz, $CDCl_3$) δ 7.71 (dd, *J* = 7.6, 0.9 Hz, 1H), 7.60 (dd, *J* = 7.9, 1.0 Hz, 1H), 7.51 (dd, *J* = 7.8, 0.8 Hz, 1H), 4.96 (s, br, 1H), 4.49 (d, *J* = 4.8 Hz, 2H); $^{13}C\{^1H\}$ NMR (101 MHz, $CDCl_3$) δ 137.6 (C), 135.0 (C), 133.1 (CH), 131.1 (C). 131.0 (CH), 119.9 (CH), 44.8 (CH_2); IR (FTIR): 3251 (br), 3079, 2921, 2850, 2790, 1449, 1391, 1307, 1210, 1167, 1147, 1101, 1059 cm^{-1}; HRMS [EI]: Exact mass calcd for $C_7H_6ClNO_2S^+$ $[M]^+$ 202.9808. Found: 202.9807.

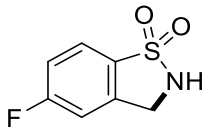

2f

*4-Fluoro-2,3-dihydrobenzo[d]isothiazole 1,1-dioxide (**2f**).* (**Table 20**). The title compound was synthesized according to general procedure **G**. *N*-(benzoyloxy)-4-fluoro-2-methylbenzenesulfonamide **1f** (0.155 g, 0.500 mmol, 1.00 equiv.) and $Ru(bpy)_3(PF_6)_2$ (0.0086 g, 0.010 mmol, 2.0 mol%) were solubilized in 1,2-dichloroethane (5.0 mL) in a microwave vial. The solution was cooled to 0 °C and purged with argon for 10 minutes, after which the reaction was heated at 85 °C in an oil bath for 22 hours. The product was isolated by column chromatography (1% Et_2O/CH_2Cl_2). ***Note:** in this case an extraction was not performed; the crude product mixture was instead directly added to a column containing silica treated with 1% triethylamine. The product was obtained as a white solid (*m* = 0.0466 g, 50% yield). TLC R_F = 0.17 in 1% Et_2O/CH_2Cl_2; ^{1}H NMR (400 MHz, $CDCl_3$) δ 7.79 (dd, *J* = 8.6, 4.7 Hz, 1H), 7.23 (td, *J* = 8.5, 2.2 Hz, 1H), 7.09 – 7.04 (m, 1H), 4.91 (s, br, 1H), 4.52 (s, 2H); $^{13}C\{^1H\}$ NMR (101 MHz, $CDCl_3$) δ 165.6 (d, *J* = 255.2 Hz, C), 140.1 (d, *J* = 9.6 Hz, C), 131.7 (d, *J* = 2.6 Hz, C), 123.9 (d, *J* = 10.1 Hz, CH), 117.5 (d, *J* = 24.1 Hz, CH), 112.0 (d, *J* = 24.0 Hz, CH), 45.5 (d, *J* = 2.4 Hz, CH_2); IR (FTIR): 3210 (br), 1613, 1592, 1476, 1394, 1306, 1278, 1260, 1237, 1202, 1163, 1116 cm^{-1}; HRMS [EI]: Exact mass calcd for $C_7H_6FNO_2S^+$ $[M]^+$ 187.0103. Found: 187.0119.

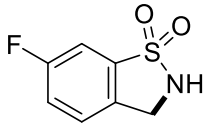

2g

*5-Fluoro-2,3-dihydrobenzo[d]isothiazole 1,1-dioxide (**2g**).* (**Table 20**). The title compound was synthesized according to general procedure **G**. *N*-(benzoyloxy)-5-fluoro-2-methylbenzenesulfonamide **1g** (0.155 g, 0.500 mmol, 1.00 equiv.) and $Ru(bpy)_3(PF_6)_2$ (0.0086 g, 0.010 mmol) were solubilized in 1,2-dichloroethane (5.0 mL) in a microwave vial. The solution was cooled to 0 °C and purged with argon for 10 minutes, after which the reaction was heated at 85 °C in an oil bath for 22 hours. The product was isolated by column chromatography (2% Et_2O/CH_2Cl_2). ***Note:** in this case an extraction was not performed; the crude product mixture was instead directly added to a column containing silica treated with 1% triethylamine. The product was obtained as a white solid (*m* = 0.0660 g, 70% yield). TLC R_F = 0.17 in 2% Et_2O/CH_2Cl_2; ^{1}H NMR (400 MHz, $CDCl_3$) δ 7.46 (dd, *J* = 6.7, 2.3 Hz, 1H), 7.38 (ddd, *J* = 8.5, 4.5, 0.8 Hz, 1H), 7.32 (td, *J* = 8.4, 2.3 Hz, 1H), 5.02 (s, br, 1H), 4.50 (s, 2H); $^{13}C\{^1H\}$ NMR (101 MHz, $CDCl_3$) δ 162.7 (d, *J* = 252.3 Hz, C), 137.2 (d, *J* = 8.4 Hz, C), 132.4 (d, *J* = 2.7 Hz, C), 126.6 (d, *J* = 8.3 Hz, CH), 121.1 (d, *J* = 23.4 Hz, CH), 108.7 (d, *J* = 25.6 Hz, CH), 45.4 (CH_2); IR (FTIR): 3254 (br), 3076, 2924, 2889, 2853, 1606, 1493, 1459, 1374, 1331, 1257, 1225, 1150 cm^{-1}; HRMS [EI]: Exact mass calcd for $C_7H_6FNO_2S^+$ $[M]^+$ 187.0103. Found: 187.0110.

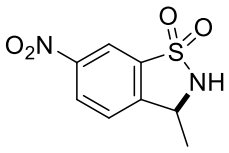

2h

*3-Methyl-6-nitro-2,3-dihydrobenzo[d]isothiazole 1,1-dioxide (**2h**).* (**Table 20**). The title compound was synthesized according to general procedure **G**. *N*-(benzoyloxy)-2-ethyl-5-nitrobenzenesulfonamide **1h** (0.175 g, 0.500 mmol, 1.00 equiv.) and $Ru(bpy)_3(PF_6)_2$ (0.0086 g, 0.010 mmol) were solubilized in 1,2-dichloroethane (5.0 mL) in a microwave vial. The solution was cooled to 0 °C and purged with argon for 10 minutes, after which the reaction was heated at 85 °C in an oil bath for 22 hours. The product was isolated by column chromatography (6% EtOAc/CH_2Cl_2). ***Note:** in this case an extraction was not performed; the crude product mixture was instead directly added to a column containing silica treated with 1% triethylamine. The product was obtained as a yellow solid (*m* = 0.112 g, 98% yield). TLC R_F = 0.12 in 20% EtOAc/hexanes. ^{1}H NMR (400 MHz, $CDCl_3$) δ 8.62 (d, *J* = 2.0 Hz, 1H), 8.50 (dd, *J* = 8.5, 2.1 Hz, 1H), 7.61 (d, *J* = 8.4 Hz, 1H), 4.92 (s, br, 1H, overlapped), 4.88 (q, *J* = 6.1 Hz, 1H), 1.69 (d, *J* = 6.7 Hz, 3H); $^{13}C\{^1H\}$ NMR (101 MHz, $CDCl_3$) δ 148.6 (C), 147.9 (C),137.7 (C), 128.2 (CH), 125.5 (CH), 117.6 (CH), 53.5 (CH), 21.2 (CH_3). ^{1}H and $^{13}C\{^1H\}$ NMR are in accordance with those reported in the literature.[246,247,362]

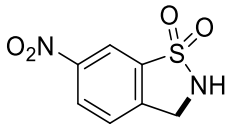

2i

*6-Nitro-2,3-dihydrobenzo[d]isothiazole 1,1-dioxide (**2i**).* (**Table 20**). The title compound was synthesized according to general procedure **G**. *N*-(benzoyloxy)-2-methyl-5-nitrobenzenesulfonamide **1i** (0.168 g, 0.500 mmol, 1.00 equiv.) and $Ru(bpy)_3(PF_6)_2$ (0.0086 g, 0.010 mmol) were solubilized in 1,2-dichloroethane (5.0 mL) in a microwave vial. The solution was cooled to 0 °C and purged with argon for 10 minutes, after which the reaction was heated at 85 °C in an oil bath for 22 hours. An ^{1}H NMR yield of 40% was obtained using 1,3,5-trimethoxybenzene as an internal standard. Isolation of this compound was difficult, and the coelution of side products and/or degraded compounds was observed.

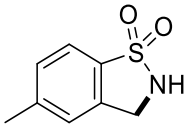

2j

*5-Methyl-2,3-dihydrobenzo[d]isothiazole 1,1-dioxide (**2j**).* (**Table 20**). The title compound was synthesized according to general procedure **G**. *N*-(benzoyloxy)-2,4-dimethylbenzenesulfonamide **1j** (0.153 g, 0.500 mmol, 1.00 equiv.) and $Ru(bpy)_3(PF_6)_2$ (0.0086 g, 0.010 mmol) were solubilized in 1,2-dichloroethane (5.0 mL) in a microwave vial. The solution was cooled to 0 °C and purged with argon for 10 minutes, after which the reaction was heated at 85 °C in an oil bath for 22 hours. The product was isolated by performing a first round of column chromatography (80% Et_2O/hexanes), followed by a second round to remove remaining impurities (70% Et_2O/toluene). The product was obtained as a white solid (m = 0.0607 g, 66% yield). TLC R_F = 0.24 in 80% Et_2O/hexanes, 0.42 in 70% Et_2O/toluene. ^{1}H NMR (400 MHz, $CDCl_3$) δ 7.67 (d, J = 8.0 Hz, 1H), 7.32 (ddq, J = 8.0, 1.5, 0.7 Hz, 1H), 7.17 (dt, J = 1.6, 0.8 Hz, 1H), 4.79 (s, br, 1H), 4.49 (s, 2H), 2.45 (s, 3H); ^{13}C{^{1}H} NMR (101 MHz, $CDCl_3$) δ 144.2 (C), 137.2 (C), 132.9 (C), 130.3 (CH), 125.1 (CH), 121.3 (CH), 45.7 (CH_2), 21.8 (CH_3); IR (FTIR): 3234 (br), 1599, 1448, 1395, 1288, 1236, 1179, 1146, 1136 cm^{-1}; HRMS [ESI]: Exact mass calcd for $C_8H_9NO_2SNa^+$ [M+Na]$^+$ 206.0252. Found: 206.0259. ***Note:** The first round of column chromatography gave 0.0730 g of the compound with greater than 90% purity by ^{1}H NMR (>0.36 mmol, >0.066 g, ~72%).

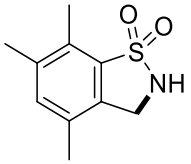

2k

*4,6,7-Trimethyl-2,3-dihydrobenzo[d]isothiazole 1,1-dioxide (**2k**).* (**Table 20**). The title compound was synthesized according to general procedure **G**. *N*-(benzoyloxy)-2,3,5,6-tetramethylbenzenesulfonamide **1k** (0.167 g, 0.500 mmol, 1.00 equiv.) and $Ru(bpy)_3(PF_6)_2$ (0.0086 g, 0.010 mmol, 2.0 mol%) were solubilized in 1,2-dichloroethane (5.0 mL) in a microwave vial. The solution was cooled to 0 °C and purged with argon for 10 minutes, after which the reaction was heated at 85 °C in an oil bath for 22 hours. The product was isolated by column chromatography (60% Et_2O/pentanes). The product was obtained as an off-white solid (m = 0.0841 g, 80% yield). TLC R_F = 0.26 in 60% Et_2O/pentanes; ^{1}H NMR (400 MHz, $CDCl_3$) δ 7.17 (s, 1H), 4.66 (s, br, 1H), 4.34 (s, 2H), 2.50 (s, 3H), 2.30 (s, 3H), 2.21 (s, 3H); ^{13}C{^{1}H} NMR (101 MHz, $CDCl_3$) δ 138.6 (C), 135.8 (CH), 134.1 (C), 132.8 (C), 131.1 (C), 129.8 (C), 43.9 (CH_2), 19.1 (CH_3), 17.0 (CH_3), 13.9 (CH_3). ^{1}H and ^{13}C{^{1}H} NMR are in accordance with those reported in the literature.[246]

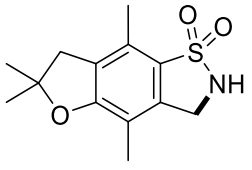

2l

*4,6,6,8-Tetramethyl-2,3,6,7-tetrahydrobenzofuro[6,5-d]isothiazole 1,1-dioxide (**2l**).* (**Table 20**). The title compound was synthesized according to general procedure **G**. *N*-(benzoyloxy)-2,2,4,6,7-pentamethyl-2,3-dihydrobenzofuran-5-sulfonamide **1l** (0.195 g, 0.500 mmol, 1.00 equiv.) and $Ru(bpy)_3(PF_6)_2$ (0.0086 g, 0.010 mmol, 2.0 mol%) were solubilized in 1,2-dichloroethane (5.0 mL) in a microwave vial. The solution was cooled to 0 °C and purged with argon for 10 minutes, after which the reaction was heated at 85 °C in an oil bath for 22 hours. This compound was isolated by column chromatography (70% Et_2O/pentanes) as the major product of the reaction. The product was obtained as a yellow-white solid (m = 0.0758 g, 57% yield). TLC R_F = 0.26 in 70% Et_2O/pentanes; ^{1}H NMR (400 MHz, $CDCl_3$) δ 4.78 (s, br, 1H), 4.31 (s, 2H), 2.96 (s, 2H), 2.44 (s, 2H), 2.03 (s, 3H), 1.49 (s, 6H); ^{13}C{^{1}H} NMR (101 MHz, $CDCl_3$) δ 161.3 (C), 137.2 (C), 128.1 (C), 128.0 (C), 125.3 (C), 112.3 (C), 88.8 (C), 44.3

(CH_2), 41.5 (CH_2), 28.6 (CH_3), 14.3 (CH_3), 10.3 (CH_3); IR (FTIR): 3298 (br), 2976, 2924, 2922, 1594, 1447, 1372, 1322, 1263, 1153, 1133, 1091 cm^{-1}; HRMS [ESI]: Exact mass calcd for $C_{13}H_{17}NO_3SNa^+$ $[M+Na]^+$ 290.0827. Found: 290.0825.

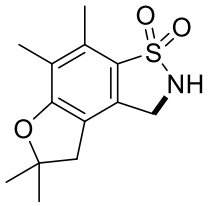

2l'

*4,5,7,7-tetramethyl-1,2,7,8-tetrahydrobenzofuro[4,5-d]isothiazole 3,3-dioxide (**2l'**).* (**Table 20**). The title compound was synthesized according to general procedure **G**. *N*-(benzoyloxy)-2,2,4,6,7-pentamethyl-2,3-dihydrobenzofuran-5-sulfonamide **1l** (0.195 g, 0.500 mmol, 1.00 equiv.) and $Ru(bpy)_3(PF_6)_2$ (0.0086 g, 0.010 mmol, 2.0 mol%) were solubilized in 1,2-dichloroethane (5.0 mL) in a microwave vial. The solution was cooled to 0 °C and purged with argon for 10 minutes, after which the reaction was heated at 85 °C in an oil bath for 22 hours. This compound was isolated by column chromatography (70% Et_2O/pentanes) as the minor product of the reaction. The product was obtained as an off-white solid (m = 0.0173 g, 13% yield). TLC R_F = 0.13 in 70% Et_2O/pentanes; ^1H NMR (400 MHz, $CDCl_3$) δ 4.64 (s, br, 1H), 4.28 (s, 2H), 2.90 (s, 2H), 2.49 (s, 3H), 2.13 (s, 3H), 1.50 (s, 6H); $^{13}C\{^1H\}$ (101 MHz, $CDCl_3$) δ 162.0 (C), 133.5 (C), 131.4 (C), 126.1 (C), 120.4 (C), 118.6 (C), 88.7 (C), 43.7 (CH_2), 40.7 (CH_2), 28.5 (CH_3), 14.3 (CH_3), 11.5 (CH_3); IR (FTIR): 3273 (br), 2980, 2921, 1597, 1457, 1410, 1373, 1317, 1271, 1134, 1090 cm^{-1}; HRMS [ESI]: Exact mass calcd for $C_{13}H_{17}NO_3SNa^+$ $[M+Na]^+$ 290.0827. Found: 290.0800.

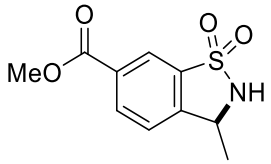

2m

*Methyl 3-Methyl-2,3-dihydrobenzo[d]isothiazole-6-carboxylate 1,1-dioxide (**2m**).* (**Table 20**). The title compound was synthesized according to general procedure **G**. Methyl 3-(*N*-(benzoyloxy)sulfamoyl)-4-ethylbenzoate **1m** (0.182 g, 0.500 mmol, 1.00 equiv.) and $Ru(bpy)_3(PF_6)_2$ (0.0086 g, 0.010 mmol, 1.00 equiv.) were solubilized in 1,2-dichloroethane (5.0 mL) in a microwave vial. The solution was cooled to 0 °C and purged with argon for 10 minutes, after which the reaction was heated at 85 °C in an oil bath for 22 hours. The product was isolated by column chromatography (85% Et_2O/hexanes). ***Note:** in this case an extraction was not performed; the crude product mixture was instead directly added to a column containing silica treated with 1% triethylamine. The product was obtained as an off-white solid (m = 0.108 g, 90% yield). TLC R_F = 0.29 in 85% Et_2O/hexanes. ^1H NMR (300 MHz, $CDCl_3$) δ 8.43 (dd, J = 1.6, 0.6 Hz, 1H), 8.30 (dd, J = 8.1, 1.5 Hz, 1H), 7.48 (d, J = 8.1 Hz, 1H), 4.83 (q, J = 6.8 Hz, 1H, overlapped), 4.83 (s, br, 1H, overlapped), 3.97 (s, 3H), 1.65 (d, J = 6.7 Hz, 3H); $^{13}C\{^1H\}$ NMR (76 MHz, $CDCl_3$) δ 165.2 (C), 146.2 (C), 136.5 (C), 134.4 (CH), 131.8 (C), 124.2 (CH), 123.1 (CH), 53.5 (CH), 52.9 (CH_3), 21.3 (CH_3). ^1H and $^{13}C\{^1H\}$ NMR are in accordance with those reported in the literature.[247,362]

Chapter 5: Spectra

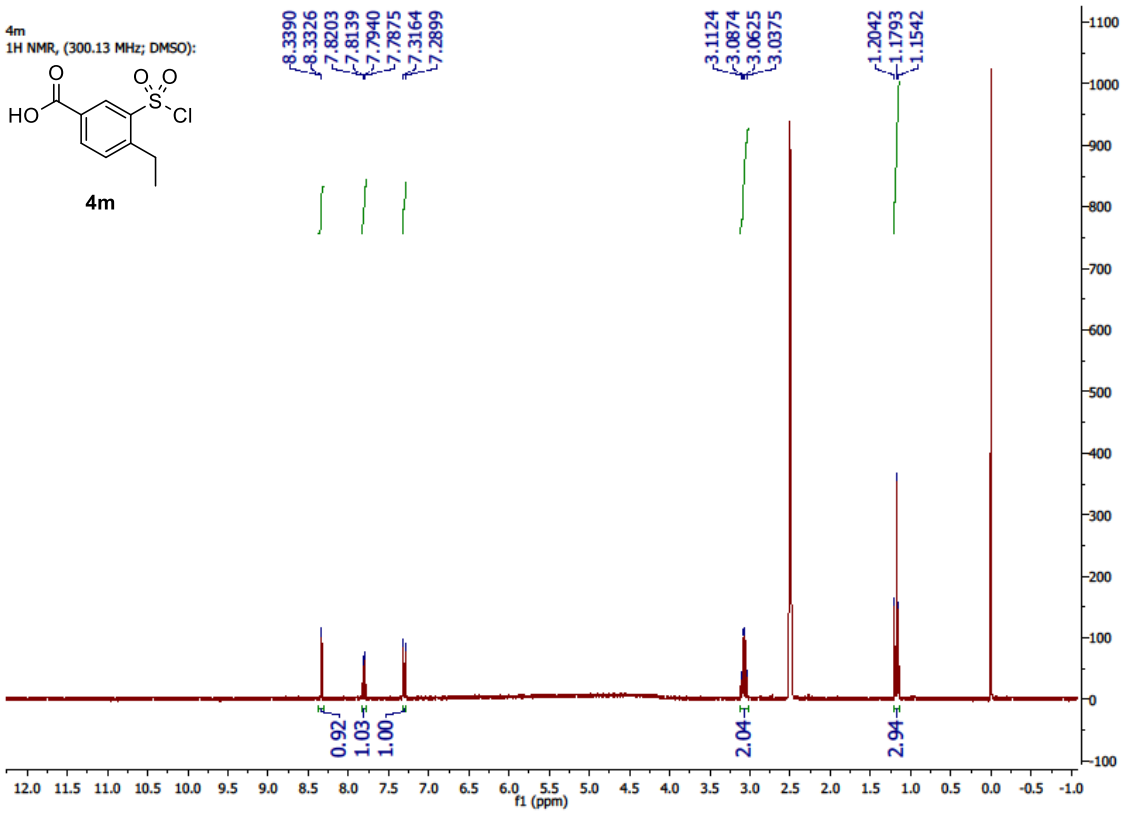
4m
1H NMR, (300.13 MHz; DMSO):
HO
O
O
O
S
Cl
4m
8.3390
8.3326
7.8203
7.8139
7.7940
7.7875
7.3164
7.2899
3.1124
3.0874
3.0625
3.0375
1.2042
1.1793
1.1542
0.92
1.03
1.00
2.04
2.94
f1 (ppm)

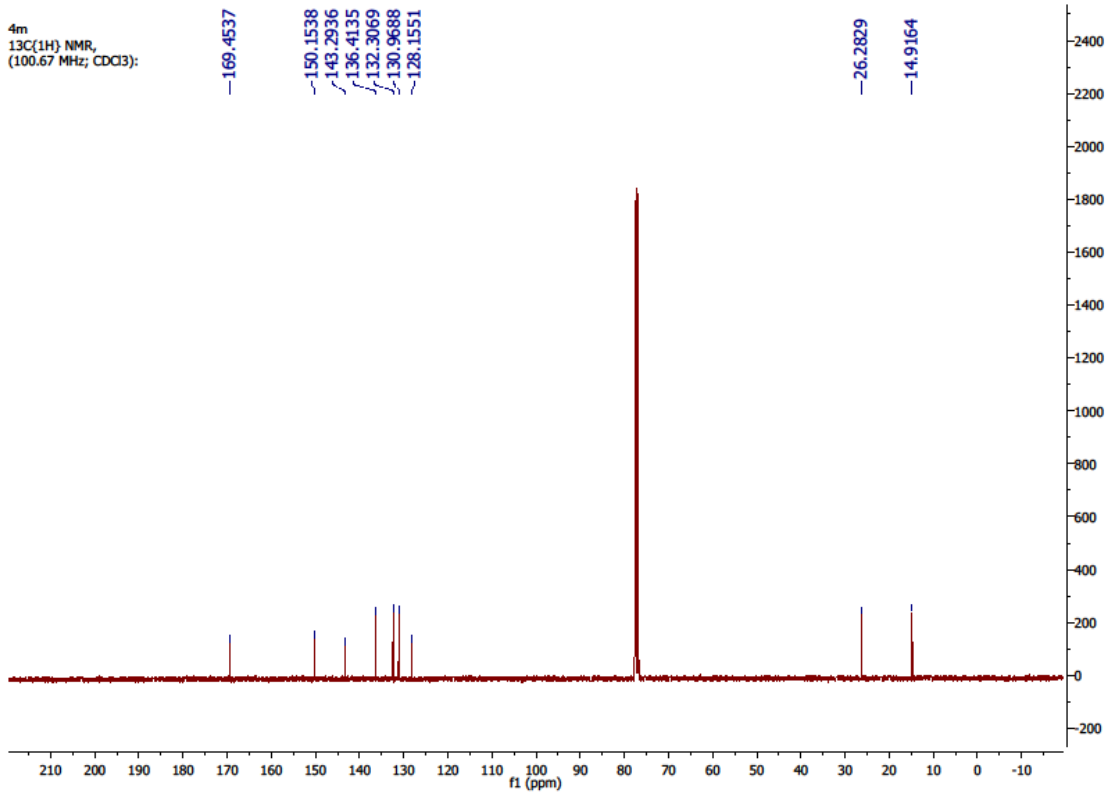
4m
13C{1H} NMR,
(100.67 MHz; CDCl3):
169.4537
150.1538
143.2936
136.4135
132.3069
130.9688
128.1551
26.2829
14.9164
f1 (ppm)

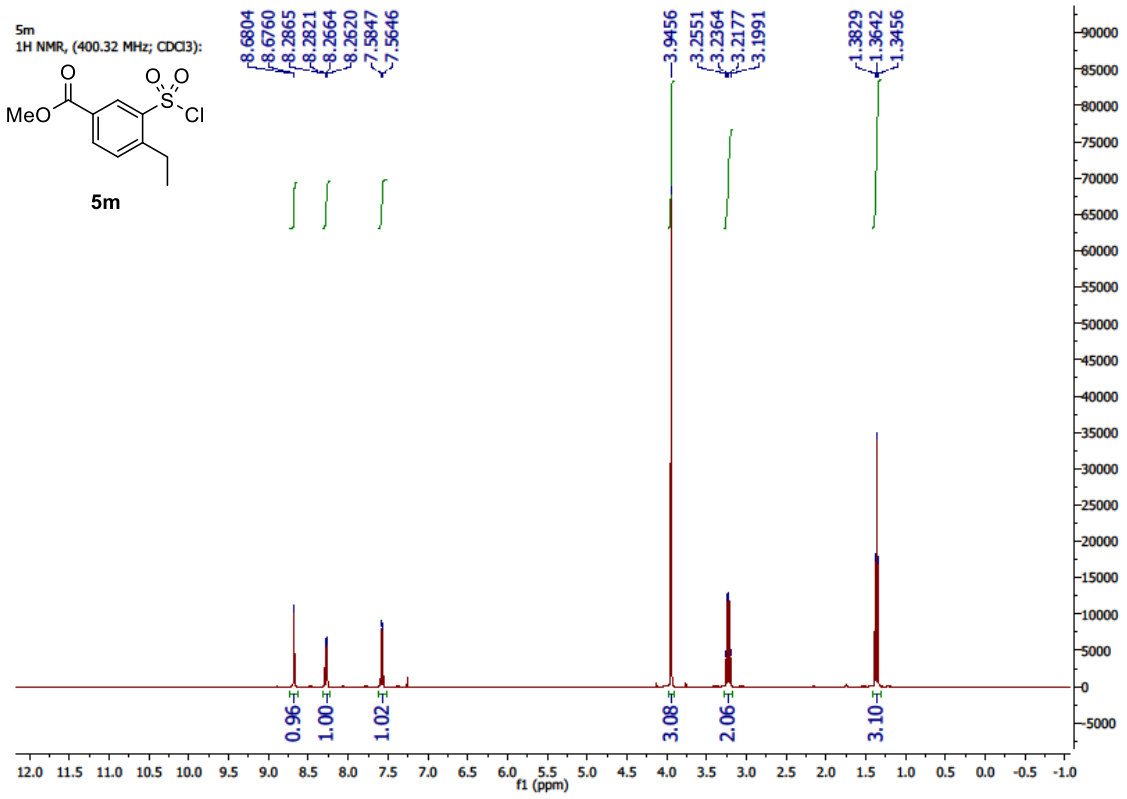
5m
1H NMR, (400.32 MHz; CDCl3):
MeO
O
O
S
O
Cl
5m
8.6804
8.6760
8.2865
8.2821
8.2664
8.2620
7.5847
7.5646
3.9456
3.2551
3.2364
3.2177
3.1991
1.3829
1.3642
1.3456
0.96
1.00
1.02
3.08
2.06
3.10
f1 (ppm)

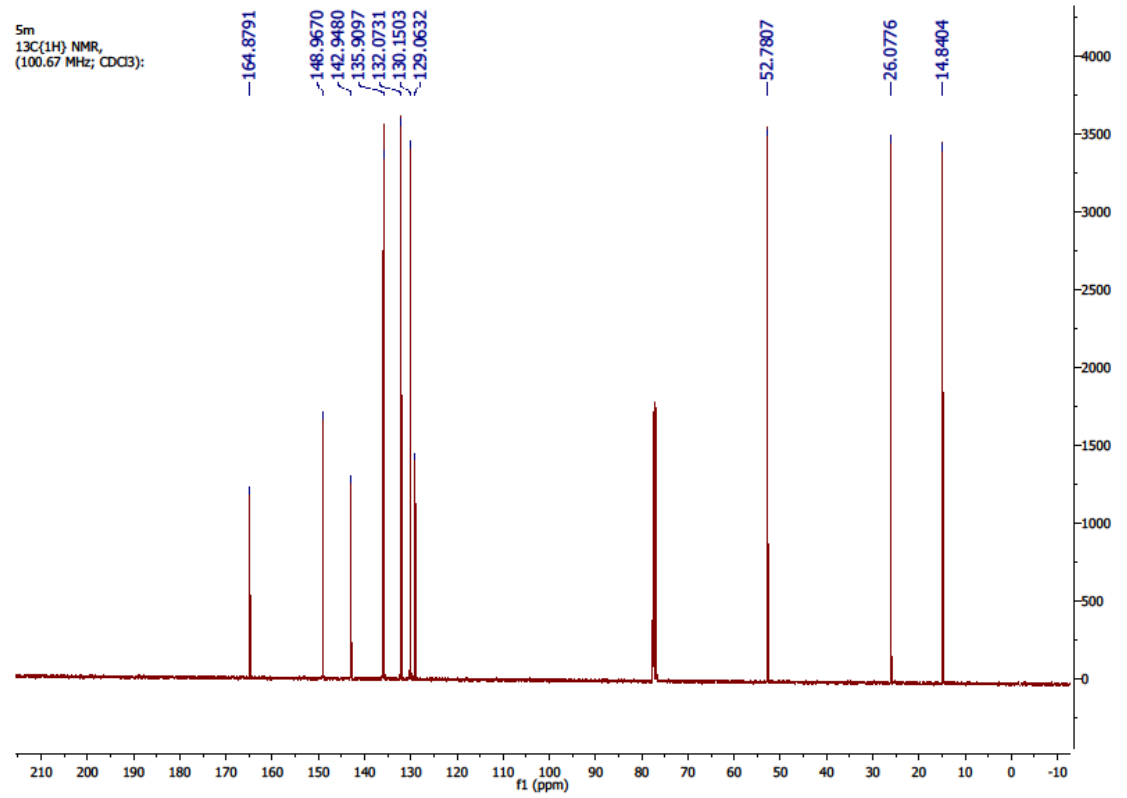
5m
13C{1H} NMR,
(100.67 MHz; CDCl3):
164.8791
148.9670
142.9480
135.9097
132.0731
130.1503
129.0632
52.7807
26.0776
14.8404
f1 (ppm)

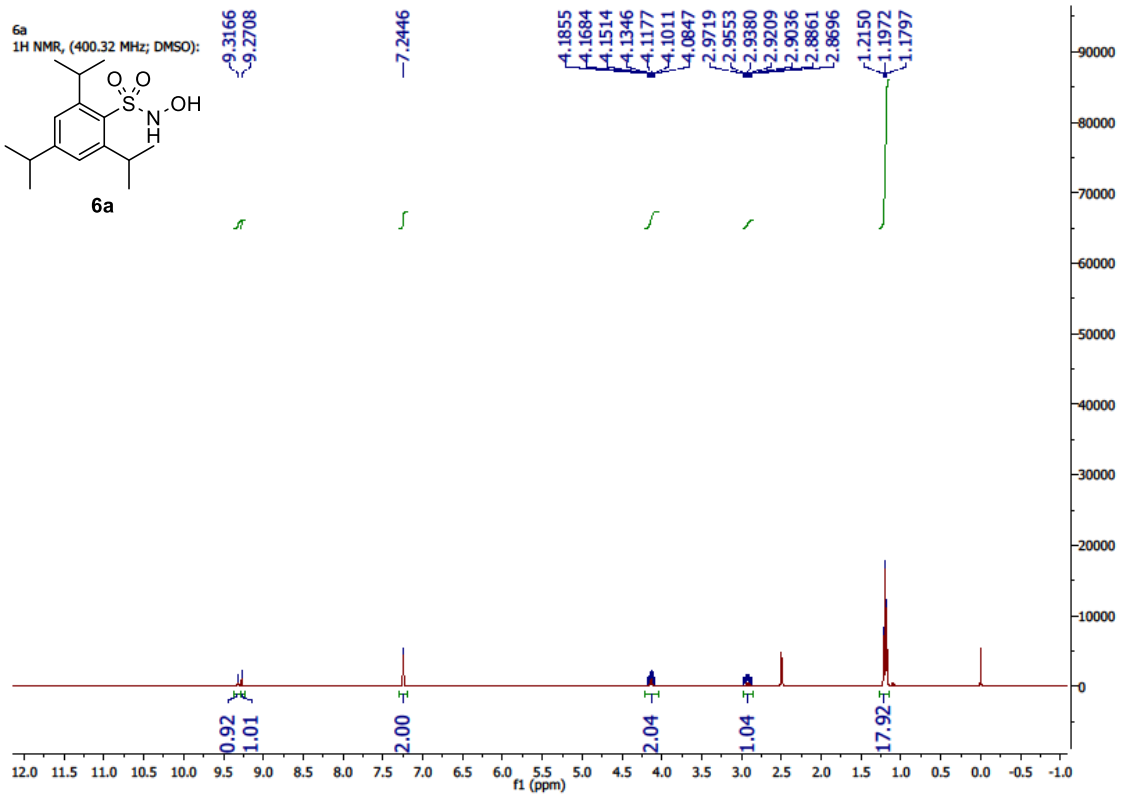
6a
1H NMR, (400.32 MHz; DMSO):
9.3166
9.2708
7.2446
4.1855
4.1684
4.1514
4.1346
4.1177
4.1011
4.0847
2.9719
2.9553
2.9380
2.9209
2.9036
2.8861
2.8696
1.2150
1.1972
1.1797
0.92
1.01
2.00
2.04
1.04
17.92
f1 (ppm)

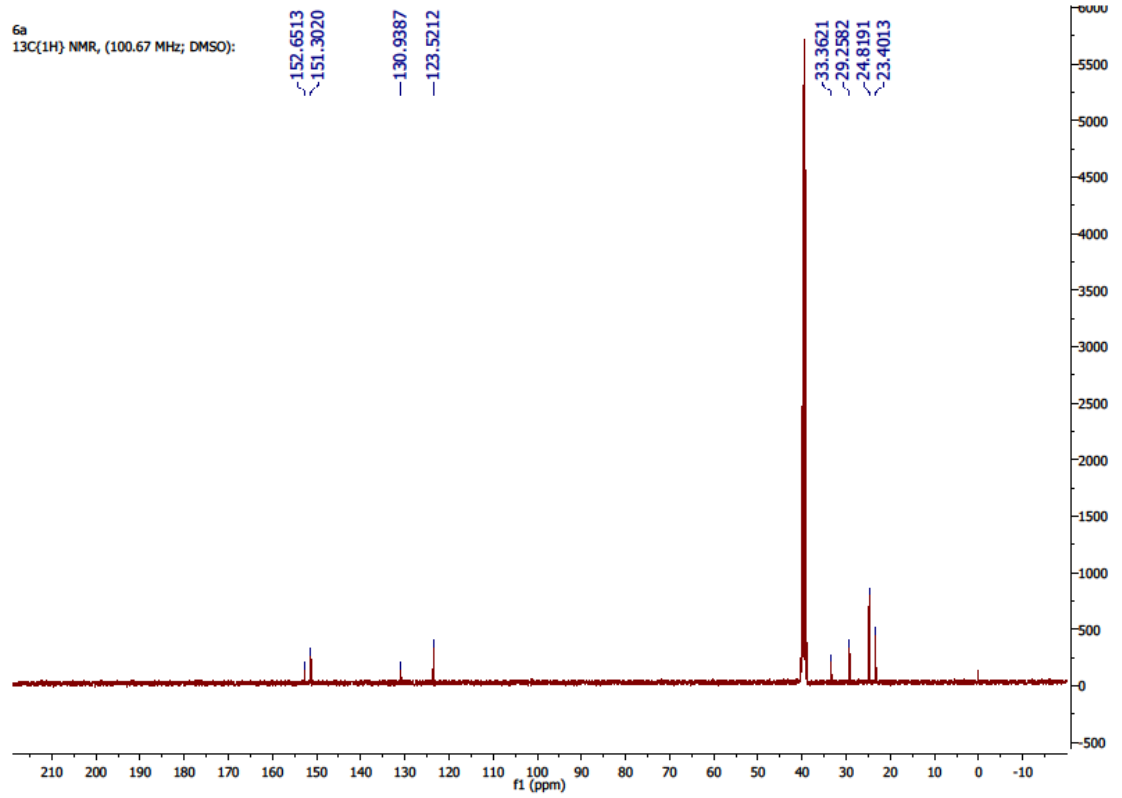
6a
13C{1H} NMR, (100.67 MHz; DMSO):
152.6513
151.3020
130.9387
123.5212
33.3621
29.2582
24.8191
23.4013
f1 (ppm)

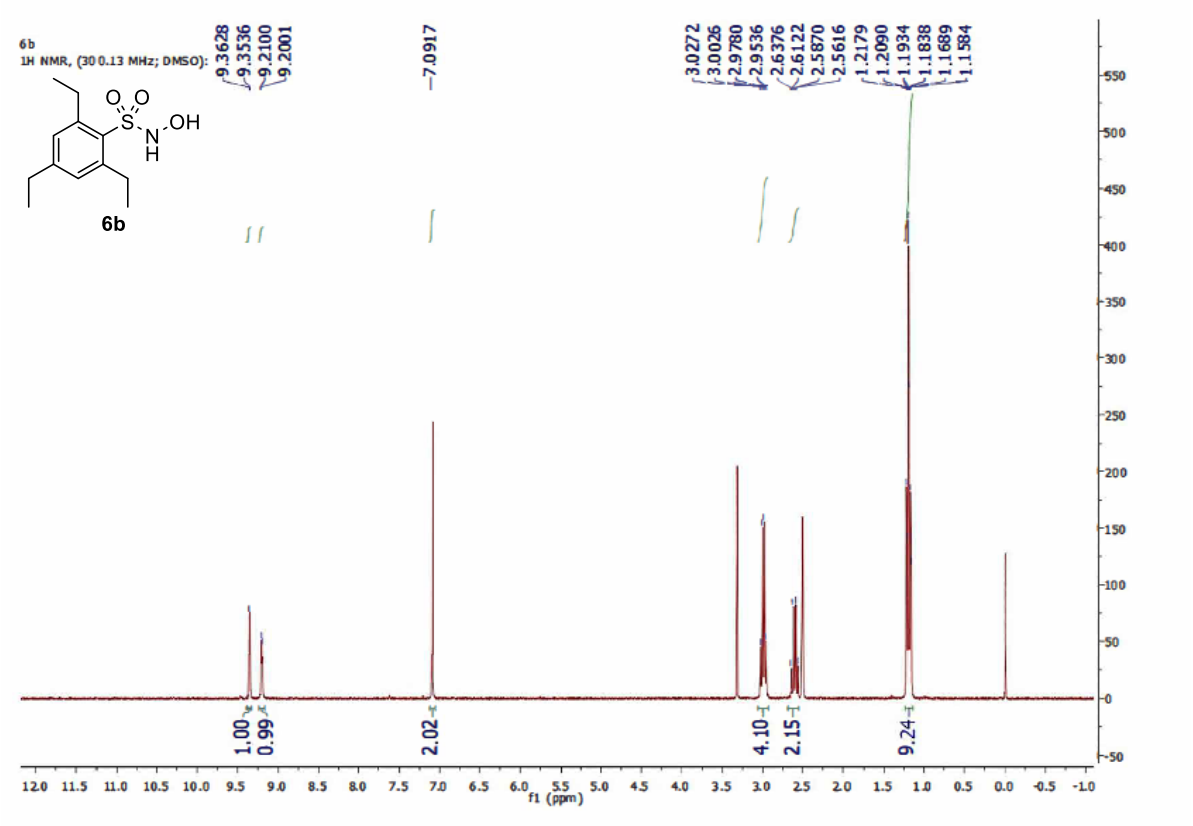
6b
1H NMR, (300.13 MHz; DMSO):
9.3628
9.3536
9.2100
9.2001
7.0917
3.0272
3.0026
2.9780
2.9536
2.6376
2.6122
2.5870
2.5616
1.2179
1.2090
1.1934
1.1838
1.1689
1.1584
1.00
0.99
2.02
4.10
2.15
9.24
f1 (ppm)

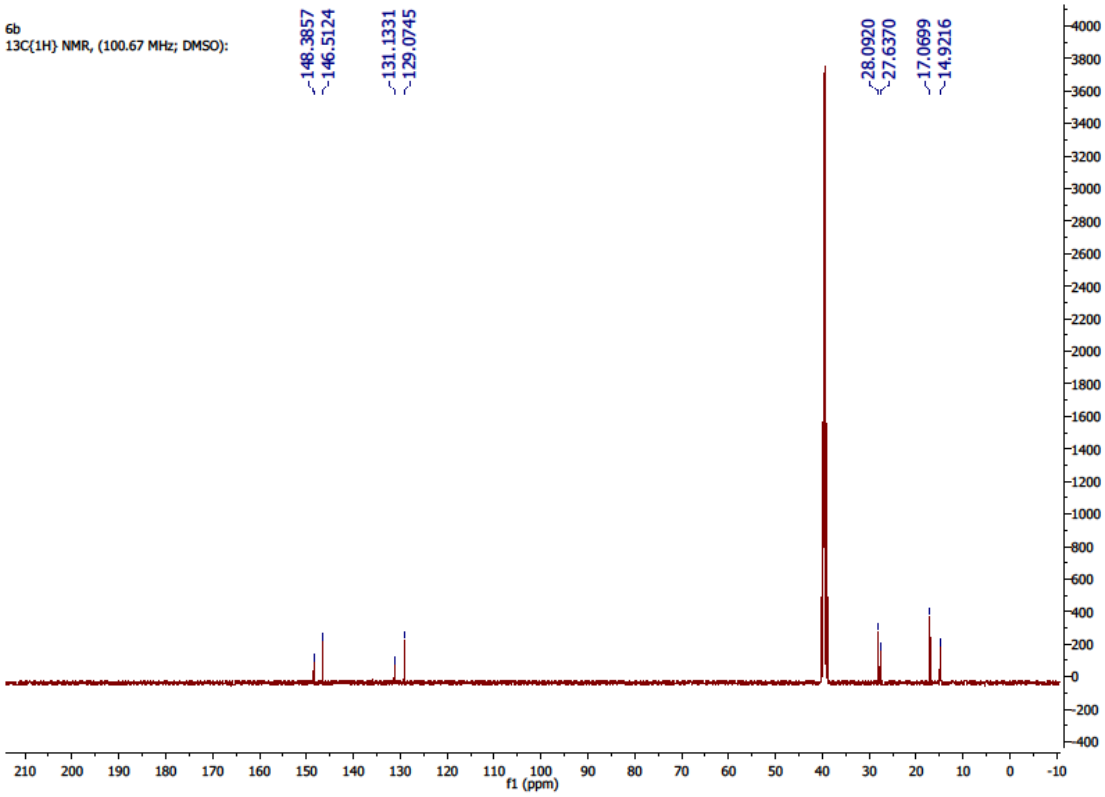
6b
13C{1H} NMR, (100.67 MHz; DMSO):
148.3857
146.5124
131.1331
129.0745
28.0920
27.6370
17.0699
14.9216
f1 (ppm)

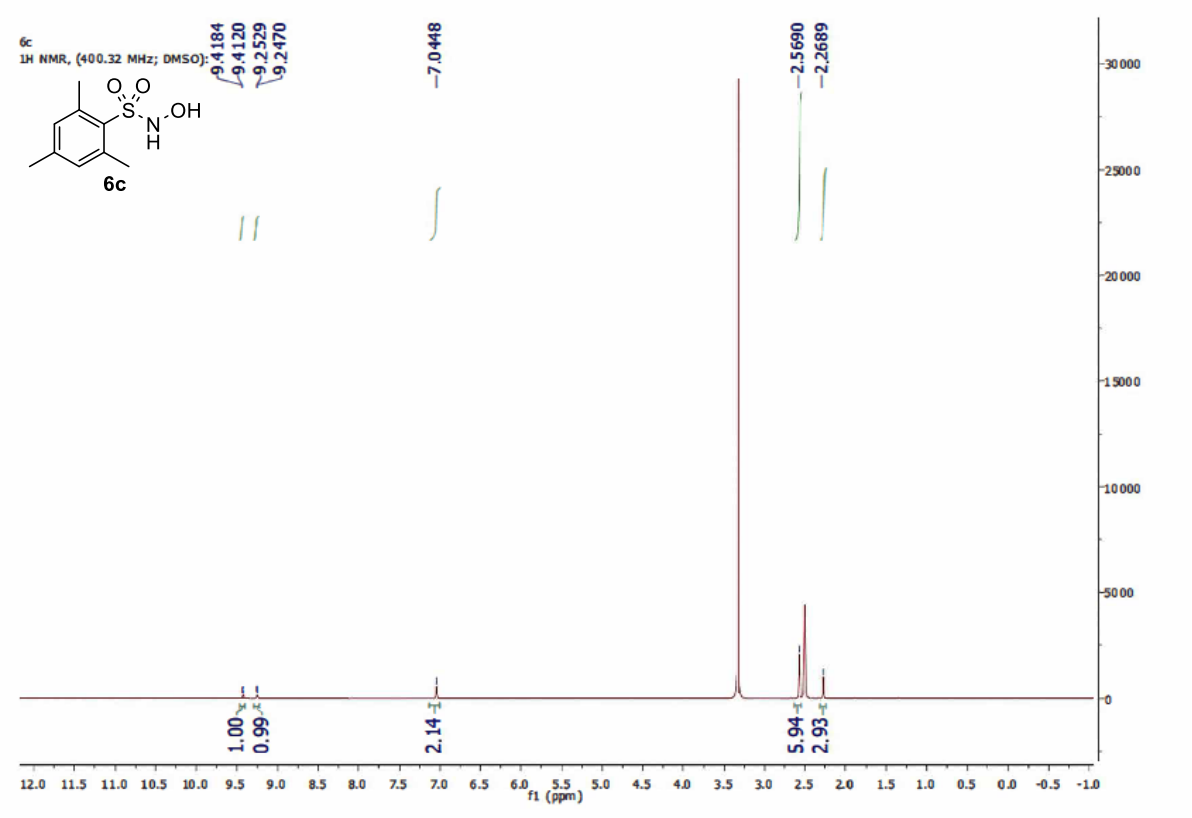
6c
1H NMR, (400.32 MHz; DMSO):
9.4184
9.4120
9.2529
9.2470
7.0448
2.5690
2.2689
1.00
0.99
2.14
5.94
2.93
f1 (ppm)

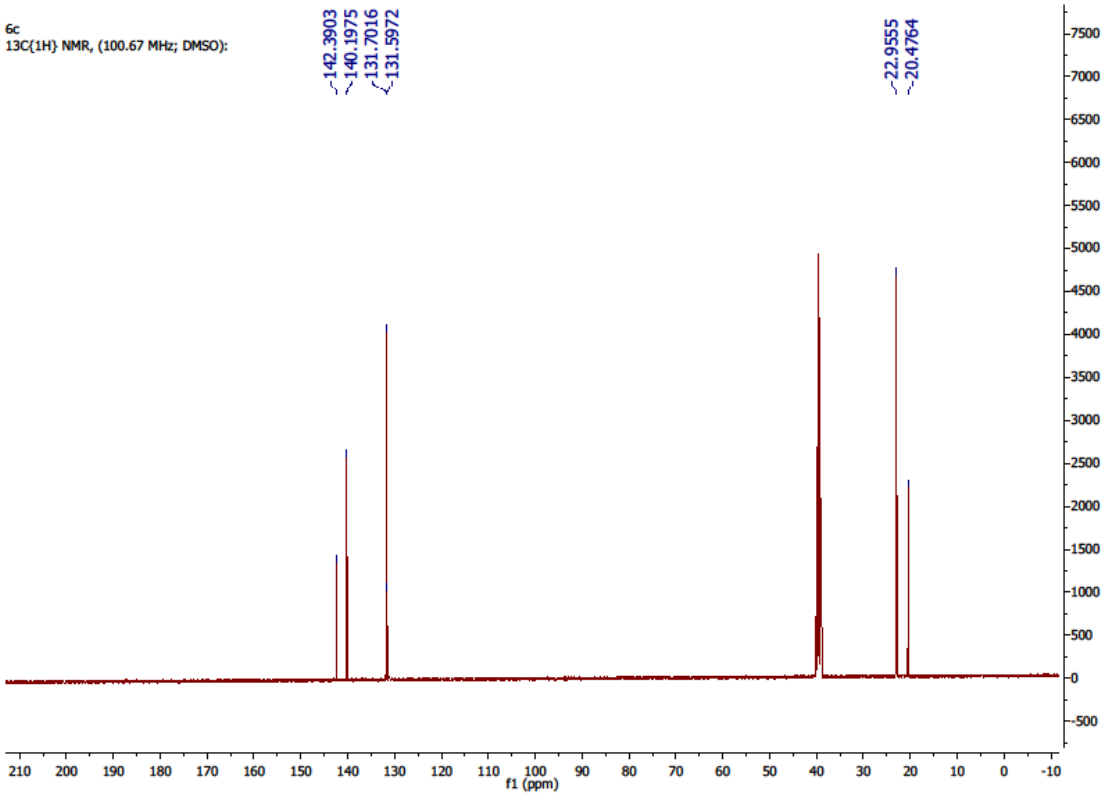
6c
13C{1H} NMR, (100.67 MHz; DMSO):
142.3903
140.1975
131.7016
131.5972
22.9555
20.4764
f1 (ppm)

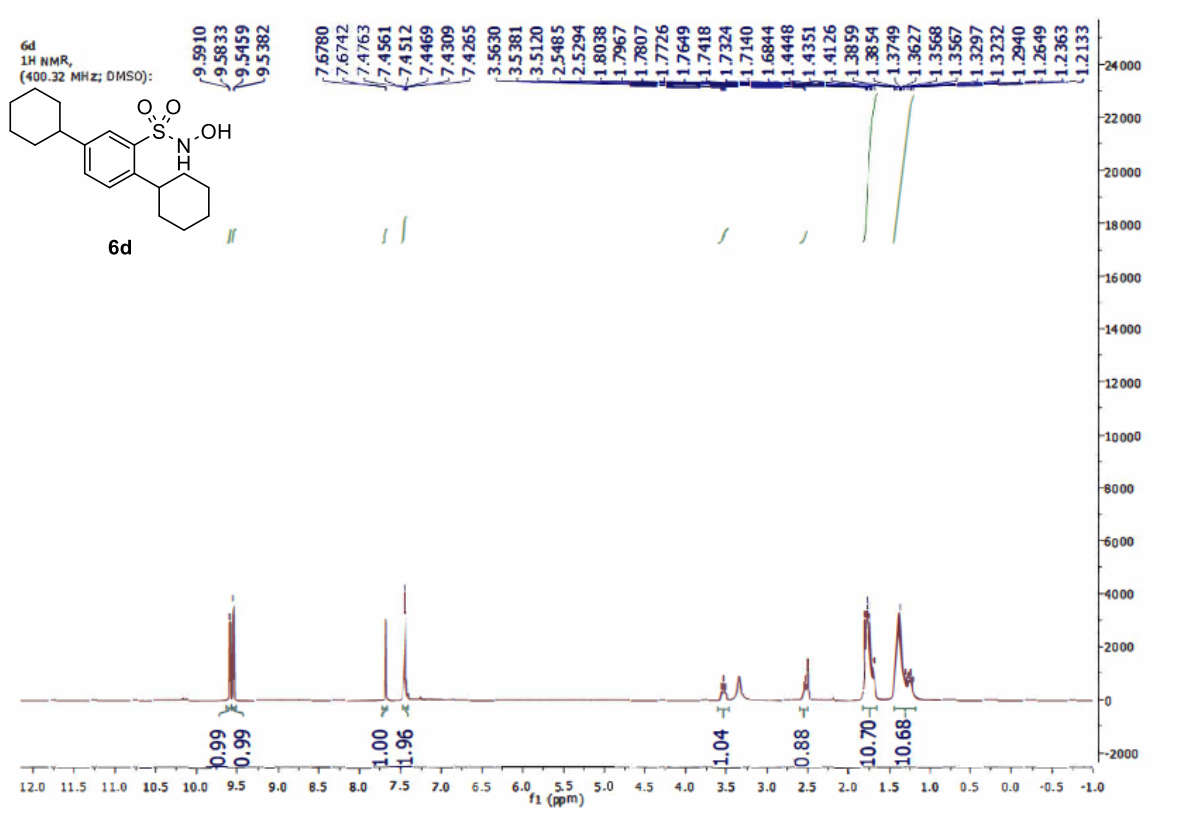
6d
1H NMR,
(400.32 MHz; DMSO):
6d
f1 (ppm)

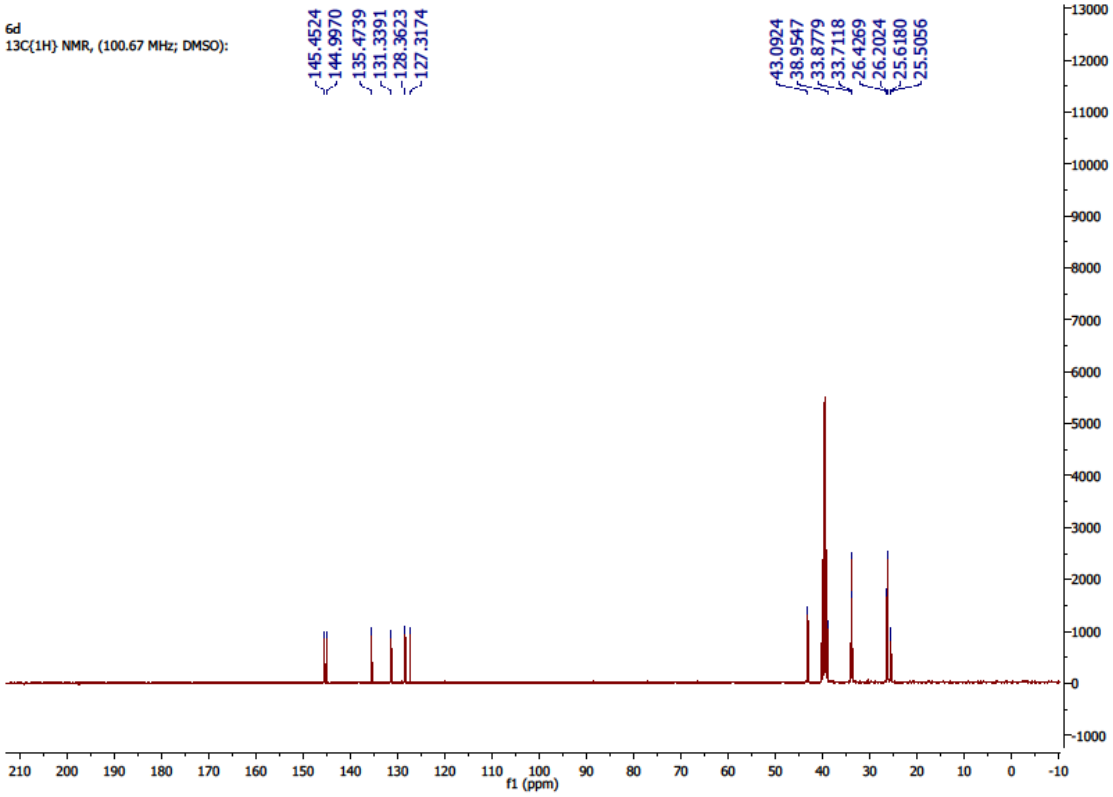
6d
13C{1H} NMR, (100.67 MHz; DMSO):
f1 (ppm)

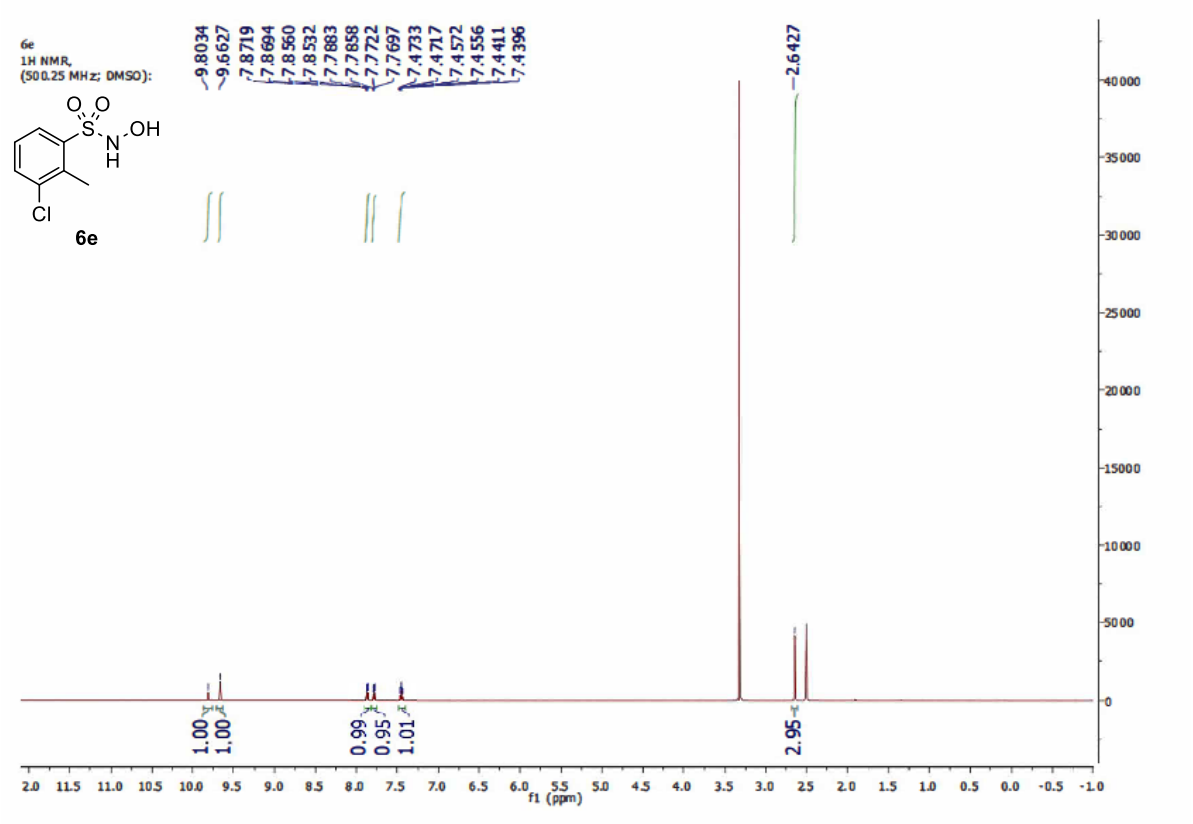
6e
1H NMR,
(500.25 MHz; DMSO):
6e
9.8034
9.6627
7.8719
7.8694
7.8560
7.8532
7.7883
7.7858
7.7722
7.7697
7.4733
7.4717
7.4572
7.4556
7.4411
7.4396
2.6427
1.00
1.00
0.99
0.95
1.01
2.95
f1 (ppm)

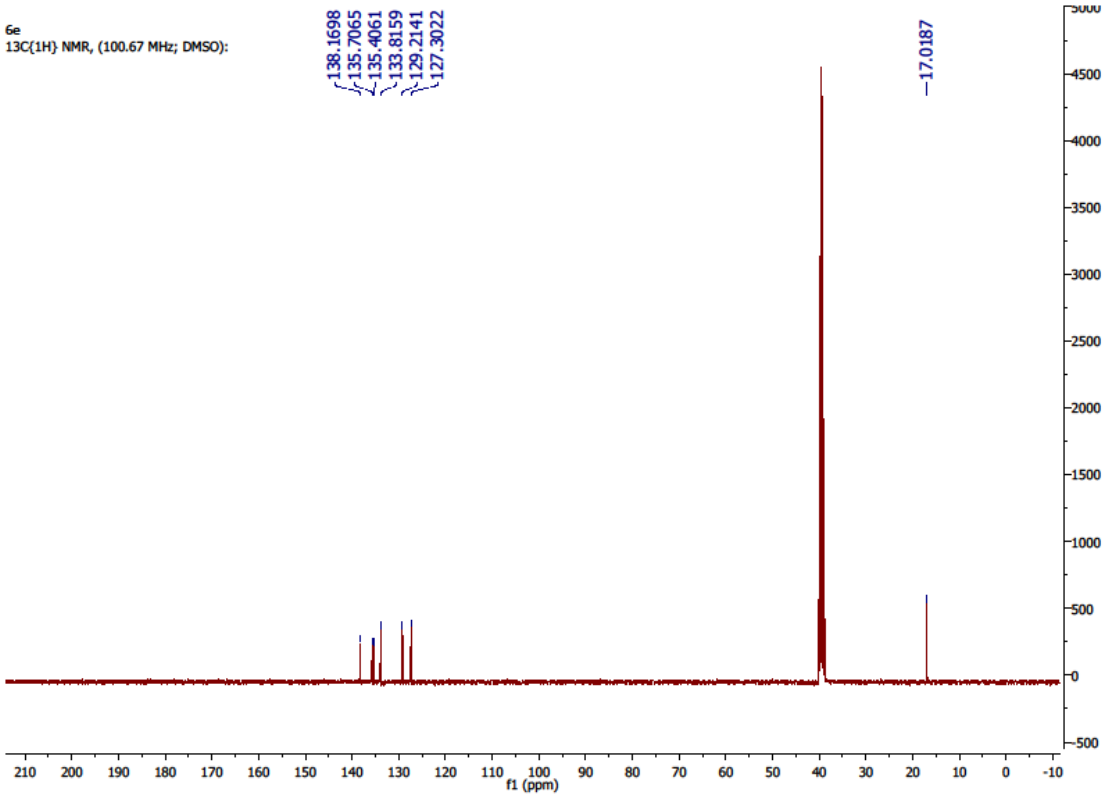
6e
13C{1H} NMR, (100.67 MHz; DMSO):
138.1698
135.7065
135.4061
133.8159
129.2141
127.3022
17.0187
f1 (ppm)

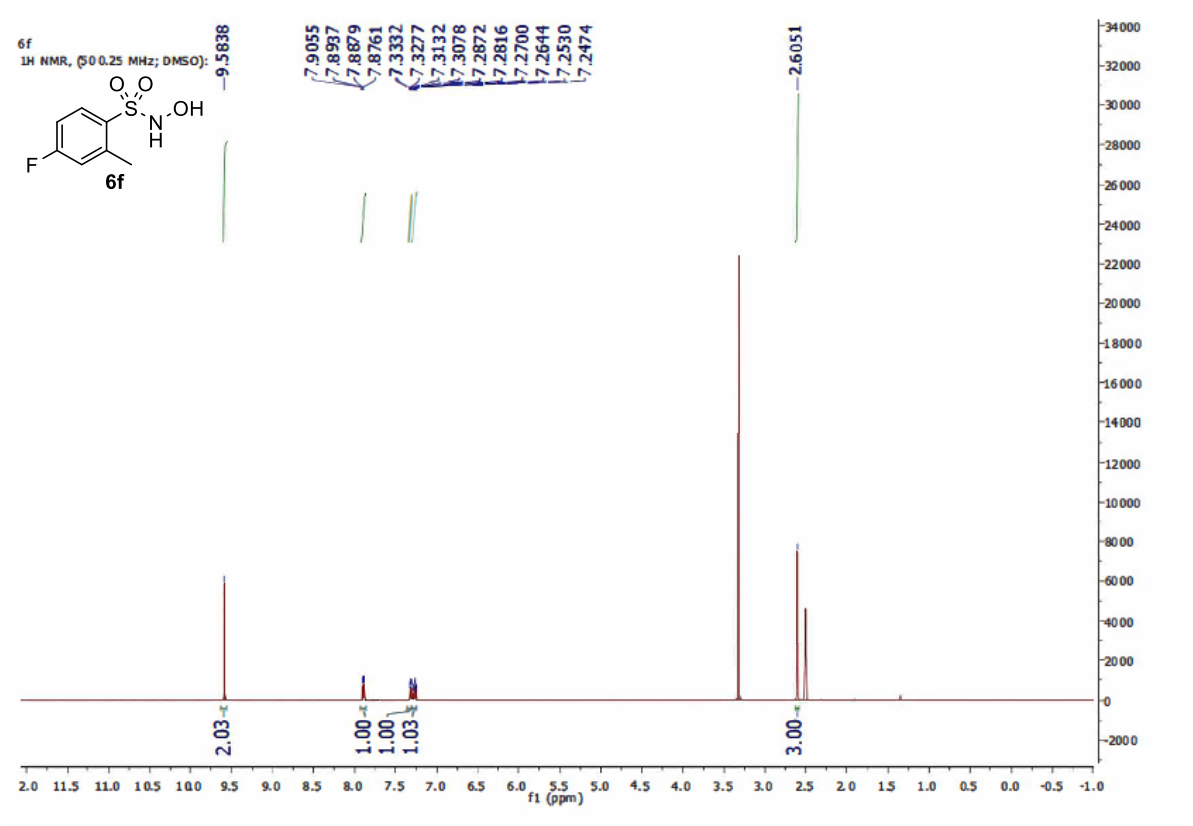
6f
1H NMR, (500.25 MHz; DMSO):
9.5838
7.9055
7.8937
7.8879
7.8761
7.3332
7.3277
7.3132
7.3078
7.2872
7.2816
7.2700
7.2644
7.2530
7.2474
2.6051
6f
2.03
1.00
1.00
1.03
3.00
f1 (ppm)

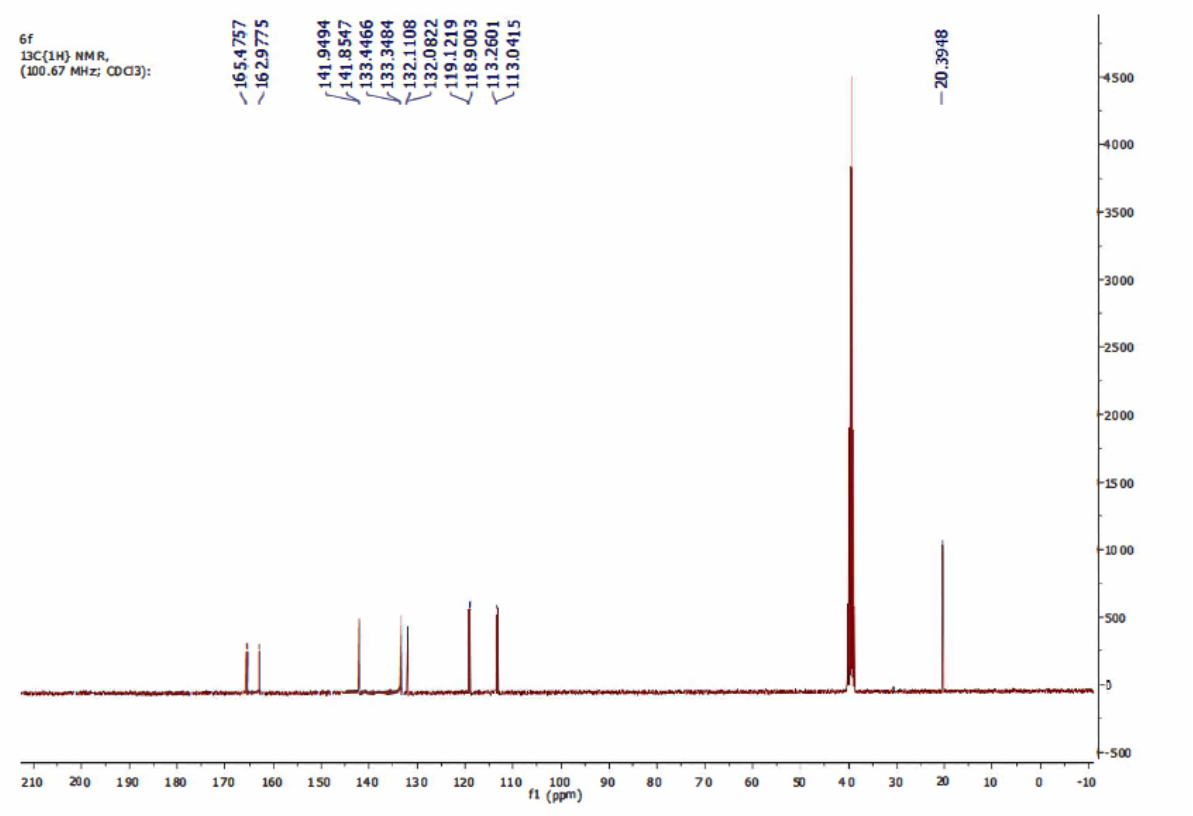
6f
13C{1H} NMR,
(100.67 MHz; CDCl3):
165.4757
162.9775
141.9494
141.8547
133.4466
133.3484
132.1108
132.0822
119.1219
118.9003
113.2601
113.0415
20.3948
f1 (ppm)

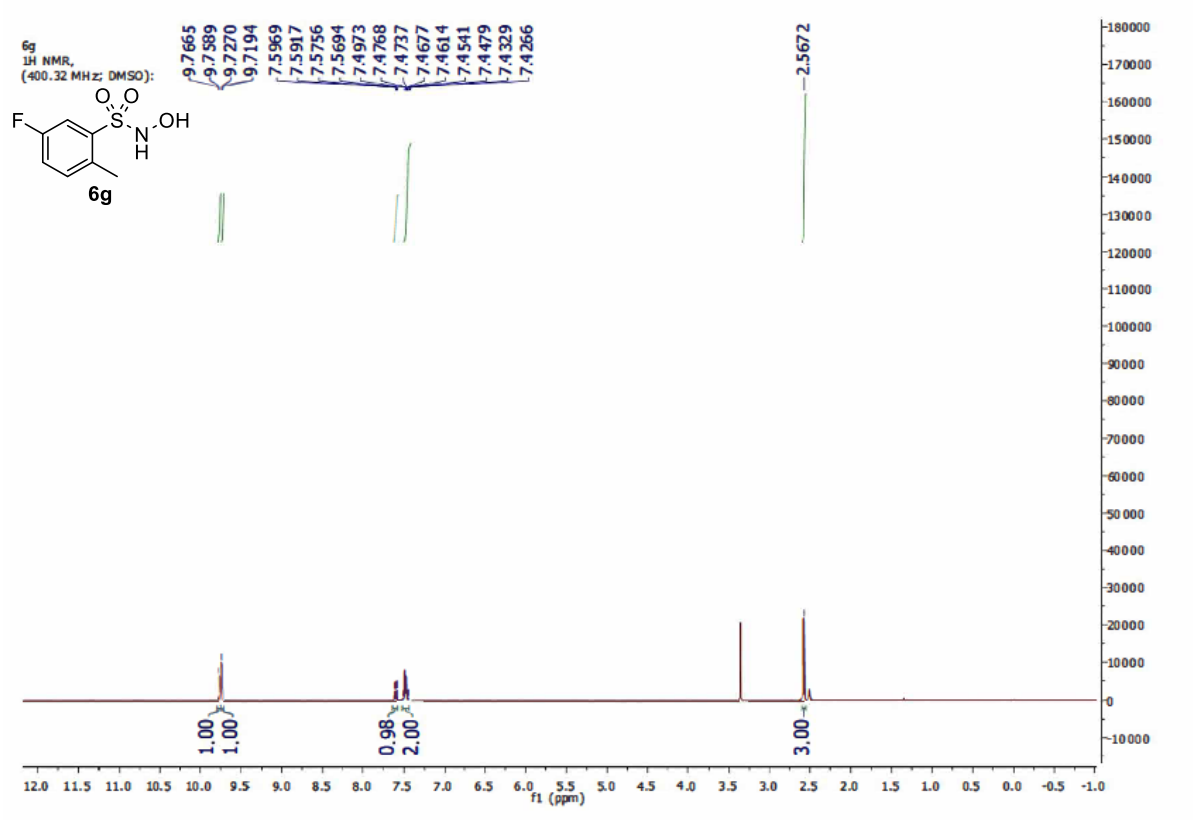
6g
1H NMR,
(400.32 MHz; DMSO):
6g
9.7665
9.7589
9.7270
9.7194
7.5969
7.5917
7.5756
7.5694
7.4973
7.4768
7.4737
7.4677
7.4614
7.4541
7.4479
7.4329
7.4266
2.5672
1.00
1.00
0.98
2.00
3.00
f1 (ppm)

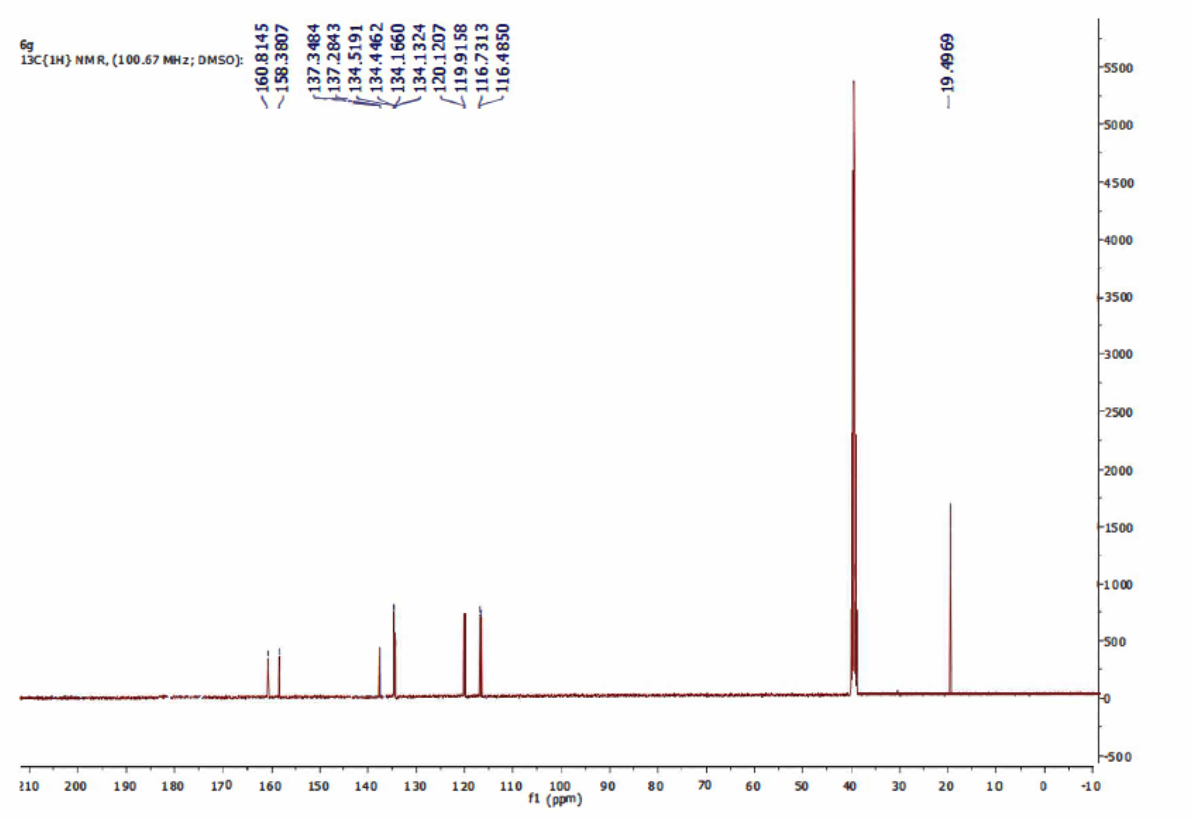
6g
13C{1H} NMR, (100.67 MHz; DMSO):
160.8145
158.3807
137.3484
137.2843
134.5191
134.4462
134.1660
134.1324
120.1207
119.9158
116.7313
116.4850
19.4969
f1 (ppm)

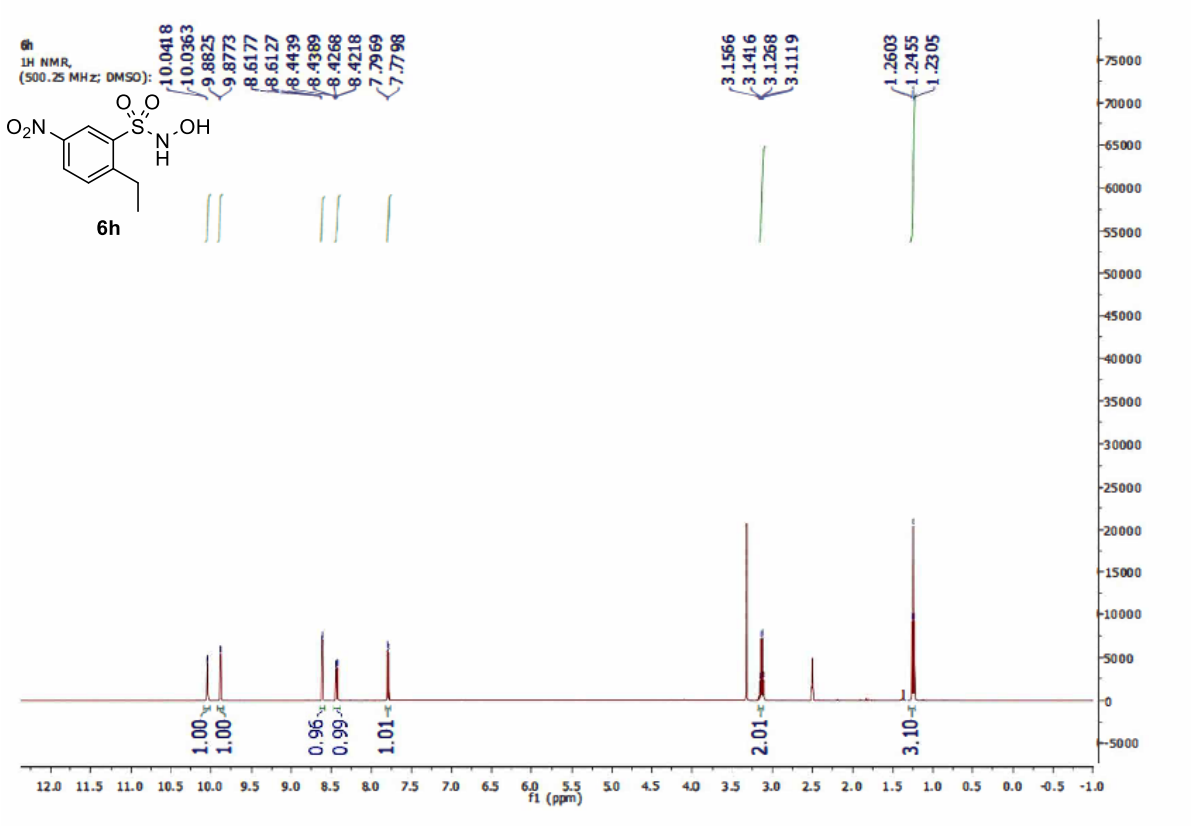
6h
1H NMR,
(500.25 MHz; DMSO):
10.0418
10.0363
9.8825
9.8773
8.6177
8.6127
8.4439
8.4389
8.4268
8.4218
7.7969
7.7798
3.1566
3.1416
3.1268
3.1119
1.2603
1.2455
1.2305
6h
1.00
1.00
0.96
0.99
1.01
2.01
3.10
f1 (ppm)

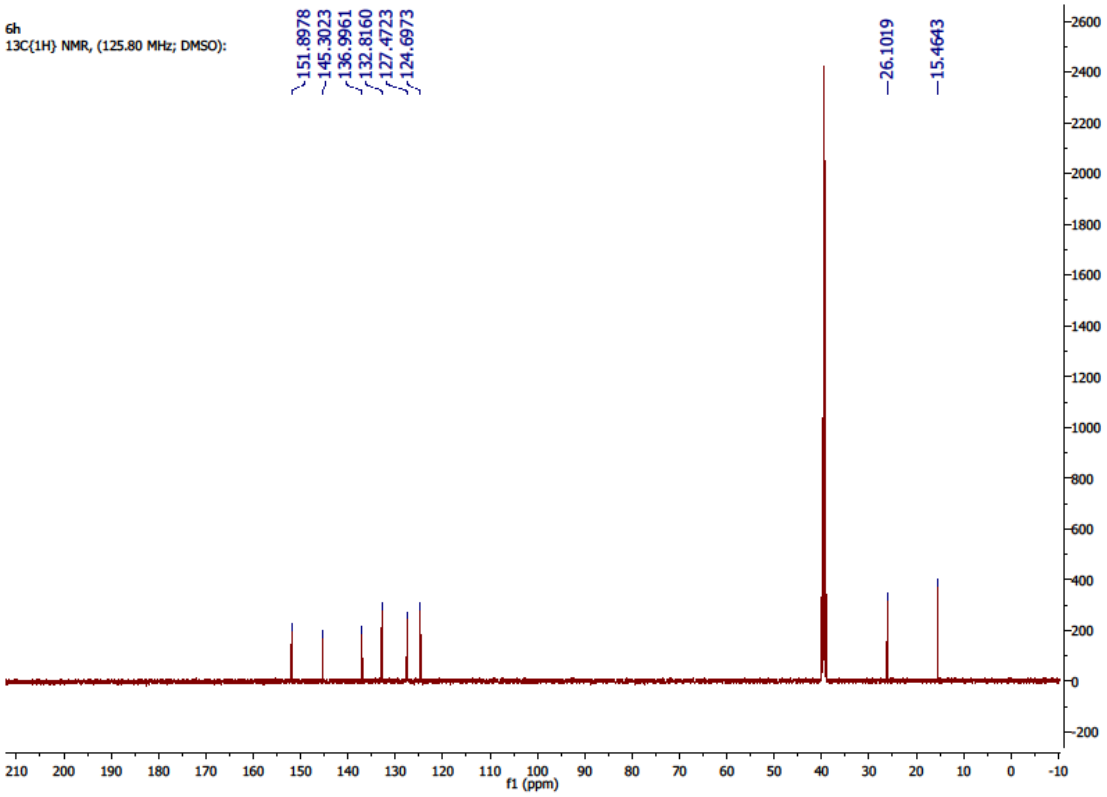
6h
13C{1H} NMR, (125.80 MHz; DMSO):
151.8978
145.3023
136.9961
132.8160
127.4723
124.6973
26.1019
15.4643
f1 (ppm)

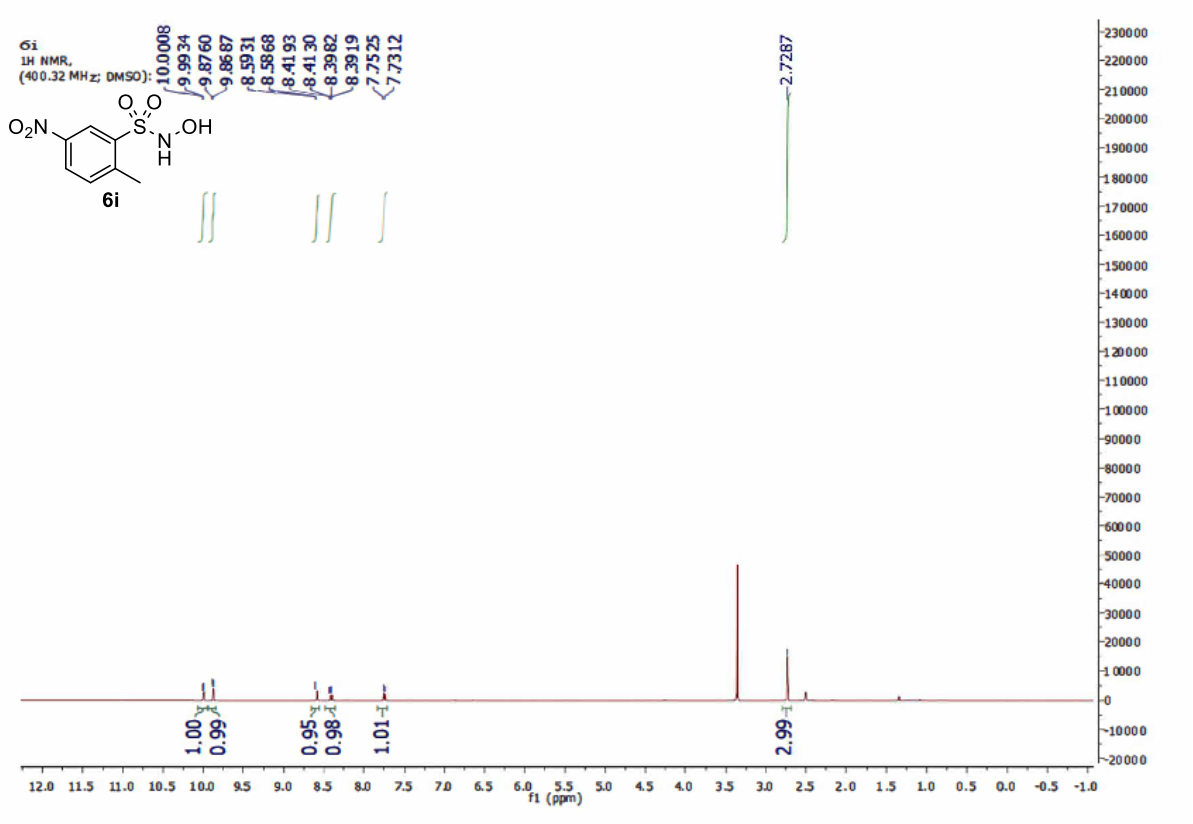
6i
1H NMR,
(400.32 MHz; DMSO):
10.0008
9.9934
9.8760
9.8687
8.5931
8.5868
8.4193
8.4130
8.3982
8.3919
7.7525
7.7312
2.7287
6i
1.00
0.99
0.95
0.98
1.01
2.99
f1 (ppm)

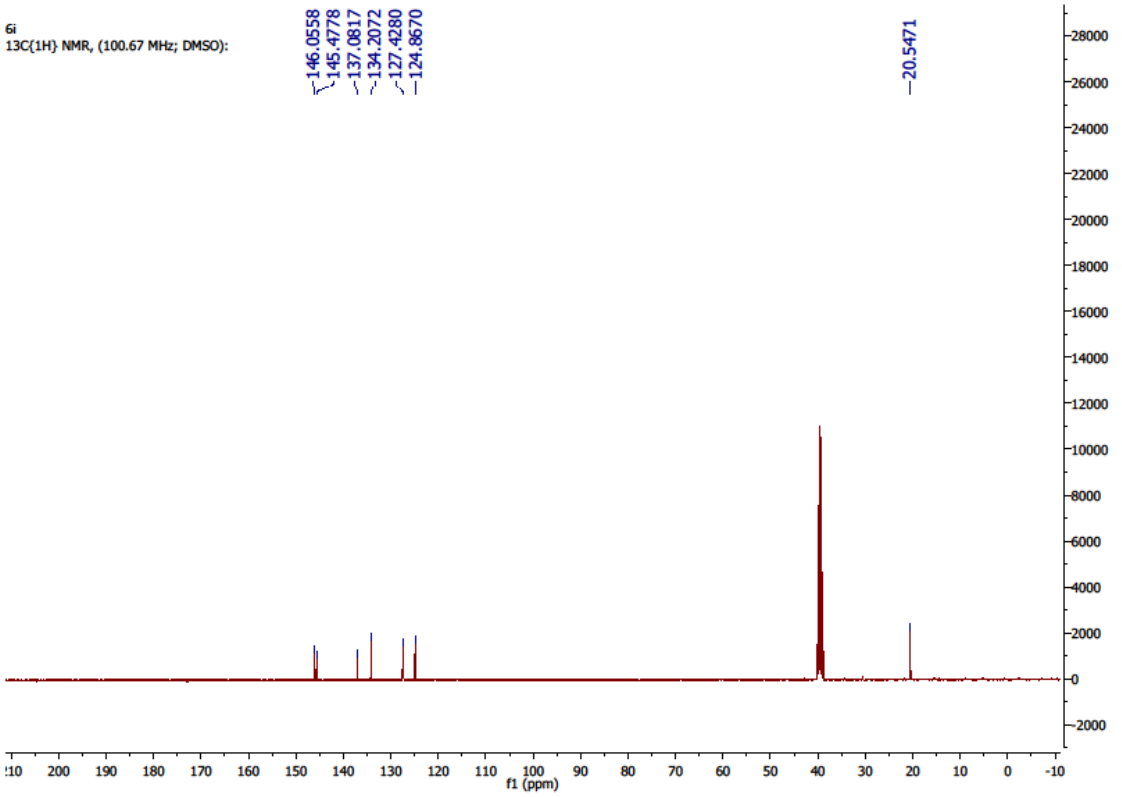
6i
13C{1H} NMR, (100.67 MHz; DMSO):
146.0558
145.4778
137.0817
134.2072
127.4280
124.8670
20.5471
f1 (ppm)

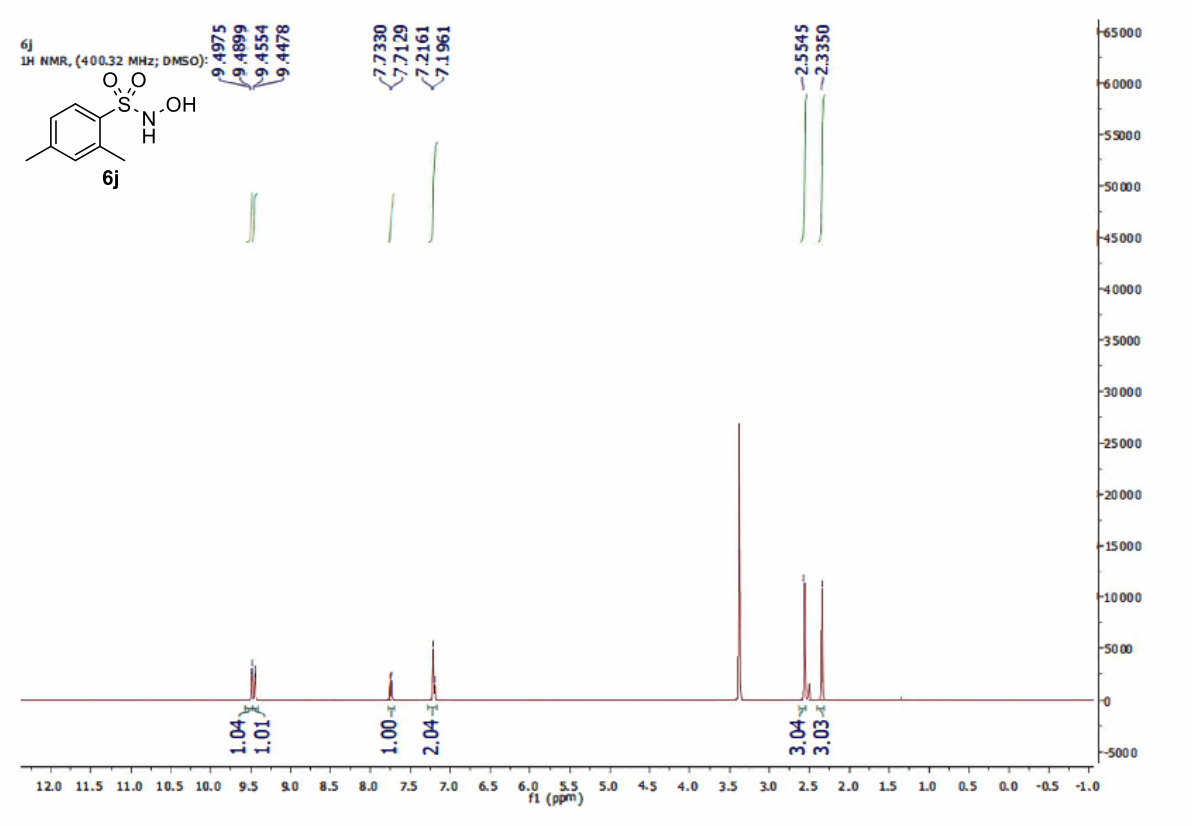
6j
1H NMR, (400.32 MHz; DMSO):
9.4975
9.4899
9.4554
9.4478
7.7330
7.7129
7.2161
7.1961
2.5545
2.3350
6j
1.04
1.01
1.00
2.04
3.04
3.03
f1 (ppm)

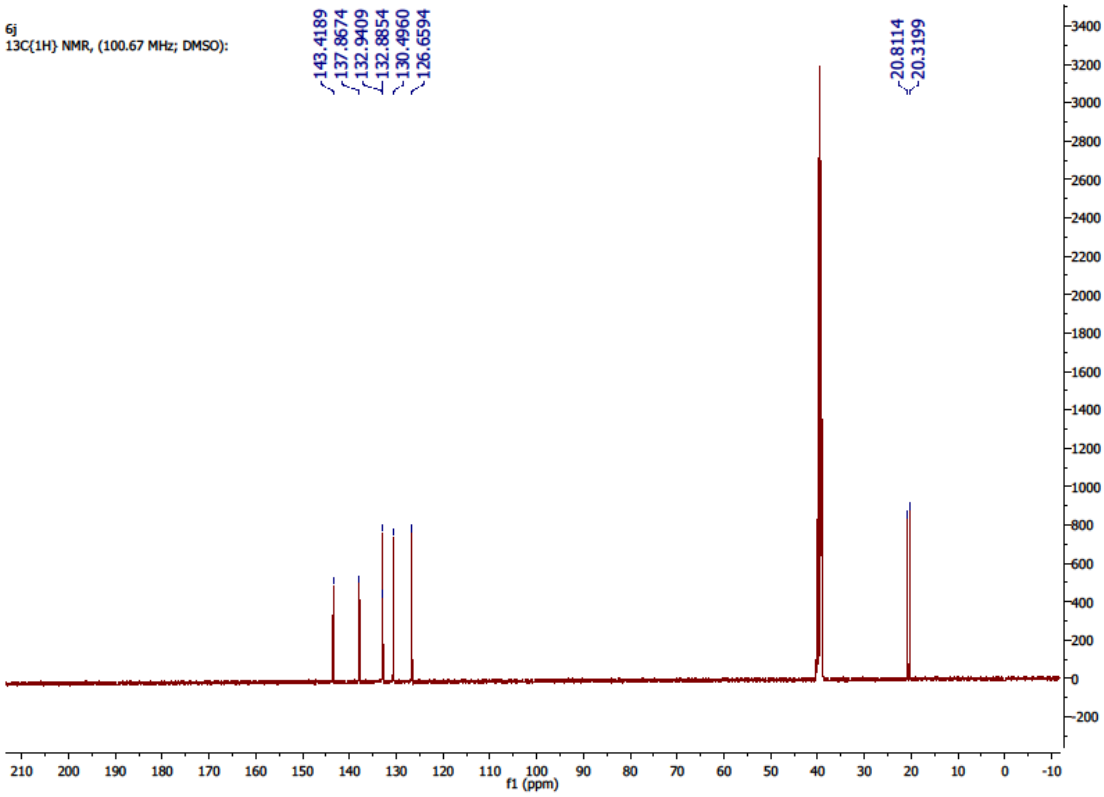
6j
13C{1H} NMR, (100.67 MHz; DMSO):
143.4189
137.8674
132.9409
132.8854
130.4960
126.6594
20.8114
20.3199
f1 (ppm)

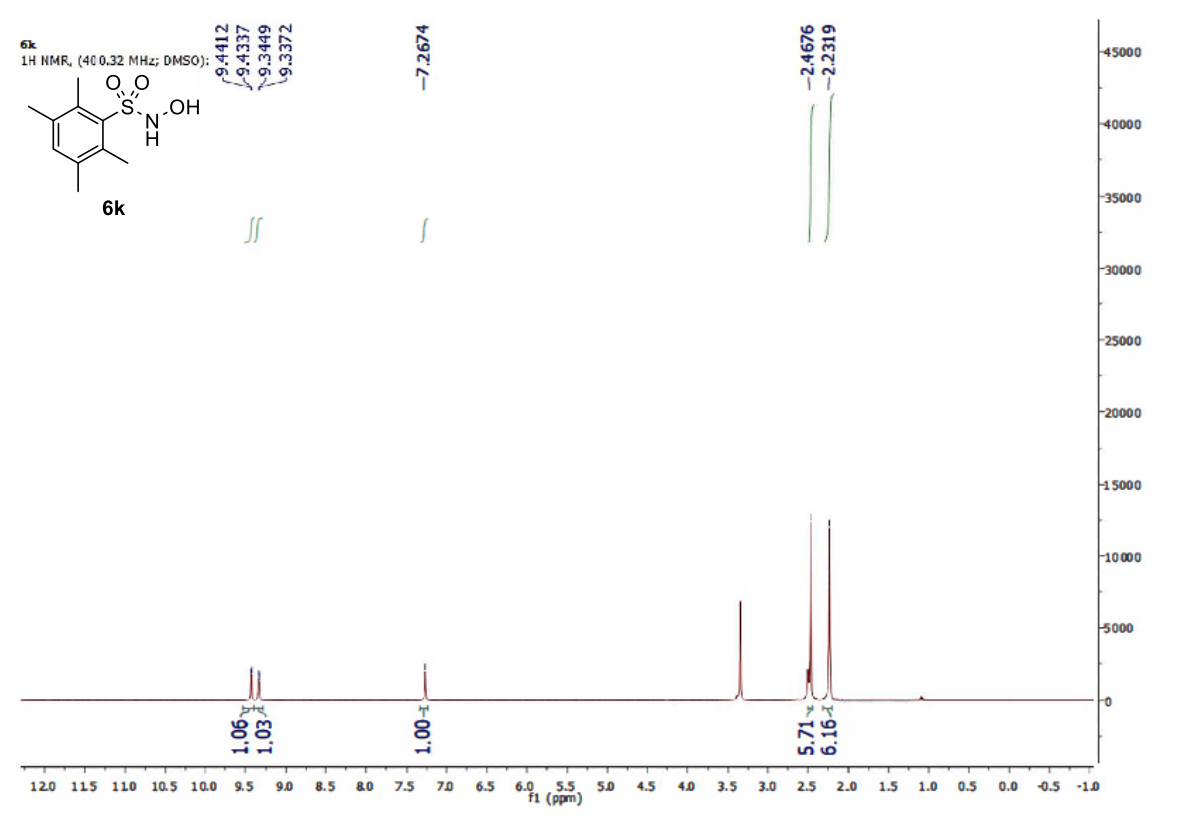
6k
1H NMR, (400.32 MHz; DMSO):
9.4412
9.4337
9.3449
9.3372
7.2674
2.4676
2.2319
1.06
1.03
1.00
5.71
6.16
f1 (ppm)

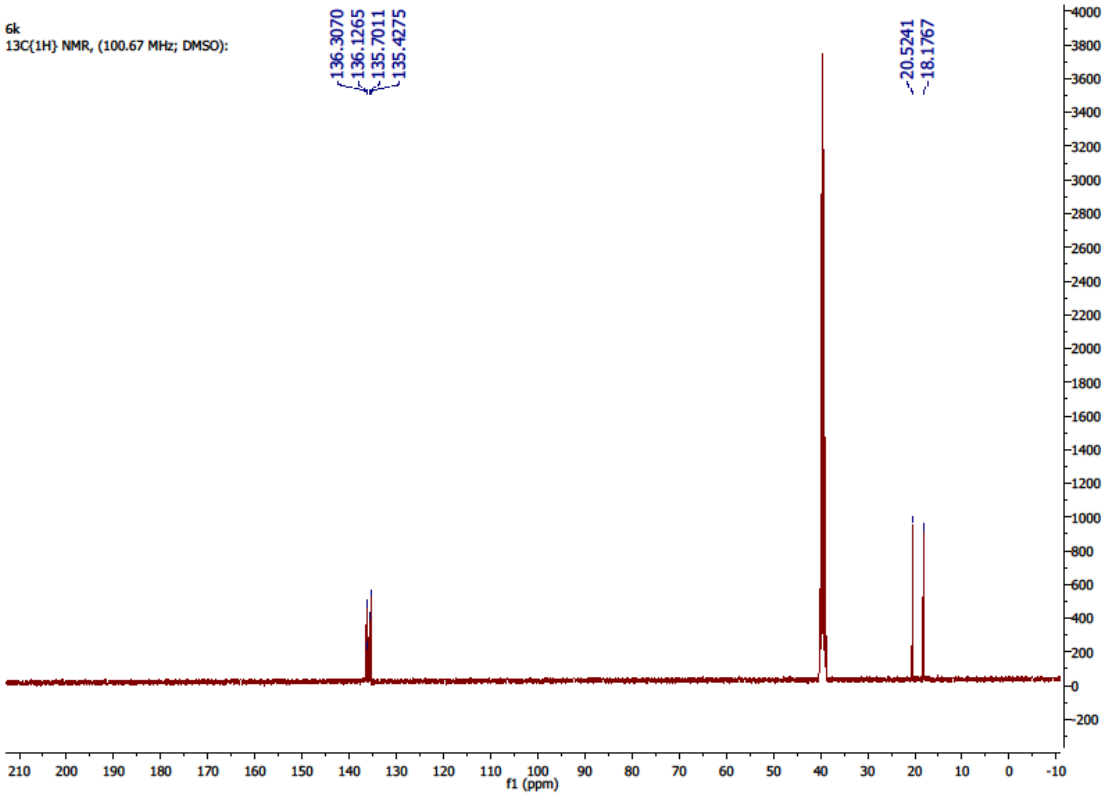
6k
13C{1H} NMR, (100.67 MHz; DMSO):
136.3070
136.1265
135.7011
135.4275
20.5241
18.1767
f1 (ppm)

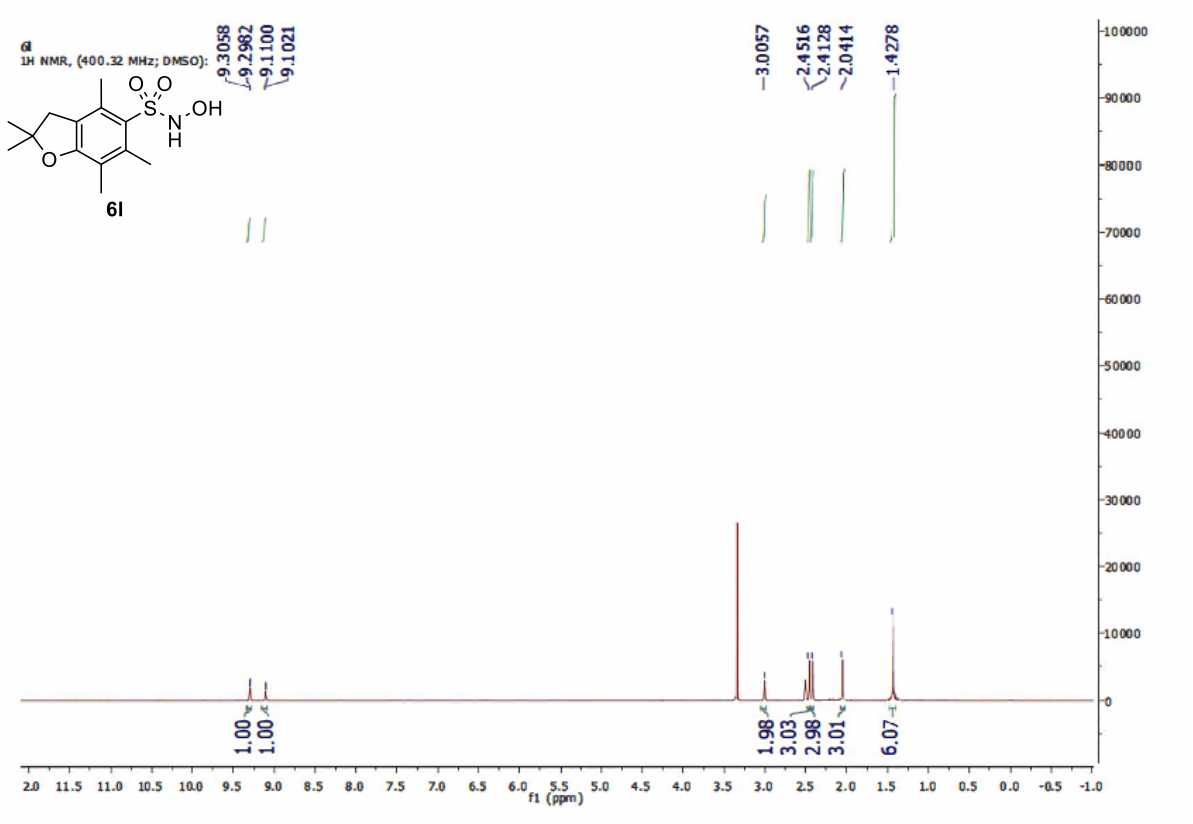
6l
1H NMR, (400.32 MHz; DMSO):
9.3058
9.2982
9.1100
9.1021
3.0057
2.4516
2.4128
2.0414
1.4278
1.00
1.00
1.98
3.03
2.98
3.01
6.07
f1 (ppm)

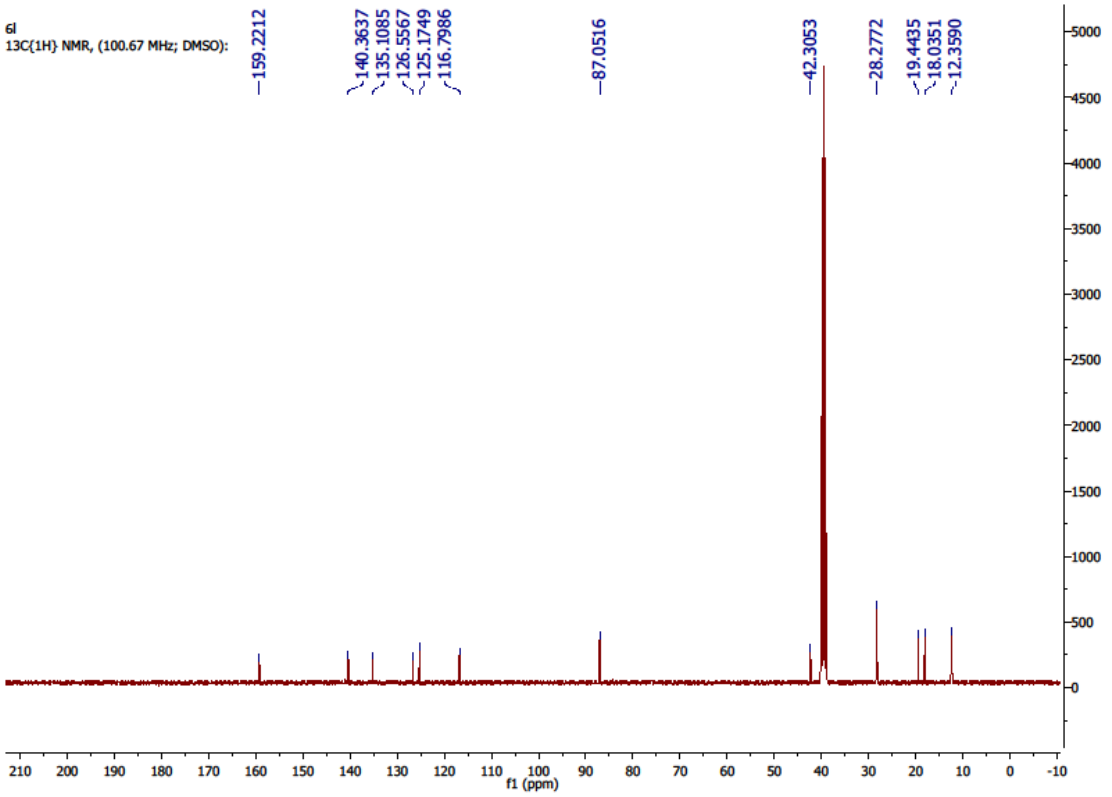
6l
13C{1H} NMR, (100.67 MHz; DMSO):
159.2212
140.3637
135.1085
126.5567
125.1749
116.7986
87.0516
42.3053
28.2772
19.4435
18.0351
12.3590
f1 (ppm)

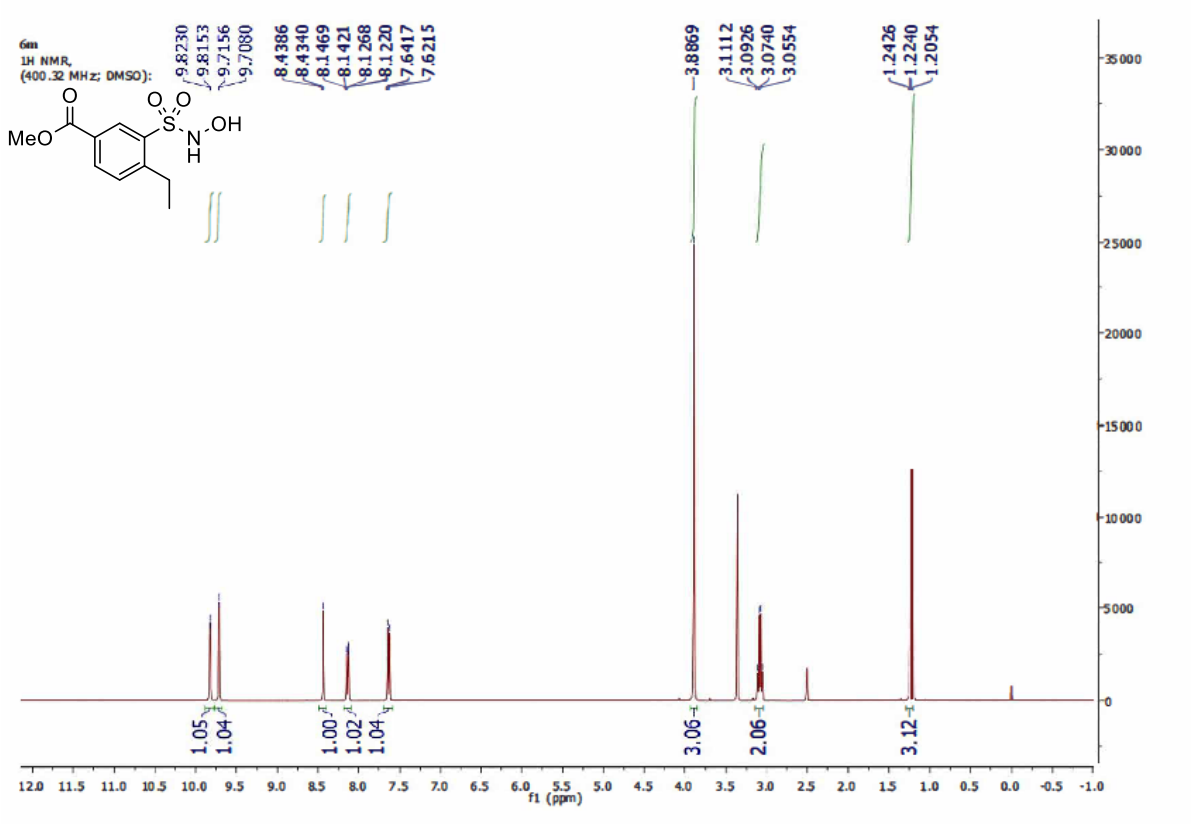
6m
1H NMR,
(400.32 MHz; DMSO):
MeO
O
O
S
N
OH
H
9.8230
9.8153
9.7156
9.7080
8.4386
8.4340
8.1469
8.1421
8.1268
8.1220
7.6417
7.6215
3.8869
3.1112
3.0926
3.0740
3.0554
1.2426
1.2240
1.2054
1.05
1.04
1.00
1.02
1.04
3.06
2.06
3.12
f1 (ppm)

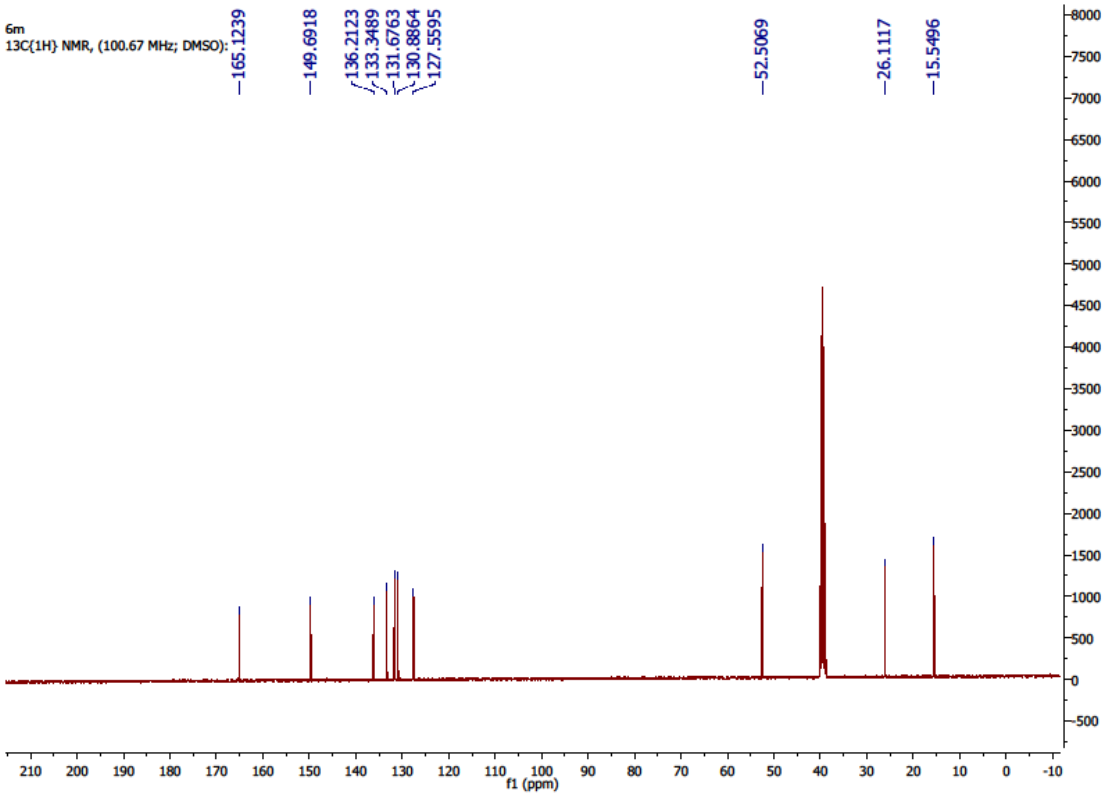
6m
13C{1H} NMR, (100.67 MHz; DMSO):
165.1239
149.6918
136.2123
133.3489
131.6763
130.8864
127.5595
52.5069
26.1117
15.5496
f1 (ppm)

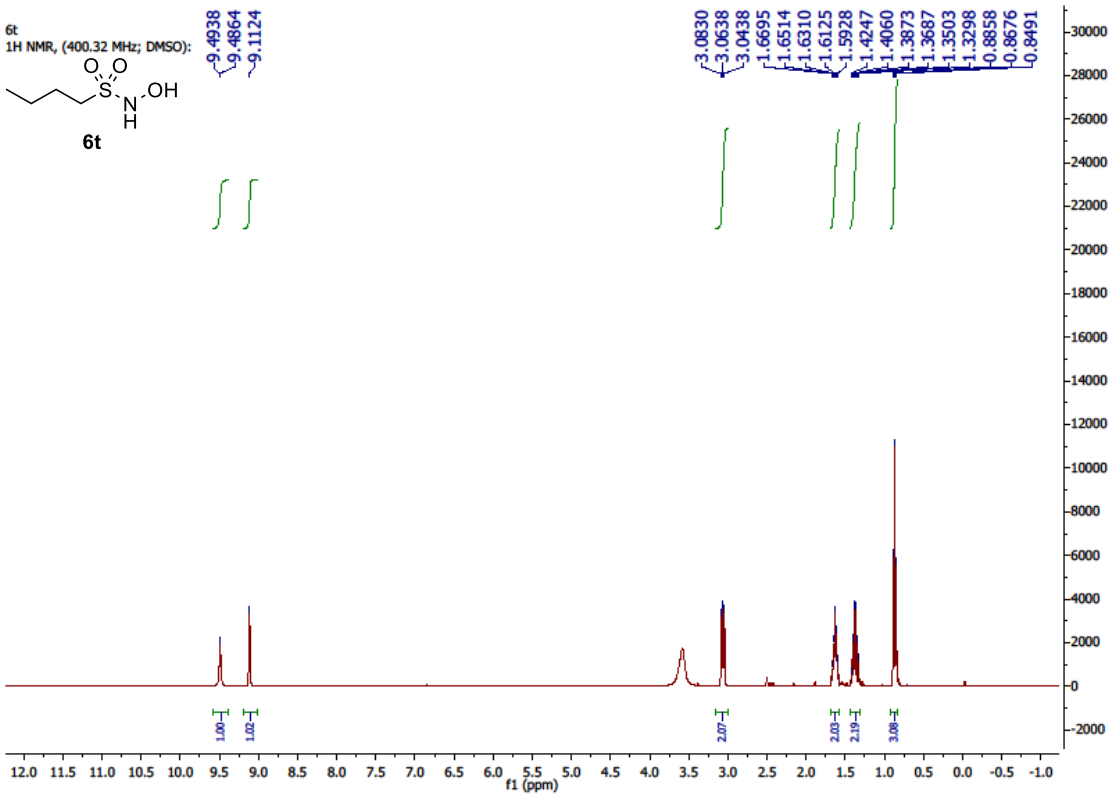
6t
1H NMR, (400.32 MHz; DMSO):
6t
9.4938
9.4864
9.1124
3.0830
3.0638
3.0438
1.6695
1.6514
1.6310
1.6125
1.5928
1.4247
1.4060
1.3873
1.3687
1.3503
1.3298
0.8858
0.8676
0.8491
1.00
1.02
2.07
2.03
2.19
3.08
f1 (ppm)

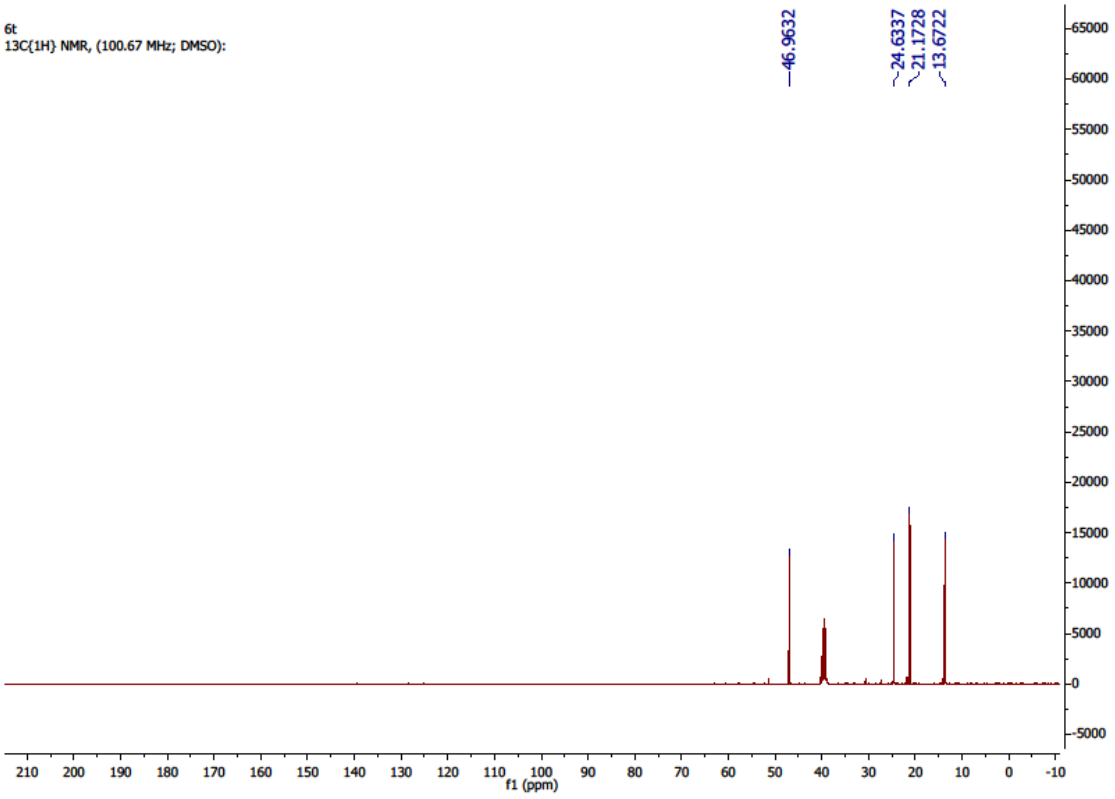
6t
13C{1H} NMR, (100.67 MHz; DMSO):
46.9632
24.6337
21.1728
13.6722
f1 (ppm)

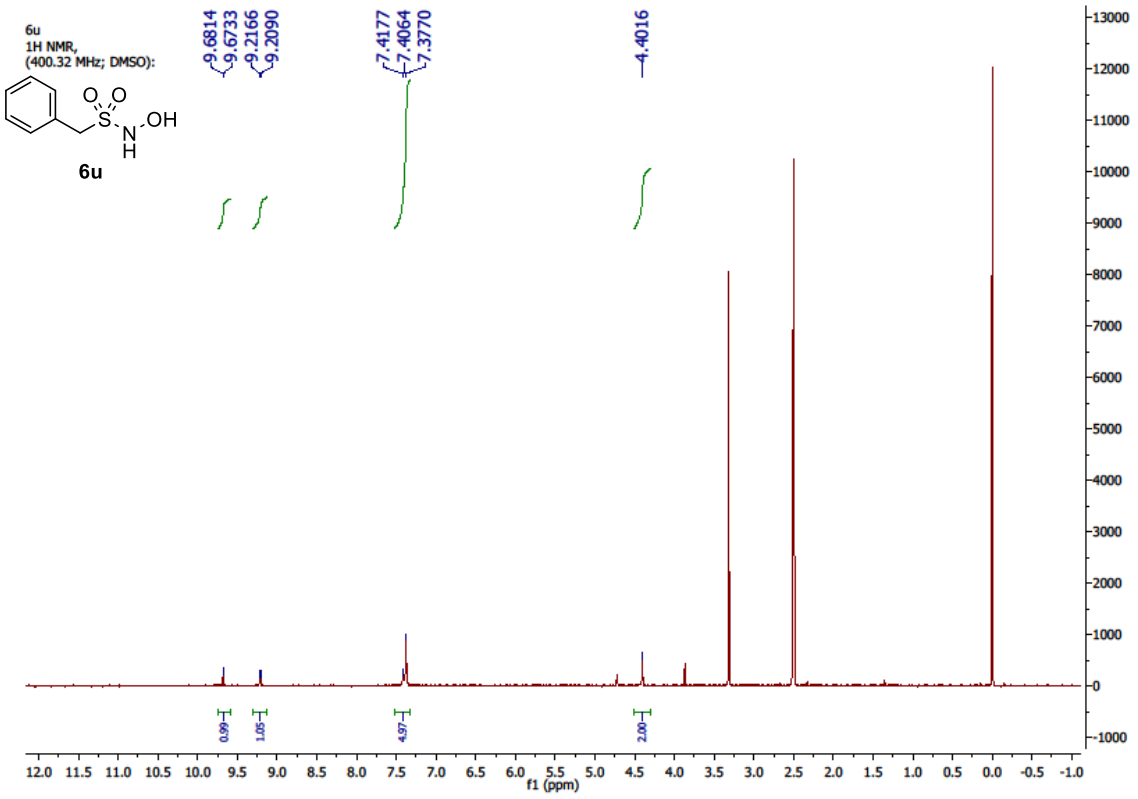
6u
1H NMR,
(400.32 MHz; DMSO):
6u
9.6814
9.6733
9.2166
9.2090
7.4177
7.4064
7.3770
4.4016
0.99
1.05
4.97
2.00
f1 (ppm)

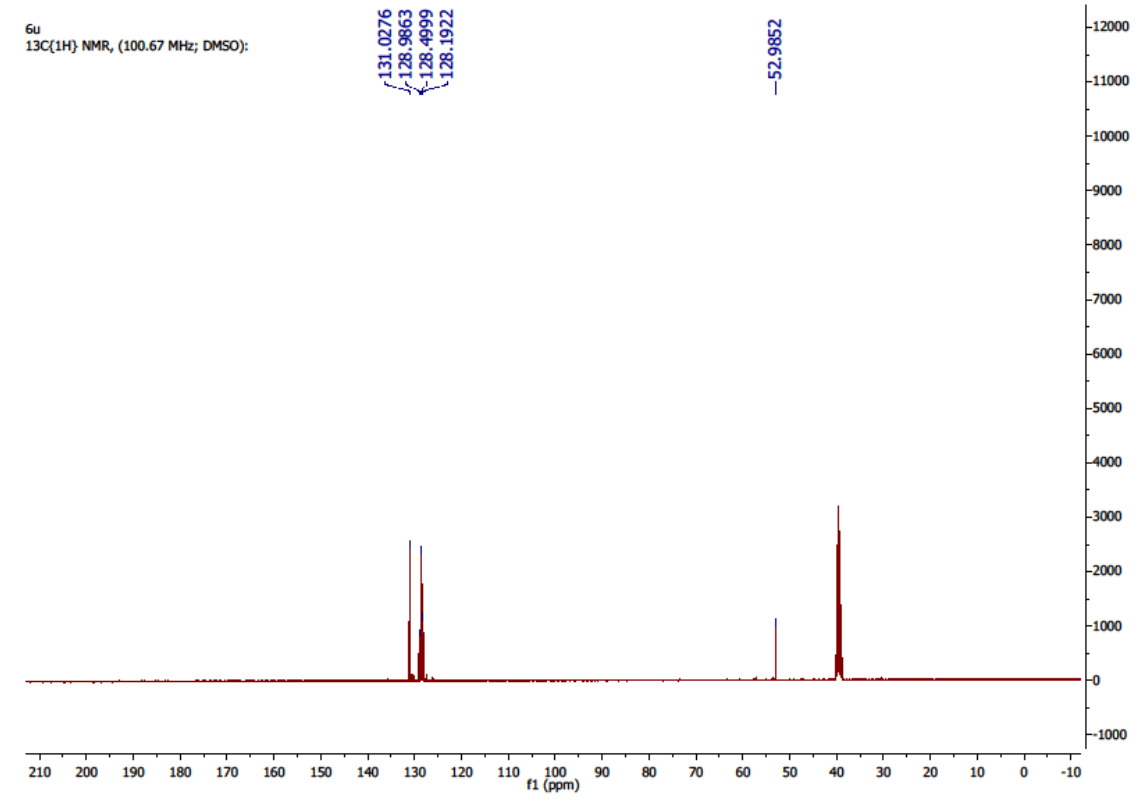
6u
13C{1H} NMR, (100.67 MHz; DMSO):
131.0276
128.9863
128.4999
128.1922
52.9852
f1 (ppm)

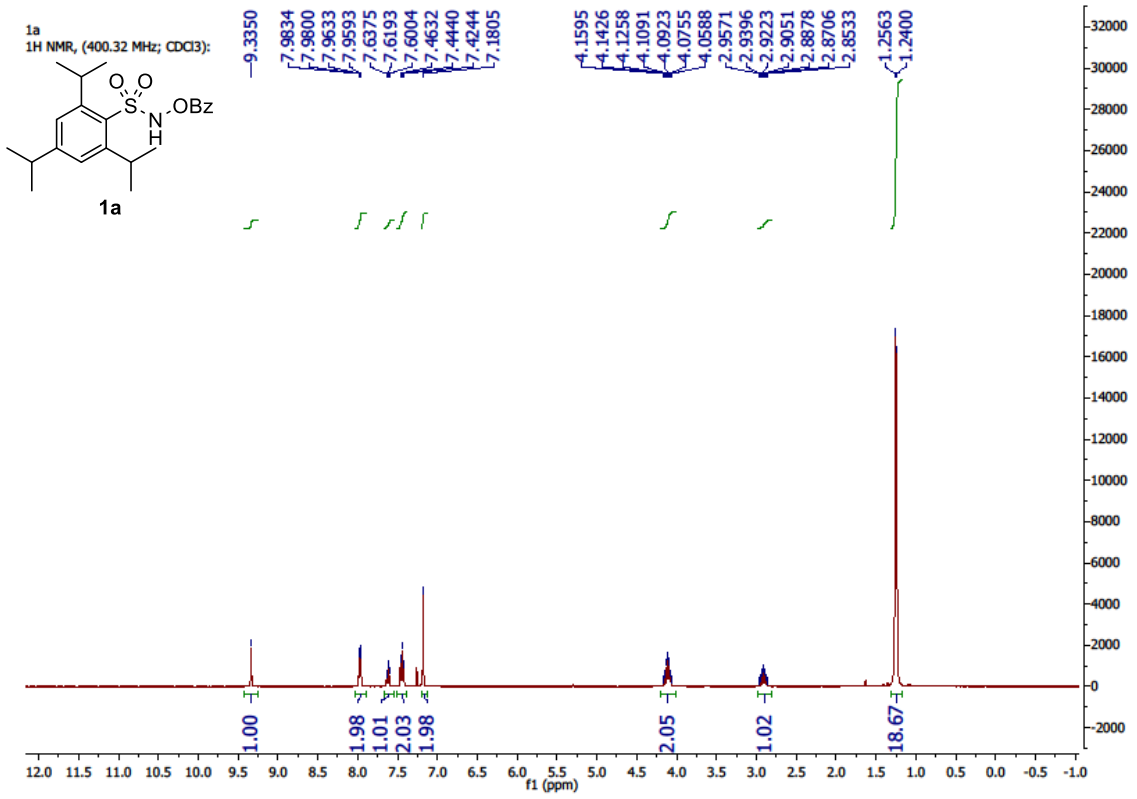
1a
1H NMR, (400.32 MHz; CDCl3):
1a
9.3350
7.9834
7.9800
7.9633
7.9593
7.6375
7.6193
7.6004
7.4632
7.4440
7.4244
7.1805
4.1595
4.1426
4.1258
4.1091
4.0923
4.0755
4.0588
2.9571
2.9396
2.9223
2.9051
2.8878
2.8706
2.8533
1.2563
1.2400
1.00
1.98
1.01
2.03
1.98
2.05
1.02
18.67
f1 (ppm)

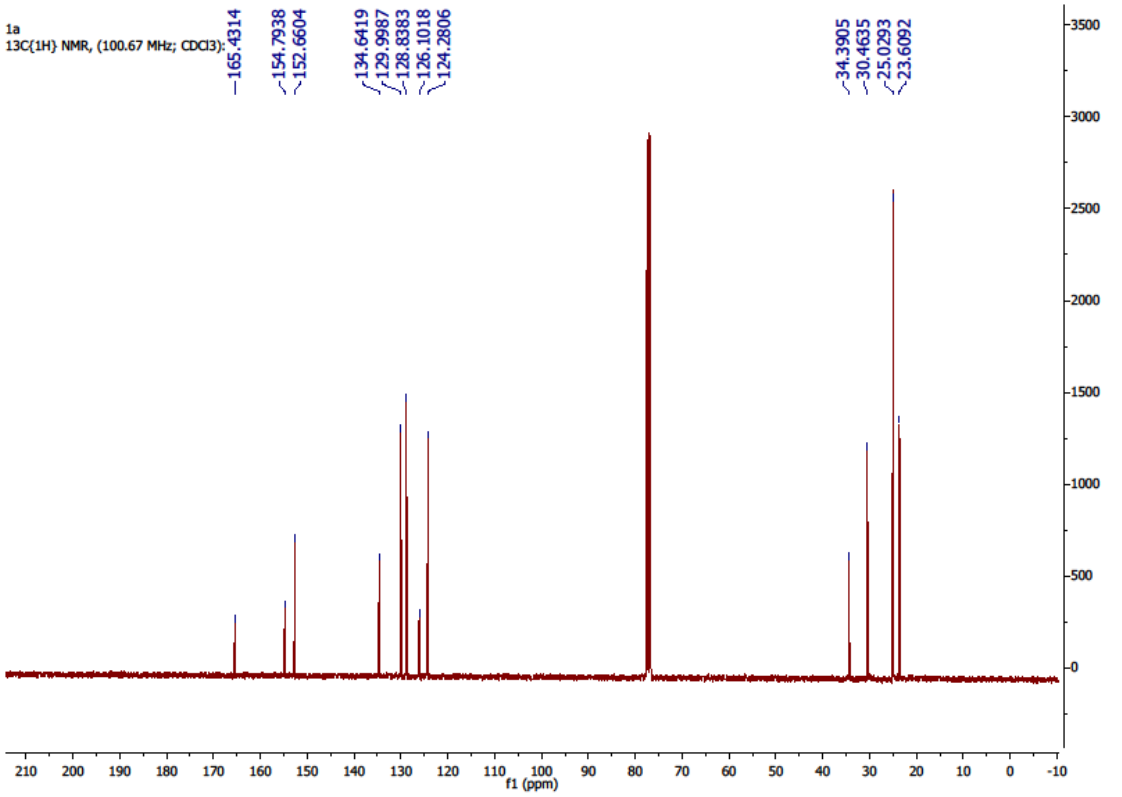
1a
13C{1H} NMR, (100.67 MHz; CDCl3):
165.4314
154.7938
152.6604
134.6419
129.9987
128.8383
126.1018
124.2806
34.3905
30.4635
25.0293
23.6092
f1 (ppm)

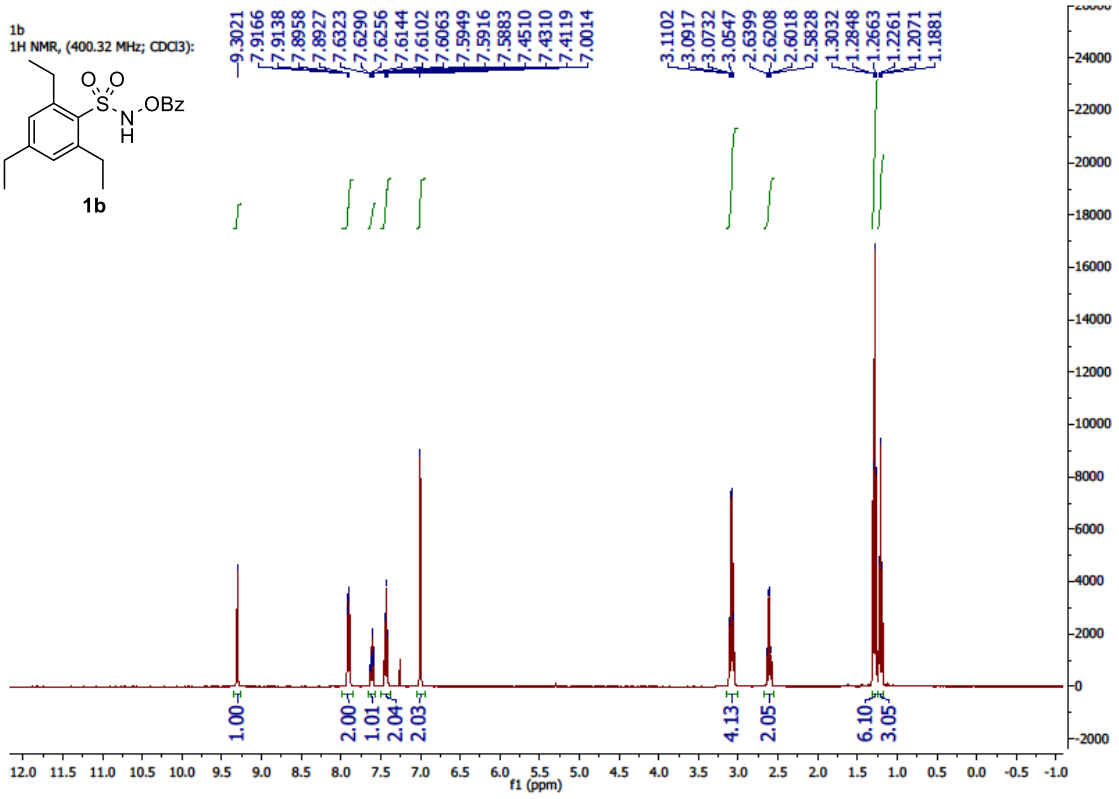
1b
1H NMR, (400.32 MHz; CDCl3):
1b
9.3021
7.9166
7.9138
7.8958
7.8927
7.6323
7.6290
7.6256
7.6144
7.6102
7.6063
7.5949
7.5916
7.5883
7.4510
7.4310
7.4119
7.0014
3.1102
3.0917
3.0732
3.0547
2.6399
2.6208
2.6018
2.5828
1.3032
1.2848
1.2663
1.2261
1.2071
1.1881
1.00
2.00
1.01
2.04
2.03
4.13
2.05
6.10
3.05
f1 (ppm)

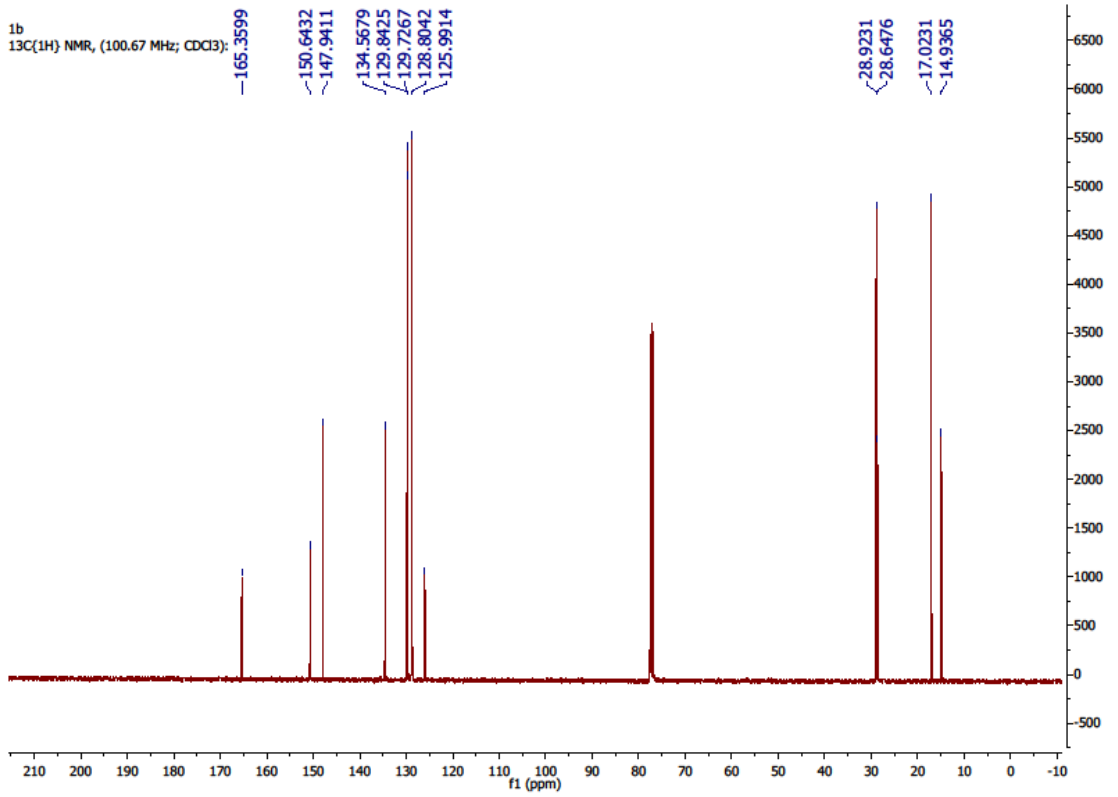
1b
13C{1H} NMR, (100.67 MHz; CDCl3):
165.3599
150.6432
147.9411
134.5679
129.8425
129.7267
128.8042
125.9914
28.9231
28.6476
17.0231
14.9365
f1 (ppm)

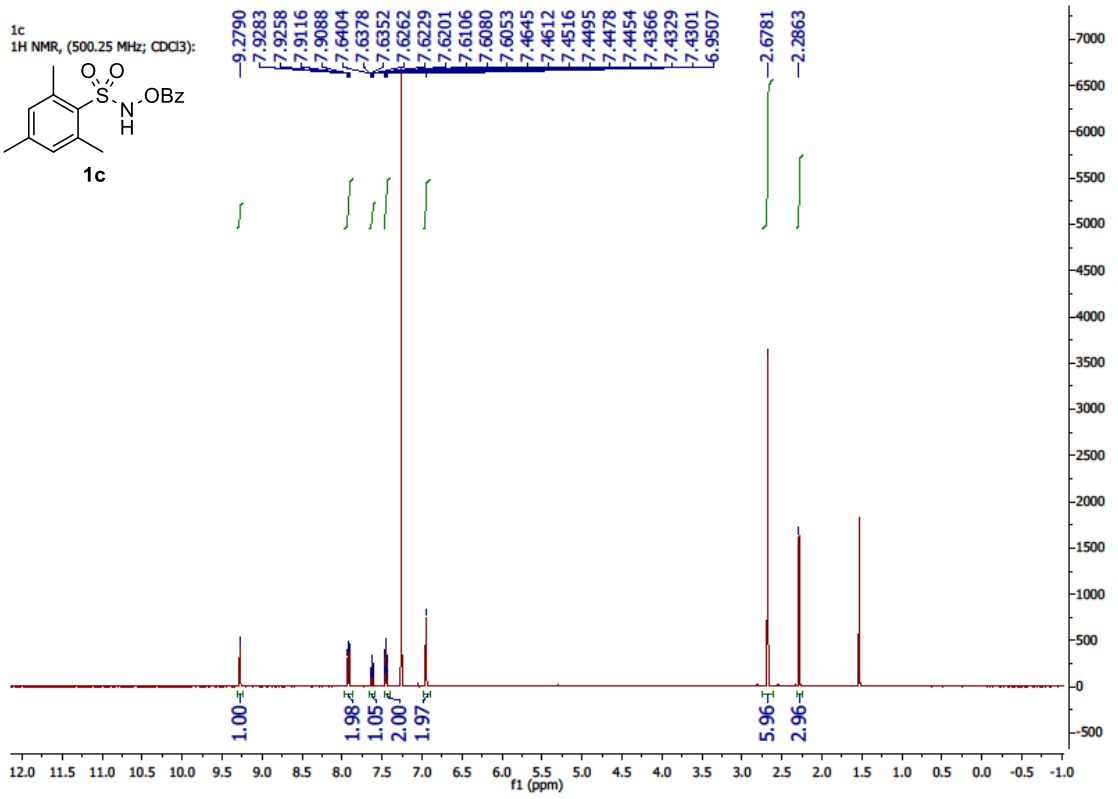
1c
1H NMR, (500.25 MHz; CDCl3):
1c
9.2790
7.9283
7.9258
7.9116
7.9088
7.6404
7.6378
7.6352
7.6262
7.6229
7.6201
7.6106
7.6080
7.6053
7.4645
7.4612
7.4516
7.4495
7.4478
7.4454
7.4366
7.4329
7.4301
6.9507
2.6781
2.2863
1.00
1.98
1.05
2.00
1.97
5.96
2.96
f1 (ppm)

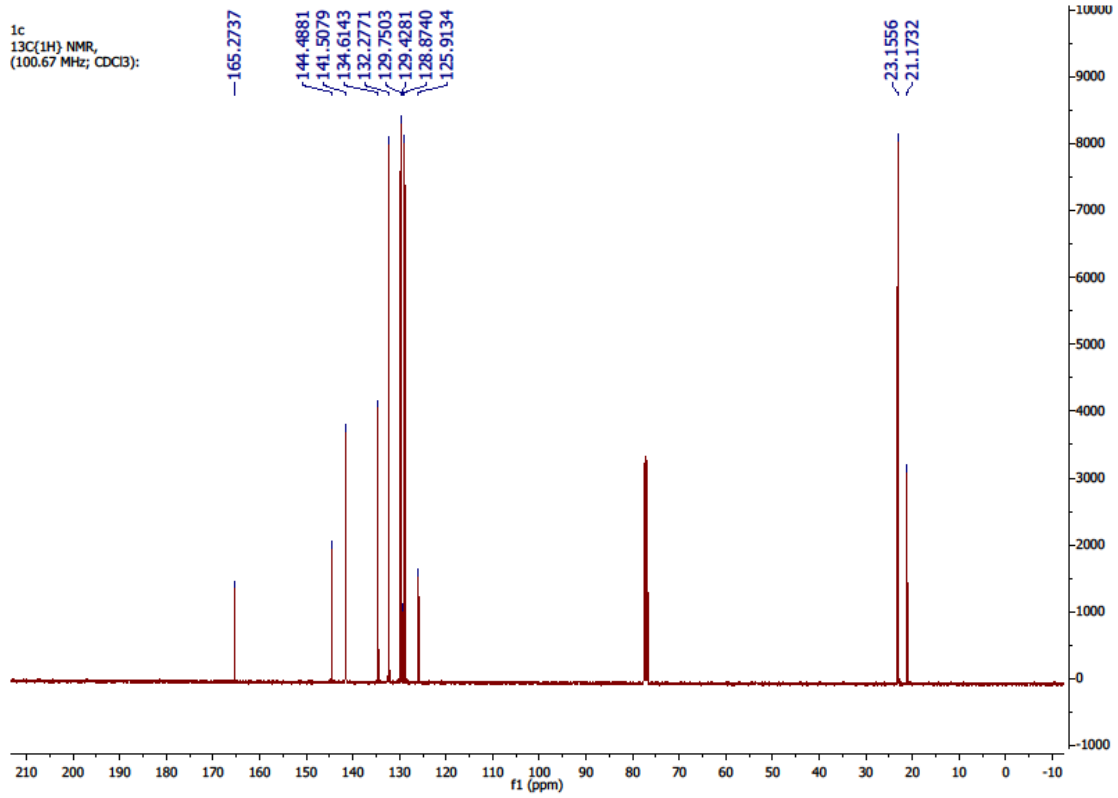
1c
13C{1H} NMR,
(100.67 MHz; CDCl3):
165.2737
144.4881
141.5079
134.6143
132.2771
129.7503
129.4281
128.8740
125.9134
23.1556
21.1732
f1 (ppm)

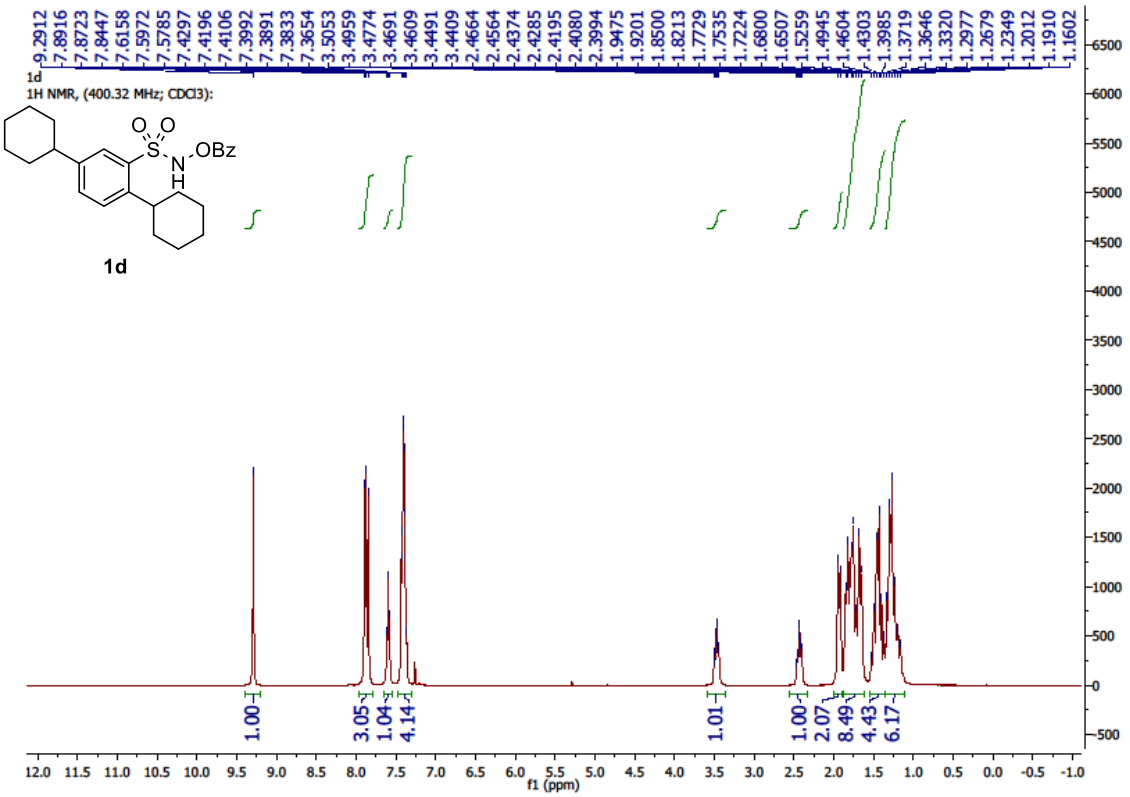
1d
1H NMR, (400.32 MHz; CDCl3):
1d
1.00
3.05
1.04
4.14
1.01
1.00
2.07
8.49
4.43
6.17
f1 (ppm)

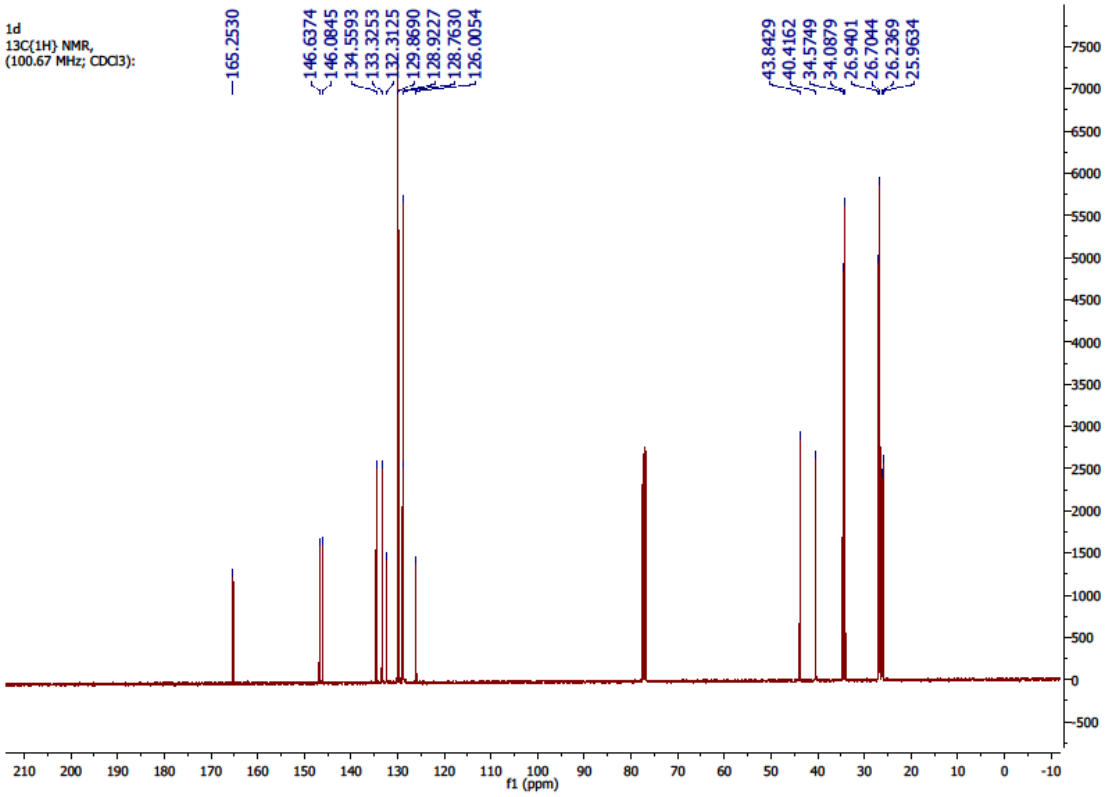
1d
13C{1H} NMR,
(100.67 MHz; CDCl3):
165.2530
146.6374
146.0845
134.5593
133.3253
132.3125
129.8690
128.9227
128.7630
126.0054
43.8429
40.4162
34.5749
34.0879
26.9401
26.7044
26.2369
25.9634
f1 (ppm)

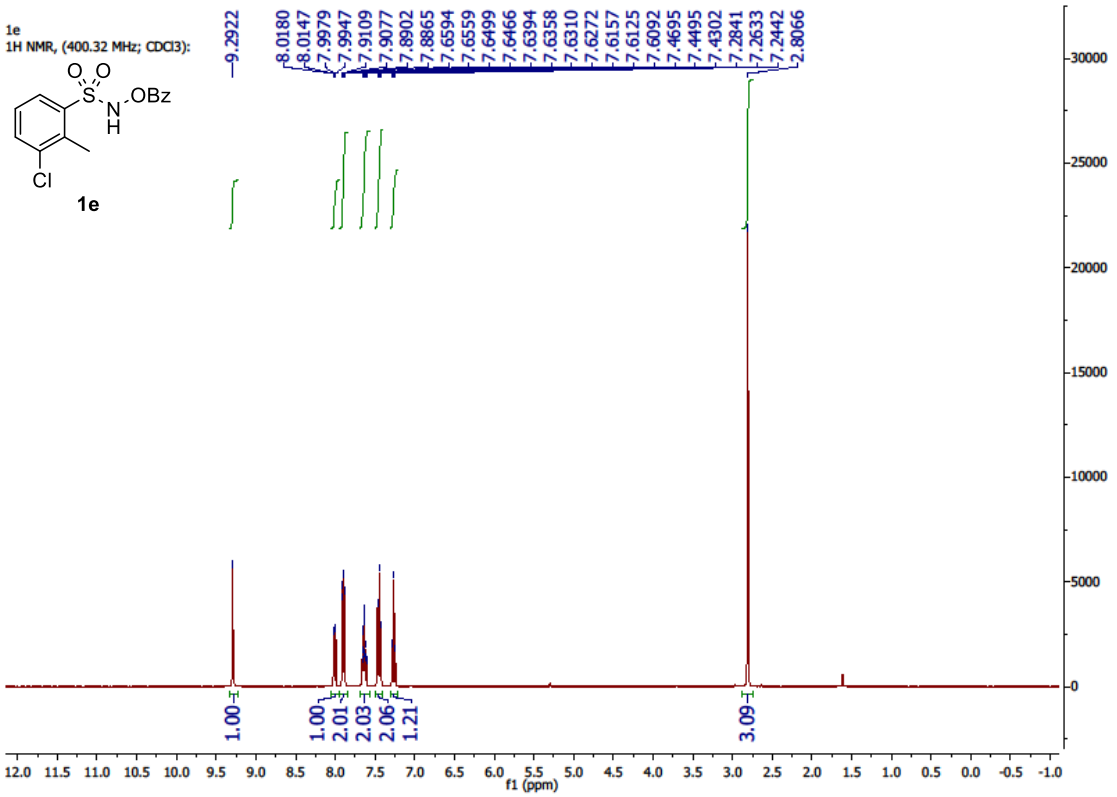
1e
1H NMR, (400.32 MHz; CDCl3):
1e
9.2922
8.0180
8.0147
7.9979
7.9947
7.9109
7.9077
7.8902
7.8865
7.6594
7.6559
7.6499
7.6466
7.6394
7.6358
7.6310
7.6272
7.6157
7.6125
7.6092
7.4695
7.4495
7.4302
7.2841
7.2633
7.2442
2.8066
1.00
1.00
2.01
2.03
2.06
1.21
3.09
f1 (ppm)

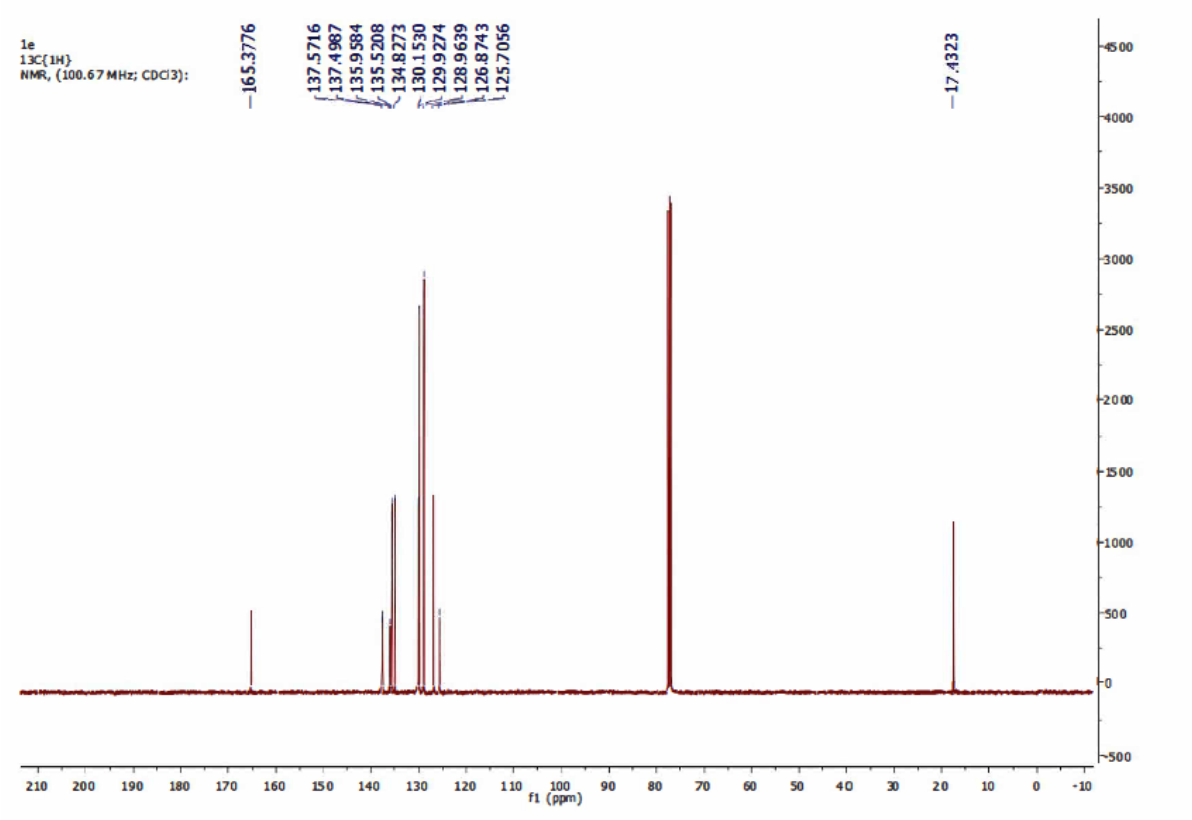
1e
13C{1H}
NMR, (100.67 MHz; CDCl3):
165.3776
137.5716
137.4987
135.9584
135.5208
134.8273
130.1530
129.9274
128.9639
126.8743
125.7056
17.4323
f1 (ppm)

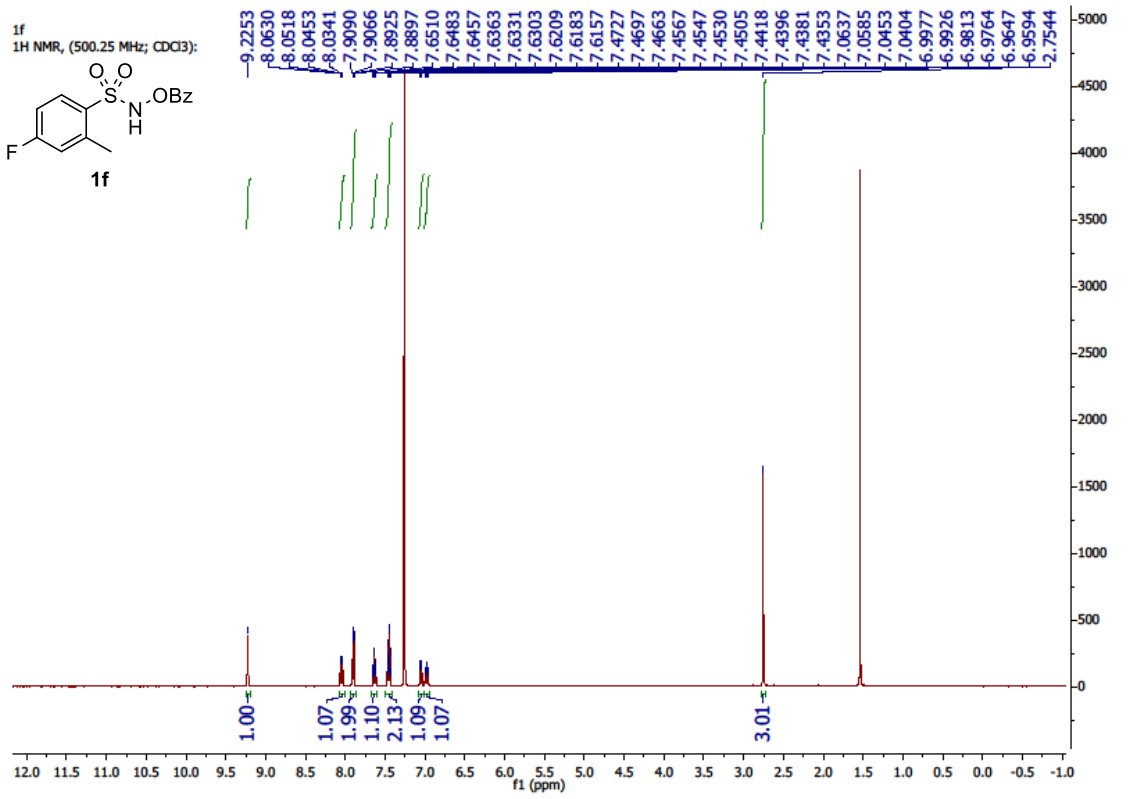
1f
1H NMR, (500.25 MHz; CDCl3):
1f
9.2253
8.0630
8.0518
8.0453
8.0341
7.9090
7.9066
7.8925
7.8897
7.6510
7.6483
7.6457
7.6363
7.6331
7.6303
7.6209
7.6183
7.6157
7.4727
7.4697
7.4663
7.4567
7.4547
7.4530
7.4505
7.4418
7.4396
7.4381
7.4353
7.0637
7.0585
7.0453
7.0404
6.9977
6.9926
6.9813
6.9764
6.9647
6.9594
2.7544
1.00
1.07
1.99
1.10
2.13
1.09
1.07
3.01
f1 (ppm)

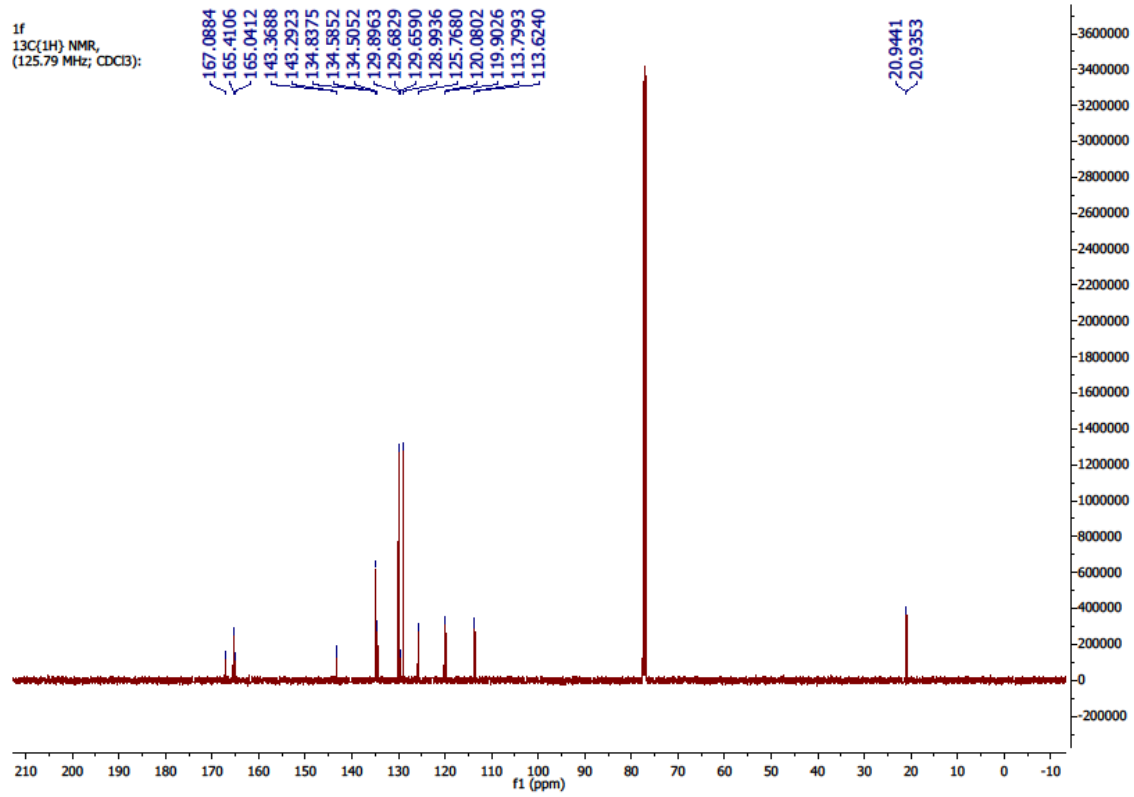
1f
13C{1H} NMR,
(125.79 MHz; CDCl3):
167.0884
165.4106
165.0412
143.3688
143.2923
134.8375
134.5852
134.5052
129.8963
129.6829
129.6590
128.9936
125.7680
120.0802
119.9026
113.7993
113.6240
20.9441
20.9353
f1 (ppm)

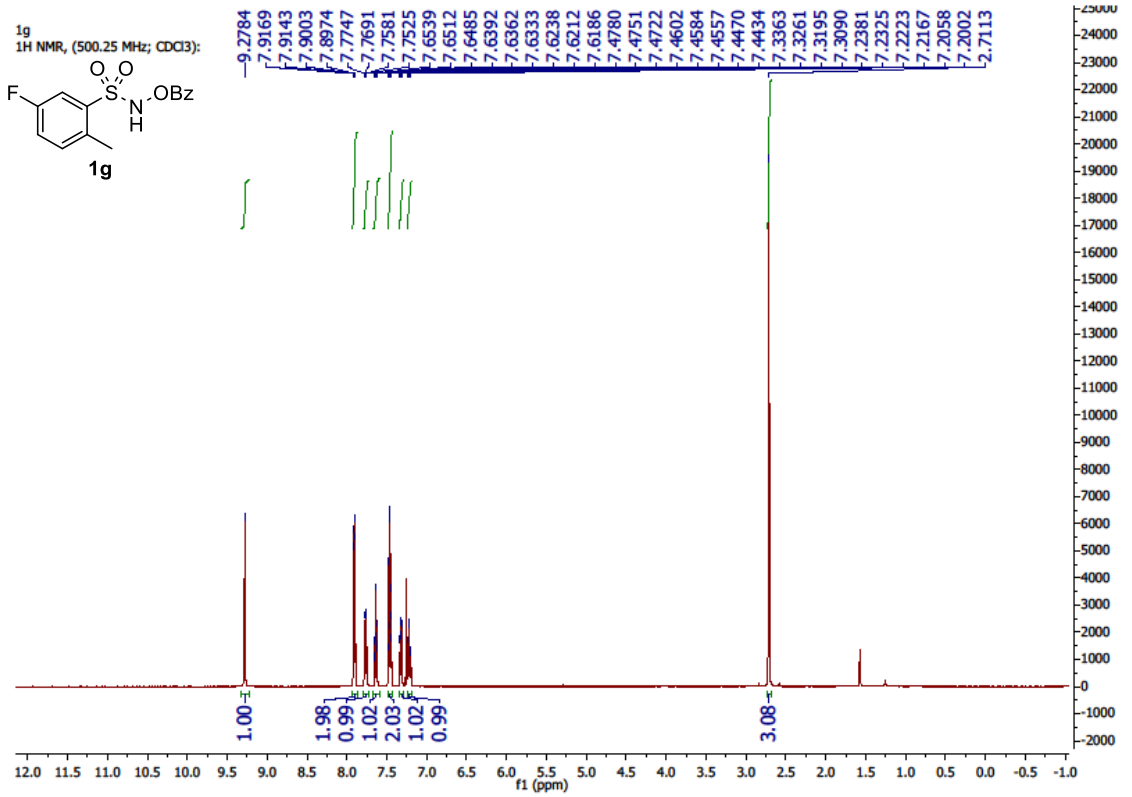
1g
1H NMR, (500.25 MHz; CDCl3):
1g
9.2784
7.9169
7.9143
7.9003
7.8974
7.7747
7.7691
7.7581
7.7525
7.6539
7.6512
7.6485
7.6392
7.6362
7.6333
7.6238
7.6212
7.6186
7.4780
7.4751
7.4722
7.4602
7.4584
7.4557
7.4470
7.4434
7.3363
7.3261
7.3195
7.3090
7.2381
7.2325
7.2223
7.2167
7.2058
7.2002
2.7113
1.00
1.98
0.99
1.02
2.03
1.02
0.99
3.08
f1 (ppm)

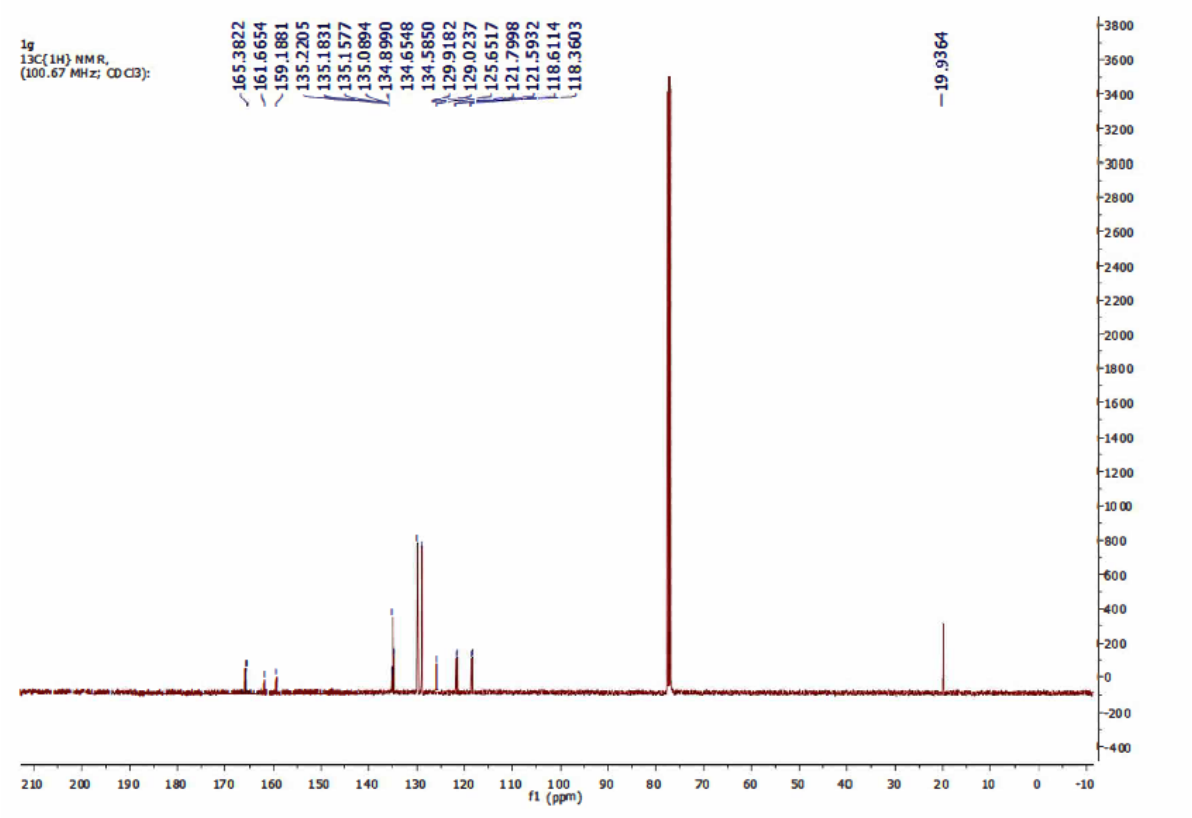
1g
13C{1H} NMR,
(100.67 MHz; CDCl3):
165.3822
161.6654
159.1881
135.2205
135.1831
135.1577
135.0894
134.8990
134.6548
134.5850
129.9182
129.0237
125.6517
121.7998
121.5932
118.6114
118.3603
19.9364
f1 (ppm)

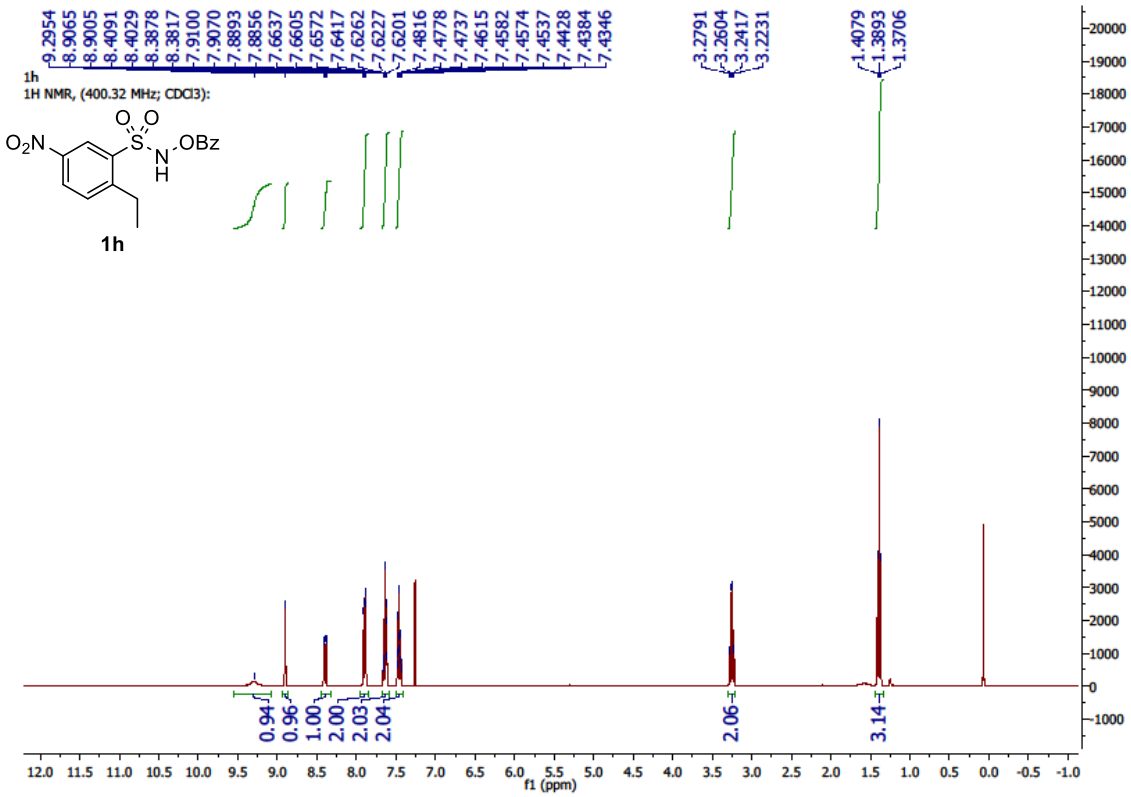
1h
1H NMR, (400.32 MHz; CDCl3):
9.2954
8.9065
8.9005
8.4091
8.4029
8.3878
8.3817
7.9100
7.9070
7.8893
7.8856
7.6637
7.6605
7.6572
7.6417
7.6262
7.6227
7.6201
7.4816
7.4778
7.4737
7.4615
7.4582
7.4574
7.4537
7.4428
7.4384
7.4346
3.2791
3.2604
3.2417
3.2231
1.4079
1.3893
1.3706
0.94
0.96
1.00
2.00
2.03
2.04
2.06
3.14
f1 (ppm)

1h

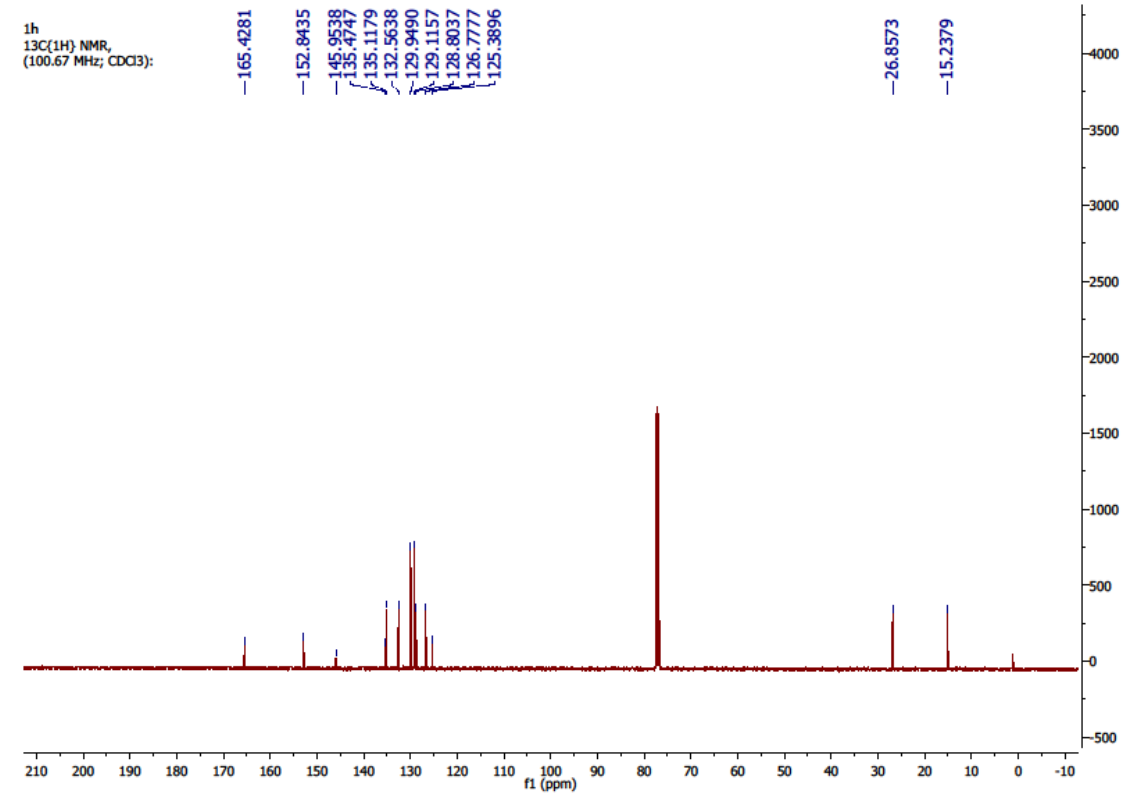
1h
13C{1H} NMR,
(100.67 MHz; CDCl3):
165.4281
152.8435
145.9538
135.4747
135.1179
132.5638
129.9490
129.1157
128.8037
126.7777
125.3896
26.8573
15.2379
f1 (ppm)

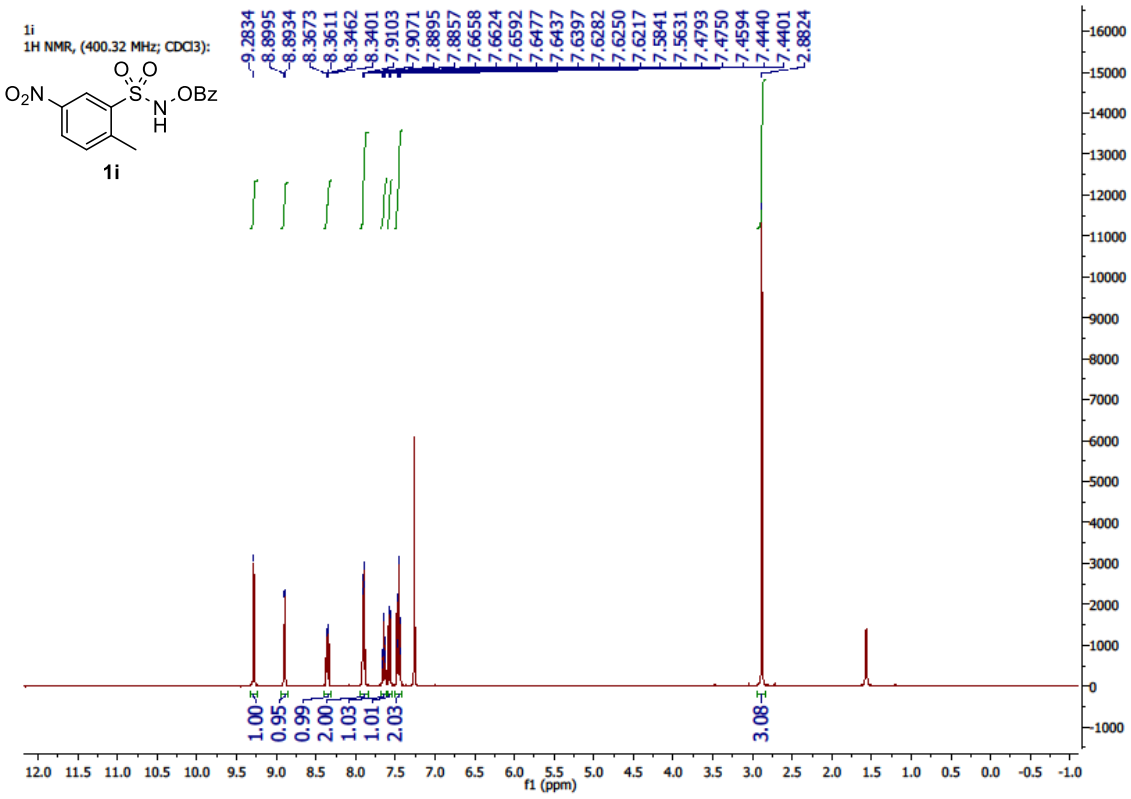
1i
1H NMR, (400.32 MHz; CDCl3):
1i
9.2834
8.8995
8.8934
8.3673
8.3611
8.3462
8.3401
7.9103
7.9071
7.8895
7.8857
7.6658
7.6624
7.6592
7.6477
7.6437
7.6397
7.6282
7.6250
7.6217
7.5841
7.5631
7.4793
7.4750
7.4594
7.4440
7.4401
2.8824
1.00
0.95
0.99
2.00
1.03
1.01
2.03
3.08
f1 (ppm)

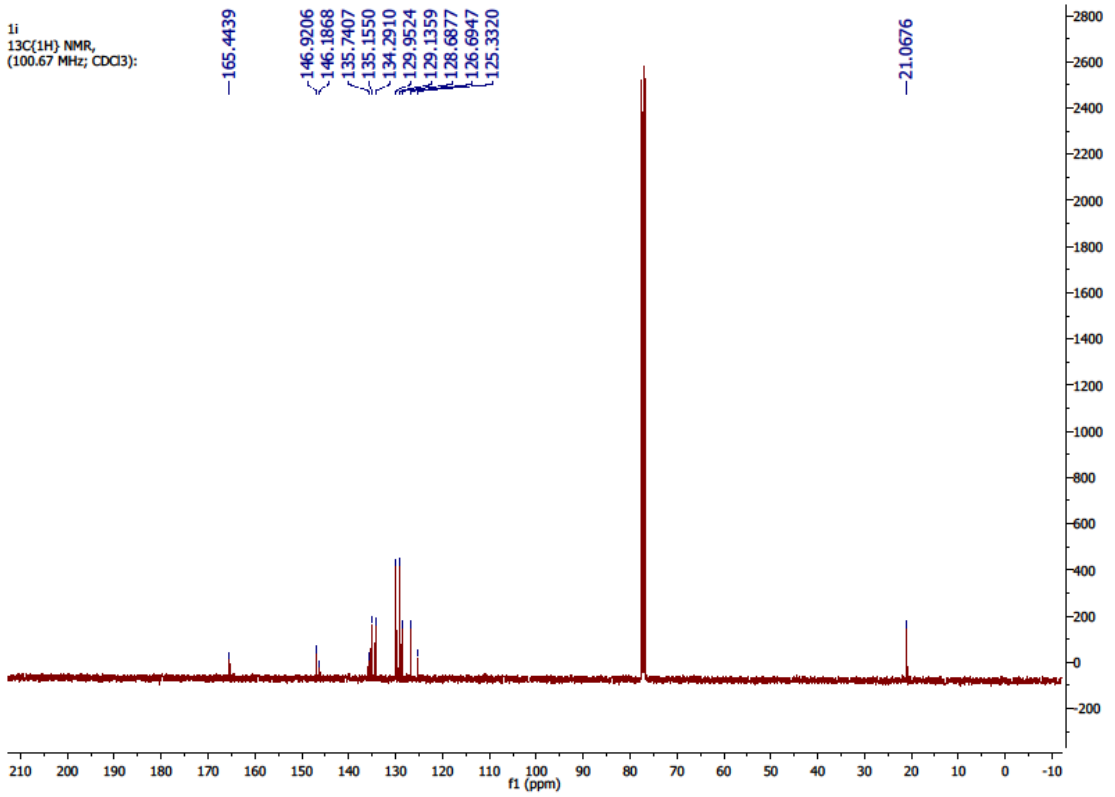
1i
13C{1H} NMR,
(100.67 MHz; CDCl3):
165.4439
146.9206
146.1868
135.7407
135.1550
134.2910
129.9524
129.1359
128.6877
126.6947
125.3320
21.0676
f1 (ppm)

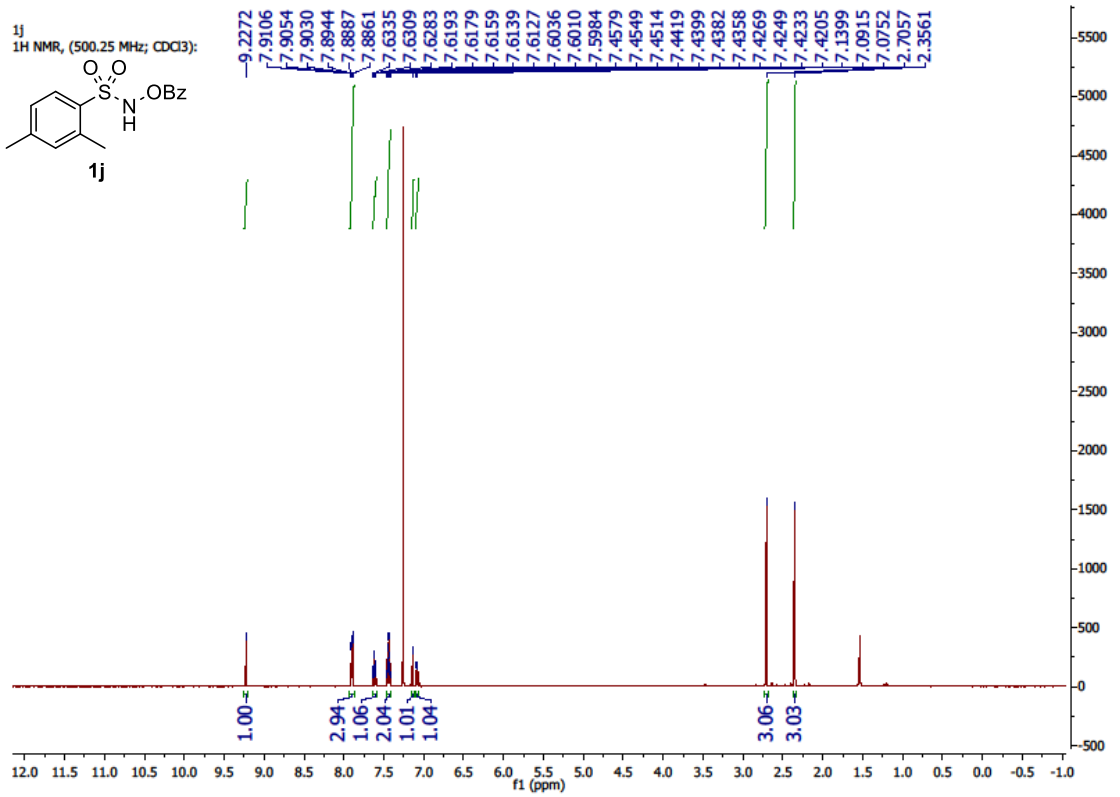
1j
1H NMR, (500.25 MHz; CDCl3):
1j
9.2272
7.9106
7.9054
7.9030
7.8944
7.8887
7.8861
7.6335
7.6309
7.6283
7.6193
7.6179
7.6159
7.6139
7.6127
7.6036
7.6010
7.5984
7.4579
7.4549
7.4514
7.4419
7.4399
7.4382
7.4358
7.4269
7.4249
7.4233
7.4205
7.1399
7.0915
7.0752
2.7057
2.3561
1.00
2.94
1.06
2.04
1.01
1.04
3.06
3.03
f1 (ppm)

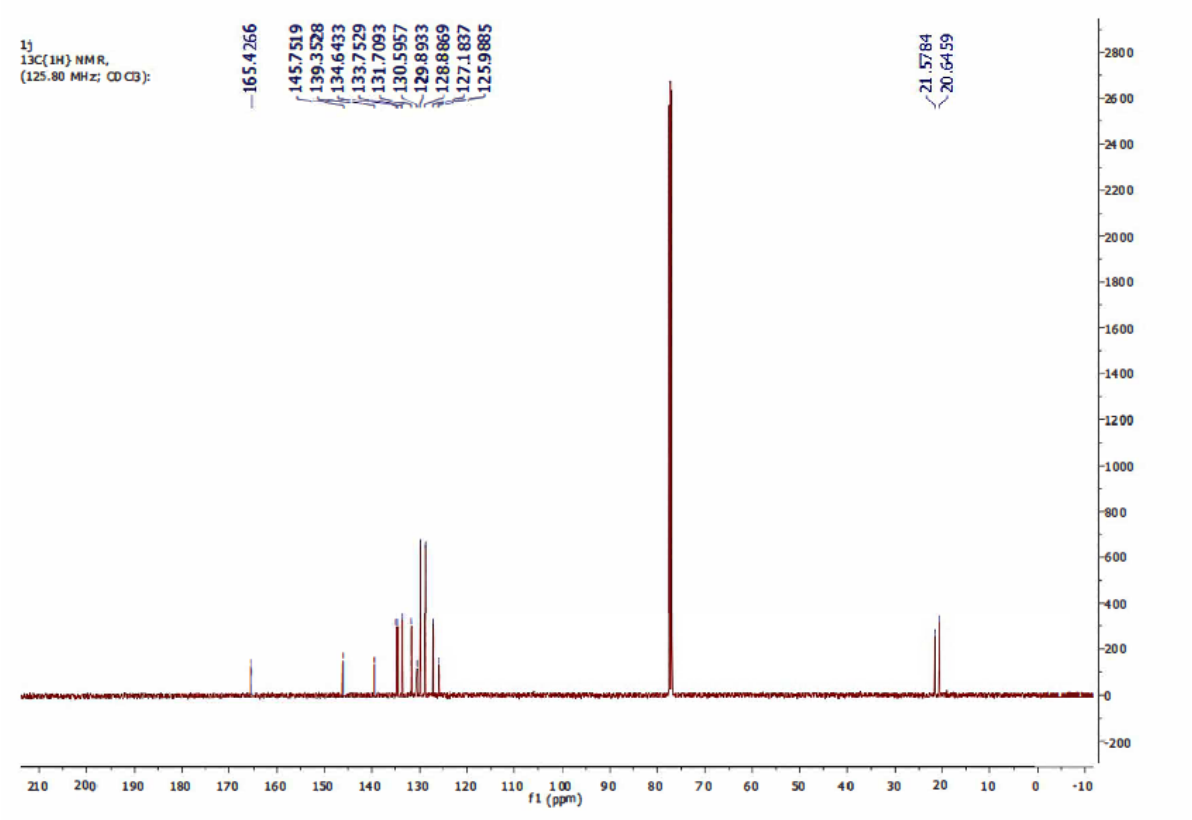
1j
13C{1H} NMR,
(125.80 MHz; CDCl3):
165.4266
145.7519
139.3528
134.6433
133.7529
131.7093
130.5957
129.8933
128.8869
127.1837
125.9885
21.5784
20.6459
f1 (ppm)

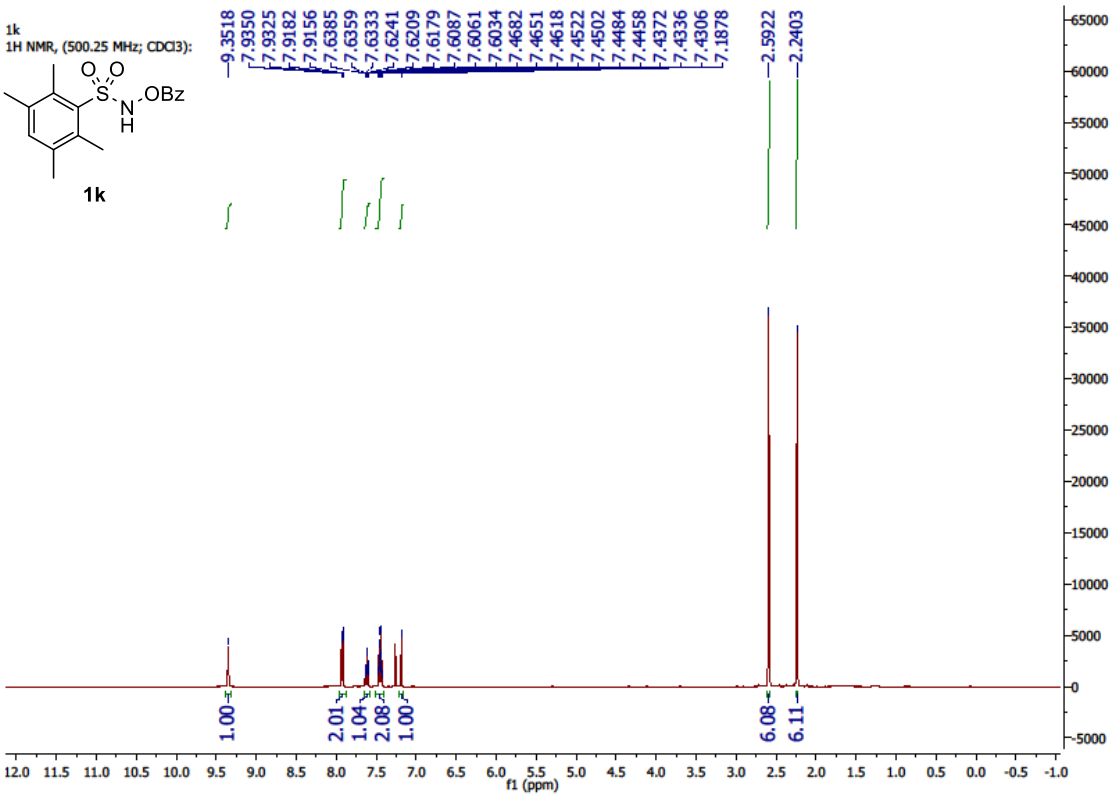
1k
1H NMR, (500.25 MHz; CDCl3):
1k
9.3518
7.9350
7.9325
7.9182
7.9156
7.6385
7.6359
7.6333
7.6241
7.6209
7.6179
7.6087
7.6061
7.6034
7.4682
7.4651
7.4618
7.4522
7.4502
7.4484
7.4458
7.4372
7.4336
7.4306
7.1878
2.5922
2.2403
1.00
2.01
1.04
2.08
1.00
6.08
6.11
f1 (ppm)

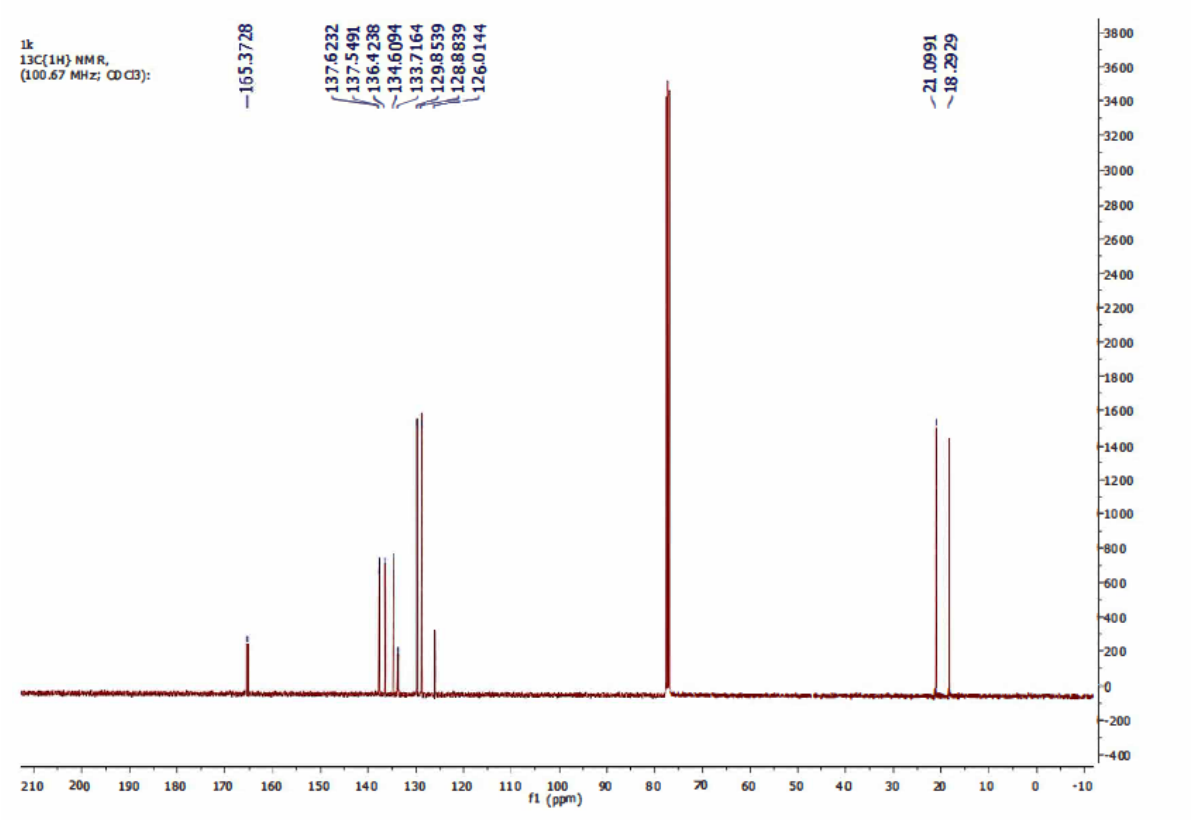
1k
13C{1H} NMR,
(100.67 MHz; CDCl3):
165.3728
137.6232
137.5491
136.4238
134.6094
133.7164
129.8539
128.8839
126.0144
21.0991
18.2929
f1 (ppm)

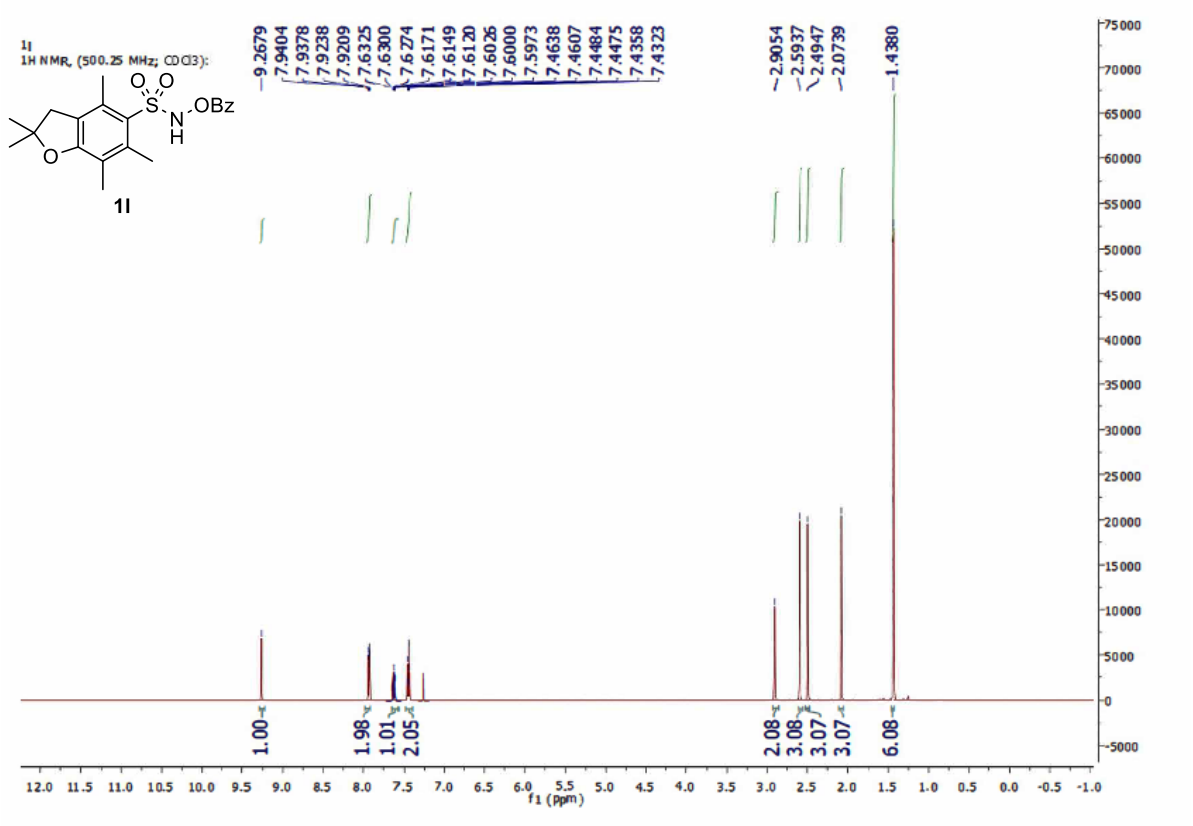
1l
1H NMR, (500.25 MHz; CDCl3):
1l
9.2679
7.9404
7.9378
7.9238
7.9209
7.6325
7.6300
7.6274
7.6171
7.6149
7.6120
7.6026
7.6000
7.5973
7.4638
7.4607
7.4484
7.4475
7.4358
7.4323
2.9054
2.5937
2.4947
2.0739
1.4380
1.00
1.98
1.01
2.05
2.08
3.08
3.07
3.07
6.08
f1 (ppm)

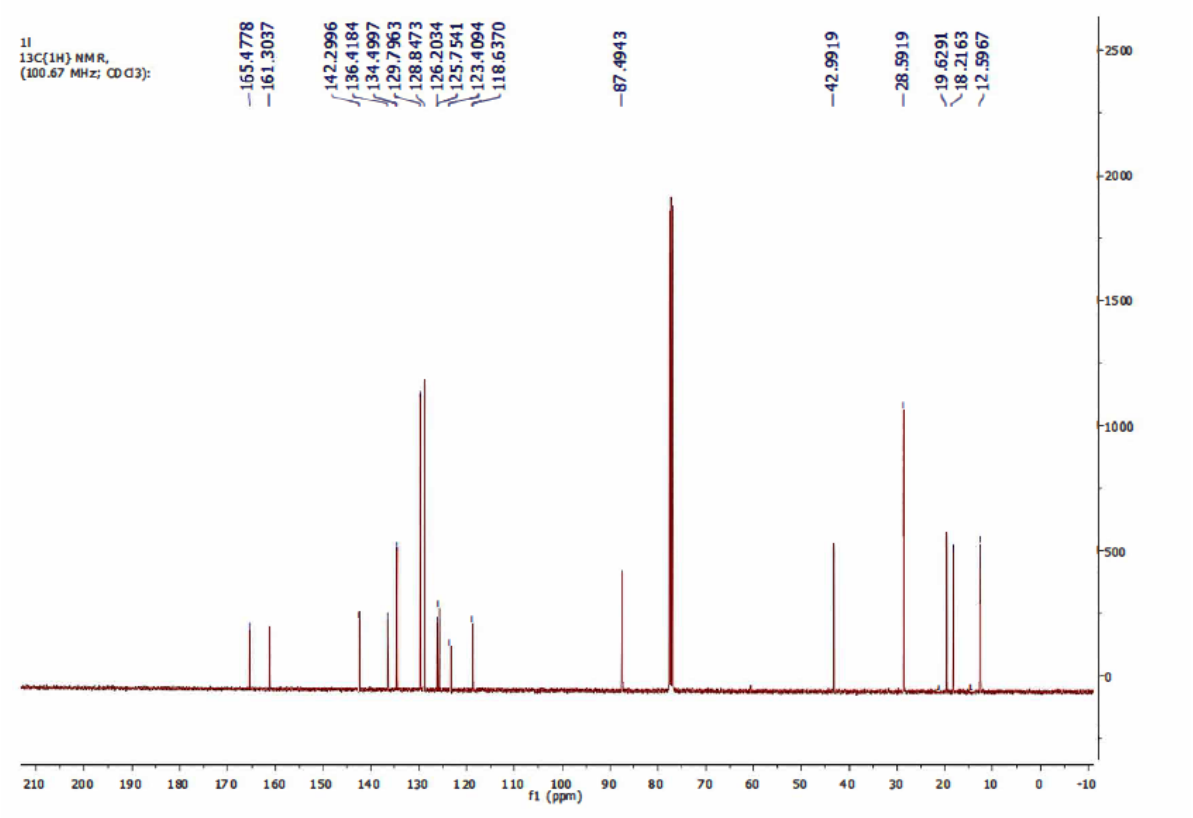
1l
13C{1H} NMR,
(100.67 MHz; CDCl3):
165.4778
161.3037
142.2996
136.4184
134.4997
129.7963
128.8473
126.2034
125.7541
123.4094
118.6370
87.4943
42.9919
28.5919
19.6291
18.2163
12.5967
f1 (ppm)

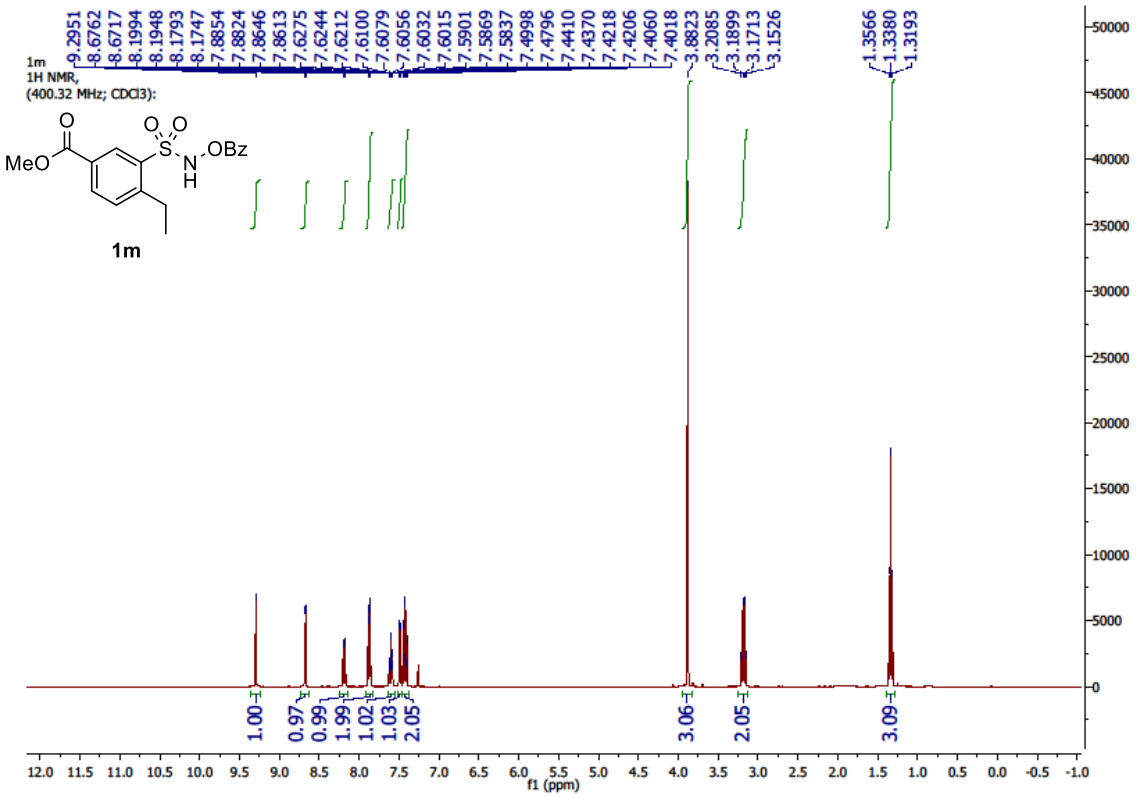
1m
1H NMR,
(400.32 MHz; CDCl3):
MeO
OBz
1m
f1 (ppm)

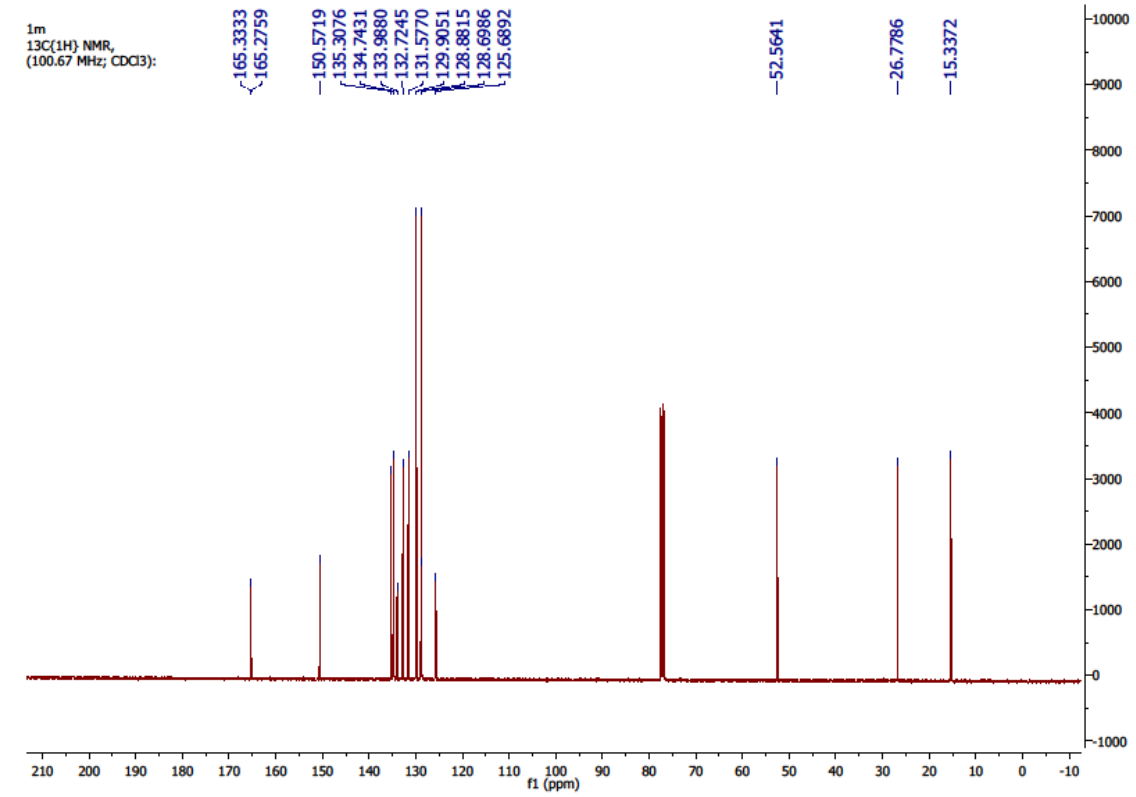
1m
13C{1H} NMR,
(100.67 MHz; CDCl3):
f1 (ppm)

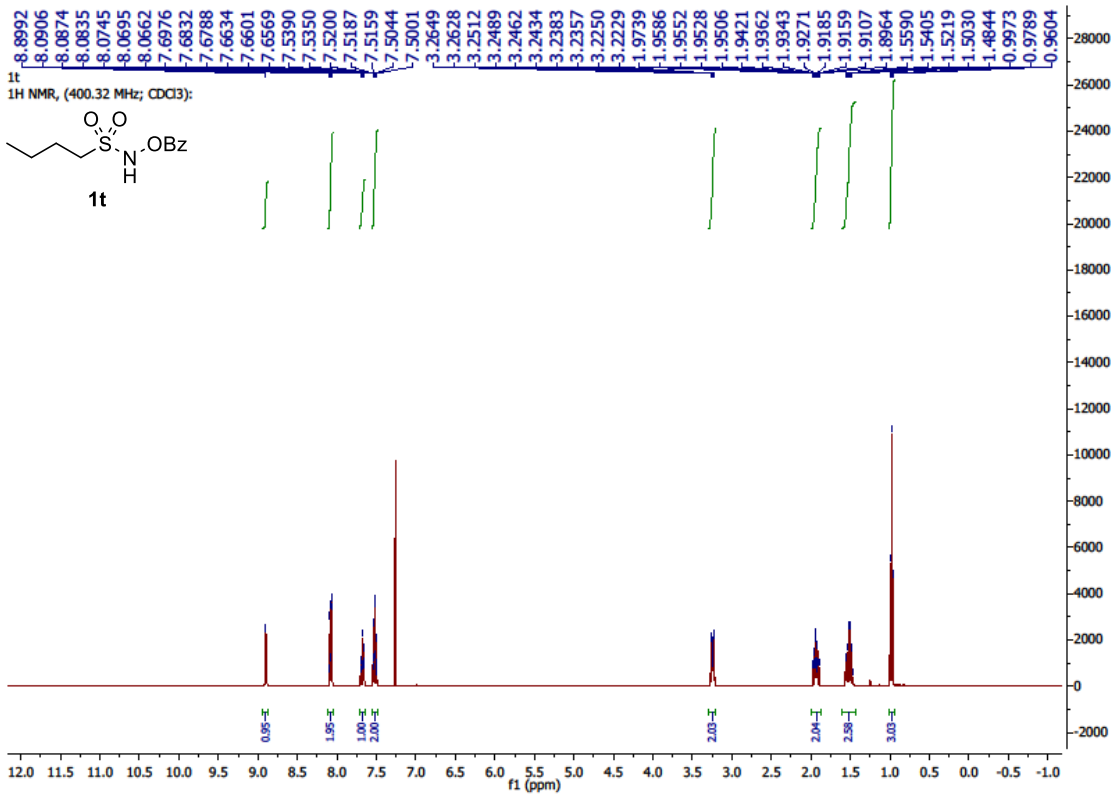
1t
1H NMR, (400.32 MHz; CDCl3):
OBz
1t
f1 (ppm)

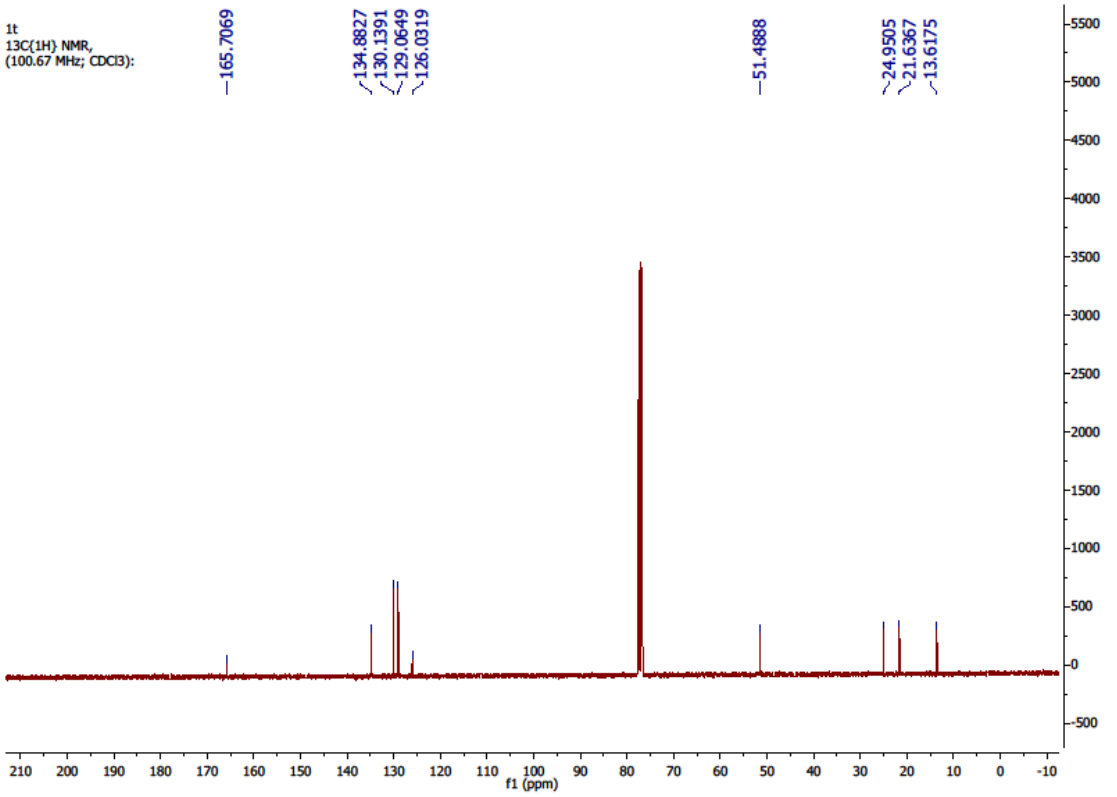
1t
13C{1H} NMR,
(100.67 MHz; CDCl3):
165.7069
134.8827
130.1391
129.0649
126.0319
51.4888
24.9505
21.6367
13.6175
f1 (ppm)

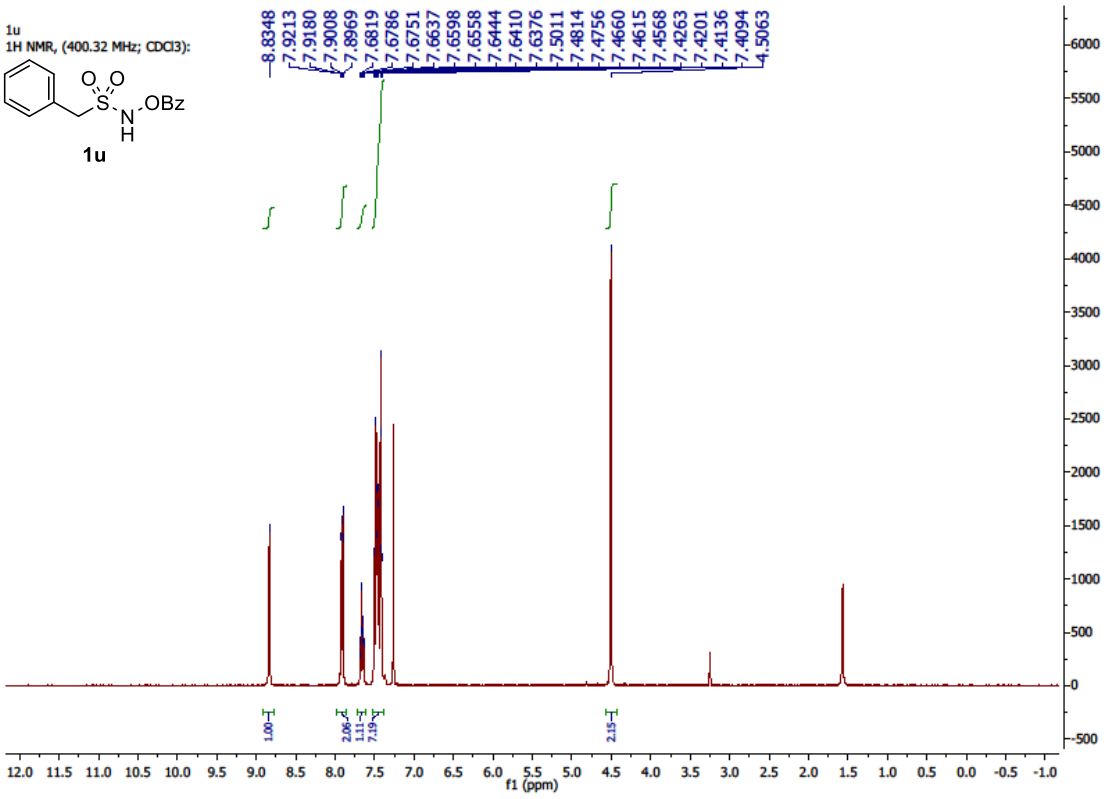
1u
1H NMR, (400.32 MHz; CDCl3):
1u
8.8348
7.9213
7.9180
7.9008
7.8969
7.6819
7.6786
7.6751
7.6637
7.6598
7.6558
7.6444
7.6410
7.6376
7.5011
7.4814
7.4756
7.4660
7.4615
7.4568
7.4263
7.4201
7.4136
7.4094
4.5063
1.00
2.06
1.11
7.19
2.15
f1 (ppm)

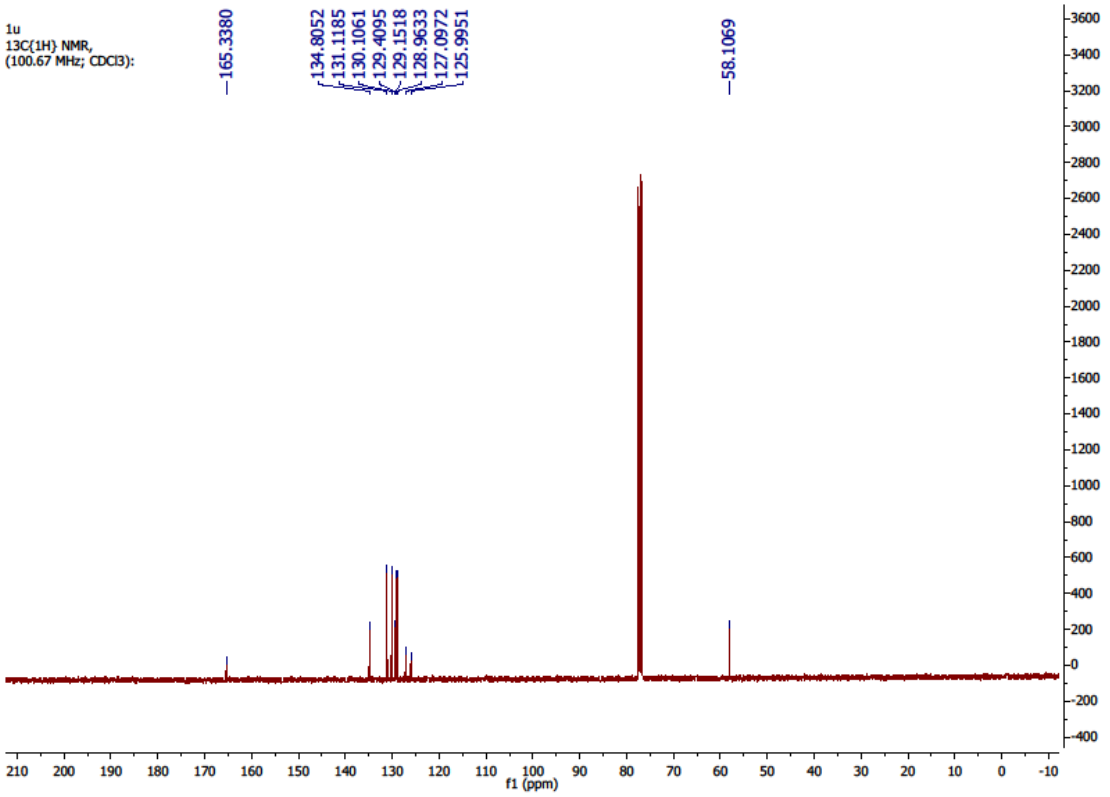
1u
13C{1H} NMR,
(100.67 MHz; CDCl3):
165.3380
134.8052
131.1185
130.1061
129.4095
129.1518
128.9633
127.0972
125.9951
58.1069
f1 (ppm)

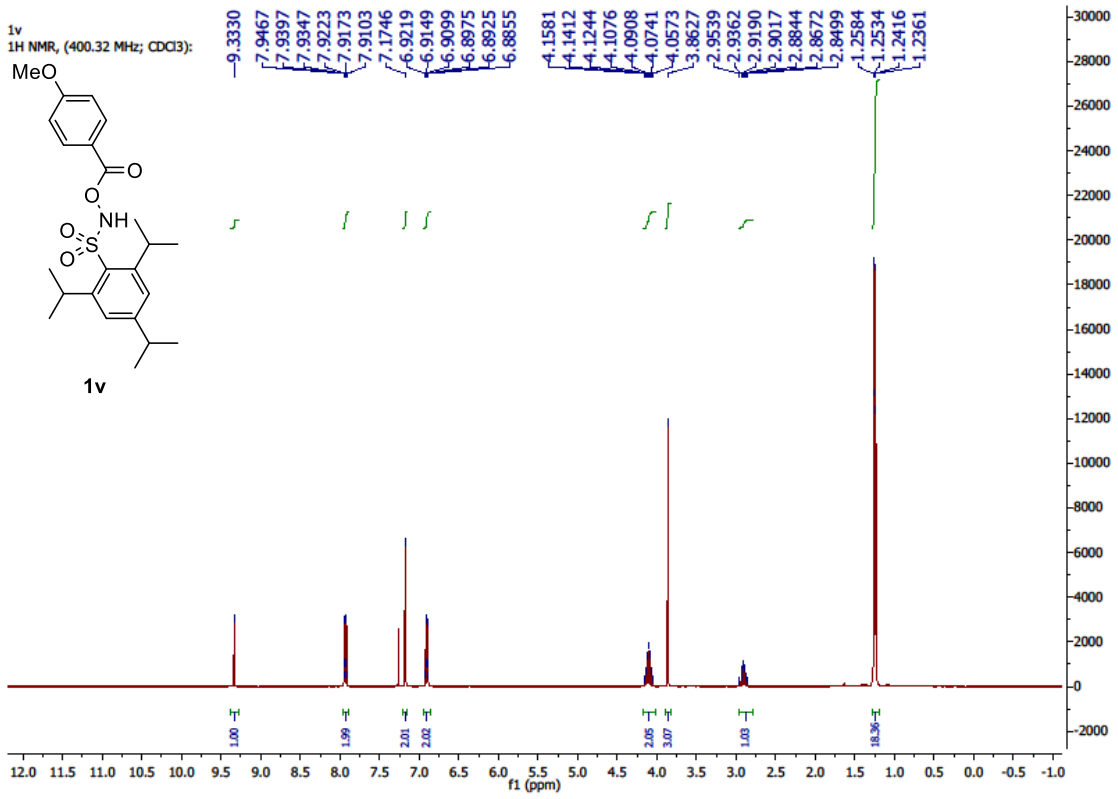
1v
1H NMR, (400.32 MHz; CDCl3):
MeO
O
O
NH
O
S
O
1v
9.3330
7.9467
7.9397
7.9347
7.9223
7.9173
7.9103
7.1746
6.9219
6.9149
6.9099
6.8975
6.8925
6.8855
4.1581
4.1412
4.1244
4.1076
4.0908
4.0741
4.0573
3.8627
2.9539
2.9362
2.9190
2.9017
2.8844
2.8672
2.8499
1.2584
1.2534
1.2416
1.2361
1.00
1.99
2.01
2.02
2.05
3.07
1.03
18.36
f1 (ppm)

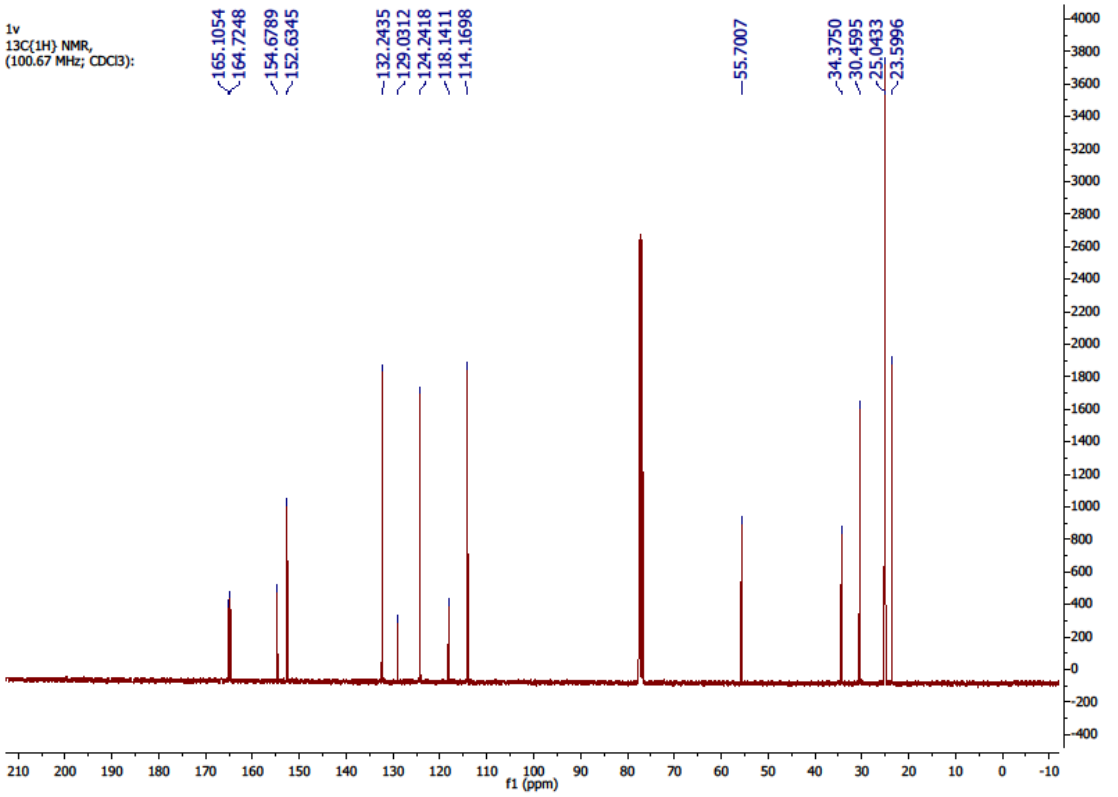
1v
13C{1H} NMR,
(100.67 MHz; CDCl3):
165.1054
164.7248
154.6789
152.6345
132.2435
129.0312
124.2418
118.1411
114.1698
55.7007
34.3750
30.4595
25.0433
23.5996
f1 (ppm)

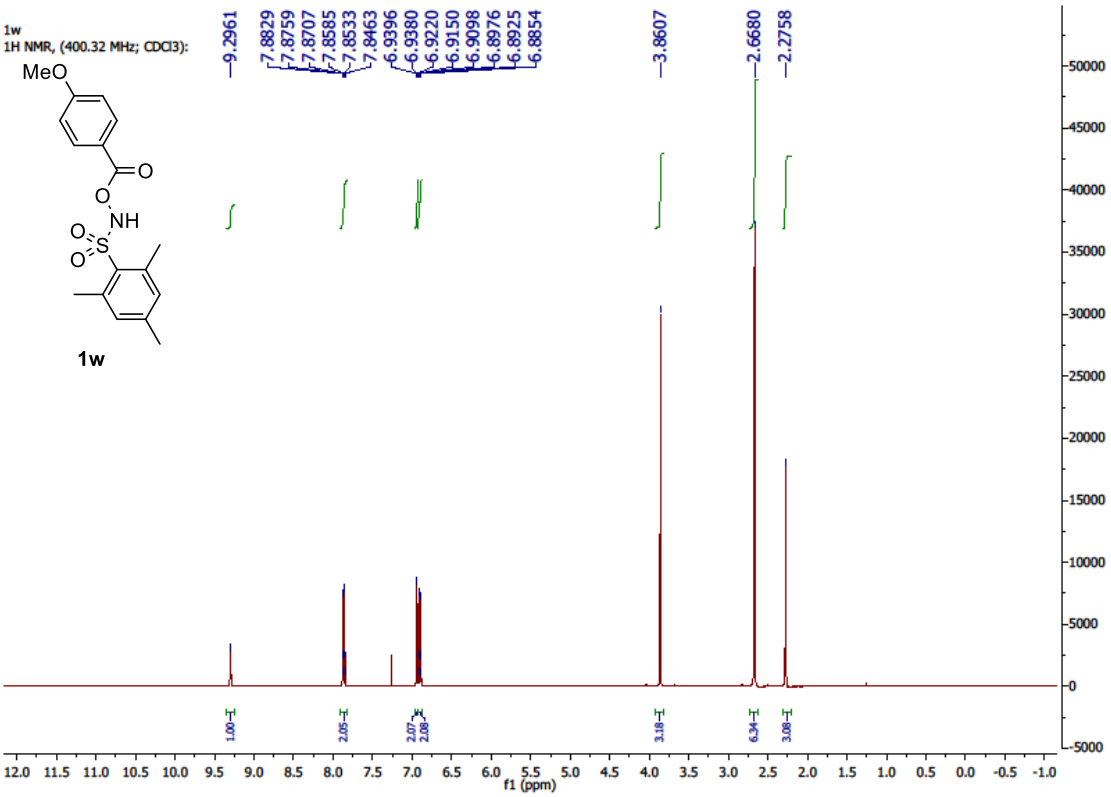
1w
1H NMR, (400.32 MHz; CDCl3):
MeO
O
O
NH
O
S
O
1w
9.2961
7.8829
7.8759
7.8707
7.8585
7.8533
7.8463
6.9396
6.9380
6.9220
6.9150
6.9098
6.8976
6.8925
6.8854
3.8607
2.6680
2.2758
1.00
2.05
2.07
2.08
3.18
6.34
3.08
f1 (ppm)

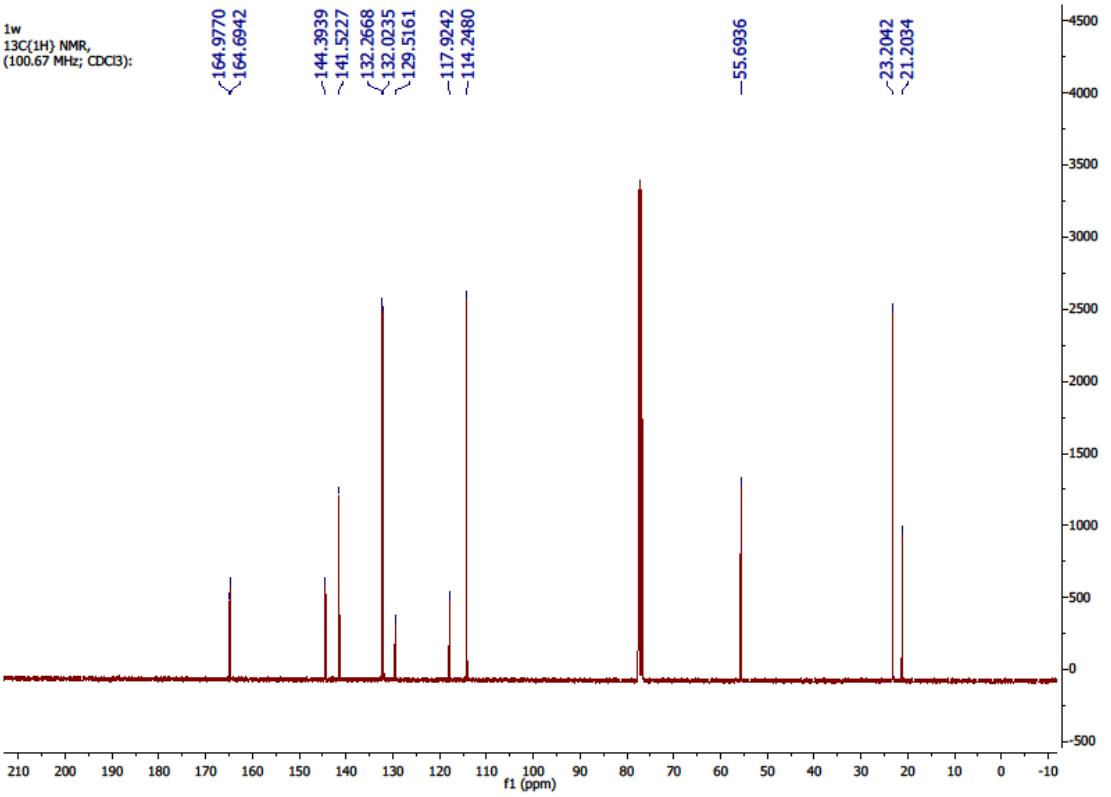
1w
13C{1H} NMR,
(100.67 MHz; CDCl3):
164.9770
164.6942
144.3939
141.5227
132.2668
132.0235
129.5161
117.9242
114.2480
55.6936
23.2042
21.2034
f1 (ppm)

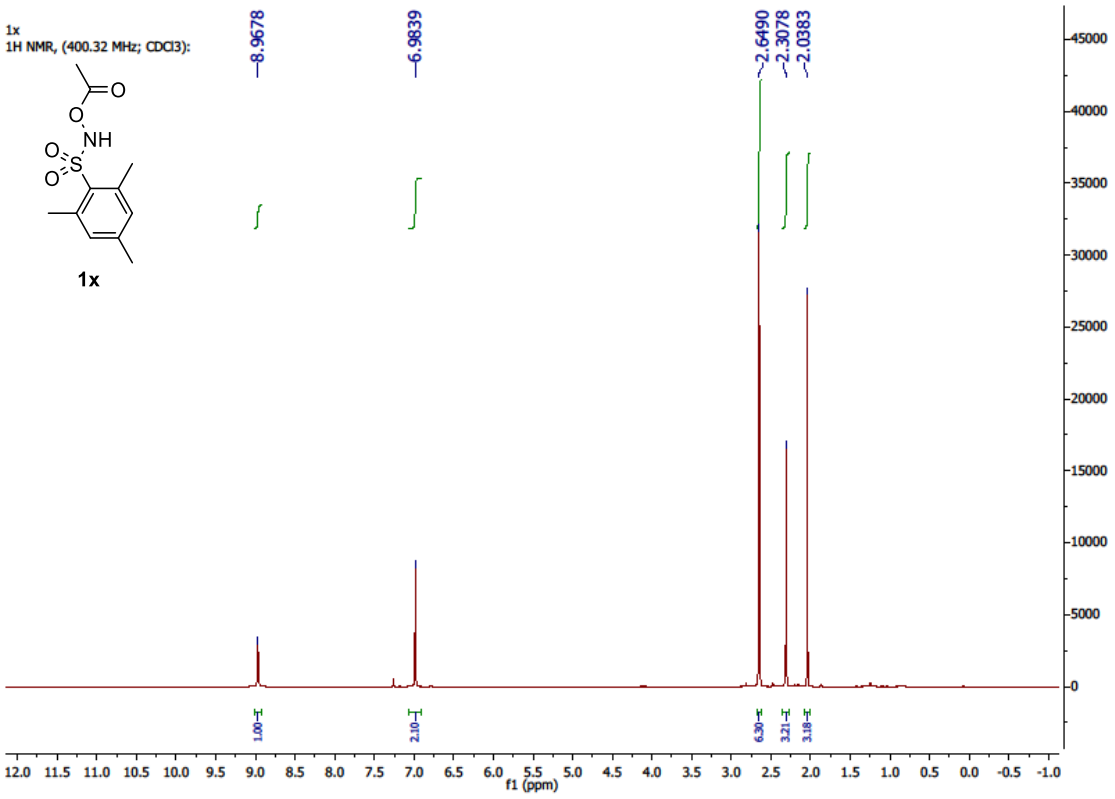
1x
1H NMR, (400.32 MHz; CDCl3):
1x
8.9678
6.9839
2.6490
2.3078
2.0383
1.00
2.10
6.30
3.21
3.18
f1 (ppm)

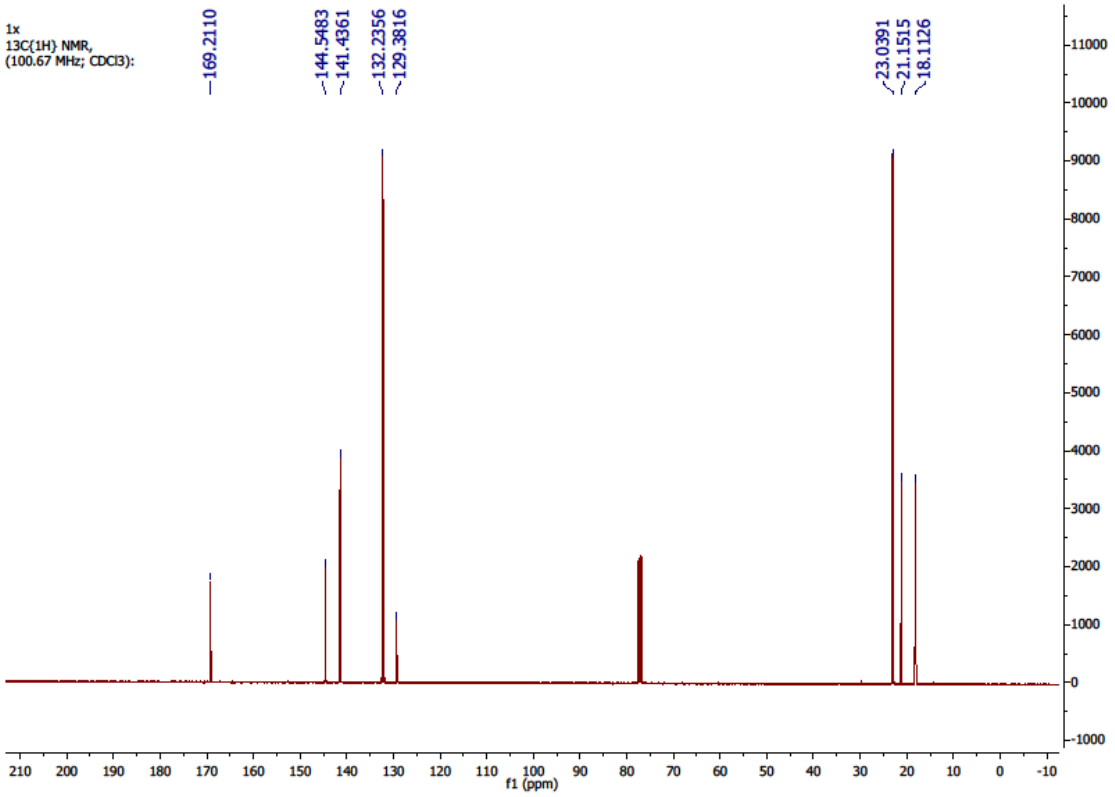
1x
13C{1H} NMR,
(100.67 MHz; CDCl3):
169.2110
144.5483
141.4361
132.2356
129.3816
23.0391
21.1515
18.1126
f1 (ppm)

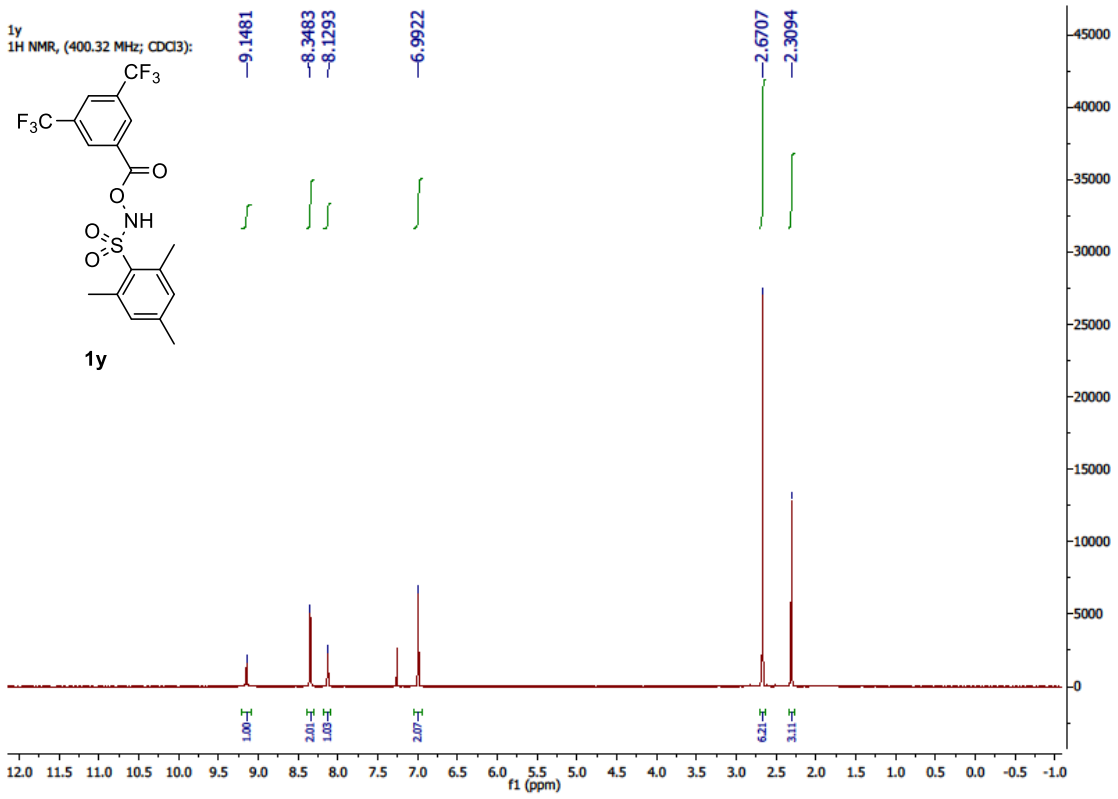
1y
1H NMR, (400.32 MHz; CDCl3):
9.1481
8.3483
8.1293
6.9922
2.6707
2.3094
1.00
2.01
1.03
2.07
6.21
3.11
f1 (ppm)

1y

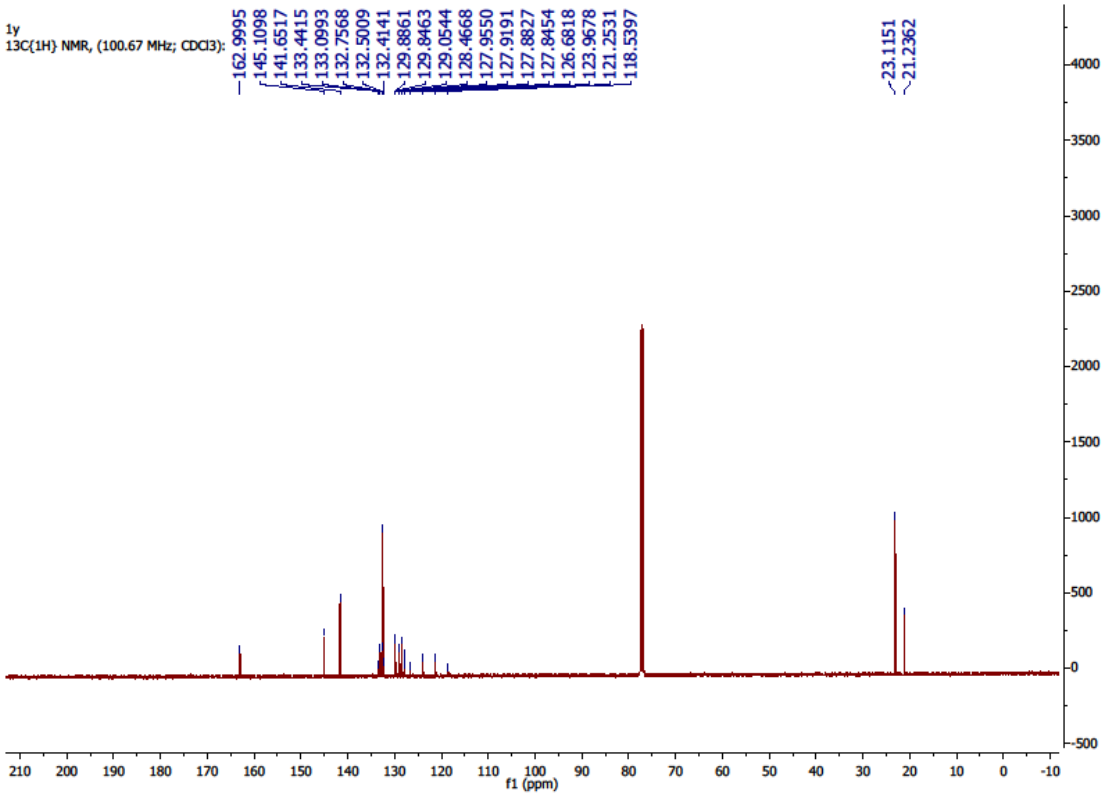
1y
13C{1H} NMR, (100.67 MHz; CDCl3):
162.9995
145.1098
141.6517
133.4415
133.0093
132.7568
132.5009
132.4141
129.8861
129.8463
129.0544
128.4668
127.9550
127.9191
127.8827
127.8454
126.6818
123.9678
121.2531
118.5397
23.1151
21.2362
f1 (ppm)

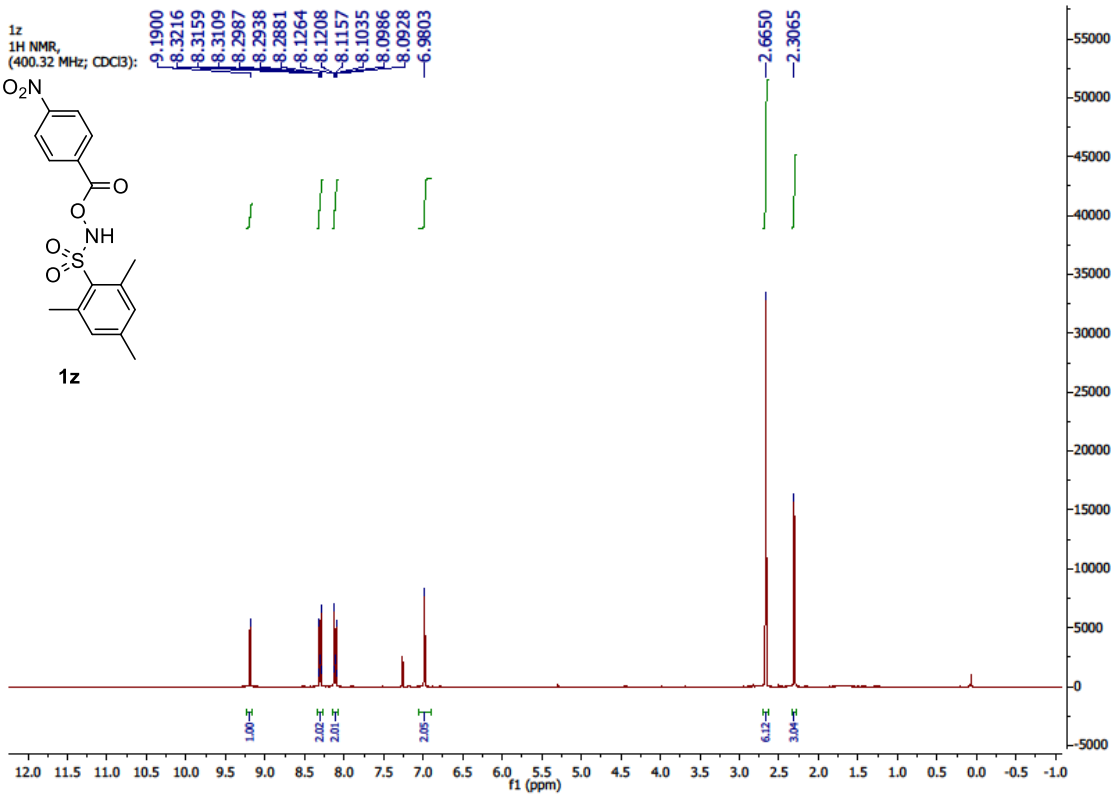
1z
1H NMR,
(400.32 MHz; CDCl3):
9.1900
8.3216
8.3159
8.3109
8.2987
8.2938
8.2881
8.1264
8.1208
8.1157
8.1035
8.0986
8.0928
6.9803
2.6650
2.3065
1z
f1 (ppm)

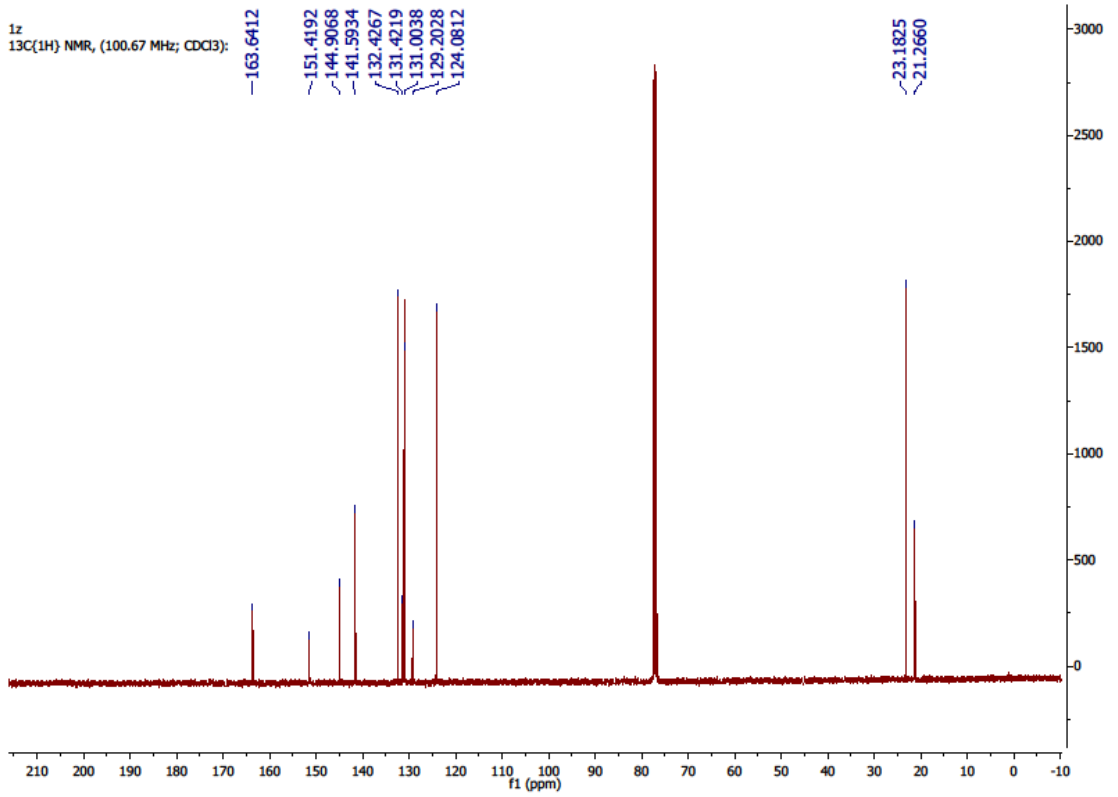
1z
13C{1H} NMR, (100.67 MHz; CDCl3):
163.6412
151.4192
144.9068
141.5934
132.4267
131.4219
131.0038
129.2028
124.0812
23.1825
21.2660
f1 (ppm)

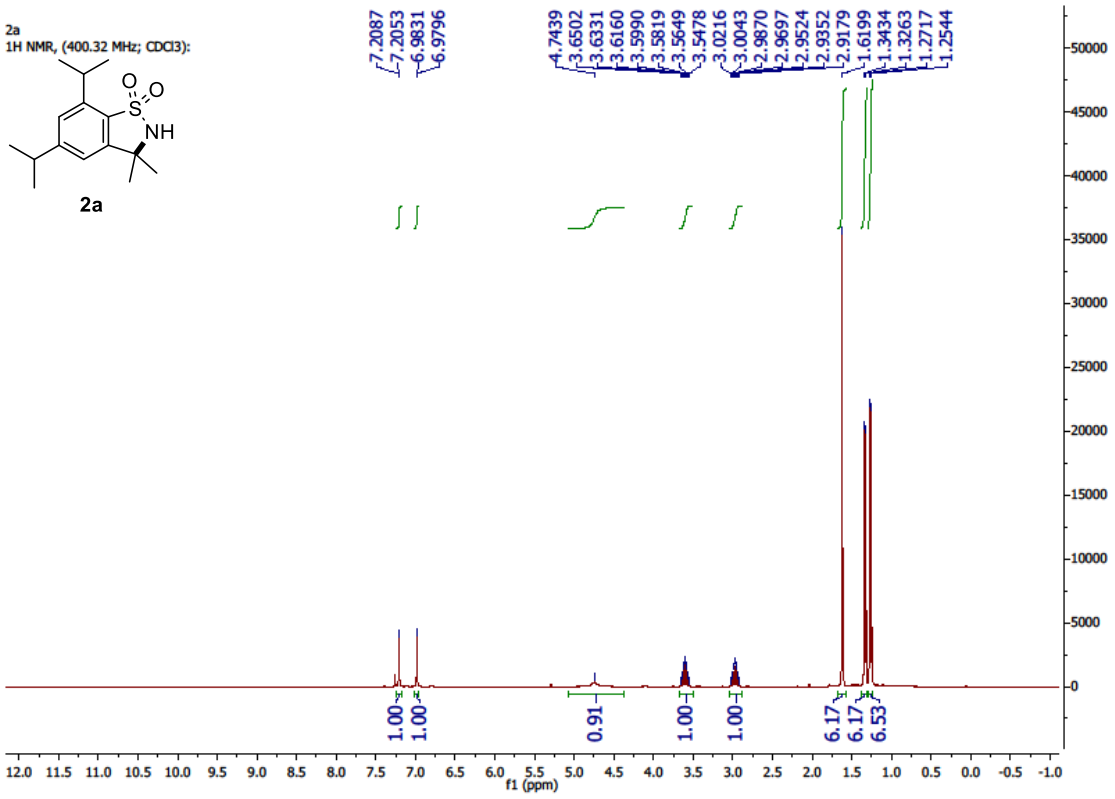
2a
1H NMR, (400.32 MHz; CDCl3):
2a
7.2087
7.2053
6.9831
6.9796
4.7439
3.6502
3.6331
3.6160
3.5990
3.5819
3.5649
3.5478
3.0216
3.0043
2.9870
2.9697
2.9524
2.9352
2.9179
1.6199
1.3434
1.3263
1.2717
1.2544
1.00
1.00
0.91
1.00
1.00
6.17
6.17
6.53
f1 (ppm)

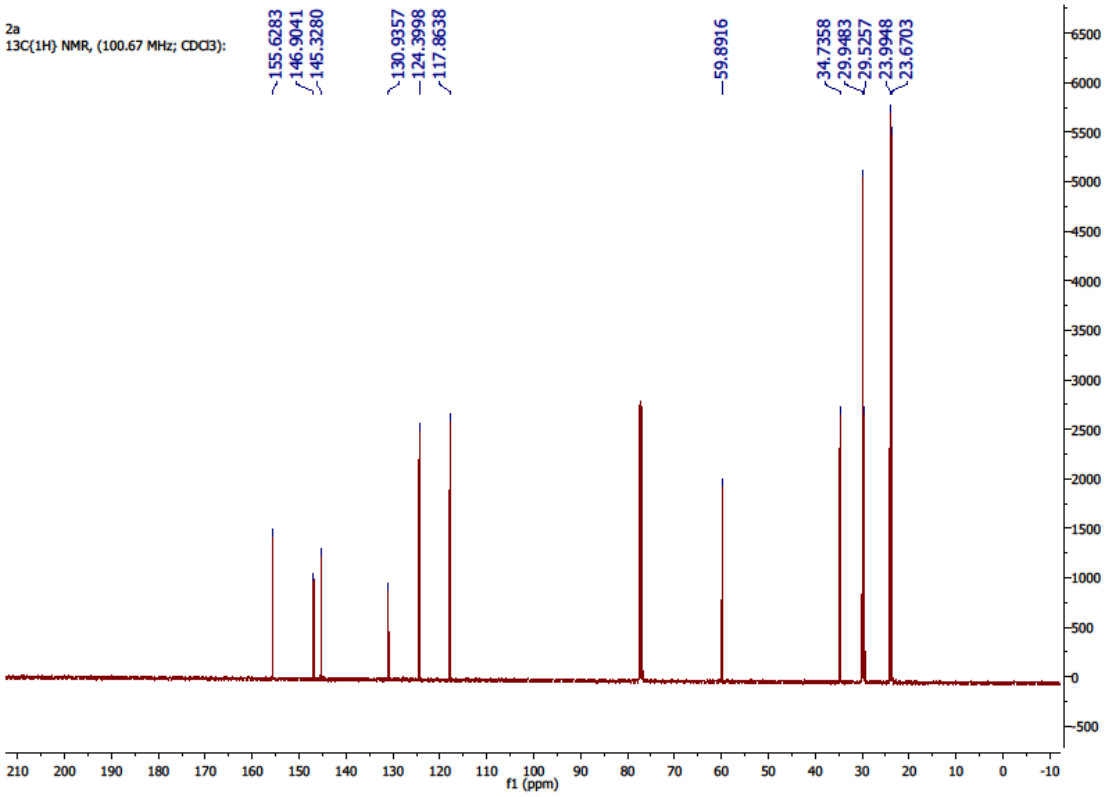
2a
13C{1H} NMR, (100.67 MHz; CDCl3):
155.6283
146.9041
145.3280
130.9357
124.3998
117.8638
59.8916
34.7358
29.9483
29.5257
23.9948
23.6703
f1 (ppm)

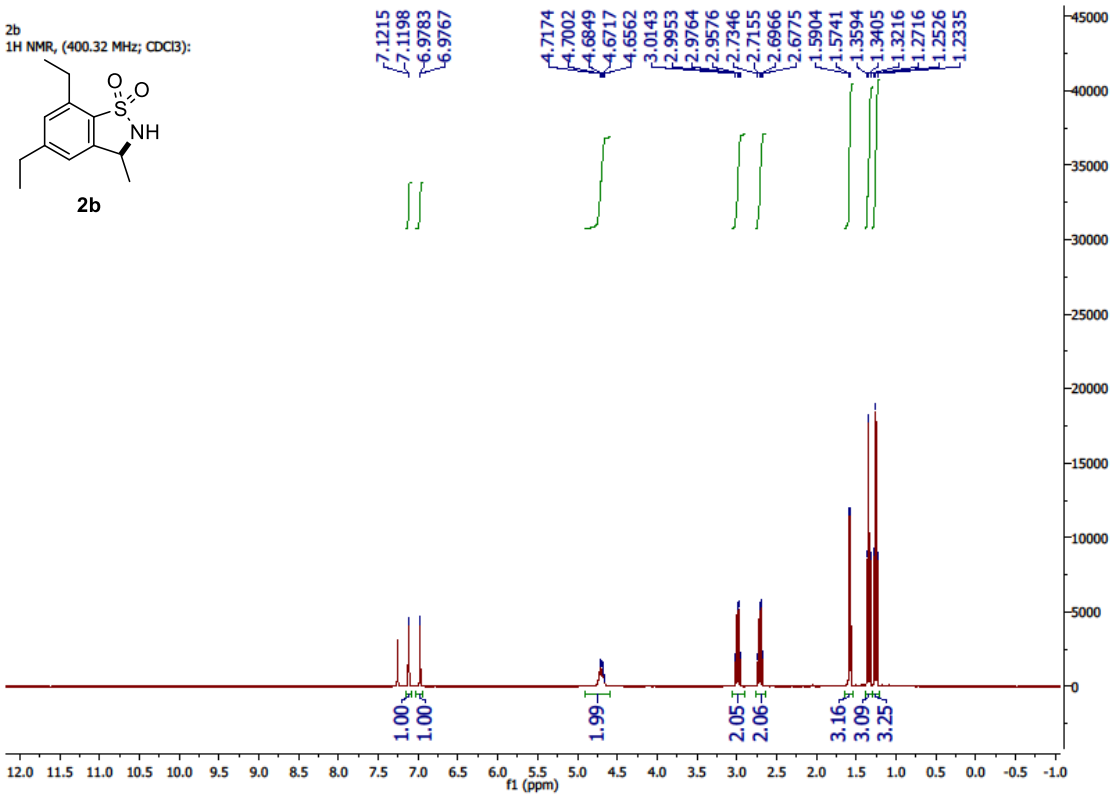
2b
1H NMR, (400.32 MHz; CDCl3):
2b
7.1215
7.1198
6.9783
6.9767
4.7174
4.7002
4.6849
4.6717
4.6562
3.0143
2.9953
2.9764
2.9576
2.7346
2.7155
2.6966
2.6775
1.5904
1.5741
1.3594
1.3405
1.3216
1.2716
1.2526
1.2335
1.00
1.00
1.99
2.05
2.06
3.16
3.09
3.25
f1 (ppm)

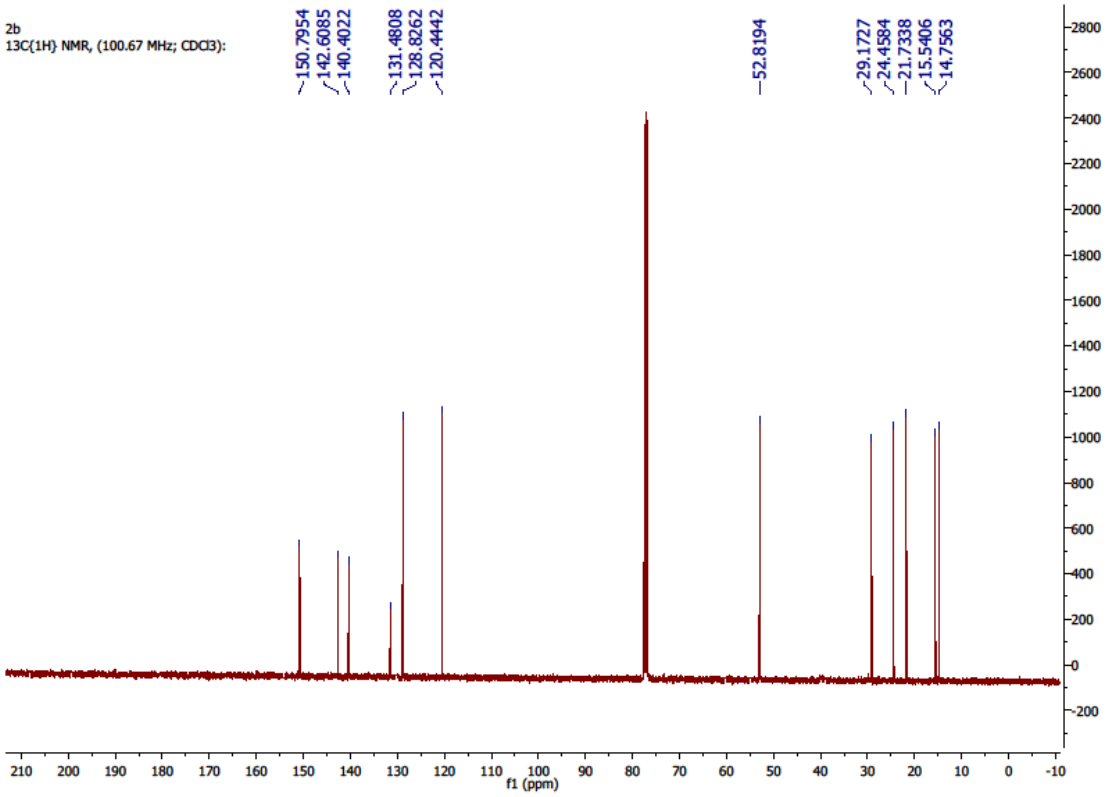
2b
13C{1H} NMR, (100.67 MHz; CDCl3):
150.7954
142.6085
140.4022
131.4808
128.8262
120.4442
52.8194
29.1727
24.4584
21.7338
15.5406
14.7563
f1 (ppm)

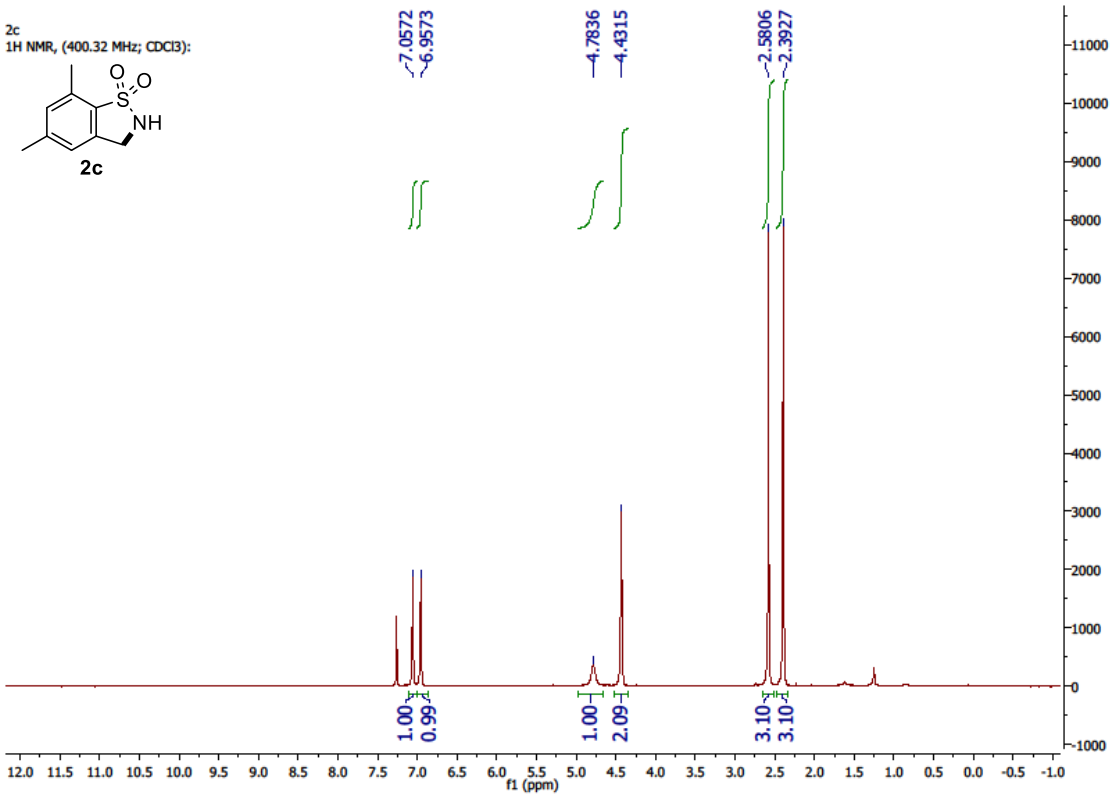
2c
1H NMR, (400.32 MHz; CDCl3):
2c
7.0572
6.9573
4.7836
4.4315
2.5806
2.3927
1.00
0.99
1.00
2.09
3.10
3.10
f1 (ppm)

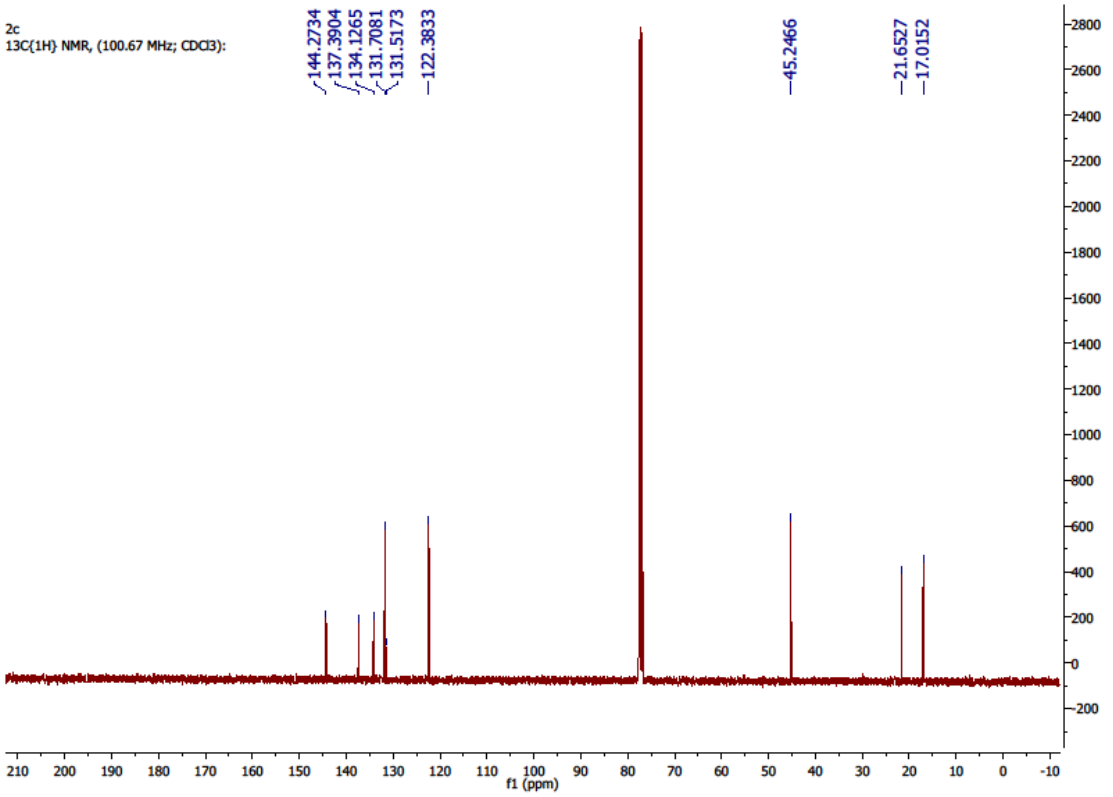
2c
13C{1H} NMR, (100.67 MHz; CDCl3):
144.2734
137.3904
134.1265
131.7081
131.5173
122.3833
45.2466
21.6527
17.0152
f1 (ppm)

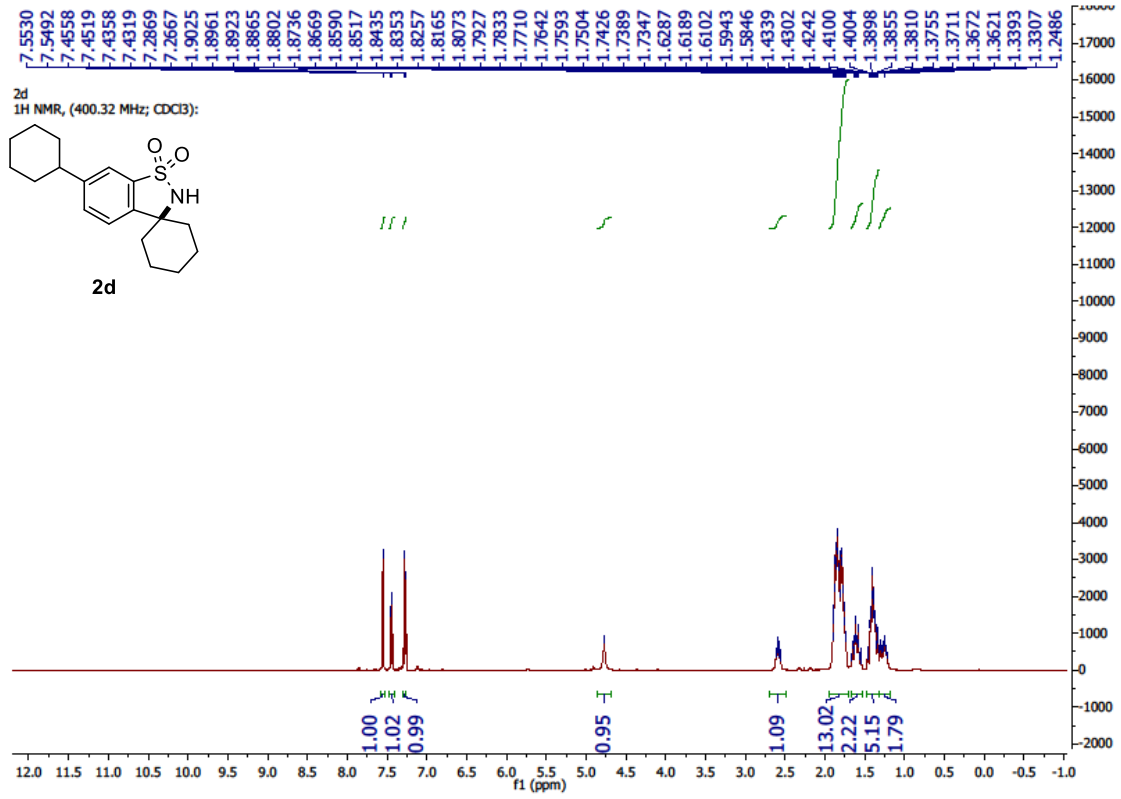
2d
1H NMR, (400.32 MHz; CDCl3):
2d
f1 (ppm)

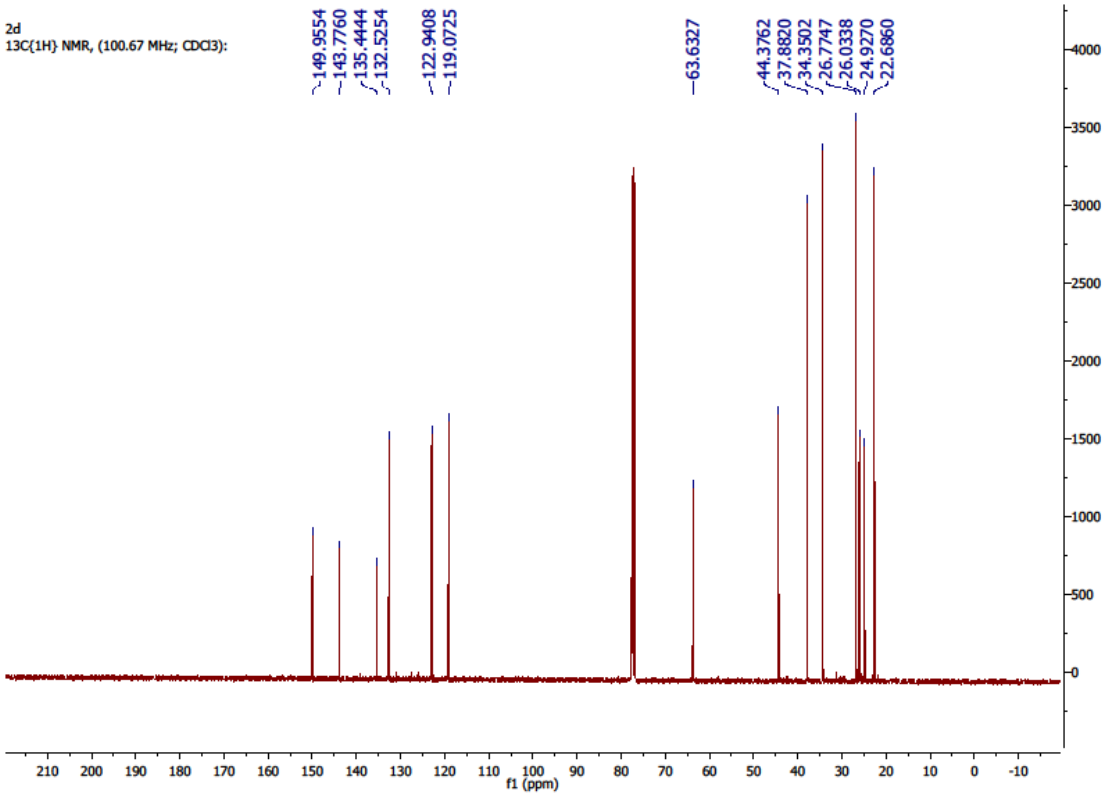
2d
13C{1H} NMR, (100.67 MHz; CDCl3):
f1 (ppm)

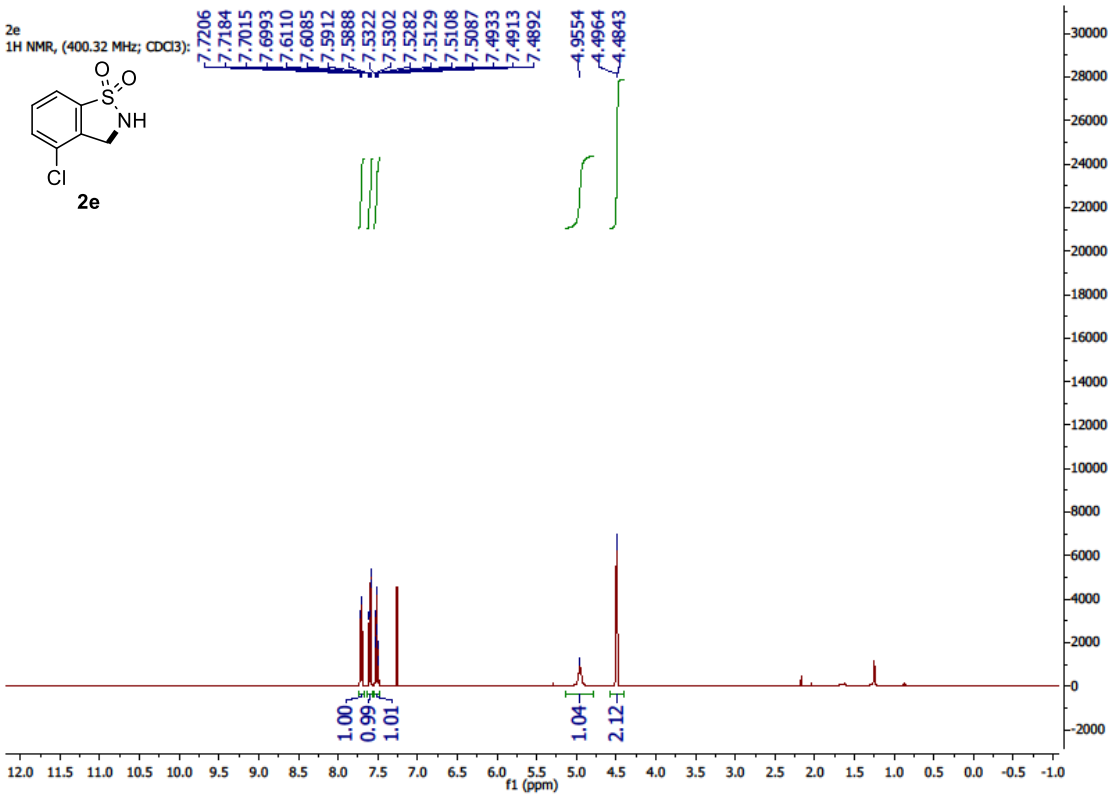
2e
1H NMR, (400.32 MHz; CDCl3):
7.7206
7.7184
7.7015
7.6993
7.6110
7.6085
7.5912
7.5888
7.5322
7.5302
7.5282
7.5129
7.5108
7.5087
7.4933
7.4913
7.4892
4.9554
4.4964
4.4843
O
O
S
NH
Cl
2e
1.00
0.99
1.01
1.04
2.12
f1 (ppm)

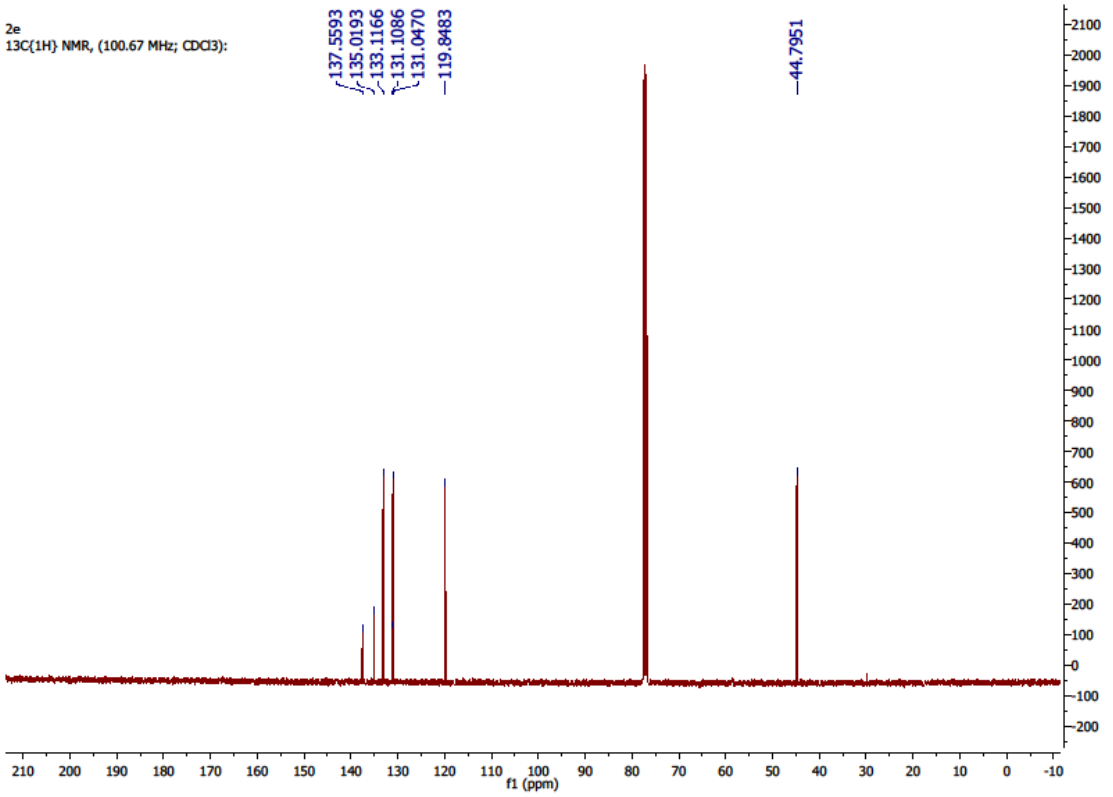
2e
13C{1H} NMR, (100.67 MHz; CDCl3):
137.5593
135.0193
133.1166
131.1086
131.0470
119.8483
44.7951
f1 (ppm)

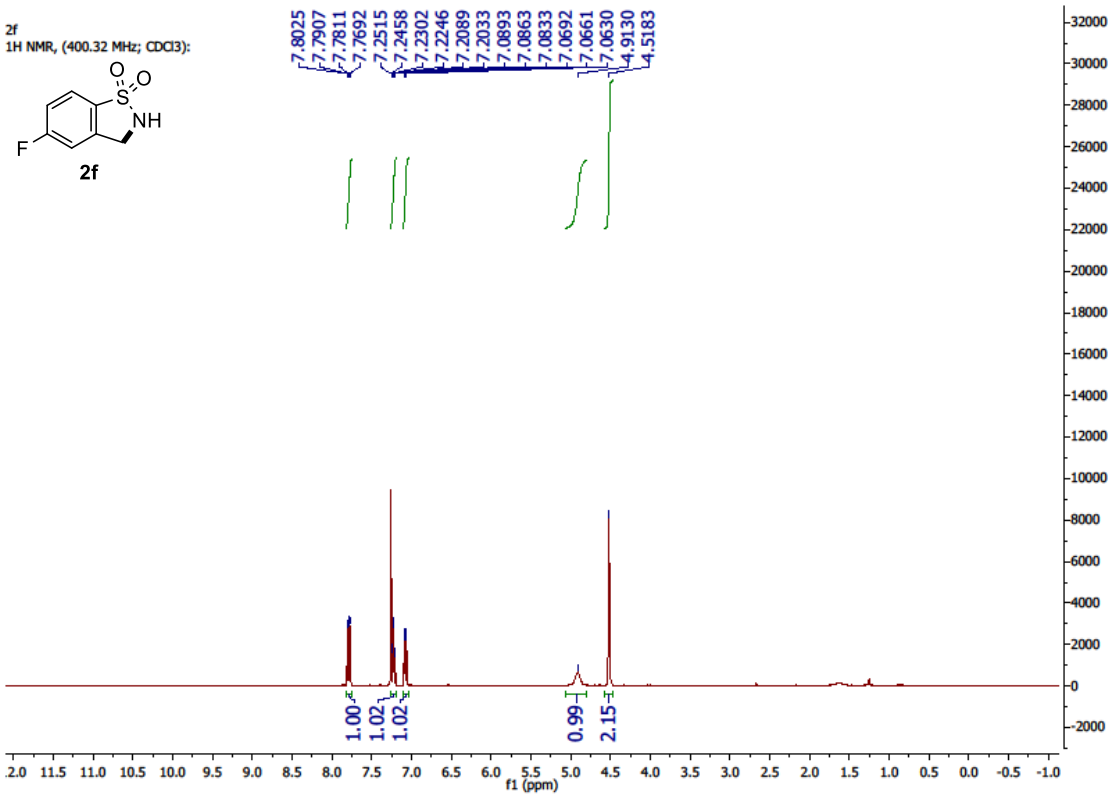
2f
1H NMR, (400.32 MHz; CDCl3):
2f
7.8025
7.7907
7.7811
7.7692
7.2515
7.2458
7.2302
7.2246
7.2089
7.2033
7.0893
7.0863
7.0833
7.0692
7.0661
7.0630
4.9130
4.5183
1.00
1.02
1.02
0.99
2.15
f1 (ppm)

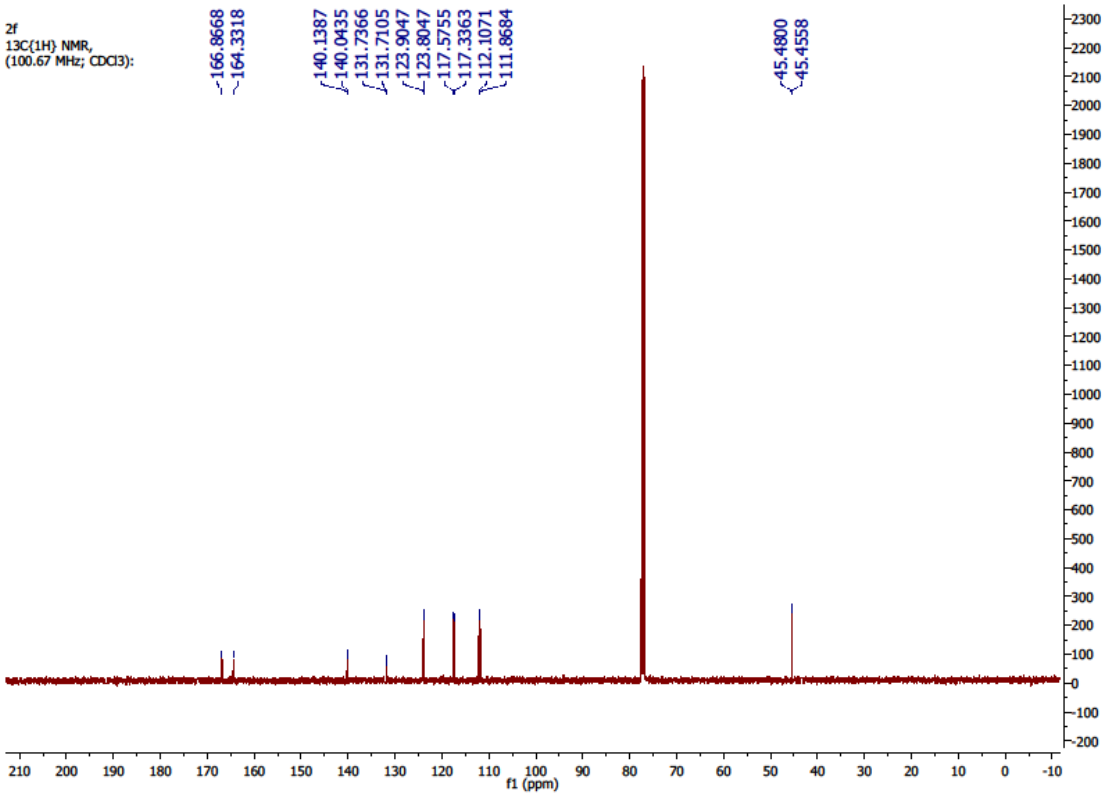
2f
13C{1H} NMR,
(100.67 MHz; CDCl3):
166.8668
164.3318
140.1387
140.0435
131.7366
131.7105
123.9047
123.8047
117.5755
117.3363
112.1071
111.8684
45.4800
45.4558
f1 (ppm)

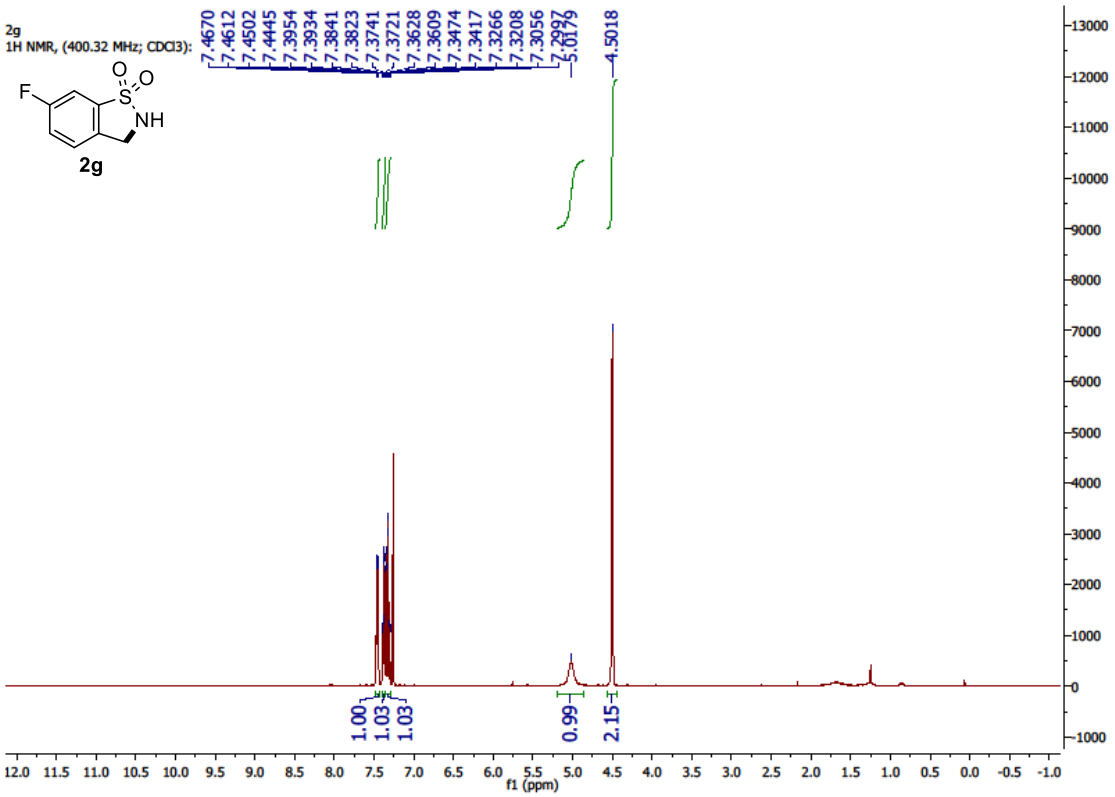
2g
1H NMR, (400.32 MHz; CDCl3):
F
O
O
S
NH
2g
7.4670
7.4612
7.4502
7.4445
7.3954
7.3934
7.3841
7.3823
7.3741
7.3721
7.3628
7.3609
7.3474
7.3417
7.3266
7.3208
7.3056
7.2997
5.0179
4.5018
1.00
1.03
1.03
0.99
2.15
f1 (ppm)

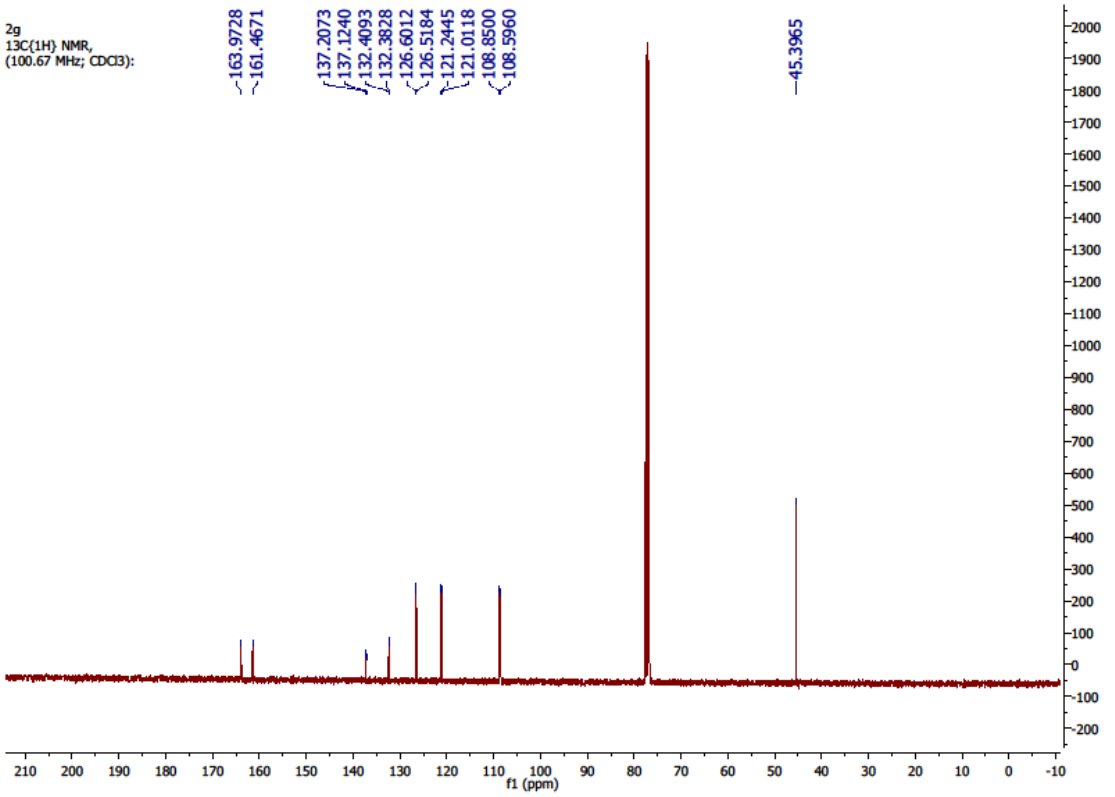
2g
13C{1H} NMR,
(100.67 MHz; CDCl3):
163.9728
161.4671
137.2073
137.1240
132.4093
132.3828
126.6012
126.5184
121.2445
121.0118
108.8500
108.5960
45.3965
f1 (ppm)

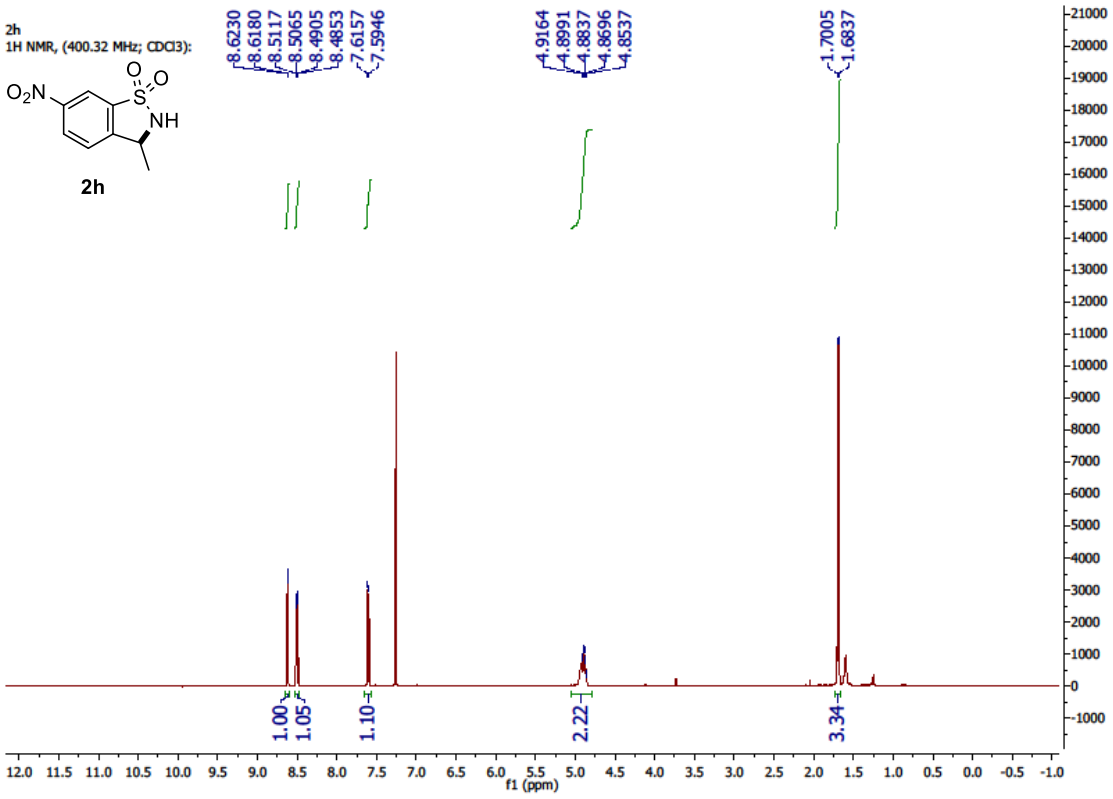
2h
1H NMR, (400.32 MHz; CDCl3):
2h
8.6230
8.6180
8.5117
8.5065
8.4905
8.4853
7.6157
7.5946
4.9164
4.8991
4.8837
4.8696
4.8537
1.7005
1.6837
1.00
1.05
1.10
2.22
3.34
f1 (ppm)

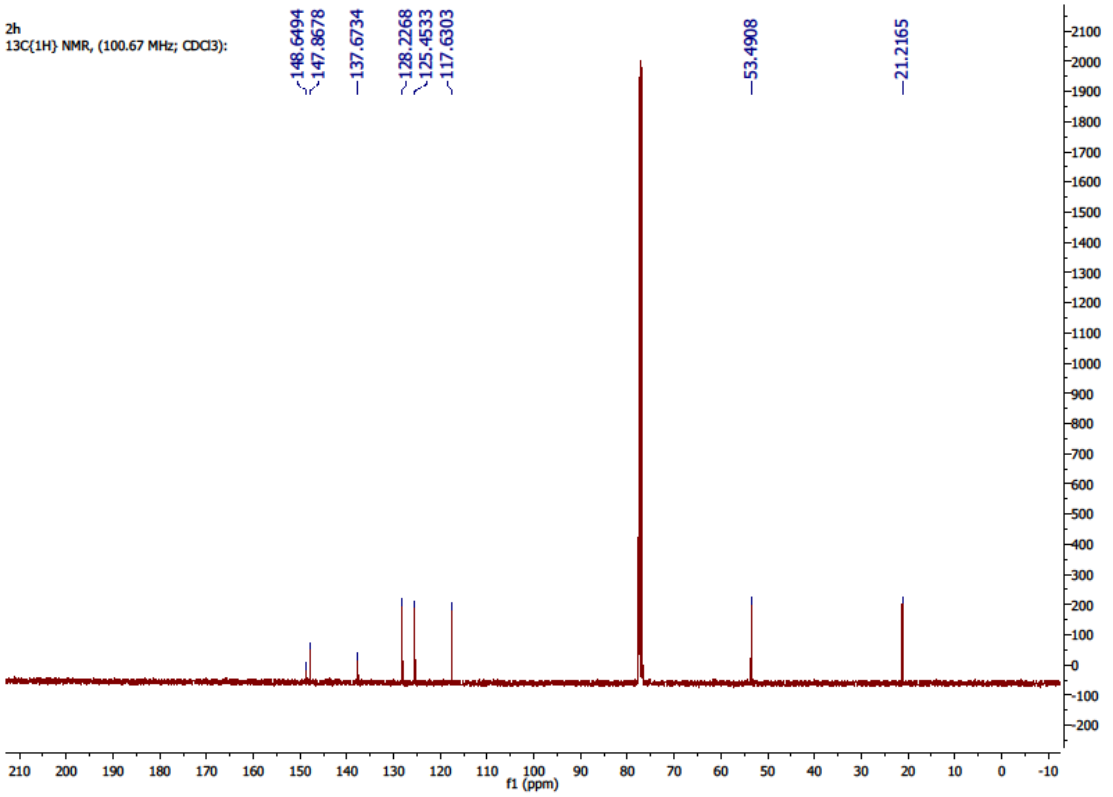
2h
13C{1H} NMR, (100.67 MHz; CDCl3):
148.6494
147.8678
137.6734
128.2268
125.4533
117.6303
53.4908
21.2165
f1 (ppm)

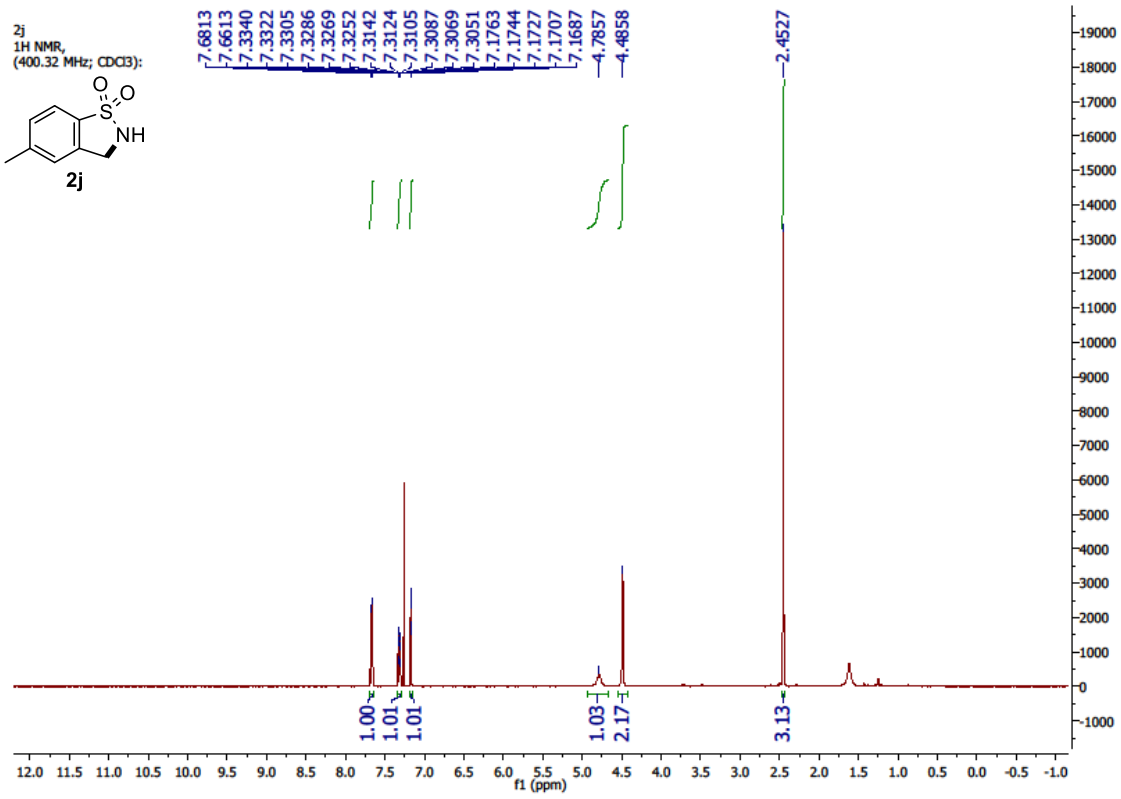
2j
1H NMR,
(400.32 MHz; CDCl3):
2j
7.6813
7.6613
7.3340
7.3322
7.3305
7.3286
7.3269
7.3252
7.3142
7.3124
7.3105
7.3087
7.3069
7.3051
7.1763
7.1744
7.1727
7.1707
7.1687
4.7857
4.4858
2.4527
1.00
1.01
1.01
1.03
2.17
3.13
f1 (ppm)

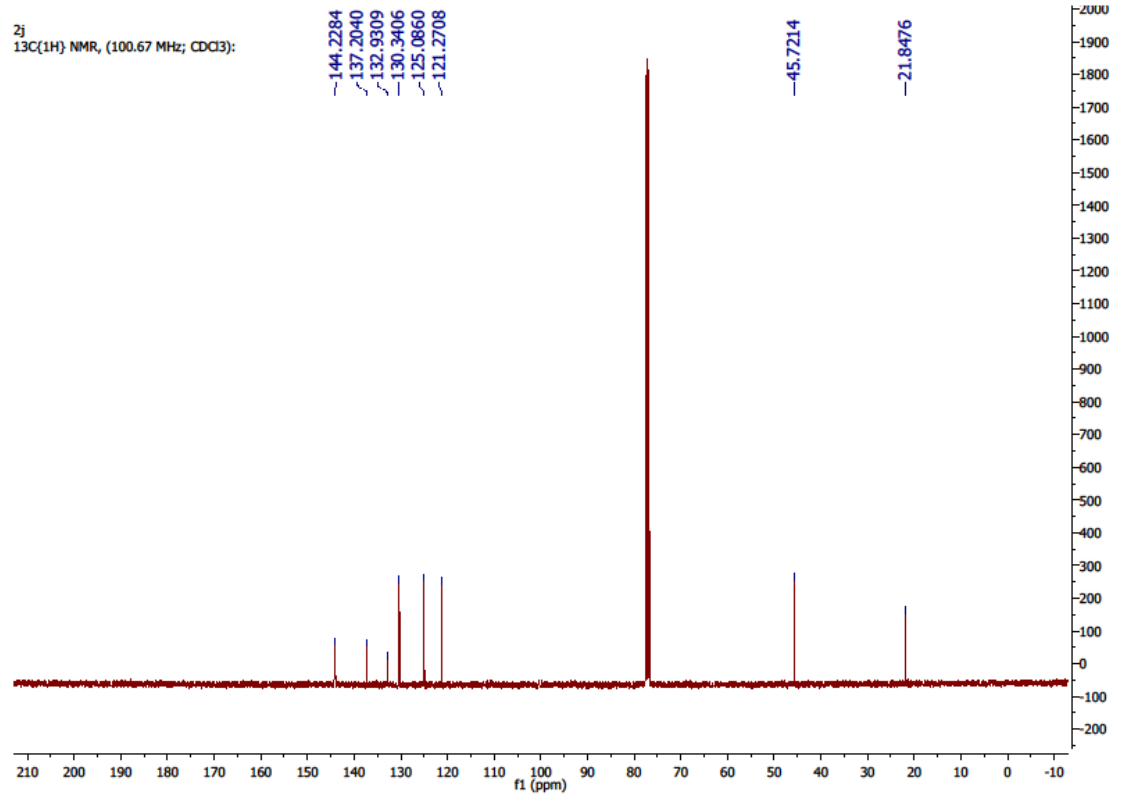
2j
13C{1H} NMR, (100.67 MHz; CDCl3):
144.2284
137.2040
132.9309
130.3406
125.0860
121.2708
45.7214
21.8476
f1 (ppm)

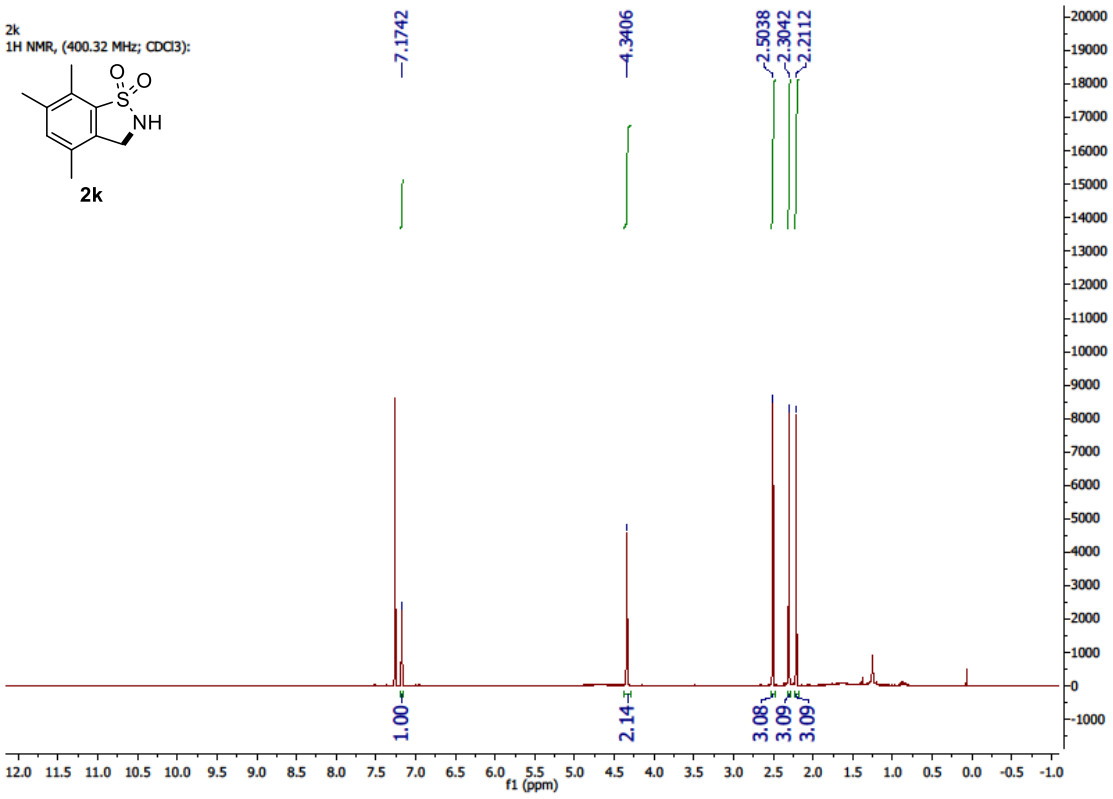
2k
1H NMR, (400.32 MHz; CDCl3):
2k
7.1742
4.3406
2.5038
2.3042
2.2112
1.00
2.14
3.08
3.09
3.09
f1 (ppm)

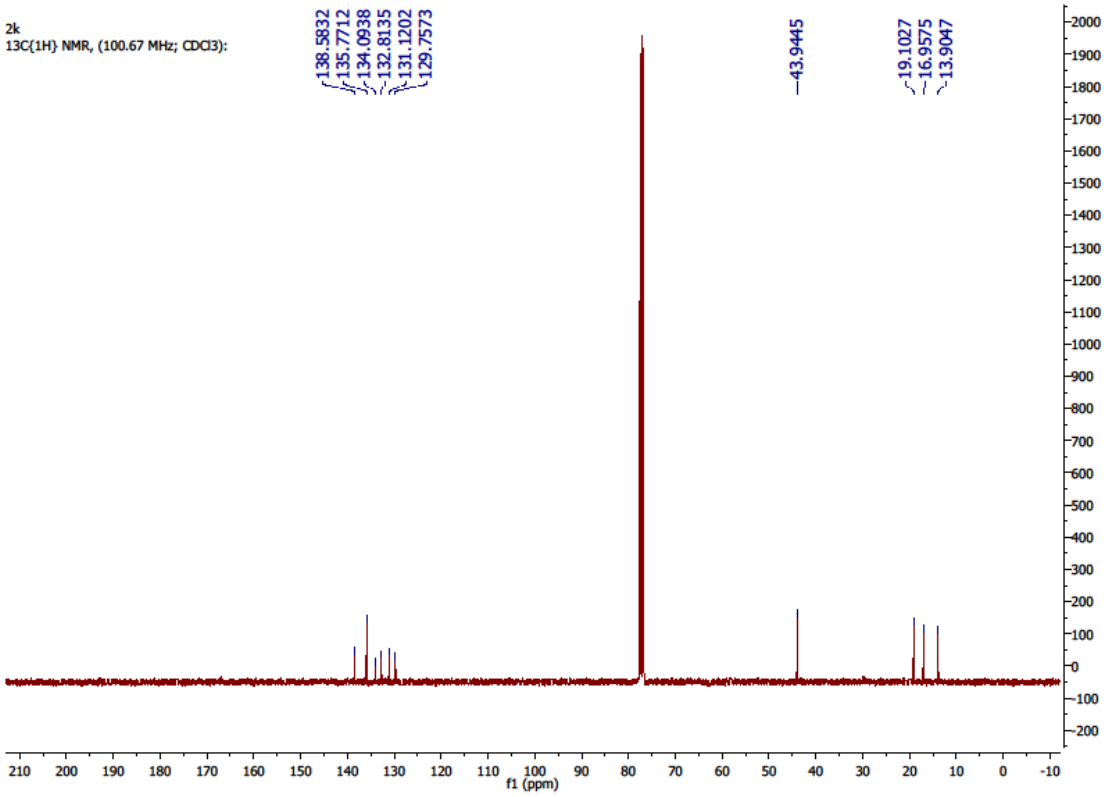
2k
13C{1H} NMR, (100.67 MHz; CDCl3):
138.5832
135.7712
134.0938
132.8135
131.1202
129.7573
43.9445
19.1027
16.9575
13.9047
f1 (ppm)

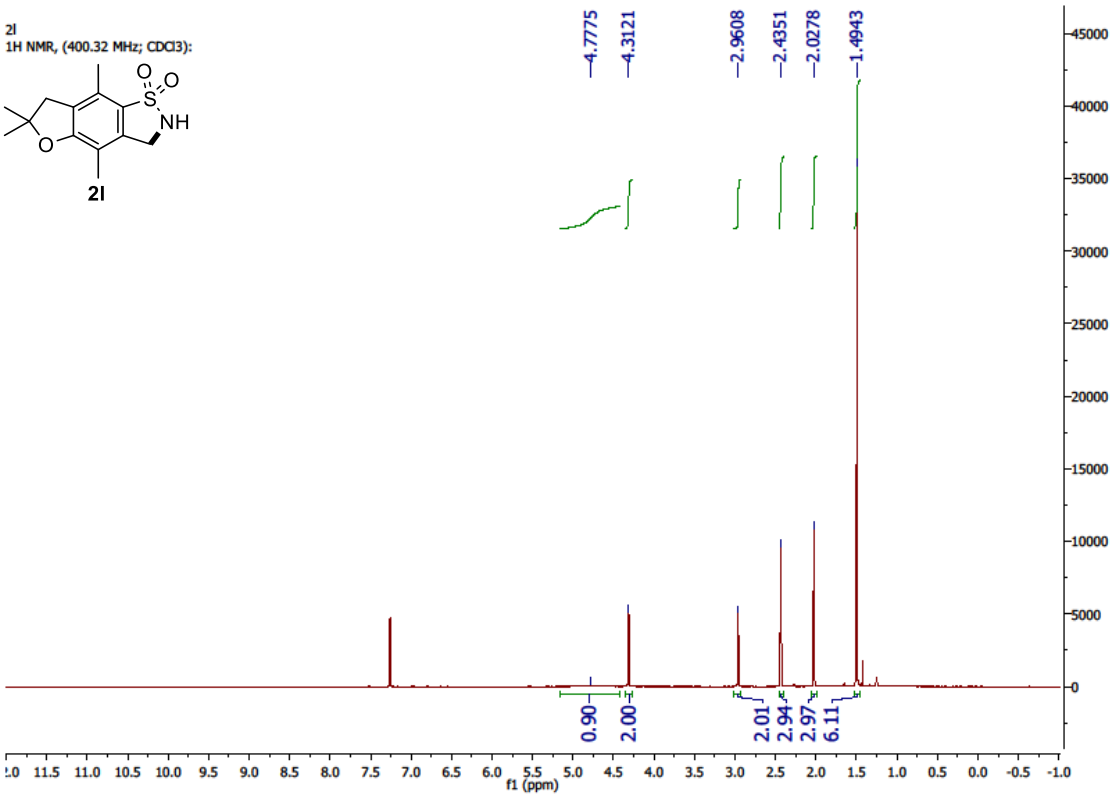
2l
1H NMR, (400.32 MHz; CDCl3):
2l
4.7775
4.3121
2.9608
2.4351
2.0278
1.4943
0.90
2.00
2.01
2.94
2.97
6.11
f1 (ppm)

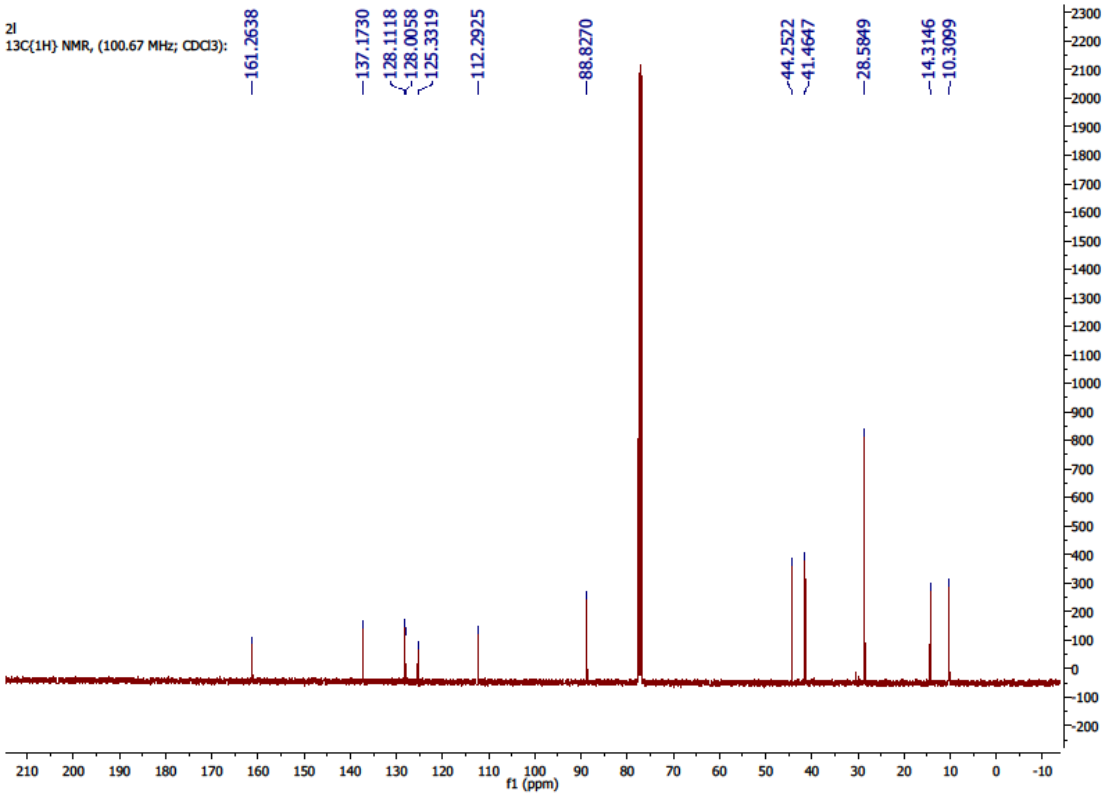
2l
13C{1H} NMR, (100.67 MHz; CDCl3):
161.2638
137.1730
128.1118
128.0058
125.3319
112.2925
88.8270
44.2522
41.4647
28.5849
14.3146
10.3099
f1 (ppm)

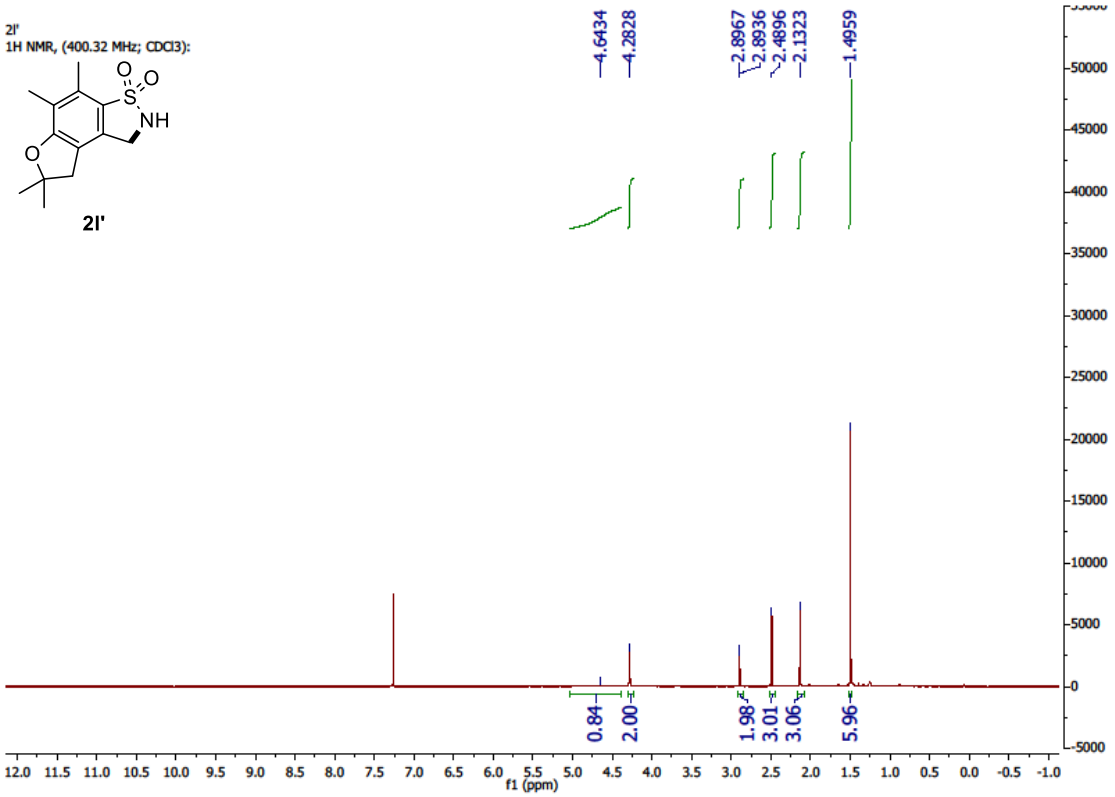
2l'
1H NMR, (400.32 MHz; CDCl3):
2l'
4.6434
4.2828
2.8967
2.8936
2.4896
2.1323
1.4959
0.84
2.00
1.98
3.01
3.06
5.96
f1 (ppm)

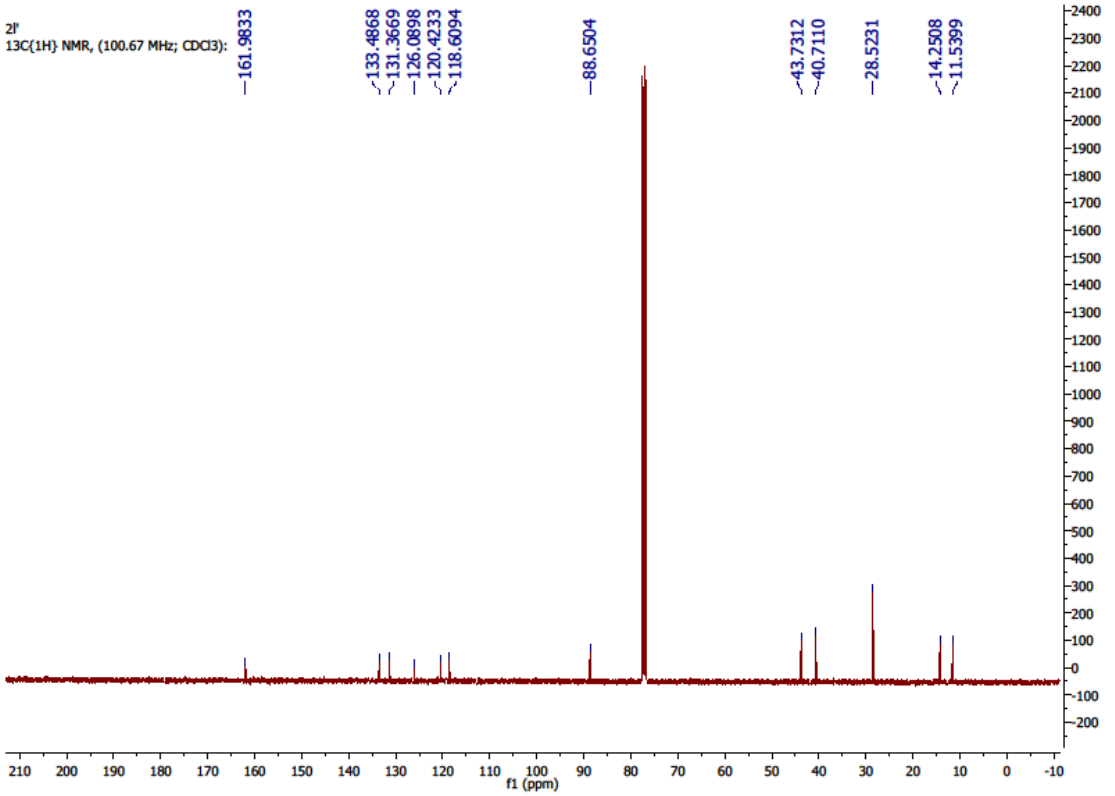
2l'
13C{1H} NMR, (100.67 MHz; CDCl3):
161.9833
133.4868
131.3669
126.0898
120.4233
118.6094
88.6504
43.7312
40.7110
28.5231
14.2508
11.5399
f1 (ppm)

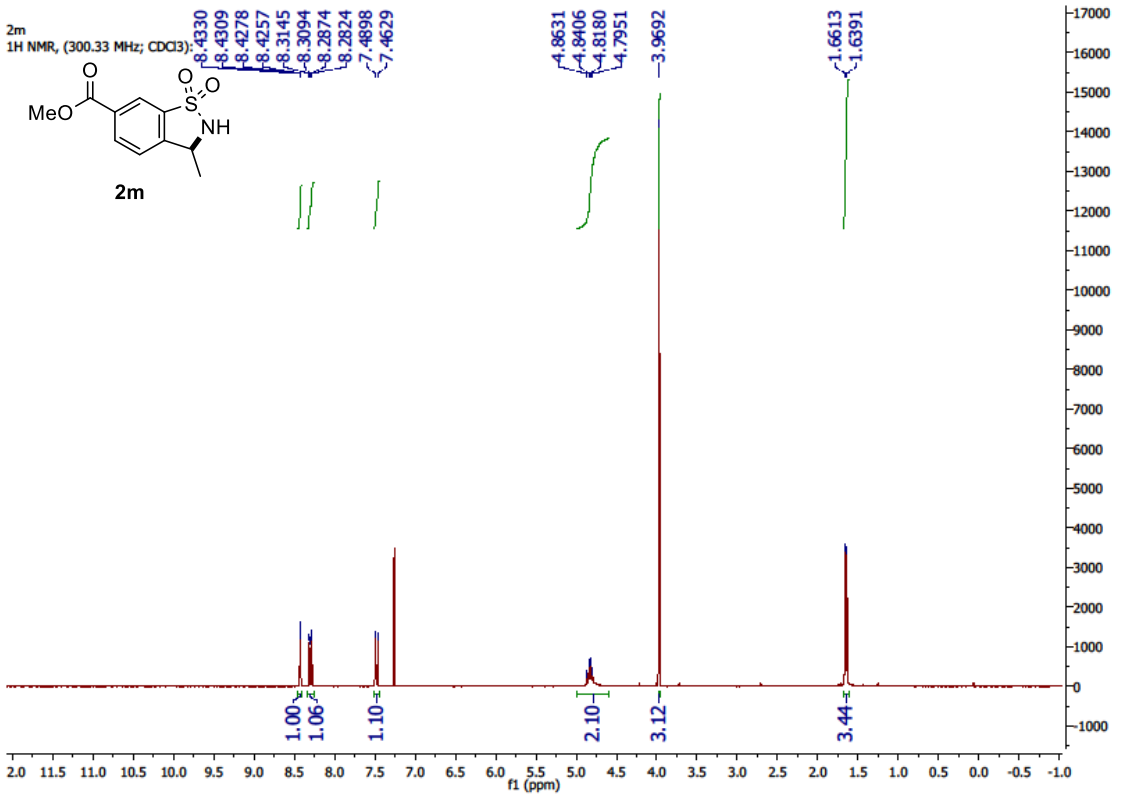
2m
1H NMR, (300.33 MHz; CDCl3):
8.4330
8.4309
8.4278
8.4257
8.3145
8.3094
8.2874
8.2824
7.4898
7.4629
4.8631
4.8406
4.8180
4.7951
3.9692
1.6613
1.6391
MeO
O
O
S
NH
2m
1.00
1.06
1.10
2.10
3.12
3.44
f1 (ppm)

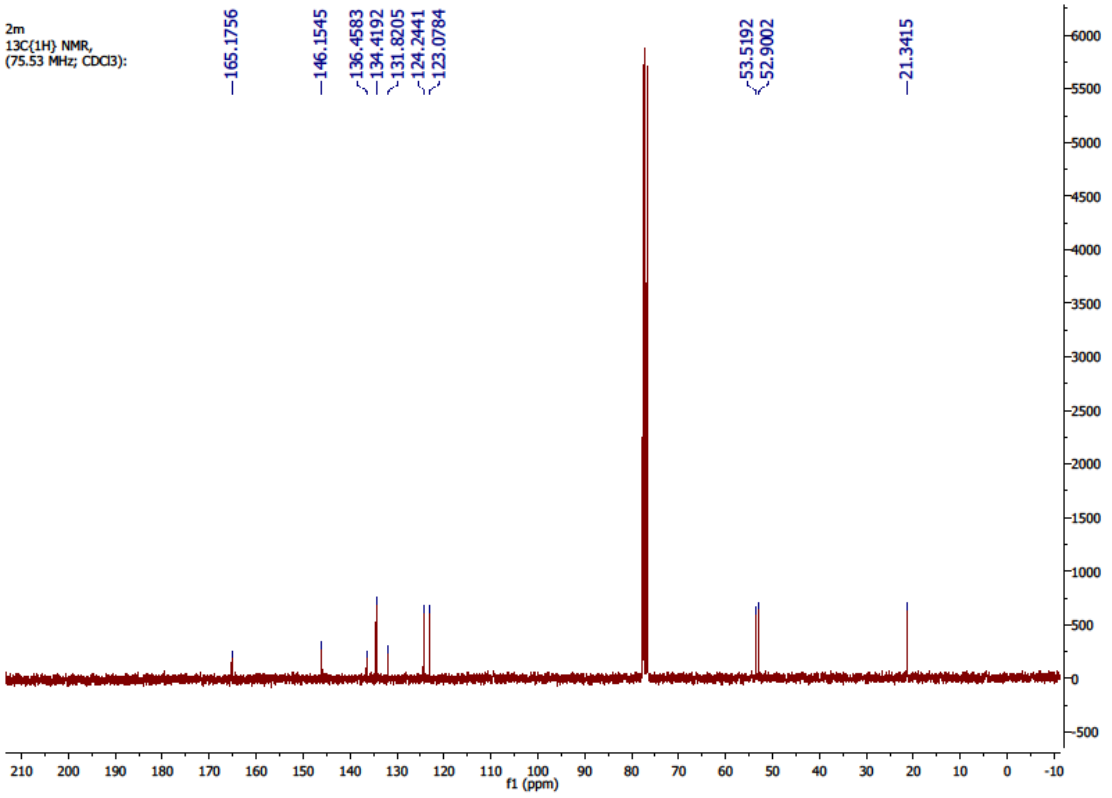
2m
13C{1H} NMR,
(75.53 MHz; CDCl3):
165.1756
146.1545
136.4583
134.4192
131.8205
124.2441
123.0784
53.5192
52.9002
21.3415
f1 (ppm)

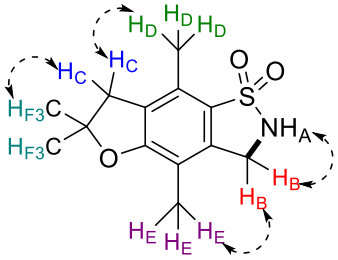

2l

Proton(s)	Δ (ppm)	NOESY Interactions
H_A	4.68	H_B
H_B	4.32	H_A, H_E
H_C	2.96	H_D, H_F
H_D	2.44	H_C
H_E	2.03	H_B
H_F	1.50	H_C

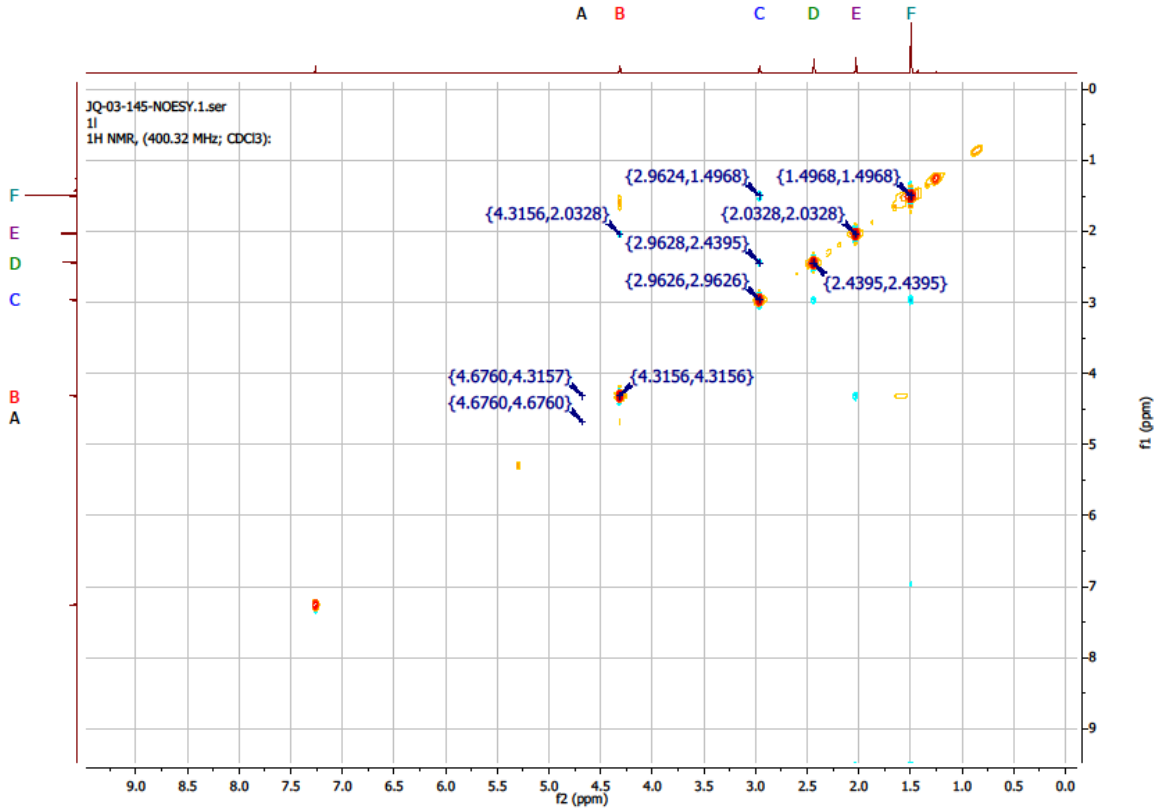

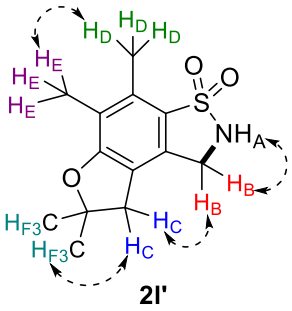

2l'

Proton(s)	Δ (ppm)	NOESY Interactions
H_A	4.64	H_B
H_B	4.27	H_A, H_C
H_C	2.88	H_B, H_F
H_D	2.47	H_E
H_E	2.11	H_D
H_F	1.48	H_C